

https://dspace.org/

The spatial distribution of trace element contaminants, associated with gold mining, in lakes, dams, and pans across Benoni, Ekurhuleni

Du Plessis, Devon Murphy

2019

https://hdl.handle.net/10539/29560

Du Plessis, Devon Murphy. (2019). The spatial distribution of trace metal contaminants, associated with gold mining, in lakes, dams, and pans across Benoni, Ekurhueni. University of the Witwatersrand, https://hdl.handle.net/10539/29560

Downloaded from a DSpace repository. https://dspace.org/



UNIVERSITY OF THE
WITWATERSRAND,
JOHANNESBURG

THE SPATIAL DISTRIBUTION OF TRACE ELEMENT CONTAMINANTS, ASSOCIATED WITH GOLD MINING, IN LAKES, DAMS, AND PANS ACROSS BENONI, EKURHULENI

DEVON MURPHY DU PLESSIS

714838

Prof. Christopher Curtis

A dissertation submitted to the Faculty of Science, in fulfilment of the requirements for the degree of Master of Science.

School of Geography, Archaeology and Environmental Studies

University of the Witwatersrand, Johannesburg

August 2019

DECLARATION

I Devon Murphy du Plessis (714838) declare that this thesis is my own unaided work. It is being submitted for the Degree of Master of Science to the University of the Witwatersrand, Johannesburg. It has not been submitted before for any degree or examination to any other University.



……..

Devon Murphy du Plessis

(2 August 2019)

ABSTRACT

The City of Benoni, like many other cities in Gauteng, is synonymous with the extensive mining of gold in the Witwatersrand region. The city has several major tailings dams and mine dumps to the centre of the area, which can pose a possible risk of trace metal contamination in the several noticeable dams and pans that can be found within the area. Through extensive fieldwork and x-ray fluorescence (XRF) analysis of various sediment samples taken from several dams and pans across the region, a comprehensive understanding of the spatial distribution of trace metals (As, Cu, Fe, Mn, Ni, Pb, and Zn) associated with gold mining was identified. Further, from this, the distribution of trace metals within each site was also analyzed to identify and consider the varying nature of individual site dynamics. In order to identify the level of pollution at each site, a geoaccumulation index was undertaken, based on natural background levels for the areas. The sites that came across as being the most contaminated across the entire region were Amata Pan, Homestead Dam and Kleinfontein Dam. Amata Pan which is situated further south of the concentration of tailings dams, was the most polluted of all sites, with the main reason being the apparent dumping of oil at the site by a large springs manufacturing company. The most likely source of trace metals at Kleinfontein dam is the large mine dump situated right on the bank of the dam. The possible sources of contamination of Homestead Dam may come from the N12 freeway that is situated south of the site and the inflow of two rivers into the dam. Due to the predominance of wind in the area, there is some contribution of trace metals, across the entire region, from the main tailings' dams and mine dumps towards the centre of the city area.

ACKNOWLEDGEMENTS

A research project as big as this one cannot be solely done by oneself and required the aid of many brilliant people. Firstly, this research could not have been possible without the help and guidance of my supervisor Prof Chris Curtis. Without him, I would not have been able to fully develop the idea that led to the creation of this research topic. He has been a mentor more than a supervisor and has constantly had provided support and knowledge over the last two year. I truly do not know where I would be without his help.

Secondly, I would like to express my appreciation to Dr Jennifer Fitchett, who has been a true help and mentor on this research, when Prof Curtis was not available. Without her help, I would not have been able to have achieved a majority of the statistical analysis that I have undertaken in this project. She made the difficult seem simple and I am grateful for this, as a good amount of statistics was required to do this research.

I would also like to show my appreciation to Dr Stefania Merlo, for helping me grapple the GIS component of this research, without her guidance I would not have completed all the bathymetric maps required for the project. She has always been willing to listen to any queries that I have had an I really appreciate her for this. I would also like to express my gratitude to Dr Mary Evans, who has also helped me when I was lost and confused and for always offering her help when I needed it. Without these three-amazing women of the geography department, I truly would have struggled with many aspects of this research.

When conducting, this research, many days of fieldwork were required to gather up samples for analysis. Without the help of Mikayla Blair, Ariel Prinsloo,

Reshoketswe Maepa, Jesse Spratt, Sarah Roffe and Kyle van Heyde, I would not have been able to complete the field work at all nine sites, I am truly thankful to all of them. I especially would like to thank Mikayla Blair, who had to pull the boat across one of the sites, and Ariel Prinsloo, who acted as the best confident during my times of stress. She really is an amazing human being. I also would like to thank Francois Stonelake and Kirsten Noome, for helping me sort through 20 years of wind data to create the wind rose diagrams. Without their help, a week job would have taken me a month.

To Jane Trembath, and the rest of Korsman's conservancy to giving me access to Korsman's in order to complete the field work. The same goes for the local springs manufacturing company for allowing me access to the Amata Pan, through their property. Without access to sites, the fieldwork and subsequent data analysis could not be completed.

Finally, I would like to express my appreciation to my friends and family, without them I would not have been able to find the mental and physical strength to complete this research. My friends have allowed me to be myself and have always provided valuable support in any endeavour that I undertake. The same goes for my family. I would love to thank them for taking my stress and being completely understanding. This truly has been an amazing experience and without them, it would not have been possible.

Table of Contents

DECLARATION ..... **i**
ACKNOWLEDGEMENTS ..... **iii**
LIST OF FIGURES ..... **ix**
LIST OF TABLES ..... **xiv**
ACRONYMS AND ABBREVIATIONS ..... **xvi**
CHAPTER 1: INTRODUCTION AND BACKGROUND **1**
1.1. Introduction **2**
1.2. Problem Statement **3**
1.3. Research Question: **3**
1.4. Aim **3**
1.5. Objectives **4**
1.6. Research Location **4**
1.6.1. Study Area 4
1.6.2. Geology of the Area 7
1.6.3. The climate of the Area 8
CHAPTER 2: LITERATURE REVIEW **11**
2.1. Introduction **12**
2.2. Characterising Pans and Dams in South Africa **12**
1.2.1. Pans – Endorheic Wetlands 13
1.2.2. Dams 16
2.3. Defining Trace Elements **18**
2.4. Sources of Trace Elements in Surface Waters and Sediments **18**
2.4.1. Trace Elements Associated with Gold Mining 19
2.4.2. Acid Mine Drainage 20
2.4.3. Other Sources of Trace Elements 20
2.5. Processes Leading to the Distribution of Contaminants **22**
2.5.1. Sediment Erosion 22
2.5.2. Legacy Contaminants 23
2.6. Spatial Distribution of Trace Elements **24**
2.6.1. Varol (2013) 24
2.6.2. Liu *et al*. (2014) 25
2.6.3. Islam *et al.* (2015) 25

2.6.4. Munyangane *et al.* (2016) 26
2.6.5. Alyazichi *et al.* (2015) 27
2.6.6. Wang *et al.* (2017) 27
2.6.7. Kříbek *et al.* (2014) 28
2.7. Further Sources of Contamination in Urban Water Bodies 28
2.8. Pollution and Toxicity Indices of Sediments 30
2.9. Water Quality Guidelines for Various Elements 32
2.10. The Impacts of Trace Elements on the Environment 34
CHAPTER 3: METHODOLOGY 36
3.1. Introduction 37
3.2. Study Site Selection and Descriptions 37
3.2.1. Study Site Selection 37
3.2.2. Study Sites Descriptions 39
3.3. Methods 57
3.3.1. Bathymetry 58
3.3.2. Wind Rose Diagrams 60
3.3.3. Sediment Sampling 61
3.3.4. Water Sampling 66
3.4. Statistical Analysis 69
3.5. Limitations and Setbacks 70
3.5.1. Fieldwork Duration 70
3.5.2. Data Collection 71
CHAPTER 4: RESULTS 73
4.1. Introduction 74
4.2. Bathymetric Maps 74
4.2.1. The Bathymetry of the Pans 75
4.2.2. The Bathymetry of the Dams 78
4.2.3. The Volume of Each Dam 83
4.3. Wind Rose Diagrams 83
4.4. Results of Water Analysis 85
4.4.1. Physical Characteristics 86
4.4.2. Chemical Characteristics 89
4.4.3. Comparisons to Water Quality Standards 92

4.5. XRF Analysis 94
4.5.1. Average Trace Element Concentrations across each Site. 94
4.5.2. Handheld XRF Error Correlation 96
4.5.3. Conventional XRF Correlation 97
4.6. Sediment Results 98
4.6.1. Understanding Trace Element Distribution across Benoni 99
4.6.2. Representing Trace Element Distribution at each Site 107
4.6.3. Understanding Trace Element Distribution across the Region 117
4.6.4. Relationships between varying Trace Elements 126
4.6.5. Trace Element Pollution and Toxicity 133
CHAPTER 5: DISCUSSION 142
5.1. Introduction 143
5.2. The Spatial Distribution of Contaminants in Water across Benoni 143
5.2.1. *In Situ* Water Characteristics 144
5.2.2. The Chemical Characteristics 145
5.3. The Spatial Distribution of Trace Elements across Benoni 146
5.3.1. The Distribution of Trace Elements within each Pan 147
5.3.2. The Distribution of Trace Elements within each Dam 149
5.3.3. Spatial Distribution Across the Entire Area 153
5.4. The Level of Trace Element Contamination in Sediments across Benoni 154
5.4.1. Contamination in the Pans 155
5.4.2. Contamination in the Dams 156
5.4.3. Contamination Across the Entire Region 157
5.5. The Possible Sources of Trace Elements Across Benoni 159
5.6. The Influence of Gold Mine Tailings' Dams and Dumps 164
5.7. The Possible Environmental Impacts 167
6. CONCLUSIONS 170
6.1. Introduction 171
6.2. Objective 1: To identify the deepest sections of the dams and pans to take sediment and limnological samples and to map each lake/dam/pan. 171
6.3. Objective 2: To identify the spatial patterns in water chemistry, associated with AMD contamination, of lakes/pans/dams. 172
6.4. Objective 3: To determine the spatial variation, of contaminants associated with AMD, in surface sediments, within lakes/pans/dams. 174

6.5. Objective 4: To establish the difference between lakes/pans/dams' trace element concentrations 176

6.6. Recommendations 177

6.7. Synthesis..... 178

REFERENCE LIST 180

References 181

APPENDICES 204

APPENDIX 1: The Initial Measured Depth Data used to Create the Bathymetric Maps……205

APPENDIX 2: The Initial (Raw) Sediment Data obtained from the Handheld XRF…….224

APPENDIX 3: Handheld XRF Data compared to the Conventional XRF Data.228

LIST OF FIGURES

Figure 1.1: A reference map to show the relation of the City of Benoni to the rest of South Africa 5
Figure 1.2: Detailed base map of the City of Benoni, Ekurhuleni 6
Figure 1.3: The lithic classification of the Benoni Area, and subsequent study sites 9
Figure 1.4: Geologic Map of the Benoni Area, and subsequent study sites 10
Figure 3.1: The study sites (dams and pans) that will be used in to conduct the research study. The number values correspond to Table 3.1 40
Figure 3.2: Map showing Korsman's Pan and relative sample points within the site ……41
Figure 3.3: Image of Korsman's Pan during fieldwork in 2017 41
Figure 3.4: Image of the boat used to conduct field work, on the banks of Korsman's Pan 422
Figure 3.5: Map showing Bullfrog Pan and relative sample points within the site 433
Figure 3.6: Image of Bullfrog Pan during field work in 2017 433
Figure 3.7: Image of birds resting on the water of Bullfrog Pan, during field work in 2017 44
Figure 3.8: Map showing Sandpan and relative sample points within the site 45
Figure 3.9: Image of Sandpan from the north of the site, during fieldwork in 2017 45
Figure 3.10: Map showing Homestead Dam and relative sample points within the site 46
Figure 3.11: Image of Homestead Dam from the large urban park on the east bank, with the N12 in the background 45
Figure 3.12: Map showing Middle Lake and relative sample points within the site 48
Figure 3.13: Image of Middle Lake, from west of the Dam, during fieldwork in 2017 48

Figure 3.14: Map showing Civic Lake and relative sample points within the site... 49
Figure 3.15: Image of Civic Lake from the south-west of the dam 50
Figure 3.16: Image of Civic Lake towards the east, with Lakeside Mall to the south 50
Figure 3.17: Map showing Kleinfontein Dam and relative sample points within the site 51
Figure 3.18: Image of Kleinfontein Dam, with the massive mine dump being reprocessed, during fieldwork in 2017 52
Figure 3.19: Image of Kleinfontein Dam from the east, with the Benoni City centre in the background 52
Figure 3.20: Map showing van Ryn Dam and relative sample points within the site 53
Figure 3.21: Image of van Ryn Dam from the boat launch at the East Rand Speedboat Club 54
Figure 3.22: Image of van Ryn Dam taken during field work in 2017 54
Figure 3.23: Map showing Kleinfontein Dam and relative sample points within the site 55
Figure 3.24: Image of Amata Pan with some of the plant life that surrounds the perimeter of the entire pan 56
Figure 3.25: Image of Amata Pan during field work in 2017 56
Figure 3.26: Image of Amata Pan with the Springs Manufacturing Company in the background 57
Figure 3.27: Map showing the relation of the O.R. Tambo Weather Station to the study sites 61
Figure 4.1: Bathymetric Map of Amata Pan 76
Figure 4.2: Bathymetric Map of Bullfrog Pan 77
Figure 4.3: Bathymetric Map of Sandpan 77
Figure 4.4: Bathymetric Map of Korsman Pan 78
Figure 4.5: Bathymetric Map of Civic Lake 80
Figure 4.6: Bathymetric Map of van Ryn Dam 81
Figure 4.7: Bathymetric Map of Kleinfontein Dam 81

Figure 4.8: Bathymetric Map of Middle Lake 82
Figure 4.9: Bathymetric Map of Homestead Dam 82
Figure 4.10: Wind rose diagram comparing the average wind speed to the average direction for a 20-year period (1997 - 1998) 84
Figure 4.11: Wind rose diagram comparing the average wind speed and direction for 2017 853
Figure 4.12: The relationship between the individual sites and the main trace elements found within them 101
Figure 4.13: The PCA expressing the relationship of various samples across the entire research area 100
Figure 4.14: The individual PCA expressing the relationship of samples and trace elements within each site (a. Amata Pan; b. Bullfrog Pan; c. Sandpan) 104
Figure 4.15: The individual PCA expressing the relationship of samples and trace elements within each site (a. Korsmans Pan; b. Homestead Dam; c. Middle Lake; d. Civic Lake; e. Kleinfontein Dam; f. van Ryn Dam) 104
Figure 4.16: Spatial distribution of 7 trace metal concentrations across Amata Pan 106
Figure 4.17: Spatial distribution of 7 trace metal concentrations across Korsman Pan 107
Figure 4.18: Spatial distribution of 7 trace metal concentrations across Bullfrog Pan 108
Figure 4.19: Spatial distribution of 7 trace metal concentrations across Sandpan 109
Figure 4.20: Spatial distribution of 7 trace metal concentrations across Homestead Dam 110
Figure 4.21: Spatial distribution of 7 trace metal concentrations across Middle Lake 111
Figure 4.22: Spatial distribution of 7 trace metal concentrations across Civic Lake 112
Figure 4.23: Spatial distribution of 7 trace metal concentrations across Kleinfontein Dam 113

Figure 4.24: Spatial distribution of 7 trace metal concentrations across van Ryn Dam 114
Figure 4.25: The ANOVA plot comparing each site to each other based on mean As (a), Cu (b), Ni (c), and Zn (d) concentrations. 116
Figure 4.26: The ANOVA plot comparing each site to each other based on mean Ca concentrations. 118
Figure 4.27: The ANOVA plot comparing each site to each other based on mean Cr concentrations..... 118
Figure 4.28: The ANOVA plot comparing each site to each other based on mean Fe concentrations..... 1121
Figure 4.29: The ANOVA plot comparing each site to each other based on mean K concentrations..... 122
Figure 4.30: The ANOVA plot comparing each site to each other based on mean Mn concentrations. 123
Figure 4.31: The ANOVA plot comparing each site to each other based on mean Pb concentrations. 123
Figure 4.32: The ANOVA plot comparing each site to each other based on mean S concentrations..... 125
Figure 4.33: The ANOVA plot comparing each site to each other based on mean Ti concentrations 125
Figure 4.34: The ANOVA plot comparing each site to each other based on mean V concentrations..... 126
Figure 4.35: An image representation of the correlations matric for trace metal concentrations from sediment samples across the entire region 126
Figure 4.36: An image representation of multiple correlation matrices for trace metal concentrations from across the four pans (a. Amata Pan; b. Bullfrog Pan; c. Korsman Pan; d. Sandpan)..... 130
Figure 4.37: Image representation of the correlation matrix done for the relationship between trace elements analysed from various sediment samples for the four dams that fall along the same river gradient (Homestead Dam; b. Middle Lake; c. Civic Lake; d. Kleinfontein Dam)..... 132

Figure 4.38: Image representation of the correlation matrix for the relationship between trace elements identified in sediments at van Ryn Dam 133

LIST OF TABLES

Table 2.1: The recommended water quality guidelines according to the SAWQS and the WHO drinking water guidelines (WHO, 2011)..... 33
Table 3.1: The study sites used for the purpose of this research..... 39
Table 3.2: The number of sampling point at each individual study site 62
Table 3.3: SQL for TEC and PEC (in PPM) for specific trace elements as set out by MacDonald *et al*. (2000)……..62
Table 3.4: The Classification of the Igeo used to identify levels of pollution in each sediment sample..... 66
Table 4.1: Average Volumes of each site based on Bathymetric Depths……..83
Table 4.2: Physical characteristics identified at the surface and depth of each site, with the YSI multi-parameter probes (S = surface; D = depth) 88
Table 4.3: The concentrations, identified with ICP-OES, of various chemical characteristics for the surface and depth samples at each site. These were the only trace elements identified using this method. 89
Table 4.4: Average trace metal concentrations of each site in ppm……...95
Table 4.5: The Correlation of the Sample means versus the Error Mean to identify the accuracy of the Handheld XRF data..... 96
Table 4.6: The correlation and significant difference of the Conventional XRF means for each trace metal versus the Handheld means to identify the similarity and subsequent accuracy of the Handheld XRF Data 98
Table 4.7: The Igeo values, based on the trace metal concentrations identified in each individual sample for all the sites considered as pans. The Igeo values are subsequently colour coded to easily identify pollution extremes and to contrast with unpolluted samples (The key to the colour coding can be identified in Table 3.3..... 139
Table 4.8: The Igeo values, based on the trace metal concentrations identified in each individual sample for three sites considered as dams, Homestead Dam, Middle Lake, and Civic Lake. The Igeo values are subsequently colour coded to

easily identify pollution extremes and to contrast with unpolluted samples (The key to the colour coding can be identified in Table 3.3)..... 140
Table 4.9: The Igeo values, based on the trace metal concentrations identified in each individual sample for two sites considered as dams, Kleinfontein Dam and van Ryn Dam. The Igeo values are subsequently colour coded to easily identify pollution extremes and to contrast with unpolluted samples (The key to the colour coding can be identified in Table 3.3)..... 141
Table A1: Depth Measurements for Korsman Pan 205
Table A2: Depth Measurements for Amata Pan 206
Table A3: Depth Measurements for Sandpan 207
Table A4: Depth Measurements for Bullfrog Pan 209
Table A5: Depth Measurements for Homestead Dam 211
Table A6: Depth Measurements for Middle Lake 214
Table A7: Depth Measurements for Civic Lake 216
Table A8: Depth Measurements for Kleinfontein Dam..... 218
Table A9: Depth Measurements for van Ryn Dam..... 2200
Table B1: The Raw sediment data from the Handheld XRF for the four pans... 224
Table B2: Raw sediment data from the Handheld XRF for the five dams 226
Table C1: Initial Data used to compare the Handheld XRF to the Conventional XRF..... 228

ACRONYMS AND ABBREVIATIONS

Al - Aluminium

ANOVA – Analysis of Variance

AMD – Acid Mine Drainage

As – Arsenic

B_n – background value

Br – Bromide

Ca - Calcium

Cd – Cadmium

Cl – Chlorine/chloride

C_n - Trace Metal concentration

Co – Cobalt

Cu – Copper

Cr – Chromium

DO – Dissolved Oxygen

F - Fluoride

Fe – Iron

FeAsS – Arsenopyrite

FS - Pyrrhotite

FeS_2 – Pyrite

Grp - Group

H_3BO_4 - Borate

HCO_3^- - Bicarbonate

Hg – Mercury

Igeo – GeoAccumulation Index

ICP-MS – inductively coupled plasma mass spectrometry

ICP-OES - inductively coupled plasma optical emission spectroscopy

K - Potassium

Ma – million years ago

MET – Minimal Effect Threshold

Mg – Magnesium

Mn – Manganese

Na - Sodium

Ni – Nickel

NOAA – National Oceanic and Atmospheric Administration

Pb – Lead

PbS - Galena

PCA – Principle Component Analysis

PEC – Probable Effect Concentrations

PET – Probable Effect Threshold

S – Sulphur

SAWS – South African Weather Service

SAWQG – South African Water Quality Guidelines

SO_4^{2-} – Sulphate

Spgrp – Subgroup

SQG – Sediment Quality Guideline

Sr – Strontium

TET – Toxic Effect Threshold

TEC - Threshold Effect Concentrations

U – Uranium

UO_2 - Uraninite

$UO_3Ti_2O_4$ – Brannerite

US EPA – The United States Environmental Protection Agency

V – Vanadium

WHO – World Health Organisation

XRF – X-ray fluorescence

Zn – Zinc

Zr - Zirconium

CHAPTER 1:

INTRODUCTION AND

BACKGROUND

1.1. Introduction

Gold has always been synonymous with the Gauteng region since the first discovery of the precious metal in the 19th century (Forstner and Wittman, 1976; Durand, 2012). This discovery led to the identification of the expansive Witwatersrand Gold Reef that can be found from the east to west of the Province (Durand, 2012). After the processing of rock and extraction of gold through the cyanide process (Rosner and van Schalkwyk, 2000; Roychoudury and Starke, 2006; Tutu *et al.,* 2008), many tailings dams and mine dumps were formed containing unusable material (Marchand and Dinkelman, 2006). Associated with such waste is pyrite, a key source of acid mine drainage (AMD), and multiple trace elements (Coetzee *et al.,* 2002; Jung *et al.,* 2005; Tutu *et al.,* 2008; Humphries *et al.,* 2017). The waste associated with gold mining produces a great number of contaminants that can eventually find their way into various forms of water systems found across the Gauteng region. Trace element contaminants can pose a major threat to the health of humans, plants and animals that come in contact with them (Wang *et al.,* 2017). Great concentrations of trace elements can make their way into water bodies such as lakes/pans/dams which can be found across the province.

The City of Benoni, best known amongst local residents for the high concentration of dams and pans across the city area, is one of the many towns that were born out of the great gold rush in the late 19th to the early 20th century. Very little is known of the actual influence of left-over tailings dams and mine dumps on the dams and pans found across Benoni and how the trace elements associated with these tailings dams are spatially distributed. The aim of this study is to identify the influence of local

sources of trace elements on the various dams and pans and how they are spatially distributed within them and across the city of Benoni.

1.2. Problem Statement

The Witwatersrand region contains many different dams built in response to the increasing gold mining that took place. Many dams were built to feed the mines while they were still operational. Combined with natural pans and wetlands found in the area, these dams offer valuable spaces for both natural and recreational purposes. Over the last century, many of these dam beds could have possibly accumulated varying concentrations of contaminants produced by AMD. Identifying concentrations of AMD contaminants in the dam and pan beds in the area has rarely been done, thus creating a knowledge gap that could be filled.

1.3. Research Question:

What is the spatial distribution of trace element contaminants associated with AMD in lakes, pans and dams in Benoni, Gauteng?

1.4. Aim

The aim of this research is to identify the possible concentrations and spatial distribution of trace metal contaminants, associated with mining activity, deposited in sediments of dams and pans across the city of Benoni, in the Ekurhuleni Metro Municipality in Gauteng. When discussing the spatial distribution of contaminants, the research aims to identify the distribution within various sites and across the study area.

1.5. Objectives

In order to achieve the aim of this research, the following objectives need to be achieved:

- To identify the deepest sections of the dams and pans to take sediment and limnology samples and to map each dam and pan.
- To identify the spatial patterns in water chemistry, associated with AMD contamination, of dams and pans.
- To determine the spatial variation, of contaminants associated with AMD, in surface sediments, within dams and pans.
- To establish the difference between dams and pans trace metal concentrations

1.6. Research Location

1.6.1. Study Area

The Metropolitan Municipality of Ekurhuleni (Fig 1.1), east of Johannesburg is host to several mining towns that make up the region, with a majority of them being based on the Eastern Reef of the Witwatersrand Gold Reef. One of these original towns in the City of Benoni (26° 9' 3.907" S 28° 22' 10.452" E) (Fig 1.2). The City of Benoni contains the New Kleinfontein Gold Mine (Forstner and Wittman, 1976), which has long since been decommissioned. The discovery of gold in the town led to the building of several dams to supply water to the mine. In addition, the region also contains several large natural pans that are possibly fed by

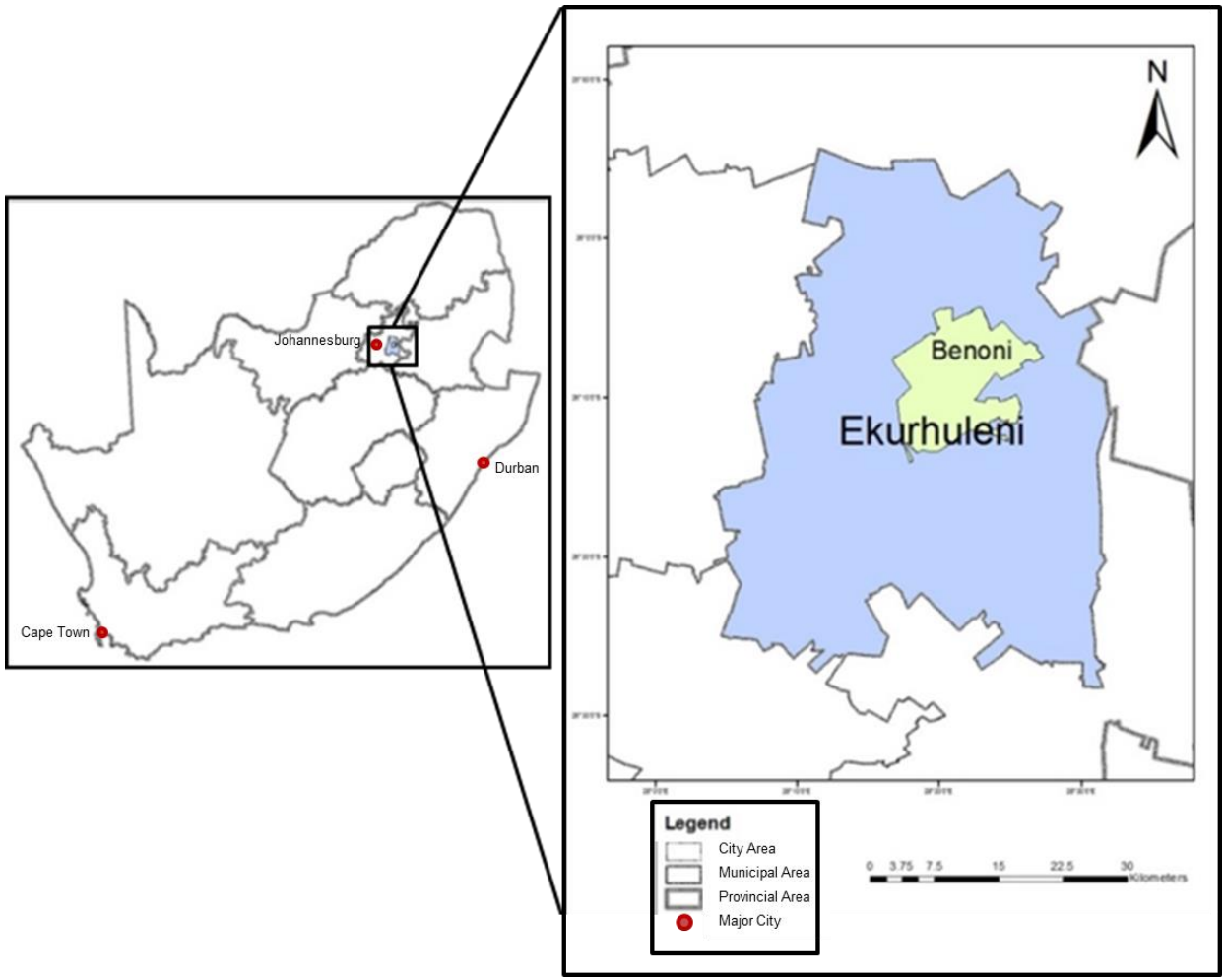


Figure 1.1: A reference map to show the relation of the City of Benoni to the rest of South Africa

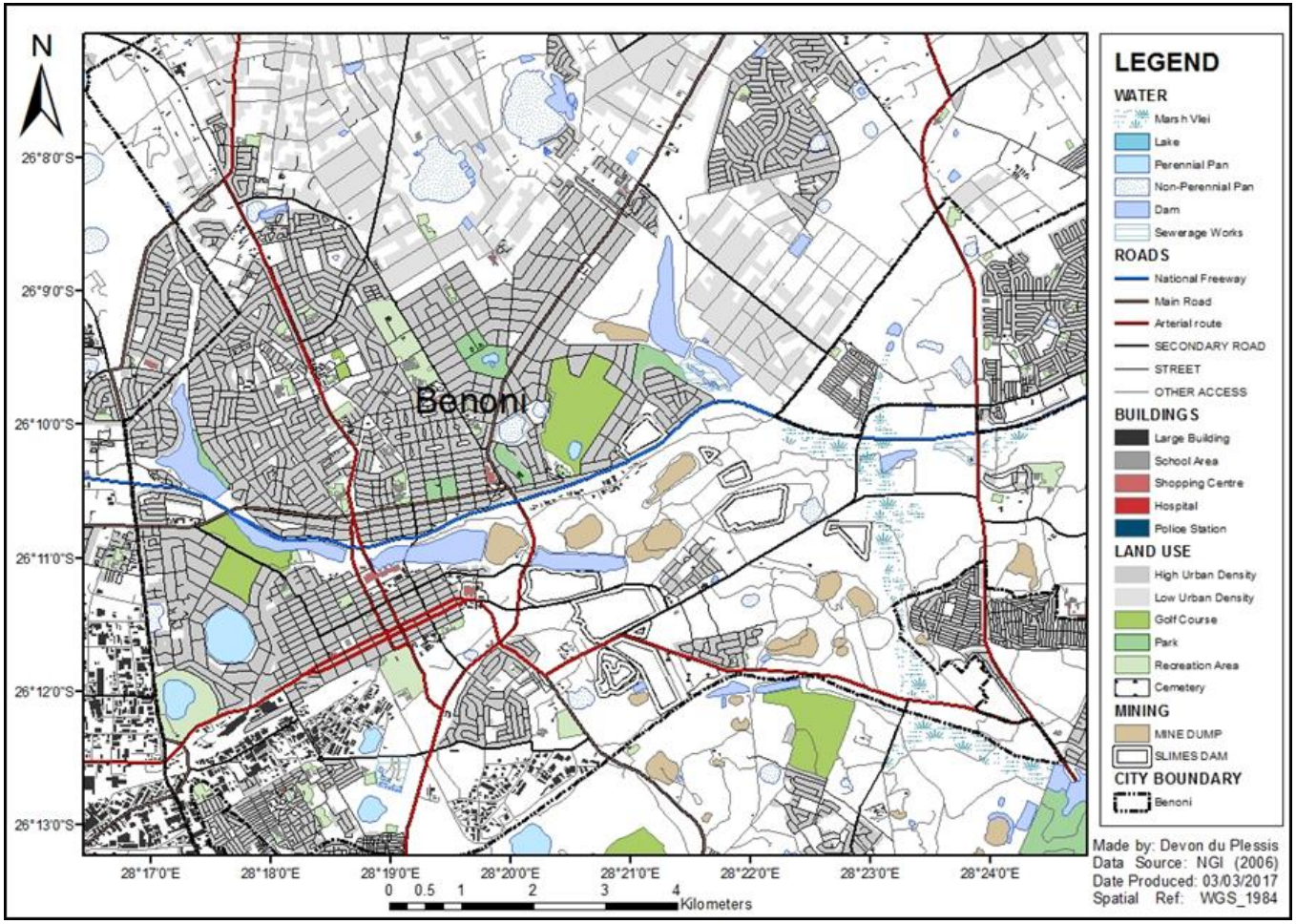


Figure 1.2: Detailed base map of the City of Benoni, Ekurhuleni

underground aquifers and precipitation. Many of the urban lakes and dams found within the city surround a large collection of tailings dumps, left over from the original mining that took place. These tailings dams and mine dumps provide a possible source of both air and water pollution to the region and thus provide a possible source of trace elements to these pans and dams.

1.6.2. Geology of the Area

The City of Benoni lies within the Eastern Basin of the Witwatersrand Basin, which was formed 360 Ma within the Kaapvaal Craton. The Witwatersrand Basin is made up of the Dominion Group, the Ventersdorp and the Witwatersrand Supergroup. The creation of the Witwatersrand Supergroup was episodic, leading to the formation of two different groups. The first of these groups was the West Rand Group, which formed 2970 – 2914 Ma, this was followed by the Central Rand Group, which formed approximately 2894 – 2714 Ma (Coward *et al.,* 1995; Robb and Meyer, 1995; Agangi *et al.,* 2015; Frimmel and Minter, 2017).

The East Rand Basin is primarily known to be made up of sedimentary strata associated with the Wits Supergroup. The Eastern Basin consist of reddish shale and alternate red-yellow sandstones, known as the Jeppestown Subgroup (Coward *et al.,* 1995; Robb and Meyer, 1995; Agangi *et al.,* 2015; Frimmel and Minter, 2017). The Witwatersrand Supergroup was then overlaid by the Ventorsdorp Supergroup, followed by the Black Reef Formation and the Dolomites of the Transvaal Supergroup (Coward *et al.,* 1995; Robb and Meyer, 1995; Agangi *et al.,* 2015; Frimmel and Minter, 2017). At the top is the Karoo Supergroup which covers more than 90% of the East Rand Basin. The East Rand Basin further consists of the

Ecca Group and Dwyka formation, which contains various shales, sandstones, and coal beds (Coward *et al.*, 1995; Robb and Meyer, 1995; Agangi *et al.*, 2015; Frimmel and Minter, 2017). Figure 1.3 and 1.4 express the lithic classification and the stratigraphic classification respectively of the study area.

1.6.3. The climate of the Area

The city of Benoni (26° 9' 3.907" S 28° 22' 10.452" E) is situated within the temperate highveld region of South Africa, which experiences a relatively temperate climate. The area experiences warm, wet summers (December to February), caused by a low-pressure trough that can be found over the central plateau, and mild, dry winters (June to August), which are caused by dominant subtropical high pressures (Dyson, 2015; Dyson *et al.*, 2015). The Average rainfall for the area, which occurs between October and March, ranges from 650 mm to 900 mm per annum (SAWS, 2017). Compared to this the average evaporation rates in the area are approximately 1651 mm per year (Dyson, 2015; Dyson *et al.*, 2015). The area is dominated mainly by northerly winds, with annual winds speeds that vary between 2 $m.s^{-1}$ to 4 $m.s^{-1}$ (SAWS, 2017; Dyson, 2015; Dyson *et al.*, 2015

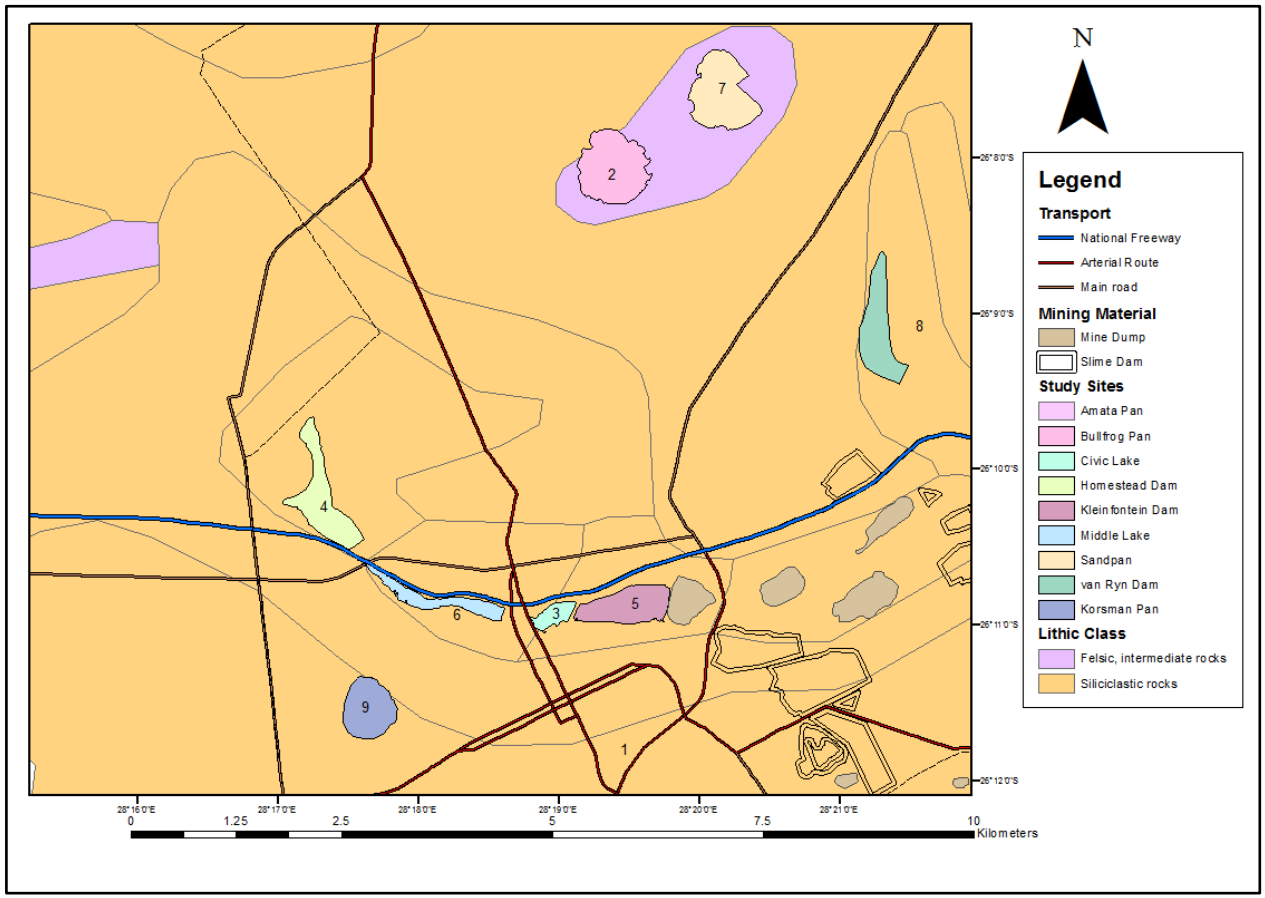


Figure 1.3: The lithic classification of the Benoni Area, and subsequent study sites

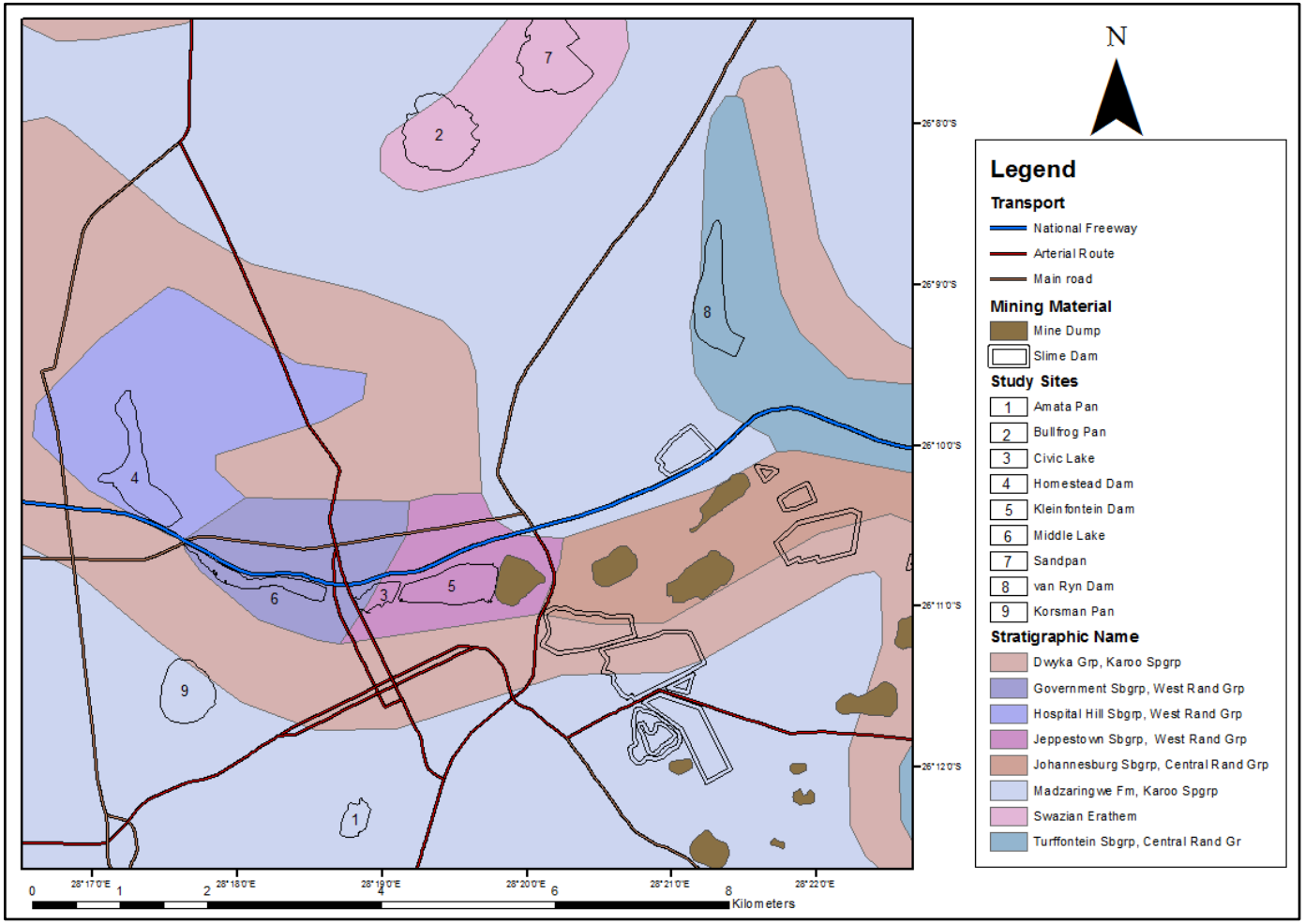


Figure 1.4: Geologic Map of the Benoni Area, and subsequent study sites

CHAPTER 2:

LITERATURE REVIEW

2.1. Introduction

The following section takes a deeper look into the current literature surrounding trace elements in dams and pans. Through this section, a better understanding of the definitions of pans versus dams will be created while expressing what makes the two types of water bodies different. Following this, a comprehensive understanding of what constitutes a trace element is laid out, with the identification of various elements that are considered to be trace elements. The review will further look into what the various sources of trace elements in surface waters and sediments of various water bodies around the world are, and how these substances are distributed across the environment. The review will then look into various other papers that have conducted similar research on the spatial distribution of trace elements across the World, followed by across Africa and then locally. Finally, the review will look at the impacts of trace elements on the environment, as well as further sources of contamination in urban water bodies.

2.2. Characterising Pans and Dams in South Africa

The research mainly focusses on how trace elements associated with AMD are spatially distributed in dams and pans across Benoni. There is a distinct difference between what constitutes a pan or dam. Identifying the difference between the various classifications for sites in this study is important for understanding how each site receives and discharges water. For the purpose of this study, a clear differentiation between dams and pans needs to be established. This allows for further comparison between natural systems and human-made systems.

1.2.1. Pans – Endorheic Wetlands

There are multiple different names associated with endorheic basins, and these are commonly related to the culture or country in which a basin can be identified (de Klerk *et al.*, 2016). In Southern Africa (de Klerk *et al.*, 2016) pans may be defined as depressional endorheic wetlands or basins (de Klerk *et al.*, 2012), that are commonly characterised by having a flat basin floor and no form of outflow points, such as rivers (de Klerk *et al.*, 2012; Ferreira *et al.*, 2012; de Klerk *et al.*, 2016; de Necker *et al.*, 2016; Burger *et al.*, 2019). Pans can either be permanent or temporary, depending on the available rainfall in the region (Hart and Appleton, 1997; Ferreira *et al.*, 2012). Natural pans are generally classified as being extremely shallow, no deeper than three metres (Ferreira *et al.*, 2012), and thus very little chemical or thermal stratification of the water column takes place (de Klerk *et al.*, 2016). Due to the lack of stratification, water columns of pans are characteristically well mixed due to wind action (de Klerk *et al.*, 2016). For a system to be considered endorheic, it must be circular, kidney or oval-shaped, have a relatively flat basin floor, contain closed drainage and be roughly 3m or less in depth (Duthie, 1999; de Necker *et al.*, 2016).

The hydrological contribution to pans occurs either through precipitation or surface and subsurface flow, or a combination of both (de Klerk *et al.*, 2016; de Necker *et al.*, 2016; Yapiyev *et al.*, 2017). Due to a lack of outflow points, water in pans can be lost either via evapotranspiration, which leads to extreme salinization or through groundwater flow (Ashton and Schoeman, 1983; de Klerk *et al.*, 2016). Though there are several characteristics that make pans similar, various pans are still classified differently.

There have been numerous attempts to classify pans, especially within South Africa, over the last 100 years. The first form of classification was done by du Toit in 1927, who classified them as either being coastal or inland. Since this first form of classification, many papers have argued and adapted classifications up until the early 1990s (du Toit, 1927; Hutchinson *et al.*, 1932; Leistner, 1967; Geldenhuys, 1982; Allan 1987; de Klerk *et al.*, 2016). de Klerk *et al.* (2016) adopt the classification set out by Allan (1987), the simplest form of classification in the literature. According to the classification set out by Allan (1987) and de Klerk *et al.* (2016), pans are organised into the following categories: Open Pans, Salt Pans, Sedge Pans, Grass Pans and Reed Pans. Identifying pans using a form of classification aids in understanding the various processes that influence water and sediment composition of those pans.

Open Pans

Open pans are often characterised as being depressional wetlands that are associated with vegetation laying along the shallow shorelines of the pan (Allan, 1987; de Klerk *et al.*, 2016). The pans also consist of very shallow soils and exposed bedrock. These characteristics lead to the pan containing open water with no vegetation found in the centre of them (Allan, 1987; de Klerk *et al.*, 2016). The main vegetation found within these pans is mainly grasses and sedges.

Salt Pans

Salt pans are a form of non-perennial open pan that consists of a saline substrate (de Klerk *et al.*, 2016). Salt pans, often found in the drier western part of South Africa, dry to reveal a white coloured substrate consisting of precipitated salts and/or saline

clays and/or mud (Seaman *et al.*, 1991; de Klerk *et al.*, 2016). The majority of salt pans found within South Africa lie above Ecca and Dwyka Shales, which are known sources of chloride, sodium, magnesium, and calcium (Seaman *et al.*, 1991; de Klerk *et al.*, 2016). Therefore, this leads to many of the pans containing salts such as sodium carbonate, sodium sulphate, sodium chloride, magnesium sulphate, and calcium sulphate. Increase in salinity is caused mainly when evaporative output exceeds precipitation input (Seaman *et al.*, 1991; de Klerk *et al.*, 2016). Gradually over time, these pans become more saline, especially if input aids in maintaining a standing water body (de Klerk *et al.*, 2016).

Sedge Pans

Sedge pans are generally perennial pans that contain vegetation along the shoreline and within the water body (de Klerk *et al.*, 2016). These small to moderately sized pans contain a substrate that can be characterised as black clay soil. The vegetation found within the pan can either be submerged or emergent or a combination of both (de Klerk *et al.*, 2016). Such plant species found within Sedge pans include *Odontelytrum abyssinicum, Eleocharis palustris,* and *Schoenoplectus corymbosus* (de Klerk *et al.*, 2016).

Reed Pans

Reed pans are considered to be the most perennial pans and thus contain high levels of water throughout the year. They generally tend to be deeper than most other types of pans and can reach depths of up to five metres (Grundling *et al.*¸ 2003; de Klerk *et al.*, 2016). Reed pans are mainly characterised by the large body of reeds found in the centre of the pan with open water found along the shoreline (Grundling *et*

al.¸2003; de Klerk *et al.*, 2016). The reed bed found at the centre of the pan is usually found to be floating above a loose organic and peat layer, while the open strip of water contains a rich diversity of other aquatic plant types (Grundling *et al.*¸ 2003; de Klerk *et al.*, 2016).

Grass Pans

Grass pans are characterised as being temporary small pans that only contain water for short periods of time. Typically, these types of pans contain fresh to somewhat saline water and are generally covered by grasses and sedges (de Klerk *et al.*, 2016). These pans usually provide good breeding environments for the African Bullfrog, *Pyxicephalus edulis*, and the Giant Bullfrog, *Pyxicephalus adspersus* (Yetman, 2018). The appearance of the pans often differs between the wet and dry seasons, and they are therefore are often overlooked due to their non-perennial nature (de Klerk *et al.*, 2016).

1.2.2. Dams

Dams, unlike pans, are not considered to be natural systems and are a result of increased human activity. For centuries, human societies have been building large impoundments to contain water (WCD 2000, Lehner *et al.*, 2011). These impoundments, known as dams, are built for a variety of purposes such as irrigation, flood control, water supply, navigation, recreation, and hydro-power generation (WCD 2000, Lehner *et al.*, 2011). Although dams have provided substantial economic benefits to human society, they also cause major issues such as displacement or resettlement, social disruption, changes in food and water security, and increased risk of various diseases. Dams also pose several threats to the local

environment in which they can be found. Dams can be identified as either small or large dams.

Large dams are characterised as being greater than 15m deep and contain a storage capacity greater than 0.5km^3 (Vörösmarty *et al*., 2003; Lehner *et al*., 2011). Compared to this, small dams are characterised as being between 5 and 15m deep with an average storage capacity of 0.003 km^3 (Mantel *et al.,* 2010). Most of the literature on dams in South Africa has focussed on the impacts of dams on the surrounding environment, with very little done on the actual threats on water quality and the environment created by these impoundments. Small dams can have a great influence on river systems around the world (Fanelli and Lautz, 2008; Mantel *et al.,* 2010). Studies have shown that small dams can influence; habitat structure through the capturing of sediments (Stanley *et al.,* 2002; Mantel *et al.,* 2010), species composition of riparian plants through poor floating capacity (Jansson *et al.,* 2000; Mantel *et al.,* 2010), reduce the density of cold-water fish, and change macroinvertebrate communities through increased average temperature below dams in summer (Lessard and Hayes, 2003; Mantel *et al.,* 2010). Mantel *et al.* (2010) aim to identify the influence of small dams on water quality and quantity in rivers in two regions across South Africa. Their study identified that a high density of small dams increased certain physio-chemical variables and reduced flow lows in two regions of South African, Mpumalanga and the Western Cape. A large amount of the literature identifies the influence of small dams on the immediate catchment they are found, but little has identified how those small dams and the relative environments they create are influenced by pollution such as trace elements.

2.3. Defining Trace Elements

Increasing anthropogenic activity has overwhelmingly increased the concentrations of toxic compounds in multiple ecosystems, threatening the health of local populations and causing a decline in species diversity (Zaaboub *et al.*, 2015). Urban sediments and waters in such ecosystems are further at a constant threat from contaminants such as trace elements (Karger *et al.,* 2015). The Oxford Dictionary of the Environment and Conservation (Park and Allaby, 2017) defines them as elements that are "naturally found in extremely small quantities in animal and plant cells and tissues, and some of which are necessary for growth". Trace elements can include aluminium (Al), arsenic (As), cadmium (Cd), copper (Cu), chromium (Cr), iron (Fe), mercury (Hg), lead (Pb), manganese (Mn), nickel (Ni), uranium (U), vanadium (V), and zinc (Zn) (Yacoub *et al.*¸ 2013; Park and Allaby, 2017). In comparison, there are several major ions found in the environment. These include bicarbonate (HCO_3^-), bromide (Br), borate (H_3BO_4), calcium (Ca), chloride (Cl), flouride (F), magnesium (Mg), potassium (K), sodium (Na), strontium (Sr), sulphur (S), and sulphate (SO_4^{-2}) (Park and Allaby, 2017). Trace elements are introduced into the environment in multiple ways. They can be introduced either directly or indirectly into soils and the water column from multiple sources.

2.4. Sources of Trace Elements in Surface Waters and Sediments

Concentrations of trace elements in sediments can generally be considered as a result of the original source material which leads to those sediments. Excessive concentrations, those that are over the natural limit, express some form of contamination and therefore represent external sources of pollution. In an urban area,

there is no shortage of possible sources of trace elements. Some of these possible sources include AMD, industrial complexes, freeways and roads, car exhaust fumes, coal power stations and domestic wastewater.

2.4.1. Trace Elements Associated with Gold Mining

After the extraction of gold through the cyanide process, gold mines leave behind large tailings dams that contain various forms of quartz, phyllosilicates, and pyrite as by-products of the mining processes (Rosner and van Schalkwyk, 2002; Roychoudury and Starke, 2006; Tutu et al., 2008). The associated tailings also consist of many more minerals, such as uraninite (UO_2) pyrite (FeS_2), arsenopyrite (FeAsS), brannerite ($UO_3Ti_2O_4$), pyrrhotite (FS) and galena (PbS) (Abiye, 2014). These minerals, when exposed to oxidised water, can lead to the distribution of trace and major elements such as; As, Cd, Co, Cu, Fe, Ni, Pb, S, U, Zn, and more (Jung et al. 2005; Roychoudury and Starke, 2006). Most of these tailings generally tend to lack vegetation, thus making them a source of dust which can be influenced by both erosion and leaching (Naicker et al., 2003; Abiye, 2014). Acid mine drainage mainly takes place when oxygenated water comes in contact with pyrite in the left-over waste material, leading to acidification taking place (Naicker et al., 2003). There are two stages to the production of acid mine drainage (Akcil and Koldas, 2006; McCarthy, 2011). The first stage involves the production of ferrous sulphate and sulphuric acid (Akcil and Koldas, 2006; McCarthy, 2011). Following this ferrous hydroxide and more sulphuric acid are produced (Akcil and Koldas, 2006; Oberholster, 2010; McCarthy, 2011: McCarthy and Humphries, 2013).

2.4.2. Acid Mine Drainage

AMD can create an adverse impact on the local environment that surrounds the tailings dams. AMD can lead to the acidification of various underground and surface water systems (Akcil and Koldas, 2006; Oberholster, 2010; McCarthy, 2011: McCarthy and Humphries, 2013). This can lead to a lower pH of the system and the addition of various trace elements that are harmful to various plant and animal species (Hui *et al.,* 2012). A lower pH can also lead to a greater mobilisation of some trace elements that would usually only be found in a solid or precipitate form. Such trace elements associated with AMD contamination include Fe, Ni, Pb, As, U, Mn, Cr, Cu, Co, Hg, V, and Zn. These contaminants can be deposited in sediments found within rivers and lakes, taken up by plant material in wetlands and can easily be bioavailable (Coetzee *et al.,* 2002; Jung *et al.,* 2005; Kossof *et al.,* 2014; Humphries *et al*., 2017). The spatial distribution of these contaminants from one single source is rarely identified, but Tutu *et al.* (2008)mapped the overall pollution levels of sites close to tailings dams across the Johannesburg region.

2.4.3. Other Sources of Trace Elements

Although AMD can provide a substantial source of trace elements in pans, lakes and dams, there are many other possible sources, especially within an urban setting such as Benoni, that provide substantial amounts of contaminants. Other possible sources of trace elements may include freeways, industrial areas, liquid industrial effluents, car exhaust fumes, coal power stations, atmospheric deposition, terrestrial runoff, and domestic wastewater effluents (Lee and von Lehmden, 1973; Herman and Neumann-Mahltau, 1985; Islam *et al.,* 2014; Alyazichi *et al.,* 2015). One of the

main sources of trace elements is fuel (Lee and von Lehmden, 1973). Trace elements in coal or oil occur naturally (Lee and von Lehmden, 1973). Fuel can contribute to contamination of soils and the water column through trace element deposition after combustion, incineration, and from other forms of industrial emissions (Lee and von Lehmden, 1973). Industrial materials that undergo grinding, smelting, blending and other various processes may lead to the production of aerosols. Once trace elements are airborne, they pose a significant threat to the contamination of soils and water, through atmospheric fallout (Lee and von Lehmden, 1973; Herman and Neumann-Mahltau, 1985; Islam *et al.*, 2014).

Once contaminated, soils also pose a significant source of trace elements through release into the water column (Islam *et al.*, 2014; Allinson *et al.*, 2015). The mobility of trace elements in soils is related to the function of metal characteristics, various properties of the soil, and the total concentrations of metals in the soil (Karger *et al.*, 2015). Contamination of water with trace elements can happen in multiple ways and is not just as a result of atmospheric fallout or contaminated underlying sediment. A study done by Alyazich *et al.* (2015) in Kagarah Bay in Australia, identified several other direct sources of trace elements into the water column of the bay. Other possible sources of contaminants include discharge points, stormwater outlets, boatyards and watercraft, gasoline fumes etc (Alyazich *et al.*, 2015). There are many sources of trace elements, especially in an urban environment. The distribution of trace elements from the original source to the water systems takes place through various geophysical processes.

2.5. Processes Leading to the Distribution of Contaminants

Trace elements can be introduced into dams by various process, such as groundwater and underground water flow, water and wind erosion and acid mine drainage (Akcil and Koldas, 2006; Blight 2007; Oberholster, 2010; McCarthy, 2011: McCarthy and Humphries, 2013, Kříbek *et al.*, 2014).

2.5.1. Sediment Erosion

Soil erosion is considered a major environmental problem both worldwide and locally (Le Roux *et al.,* 2012; Seutlaoli and Beckedahl, 2015). Erosion is the process where soil particles are detached and transported by either wind or water (Le Roux *et al.,* 2007; Le Roux *et al.,* 2008). Water erosion can take place in mainly three ways, as rain splash, concentrated flows of rill and/or gully erosion, and as sheet flow (Le Roux *et al.,* 2008; Le Roux *et al.,* 2012; Seutlaoli and Beckedahl, 2015). For dams and pans closer to the tailings dams, the most likely possible method of transport of trace elements is through water erosion. Deposition by atmospheric fallout is likely to be the main cause of trace elements within the sites. In order for trace elements to get into the atmosphere, wind erosion needs to take place (Kříbek *et al.,* 2014). Particles from tailings dams may differ in size, with different sizes being deposited at different distances.

The study by Kříbek *et al.* (2014) identified the spatial distribution of trace elements from a mining area in Namibia. Particles from tailings dams were generally deposited within a 5km radius of the source of the material (Kříbek *et al.*, 2014). Particle of material from mine dumps and tailings dumps occur in two different sizes, sand and silt, which are deposited in different stages (Blight, 2007). Particle size is

important as it has an influence on properties such as vulnerability to entrainment, transport and deposition, permeability, porosity, load strength and chemical reactivity (Blott and Pye, 2012). The first particles to be deposited from mine waste dumps are sand particles (Blight, 2007), which consist of particle sizes between 63 µm to 2 mm (Boggs, 2011). This is followed by silt particles (Blight, 2007), which consist of particles sizes between 2 µm to 63 µm (Blott and Pye, 2012). The silt particles are usually winnowed out by the wind and thus are carried further (Blight, 2007). Kříbek *et al.*, 2014 identified that 25% of particles from tailings dams, consisting of a particle size smaller than 10 µm were deposited at least 5 km away from the source. The distribution of sediments containing trace elements into various water systems such as rivers, lakes, dams, and pans has been identified by a study published in three papers by Kossoff *et al.* (2011; 2012[a]; 2012[b]). Therefore, it is safe to assume that any tailings dams found within the study area can act as a source of trace elements.

2.5.2. Legacy Contaminants

Other possible ways in which trace elements could be distributed within each site is through legacy contaminants. Legacy contaminants are generally contaminants that pre-existed within the site and across the entire catchment (Yang *et al.* 2002; Gewurtz *et al.*, 2008; Combi *et al.*, 2016; Mustajärvi *et al.*, 2017; Olsen *et al.*, 2019). Once they have remobilised they can then be redistributed across the catchment and the water bodies (Yang *et al.* 2002). Legacy contaminants would especially be a plausible source of contaminant to the dams that are located along the same gradient, as legacy contaminants from subsequent dams upstream may provide further contamination downstream.

2.6. Spatial Distribution of Trace Elements

There has been much research done on the various forms of influences gold mining and the associated tailings dams and mines dumps have on water sources in the Johannesburg region (Rosner and van Schalkwyk, 2002; Akcil and Koldas, 2006; Roychoudury and Starke, 2006; Tutu et al., 2008; Oberholster, 2010; McCarthy, 2011: McCarthy and Humphries, 2013, Humphries *et al.,* 2017). There is also a reasonable body of literature on trace metal contaminants in surface sediments and waters of rivers, lakes and dams. Very little research, however, has focussed on the spatial distribution of trace elements across different individual sites across one area. A deeper look into literature that is similar in terms of investigating spatial distribution will be presented. The reason for the limited selection of papers is because there is a lack of specific literature on the spatial distribution of trace elements. Due to the lack of literature, a more in-depth look at each paper was required.

2.6.1. Varol (2013)

Varol (2013) evaluated dissolved heavy metal concentrations in the Batman, Dircl and Kralkızı dams which can be found within the Tigris River basin of Turkey. The results of the study identified that concentrations reflected natural background levels, where the lowest concentrations were identified towards the dam walls. The highest concentrations of trace elements were located at stream entrances to the dams. Varol's (2013) study identified that the most abundant trace elements were Fe, Cr and Ni, whereas the lowest trace metal concentrations included As and Cd. The study concluded that the dissolved heavy metals in each dam were controlled by

natural sources, such as weathering of parent rock and subsequent soil formation (Varol, 2013.)

2.6.2. Liu *et al*. (2014)

Liu *et al.* (2014) conducted a study that sought to identify the spatial variation of heavy metals, upstream and downstream of the Manwan Dam, in the Lancang River, China. The study wanted to identify if there was a significant impact of hydroelectricity on concentrations of heavy metals in sediments found upstream and downstream. A total of 117 sediment samples were collected in December 2011, and analysed for metals such as Cd, Cr, Cu, Ni, Pb, and Zn, using inductively coupled plasma atomic emission spectroscopy (ICP-AES) (Liu *et al.*, 2014). Some elements were identified to be greater upstream, compared to downstream, with As and Cd exceeding the recommended soil quality guidelines (Liu *et al.*, 2014). Through principal component analysis, the research identified that sources of trace elements were either anthropogenic, in the form of fertilizers, pesticides, and from pigment and electroplating industries, in the region, or from natural sources (Liu *et al.*, 2014). The research concluded that there was a difference in trace metal concentrations and sources upstream and downstream of the dam.

2.6.3. Islam *et al.* (2015)

An assessment of trace metal concentrations in surface sediments and waters in an urban river in Bangladesh was conducted by Islam *et al.* (2015). The study mainly focused on the identification of concentrations for six trace elements; As, Cd, Cr, Cu, Ni, and Pb. Islam *et al.* (2015) identified that the associated levels for the trace elements studied exceeded safe drinking water limits, except for Cd and Pb, which

were found to have very little metal mobility. Using a geoaccumulation index and contamination factor, the research identified that sediment samples were moderately to heavily contaminated with Cr, As, Cd and Pb respectively (Islam *et al.*, 2015). The study concluded that the pollution of the river with heavy metals was mainly due to anthropogenic sources such as industrialisation, dumping of urban waste etc. and, should be of great concern for local biota and inhabitants along the river.

2.6.4. Munyangane *et al.* (2016)

The next study, done by Munyangane *et al.* (2016), conducted an assessment on trace element occurrence and distribution in borehole water for the Greater Giyani area in Limpopo, South Africa. Munyangane *et al.* (2016) collected samples from boreholes during the wet and dry season from 2012 to 2013, and analysed for trace elements such as Cd, Cr, Se, and Pb using inductively coupled plasma mass spectrometry (ICP-MS). They identified evidence that expressed seasonal fluctuations in concentrations of all analysed elements, apart from As (Munyangane *et al.*, 2016). Compared to this, concentrations of Cr and Se were below the South African national standards permissible limits for safe drinking water. Four of the boreholes studied exceeded the average water quality guidelines for As, with two of these sites being five times over the recommended limit (Munyangane *et al.*, 2016). Munyangane *et al.* (2016) concluded that main source of the contamination came from underlying bedrock and As mineralisation and that there were severe health implications for the local communities that rely on these boreholes for drinking water.

Most of these studies have mainly focussed on the concentrations of trace elements in surface waters and sediments, with few focussing on the spatial distribution of

such metals. The following three studies provide specific examples of the spatial distribution of trace elements within one site.

2.6.5. Alyazichi *et al.* (2015)

The research conducted by Alyazichi *et al*. (2015) investigated the spatial and temporal distribution of trace metal concentrations of water and sediment factions within Kogarah Bay, Australia, to identify the possible sources of such trace elements. A total of 59 surface sediments samples and six subsurface samples were taken. Alyazichi *et al.* (2015), identified the study area to be uncontaminated with Cr and Ni, moderately contaminated with As and heavily contaminated with Cu, Zn and Pb. The highest concentrations of metals, Cu, As and Pb, were found in the southeast, north, and northeast of the bay (Alyazichi *et al.*, 2015). The spatial distribution of heavy metals was strongly related to organic matter and muddy particles (Alyazichi *et al.*, 2015). Temporal distribution expresses a decline in trace elements with an increase in depth, which coincides with the settlement of Europeans in the area. The research finally identified the sources of trace elements to be stormwater outlets, gasoline fumes, boatyards and various other human activities (Alyazichi *et al.*, 2015).

2.6.6. Wang *et al.* (2017)

Compared to these studies Wang *et al.* (2017) identified the spatial distribution and seasonal variation of heavy metals, such as Cu, Zn, Cr, Cd and Hg, in surface waters of the Liaohe River, in China. Wang *et al.* (2017) analysed 324 surface water samples, collected between 2009 and 2010. The study identified that there was a significant impact on Cu and Zn concentrations due to spatial and seasonal

differences (Wang *et al.*, 2017). The greatest concentrations of Cr and Hg were identified during the wet period, whereas the greatest concentrations of Cu and Cd were found during the standard water levels and Zn during the dry season (Wang *et al.*, 2017). Wang *et al.* (2017) identified that there was an increase in health risks from upstream to downstream of the main river, and that of all the metals analysed, Cr posed the greatest single health risk to the local population.

2.6.7. Kříbek *et al.* (2014)

Compared to the two studies conducted on spatial distribution in water, the study conducted by Kříbek *et al.* (2014) identified the spread of trace metal contaminants from tailings dams at a site in Namibia. Although the study did not look at the specific concentrations within water sources, the paper looked at the spatial distribution of such contaminants. Kříbek *et al.* (2014) specifically looked at the major threat of trace elements from tailings dams and ore treatment plants to the town of Rosh Pinah, Namibia. The study identified that the air in the region contained high levels of Cu, Mn, and Zn, with lesser amounts of As and Cd (Kříbek *et al.*, 2014). The dust mainly followed the levels of prevailing winds leading to deposition being in a northwest direction, thus affecting the eastern and north-eastern parts of the town (Kříbek *et al.*, 2014). The distribution of such trace elements has a major influence on the local environment and systems they contaminate.

2.7. Further Sources of Contamination in Urban Water Bodies

The geographical location of the Johannesburg region is unique in that the city is not situated near a major water source, such as a river or lake (Turton, 2006). The city lies on the continental Witwatersrand watershed, where water north of the watershed

flows into the Indian Ocean via the Limpopo River and water south of the watershed flows, through the Vaal-Orange, into the Atlantic Ocean (Turton, 2006; Oelofse *et al.*, 2007; Oberholster and Ashton, 2008; Oberholster, 2010). This leads to the city providing multiple sources of contamination for lakes and dams situated within the watershed. Apart from AMD, other possible impacts on water quality in urban lakes and dams include eutrophication, salinization, increased effluent discharge, industrial waste, inorganic compounds and more. These forms of pollution all provide various forms of contaminants into lakes and dams across the city.

Various other forms of pollution, such as eutrophication and salinization can be represented in the form of nutrients and minerals. Eutrophication is often associated with increased input of nutrients such as nitrates, nitrites and phosphates (Oberholster, 2010; Harding, 2015). Increased nutrient intake can lead to an increase in algal blooms and the development of cyanobacteria that is toxic to many different species. Common contributors to nutrients are the agricultural industry, failing wastewater treatment works and wastewater from urban township areas (Harding, 2015).

Compared to this salinization leads to the increase in salts such as sodium chloride into the water system, which in turn leads to an increase in both the pH and conductivity of the water (van Niekerk *et al.*, 2009; Oberholster, 2010). High conductivity can occur naturally when the water is situated over a dolomitic rock or from the treatment of AMD or from intensive agriculture along the river system. Issues associated with water quality in Johannesburg are mainly due to the increased industrialisation and urbanisation the region has seen over the last 100 years. Due to the increase in impervious surfaces associated with urban areas, most of the

precipitation found within the city is unable to infiltrate the ground, therefore leading to an increase in surface runoff, allowing it to become polluted before it reaches the various water systems such as rivers and dams (Paul and Meyer, 2001).

The sites located to the east of Johannesburg, in the city of Benoni, like many other lakes, dams and pans across the region, would have been exposed to the various forms of contamination found within urban regions. Such possible forms of contamination include gold mining, industrial effluent, wastewater, suburban effluent and more. In order to identify the extent to which these sites vary, in terms of sediment and hydrological dynamics, and have been affected by the urban environment that they are found within, a spatial sampling programme was designed.

2.8. Pollution and Toxicity Indices of Sediments

There are several indices to identify the level of trace element pollution and toxicity in sediments found within the literature. Of the main contamination indices, three are commonly used, GeoAccumulation Index (*Igeo*), enrichment factor (EF) and metal pollution index (MPI). All three of these indexes rely on some form of background value, allowing for a greater distinction between natural trace elements from parent soil and anthropogenic sources (Barbieri, 2016).

Igeo, first proposed by Müller (1981), is a calculation that aids in identifying the level of probable pollution of trace elements in sediments (Ruiz, 2001; Burton, 2002; Roychoudury and Starke, 2006; Barbieri, 2016). *Igeo* is an indicator that is used to assess the concentrations of anthropogenic contaminant deposition in sediments. Igeo is calculated according to the normalisation of the trace element concentration, in the sediment, to the concentrations of the natural background levels of that trace

element (Müller, 1981: Ruiz, 2001; Burton, 2002; Roychoudury and Starke, 2006; Barbieri, 2016). Compared to this EF requires the use of a normalization element in order to identify the difference between natural and anthropogenic concentrations of trace metals (Burton, 2002; Roychoudury and Starke, 2006; Hanif *et al.*, 2015; Barbieri, 2016). Pollution indices do not equate to level of toxicity of each trace element in the sediment, and thus should not be confused with predicting the level of toxicity to various species.

Sediment quality guidelines (SQG) are the most common ways of identifying toxicity in various species. Several SQGs, based on numerical data from freshwater systems, have been developed globally, with the majority coming from the United States Environmental Protection Agency (USEPA), National Oceanic and Atmospheric Administration (NOAA)(Long and Morgan, 1990), and the Ontario Ministry of Environment and Energy (Persaud *et al.,* 1993). These SQGs have also been extensively consolidated in papers by MacDonald *et al.* (2000) and Burton (2012). Numerical SQGs are generally separated into three categories (depending on which paper you read): minimal effect threshold (MET), probable effect threshold (PET), and toxic effect threshold (TET). The three categories provide a range from no effect to concentrations that are toxic to various species. These guidelines provide a good range for comparing trace element concentrations identified in freshwater systems but may not be necessarily accurate for systems found in southern Africa. Gordon and Muller (2010) set out the need for a more local guideline for sediment quality in South Africa. To date, there is still no current framework for sediment quality guidelines in South Africa.

2.9. Water Quality Guidelines for Various Elements

Like sediments, there are many varying ways to determine the level of pollution in water. The main way to identify levels of contamination is to compare concentrations of various contaminants in fresh water to water quality guidelines and standards. Globally many papers (e.g. Oberholster and Ashton, 2008; Bains *et al.,* 2012; Edokpayi *et al,* 2016; Haydar *et al.,* 2016) compare trace element and major ion concentrations to the standards set out by the World Health Organisation (WHO 2011), while locally, South Africa has set out its own standards (South African Water Quality Guidelines) for varying forms of use, e.g. freshwater ecosystems, agricultural, industrial, and domestic use (DWAF, 1996). The main focus for this research would be to use the guidelines set out by the SAWQG for freshwater systems. The guidelines set out the maximum acceptable levels of varying trace elements and major ions in freshwater systems across the country, and are in line with the standards set out by the WHO. Using these guidelines would be in line with many studies done on freshwater systems across South Africa (Ncube and Schutte, 2005; Oberholster and Ashton, 2008; Palamuleni and Akoth 2015; Edokpayi *et al*, 2016; Nolakane *et al.*, 2017).

Table 2.1: The recommended water quality guidelines according to the SAWQS and the WHO drinking water guidelines (WHO, 2011)

Characteristics	South African Standard		WHO Drinking Water Guidelines
	Ecosystem Range	Domestic Use	
Temperature (ºC)	Cannot be >10% of the daily average	N/A	N/A
DO (%/L)	80-120	N/A	N/A
Conductivity (µS/cm)	N/A	N/A	N/A
pH	6-8	6-9	6.5-8
Chloride (mg/L)	N/A	0-100	250
Phosphate (µg/L)	< 5 (Oligotrophic) 5-25 (Mesotrophic) 25-250 (Eutrophic) > 25 (Hypertrophic)	N/A	N/A
Nitrate (mg/L)	< 0.5 (Oligotrophic) 0.5 - .5(Mesotrophic) 2.5 - 10 (Eutrophic) > 10 (Hypertrophic)	0-6	50
Sulphate (mg/L)	N/A	0-200	500
Aluminium (mg/L)	0.005	0-0.15	0.1-0.2
Arsenic (mg/L)	0.01	0-0.01	0.01
Cadmium (mg/L)	N/A	N/A	0.003
Chromium(mg/L)	0.007	0-0.05	0.05
Copper (mg/L)	0.0003	0-1	2
Cobalt (mg/L)	N/A	N/A	N/A
Iron (mg/L)	N/A	0-0.1	0.5-50
Lead (mg/L)	0.002	0-0.01	0.01
Magnesium (mg/L)	N/A	0-30	N/A
Manganese (mg/L)	0.18	0-0.05	0.4
Mercury (mg/L)	0.04	0-0.001	0.001
Nickel (mg/L)	N/A	N/A	0.02
Sodium (mg/L)	N/A	0-100	200
Sulphur (mg/L)	N/A	N/A	N/A
Uranium (mg/L)	N/A	N/A	0.015
Vanadium (mg/L)	N/A	0-0.1	N/A
Zinc (mg/L)	0-0.002	0-3	0.01-0.05

2.10. The Impacts of Trace Elements on the Environment

Once contaminants have been identified, they pose a serious threat for both the local biodiversity and human population. Even though trace elements may be significantly important for the growth of living organisms they cause severe effects when intake exceeds the recommended natural amount. Trace elements can influence both the food chain and drinking water. They can also have a severe impact on plant species, fish species, and other aquatic micro-organisms, especially because they are easily bioavailable (Coetzee *et al.,* 2002; Jung *et al.,* 2005; Humphries *et al.,* 2017; La Colla *et al.*, 2017). This being said, metal toxicity is dependent on bioavailability, metal speciation, and organism uptake, accretion and secretion (Benson *et al.,* 2017). A study by Alamdar *et al.* (2017) identified that carnivorous fish species less readily accumulated trace elements when compared to herbivorous fish species. Generally, an increase in the concentration of trace elements can lead to increased risk of cancer in most species and humans. Some specific health effects, however, are associated with individual trace elements.

Pb can cause nephrotoxicity, neurotoxicity and many other adverse health effects, such as immune, renal, cardiovascular, gastrointestinal and endocrine issues (Munyangane *et al.,* 2016; La Colla *et al.*, 2017), while an increase in Mn can cause severe neurological effects (La Colla *et al.*, 2017). Compared to this, an increase in As intake can lead to shortness of breath, a rise in skin lesions, hyperpigmentation of the skin, and the onset of various cancers, such as skin, bladder and lung cancer (Kavcar *et al.* 2009; Munyangane *et al.,* 2016). Other substances such as increased Fe can also lead to a greater risk of chronic disease (La Colla *et al.,* 2017). Cd intoxication can cause issues such as the softening of bones and renal dysfunction

(Umemura and Wako, 2006; Munyangane *et al.,* 2016), and exposure to increased Cr may cause cancer, respiratory disease, perforations of the nasal membranes, and ulcerations (Linos *et al.,* 2011; Munyangane *et al.,* 2016). Contaminated fish and drinking water pose a great health risk to human populations once consumed. Contaminated water systems pose a greater threat especially if trace element pollution is not the only form of pollution found within them. There is a greater body of literature on this topic, but the actual health impacts are not the main focus of this research.

CHAPTER 3:

METHODOLOGY

3.1. Introduction

To identify the spatial variation within, and between, dams and pans across Benoni, various sites had to be identified. This chapter will set out the various methods used to determine the research objectives. First, the chapter will lay out the criteria used to identify the various sample sites within the region, and more importantly the sample points within each site. Following the identification of the sites and sample strategy, a detailed look into the bathymetric assessment of each site will be done. Finally, this section will identify the various methods involved in taking and analysing the various water (inductively coupled plasma optical emission spectroscopy - ICP OES) and sediment (X-Ray fluorescence - XRF) samples at each site.

3.2. Study Site Selection and Descriptions

3.2.1. Study Site Selection

The aim of this research study was to identify the spatial distribution of trace element contaminants from local sources of pollution in the Benoni area. A total of 9 sites were used for this study, each site was determined using various criteria from the literature (Galloway *et al.*, 1982; Kříbek *et al.*, 2014). Sample sites were selected based on two main criteria:

1. Sites were identified if they fell within the boundaries of the Benoni City region and

2. If they fell within a 5km – 10km radius of the centroid of a collection of tailings dams and mine dumps, that can be found to the east of the Benoni central business district (Fig 3.1).

The determination of a 5km radius to identify sites was based on the distance various particles can travel and last in the atmosphere. Various particle sizes have a different residence time in the atmosphere. There are few papers which talk about the transport distances of various trace elements and thus identification of sites will be determined based on the longest possible distance in which a trace element can stay in the atmosphere (Galloway *et al.,* 1982). Galloway *et al.* (1982) conducted a review and assessment of trace elements in atmospheric deposition. According to Galloway *et al.* (1982), most particulates containing trace elements can be deposited in areas several kilometres away from the source. For this research, sites were determined based on a southern African example (Kříbek *et al.,* 2014) and were identified within a 5km radius of local tailings dams.

Determining the point at which the 5km radius starts was based on the following method. A collection of tailings dams and mine dumps can be found to the east of the Benoni CBD. A centroid was determined based on these tailings dams and mine dumps. The majority of the dams and pans, identified within a 5km to 10km radius of the centroid, were then narrowed down through other minor criteria, such as size and location. The addition of 10 km was done to compensate for sites that still fell within 5km of the perimeter of the collection of tailings dams and mine dumps (Fig 3.1). This led to the original identification of ten sites for this study. Following further site inspections, to identify access points, one site, Glenshaft Pan, was identified as being inaccessible as well as being unsafe, for security reasons.

Following this, the site was dropped. No other site, however, fell within the determined criteria and thus only nine sites were used to conduct this research. Based on this information, the following dams and pans were identified as study sites (Table 3.1; Fig 3.1).

Table 3.1: The study sites used for the purpose of this research

Site Name	Type of Site
1. Amata Pan	Perennial Pan
2. Bullfrog Pan	Non-Perennial Pan
3. Civic Lake	Dam
4. Homestead Dam	Dam
5. Kleinfontein Dam	Dam
6. Middle Lake	Dam
7. Sandpan	Non-Perennial Pan
8. van Ryn Dam	Dam
9. Westdene/Korsmans Pan	Perennial Pan

3.2.2. Study Sites Descriptions

Four of the sites are natural pans while the other five are manmade dams. This allows for a comparison of contaminant variation in pans and dams. These sites are all situated within different parts of the Benoni City area, and thus are subjected to many other possible sources of contaminants.

Korsman Pan

Korsman Pan is situated west of the Benoni city centre and the tailings dams, in the affluent suburb of Westdene; the Korsman Conservancy run the pan (Fig 3.2 - Fig 3.4). Korsman's measures 643m from north to south and 642m from west to east. The site is completely fenced off to protect the birds that inhabit the site from people, and their dogs, which run and walk around the area.

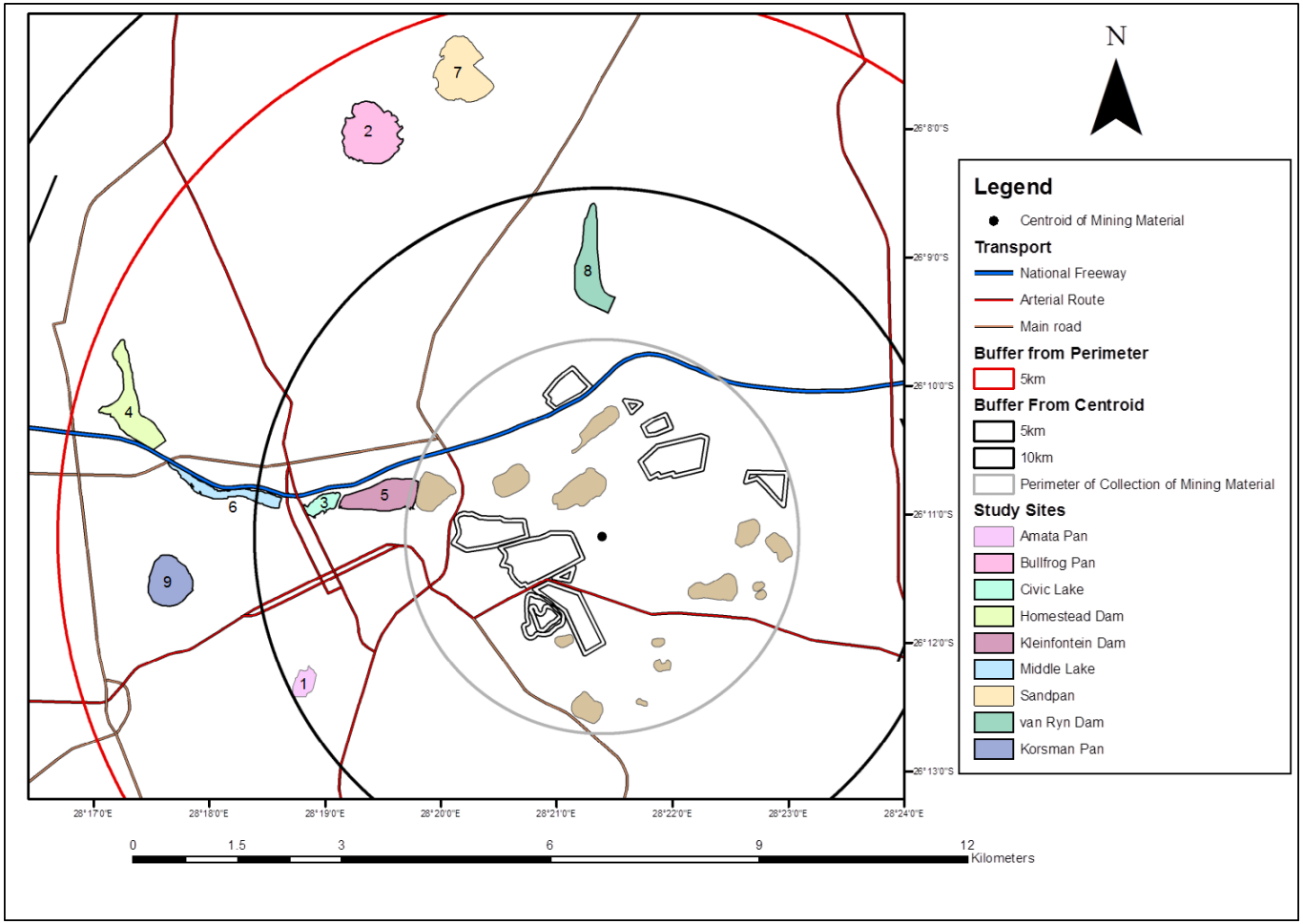


Figure 3.1: The study sites (dams and pans) that were used to conduct the research study. The site number corresponds to Table 3.1

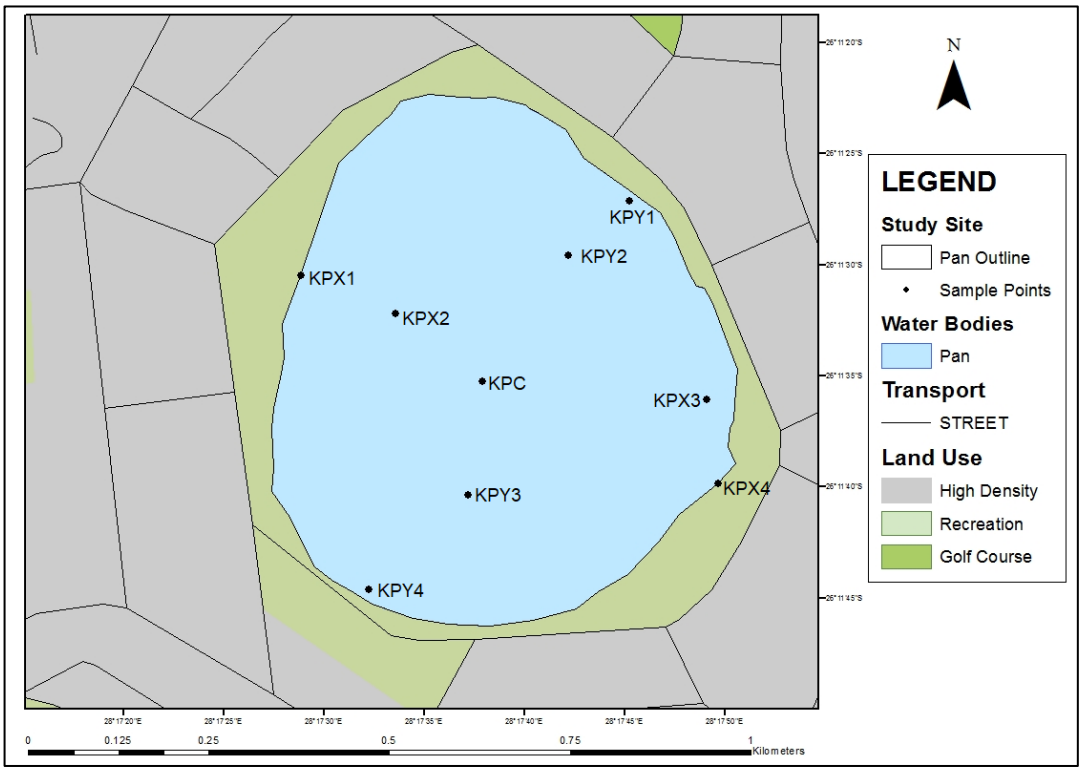


Figure 3.2: Map showing Korsman's Pan and relative sample points within the site



Figure 3.3: Image of Korsman's Pan during fieldwork in 2017



Figure 3.4: Image of the boat used to conduct fieldwork, on the banks of Korsman's Pan

Bullfrog Pan

Bullfrog Pan, which is 858m by 904m across, is one of the larger natural pans to be used in this study and is created by a natural depression in the landscape (Fig 3.5 - Fig 3.7). The pan is home to several bird species and the large African bullfrog. The site falls to the north of the tailings dams and mine dumps and falls within the Rynfield Agricultural Holdings, which is an area in Benoni made up of large pieces of former agricultural land.

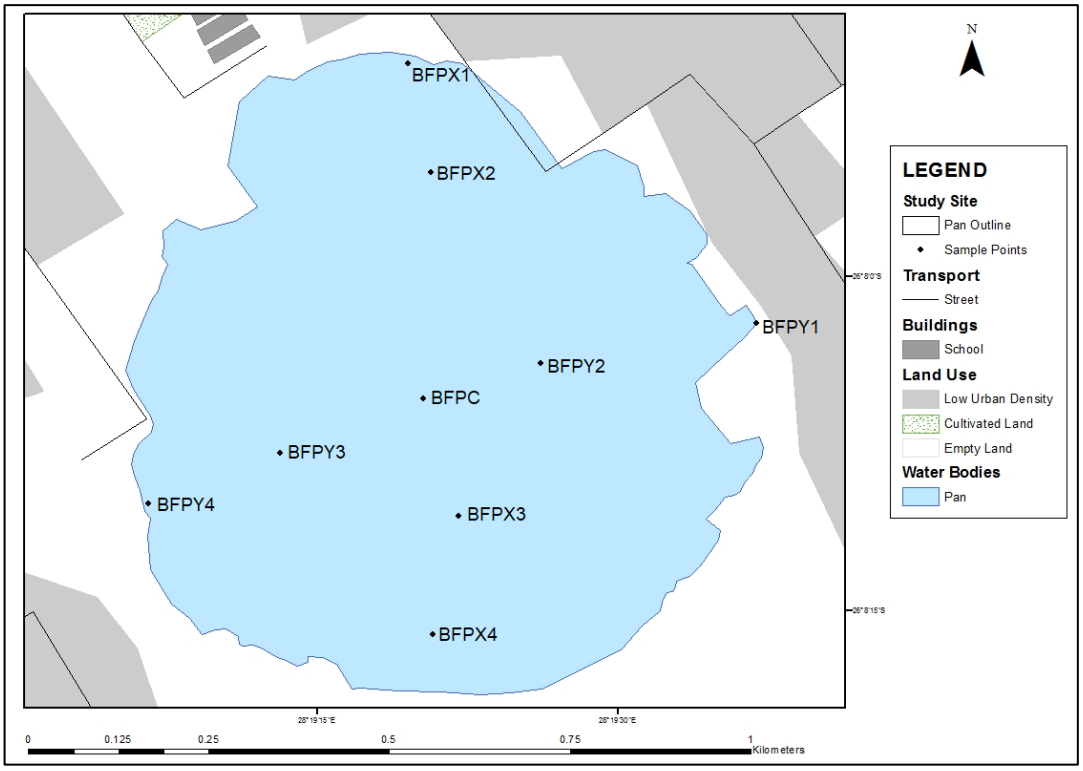


Figure 3.5: Map showing Bullfrog Pan and relative sample points within the site



Figure 3.6: Image of Bullfrog Pan during fieldwork in 2017



Figure 3.7: Image of birds resting on the water of Bullfrog Pan, during fieldwork in 2017

Sandpan

Sandpan, situated north of Benoni, is the second largest natural pan and measures 886m by 797m across (Fig 3.8 – Fig 3.9). The pan is relatively flat and falls on the border of the Rynfield Agricultural holdings, and the middle-income suburbs of Rynfield and Boat Lake Village. Like the other two pans already mentioned, this site is also home to the large African bullfrog and many other bird and fish species. The site is also surrounded by smaller pools of water that are not connected to it. The site is mainly managed by the Sandpan Conservancy.

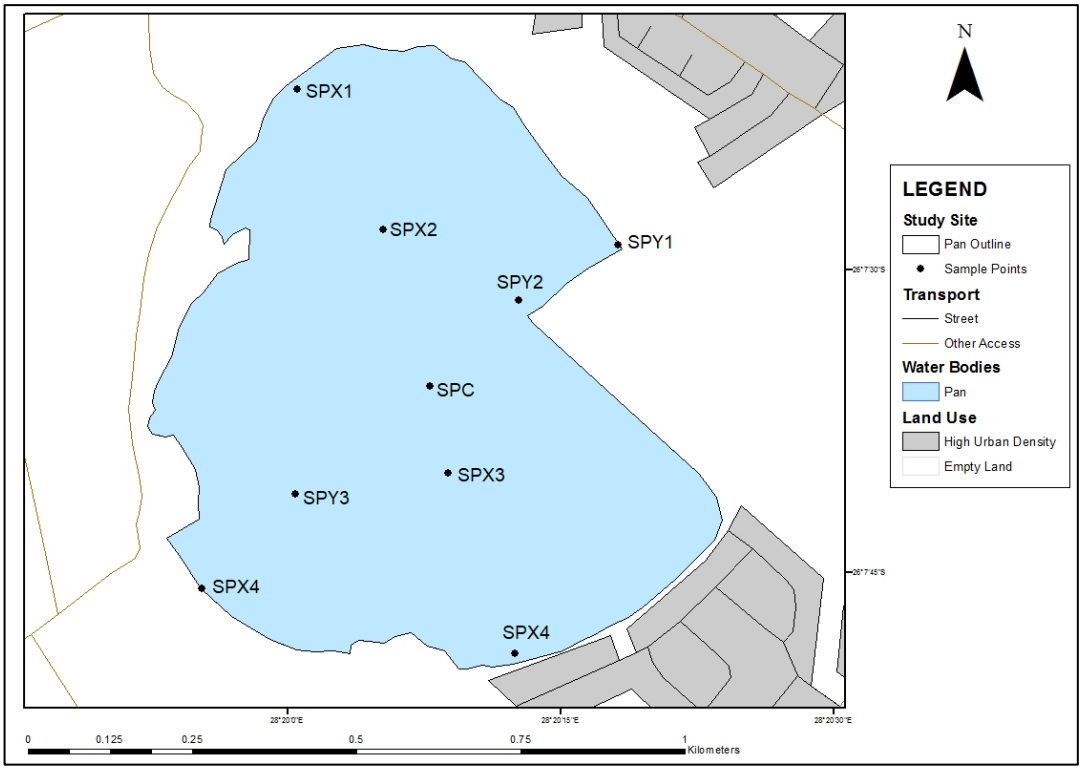


Figure 3.8: Map showing Sandpan and relative sample points within the site



Figure 3.9: Image of Sandpan from the north of the site, during fieldwork in 2017

Homestead Dam

Homestead Dam, measuring 1691m by 565m across, is one of four dams that fall along a tributary of the Bronkhorstspruit River (Fig 3.10 – Fig 3.11). The dam is also home to various bird and fish species. The site is mainly used for recreational activities, such as fishing, exercising, canoeing, rowing, and more. The dam sits within a middle-income suburb with one small and one major park situated alongside it. Towards the south of the dam, runs the N12 freeway. It is the farthest upstream of the four dams along the single gradient that runs towards the collection of mine dumps and tailings dams.

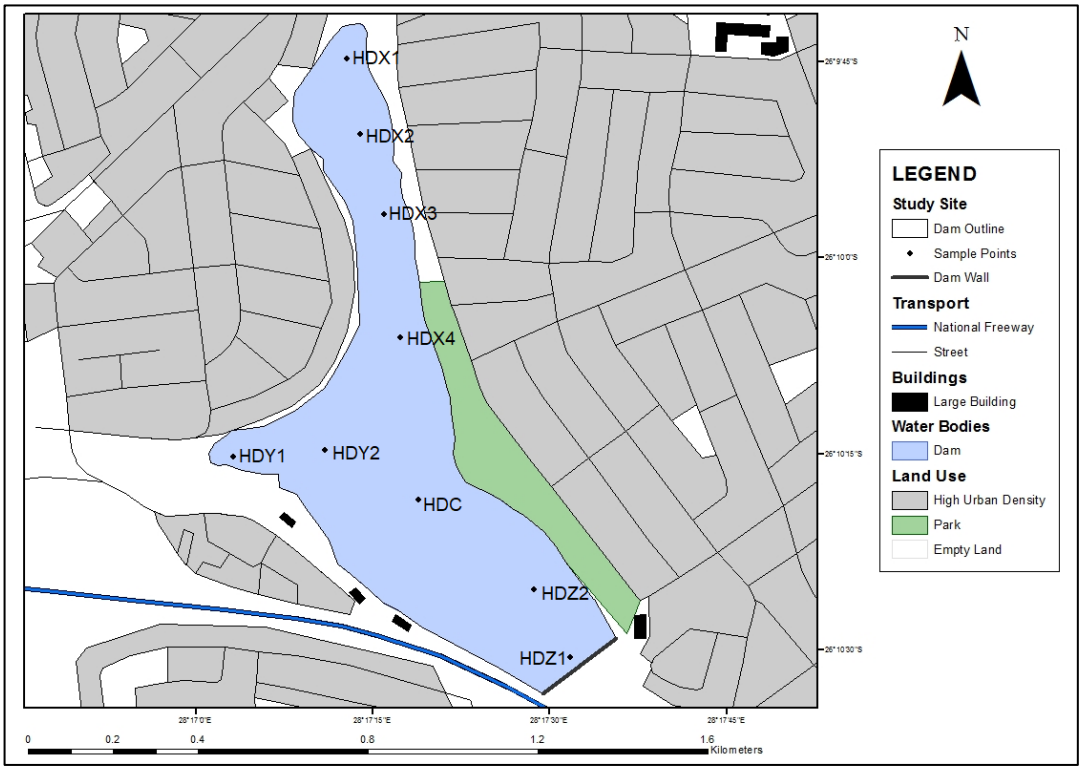


Figure 3.10: Map showing Homestead Dam and relative sample points within the site



Figure 3.11: Image of Homestead Dam from the large urban park on the east bank, with the N12 in the background

Middle Lake

The second dam along this gradient is Middle Lake (Fig 3.12 – Fig 3.13). The dam which measures 1635m by 191m, is situated between a golf course and hotel on the southern side and the N12 freeway along the northern side. The dam is not used as often as Homestead, but is home to a ski school, which uses it for water skiing. The site is also used for recreational fishing by local residents.

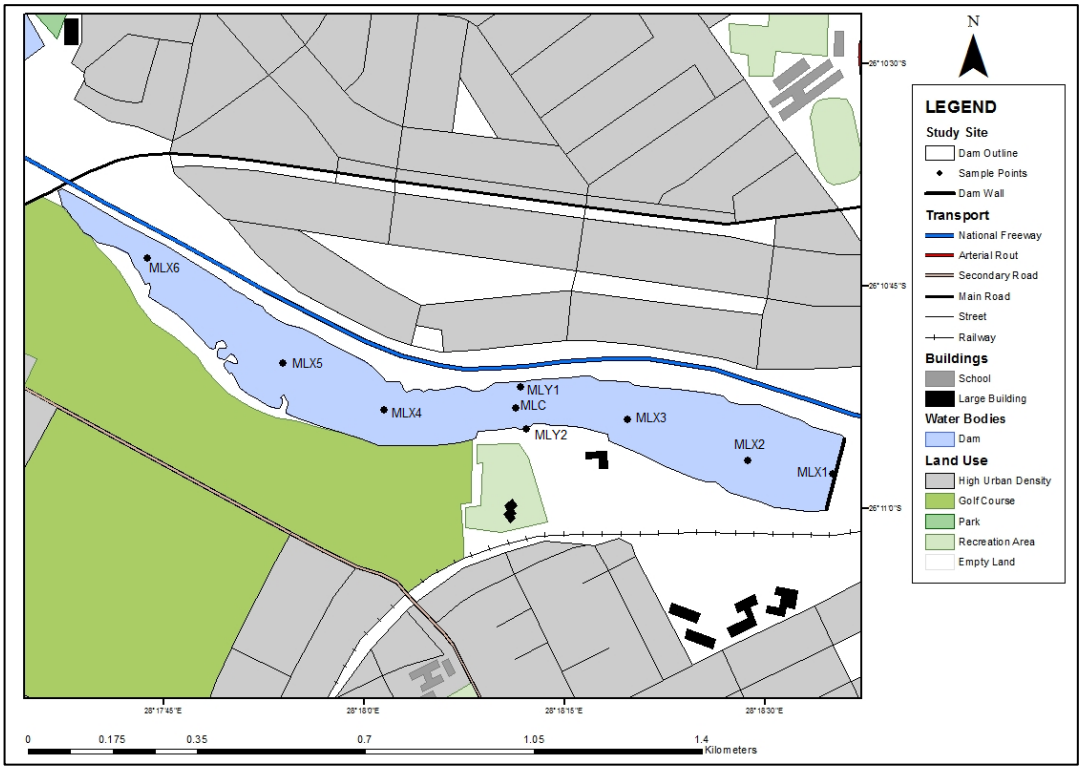


Figure 3.12: Map showing Middle Lake and relative sample points within the site



Figure 3.13: Image of Middle Lake, from west of the Dam, during fieldwork in 2017

Civic Lake

The third dam along the gradient, and second closest site to the collection of tailings dams and mine dumps, is Civic Lake (Fig 3.14 – Fig 3.16). The site, measuring 510m by 211m, is not easily accessible and thus is rarely used for any form of recreational activities. The dam is situated between a railway line and Lakeside mall, the largest mall in the city to the north and south respectively, with the east and west sides of the lake being bordered by to major roads leading into the inner city of Benoni. The road to the east of the dam is what separates this site from Kleinfontein Dam.

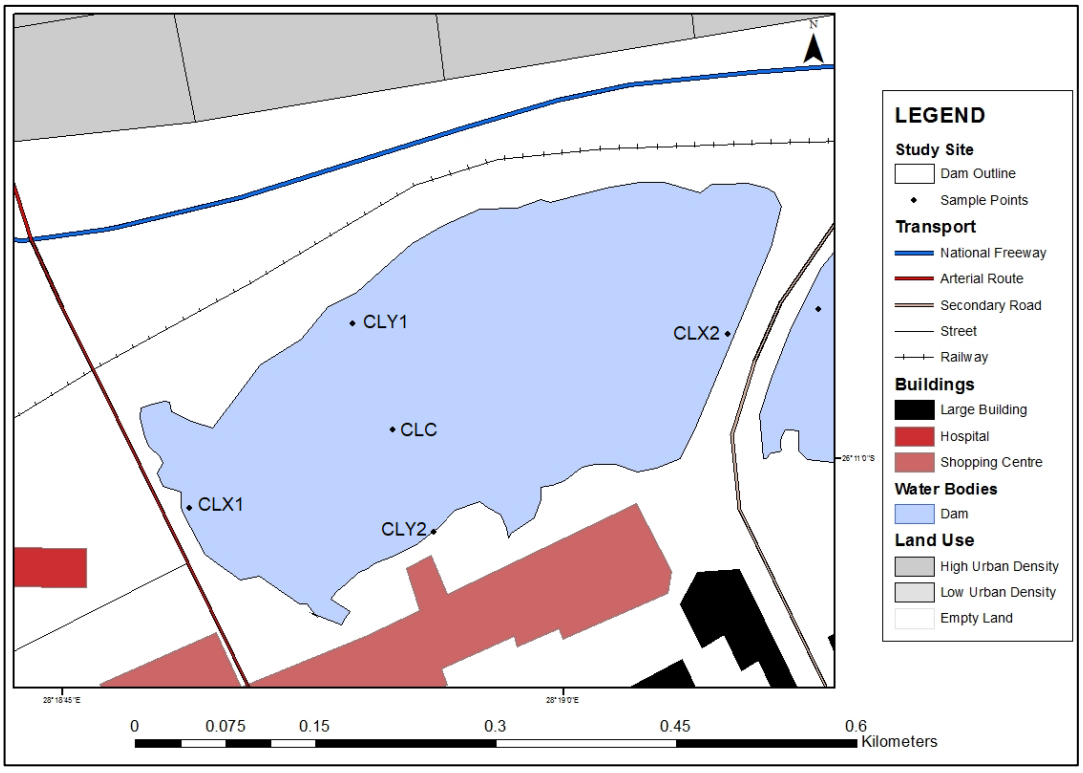


Figure 3.14: Map showing Civic Lake and relative sample points within the site



Figure 3.15: Image of Civic Lake from the south-west of the dam



Figure 3.1: Image of Civic Lake looking towards the east, with Lakeside Mall to the south

Kleinfontein Dam

Kleinfontein dam, measuring 1110m by 4833m across, is the last dam along the gradient and is the closest site to the collection of tailings and mine dumps (Fig 3.17 – Fig 3.19). The site is mainly unused, apart from the occasional boat tests done by a local boat company found across the road from the dam. The site is mainly vacant to the north, where a piece of unused land is situated. To the south of the site is the Benoni central business district, and to the east, right along the dam, is one of the larger mine dumps in the area, which is currently being repurposed for gold extraction.

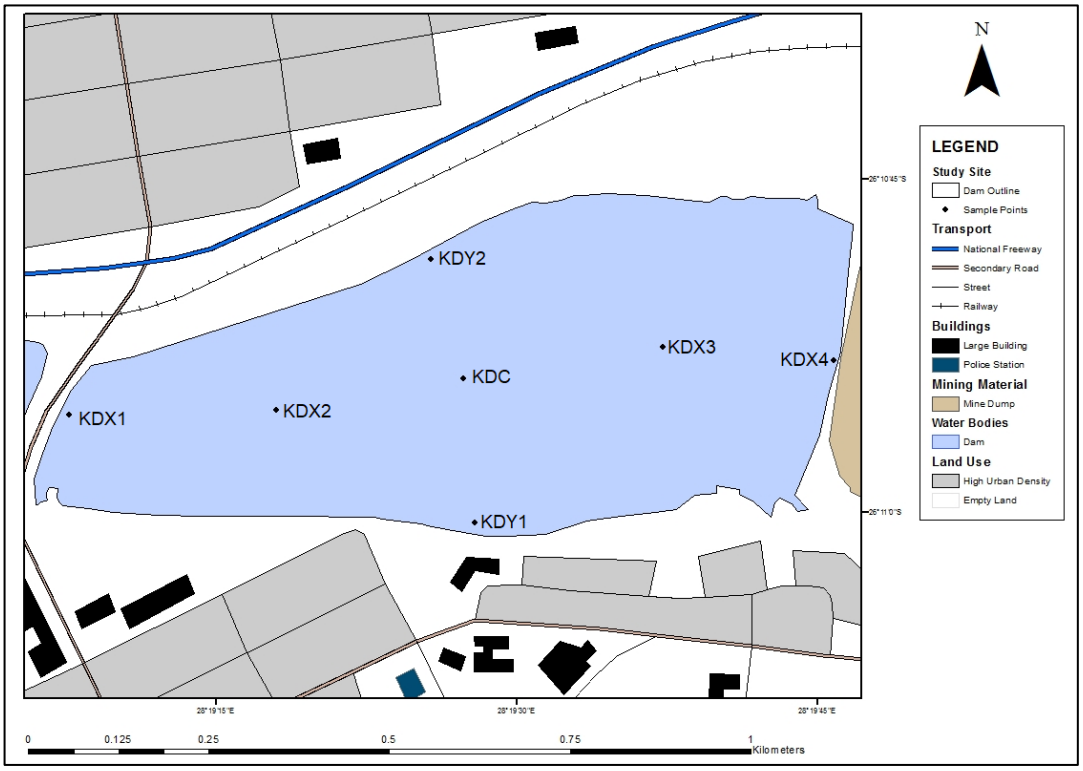


Figure 3.17: Map showing Kleinfontein Dam and relative sample points within the site



Figure 3.18: Image of Kleinfontein Dam, with the massive mine dump being reprocessed, during fieldwork in 2017



Figure 3.19: Image of Kleinfontein Dam from the east, with the Benoni City centre in the background

van Ryn Dam

The last of the five dams which will be studied in this research, van Ryn dam is situated in the upper-income golf estate of Ebotse and was measured to be 1740m by 433m across (Fig 3.20 – Fig 3.22). It is the only dam situated by itself on a separate tributary and used to be situated right next to a mine dump. The site is predominantly used by members of the East Rand Speedboat club. The site is also situated close to a wastewater treatment works.

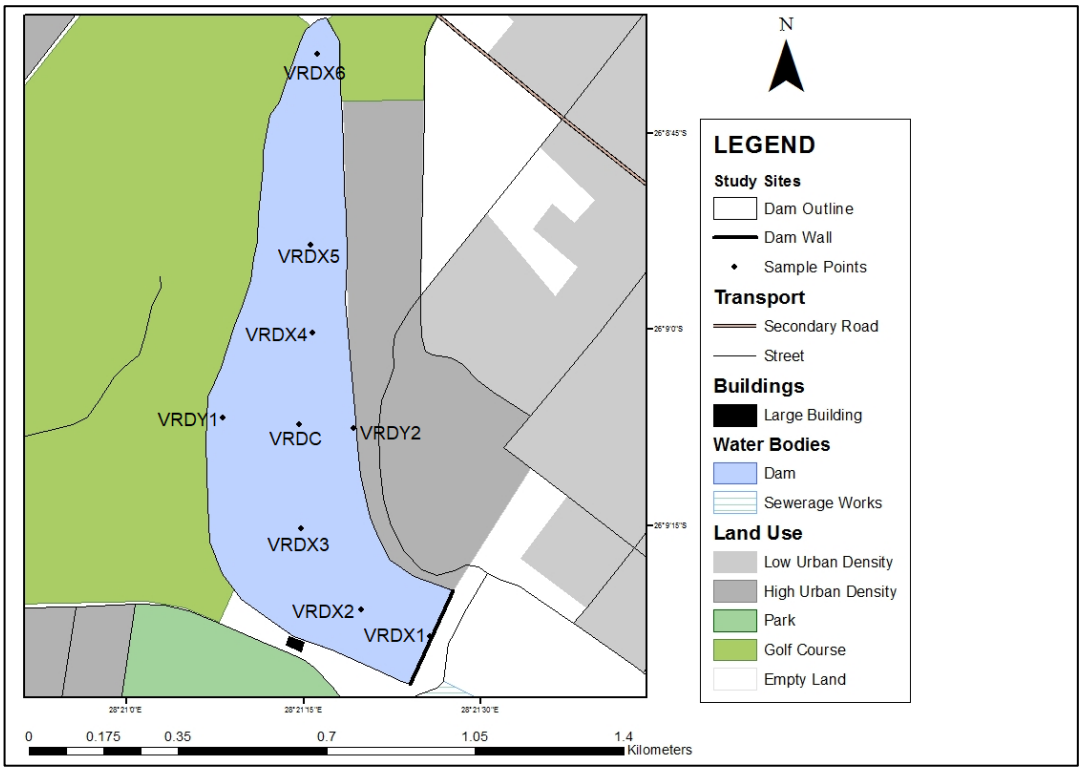


Figure 3.20: Map showing van Ryn Dam and relative sample points within the site



Figure 3.21: Image of van Ryn Dam from the boat launch at the East Rand Speedboat Club



Figure 3.22: Image of van Ryn Dam taken during fieldwork in 2017

Amata Pan

The last site to be monitored for this study is Amata Pan (Fig 3.23 – Fig 3.26). The pan, measuring 317m by 260m across, is situated in an industrial area, south of the inner city, right next to the L&P Springs South Africa. It is also south of the collection of the tailings dams and is the smallest pan to be monitored in this study. The entire pan is surrounded by sedges except for one point right next to the factory of L&P Springs South Africa.

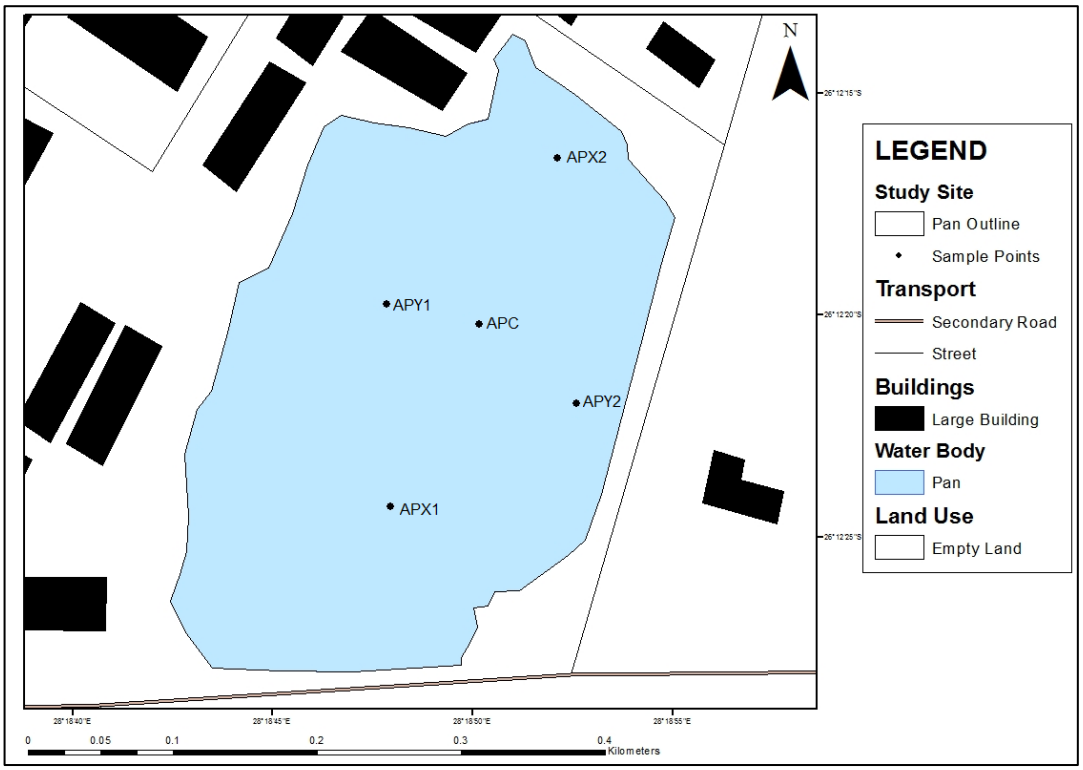


Figure 3.2: Map showing Amata Pan and relative sample points within the site



Figure 3.24: Image of Amata Pan with some of the plant life that surrounds the perimeter of the entire pan



Figure 3.3: Image of Amata Pan during fieldwork in 2017



Figure 3.4: Image of Amata Pan with the Springs Manufacturing Company in the background

3.3. Methods

In order to identify the spatial distribution of trace elements at each site, and across the entire area, the following methods were used to gather and analyse samples. Samples were taken at equal intervals along the centre transect of the dam/lake/pan. This transect was taken along the horizontal axis of each site, while a second lot of samples were taken along a vertical axis of the site. The numbers of samples for each site were dependant on the length of the main transect line and the perpendicular transect line. Therefore, approximately only five to ten samples per site were taken for surface sediment samples (table 3.2). Only two water samples, one at the surface and one at the deepest depth, for each site, were taken at the central point.

3.3.1. Bathymetry

Understanding the depths of water bodies is extremely important for anthropogenic processes, such as recreational activities and resource use. Understanding water depths allows one to identify the best possible places to construct, ports, docks, for dredging, identify waterways etc. (Ferreira *et al.*, 2017). Understanding water topography is also important for modelling of hydrological processes such as water quality, sediment transport, and hydrodynamics (Legleiter *et al.*, 2011; Curtarelli *et al.*, 2015; Andes and Cox, 2017). Bathymetry is the process of measuring the depths of water bodies and producing the actual topography underwater (Bello-Pineda and Hernandez-Stefanani, 2007). Bathymetry is important as it provides an understanding of the depth range within each site, and ensures that a greater range of depths, from the shoreline to the deeper water, can be sampled. Understanding variations in site depths is important for understanding whether or not sites stratify, further influencing redox and sediment geochemistry.

Sampling

Bathymetric surveys were done to map the various depths of each site. Identifying the depths of the lakes was done using an echo-sounder which uses sound echoes, to determine the depths of various water bodies (Moreno-Amich and Garcia-Berthou, 1989). The device was placed at the surface of the water, and the depth recorded. This was done along transects in order to give a basic map of the individual pan and dam depth. These transects were done arbitrarily, rowing or using the outboard motor to move back and forth from one end of the site to the other with as many points taken to cover as much of each site as possible. At these points, the GPS coordinates

were also taken. These coordinates were used to create bathymetric maps in ArcMap. Understanding lake depths can give a better indication of how the trace elements are distributed within the sediment at the bottom of the dams pans.

GIS

Each sample point was first projected, on *ArcGIS,* under the geographical coordinate system WSG 1984, following this, the data was then re-projected in the projected coordinate system WGS 1984 UTM Zone 35s, which allows for better representation in metres. The data for each site was then interpolated, using a one by one-metre cell size based on the smallest site, to create bathymetric maps. There are multiple methods for interpolating lake depths to identify the topography underwater. These methods include inverse distance weighting (IDW), kriging, spline, nearest neighbour (NN) and trend. For the purpose of this research, ordinary kriging was used to create bathymetric maps of each site.

Kriging is a form of geostatistical analysis that identifies (extrapolates) data for sample areas where there is little to no existing data available (Bello-Pineda and Hernandez-Stefanani, 2007; Curtarelli *et al.,* 2015; Andes and Cox, 2017; Ferreira *et al.*, 2017). Kriging works by identifying the spatial structure of the sample area based on the distance between measured points. Therefore, Kriging created its own maximum height based on the sample data provided. Kriging is generally ideal for representing spatial data as it usually produces a lower mean error and therefore produces more accurate maps (Bello-Pineda and Hernandez-Stefanani, 2007; Curtarelli *et al.,* 2015; Andes and Cox, 2017; Ferreira *et al.*, 2017). It is for this reason that kriging was undertaken to produce each map. Once each individual map

was created, the deepest points and area of each site were multiplied together to determine the average volume of each site.

3.3.2. Wind Rose Diagrams

Wind rose diagrams were created to identify the predominant wind direction and speed in the Benoni Area. Data were retrieved from the South African Weather Services (SAWS), O.R. Tambo International Airport station, from 1997 up to 2017 (Fig 3.27). Two wind rose diagrams were constructed, one for the entire 20-year period, and the other for the year 2017. The 20-year period wind rose diagram will aid in helping understand the dynamics that have been taking place for a prolonged period of time, whereas the 2017 wind rose diagram will give a better understanding as to what the conditions in the region have been for the year in which the research was conducted. The wind rose diagrams were constructed in Microsoft Excel. The wind rose diagrams were used to identify if there is a relationship between the trace elements at each site and the tailings dams and mine dumps in the area.

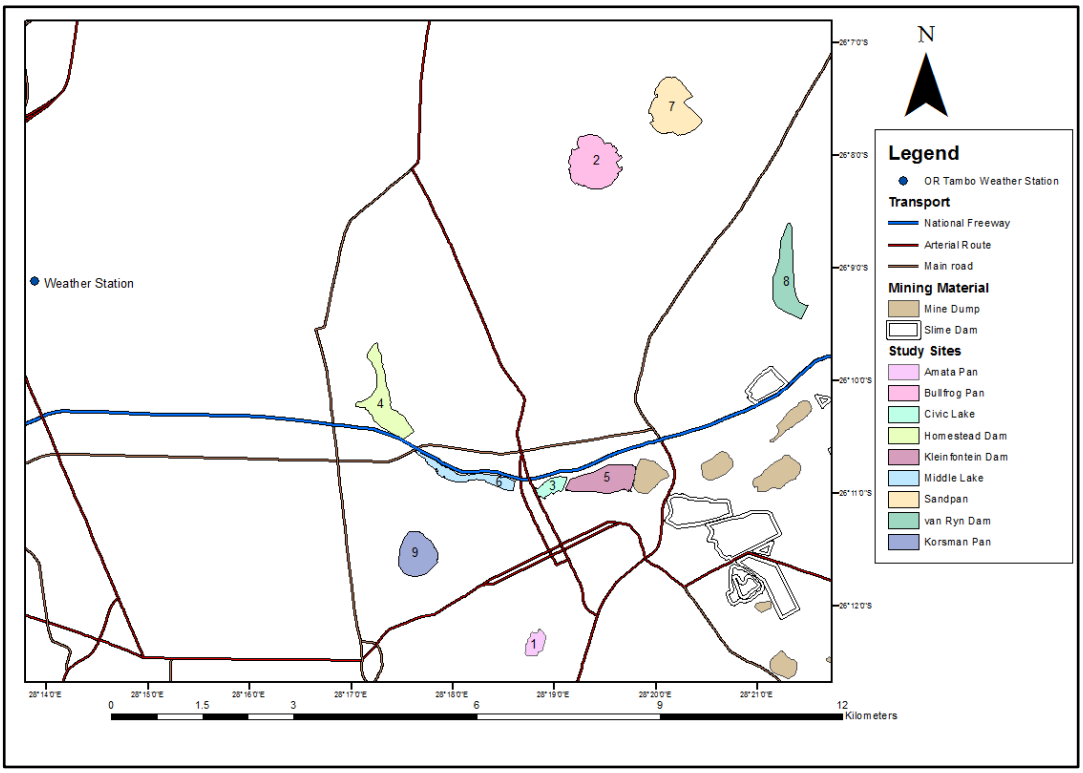


Figure 3.27: Map showing the relation of the O.R. Tambo Weather Station to the study sites

3.3.3. Sediment Sampling

Sample Collection and Preparation

Sediment Samples were taken at equal intervals along two axes at each site, apart from one, Homestead Dam, where three axes were used. The number of samples, taken at each site, were dependent on the size of the sites, with the number ranging from a minimum of five samples to a maximum of 10 samples (Table 3.2). Surface sediment samples were taken using a sediment grab, which only lifts approximately 10 cm off the top of surface sediments. The approach may seem coarse but was rapid and thus allowed for the integration of a longer period of time, as well as for multiple repeat sampling on a given date. These samples were then transferred to plastic zip-locked bags, to prevent any cross-contamination, and stored in the fridge until all the sampling was completed.

Table 3.2: The number of sampling points at each individual study site

Site Name	Number of Samples
Korsmans Pan	9
Sandpan	9
Bullfrog Pan	9
Amata Pan	5
Homestead Dam	9
Middle Lake	9
Civic Lake	5
Kleinfontein Dam	7
van Ryn Dam	9

Once samples were collected from all sites, the sediment samples were put into individual trays and dried out in an oven at 120°C for approximately 24 hours or until the samples were completely dry. These samples were then processed, using a pestle and mortar, into a fine powder of about 100 microns. One sample from the centre of each study site, was then pressed into a pellet to be analysed using the conventional lab XRF.

Analysis - XRF

Once the sediments had been retrieved, they were prepared for XRF scanning. X-ray fluorescence or XRF is a process where electrons are displaced from their atomic orbital positions. This process leads to the release of a burst of energy that is characteristic of a specific element. The energy release is then identified by the detector in the instrument, which in turn categorises the energies by element (Bruker 2018). XRF allows one to identify the concentrations of various elements, such as trace elements, present in the sample. XRF allows for non-destructive measurement of near continuous records of trace element concentrations from the sediment samples (Richter *et al.,* 2006; Weltje and Tjallingi, 2008). This method, which can

be applied in a laboratory or in the field, also allows for the analysis of various different elements, such as trace elements.

For the purpose of this research, the concentrations of the following trace elements were identified: arsenic (As), copper (Cu), cobalt (Co), iron (Fe), manganese (Mn), nickel (Ni), lead (Pb) and zinc (Zn). These trace elements are the most common contaminants, associated with gold mining, identified in the literature. Analysis of sulphur (S) was also done, as it is a common by-product of gold mining, especially AMD. The Thermo Scientific Niton XL3t Goldd+ (referred to as handheld XRF) was used for this study, as it allows for more samples to be analysed at minimal cost. In order to ensure accuracy though, 10 samples, one from each site, were analysed using the Axios Max Panalytical (referred to as the conventional XRF) at the University of the Witwatersrand Earth Science Laboratory. Two methods were taken to identify major and trace elements.

Samples were analysed for major and trace elements using the following methods, outlined by the Wits Geoscience Lab. Major elements were identified using the Norrish Fusion (Norrish and Hutton, 1969) technique, in-house correction procedures, and the Axios Max Panalytical X-ray fluorescence spectrometer. 0.35 g of each sample was used, and 2.5 g flux weight. At 1100°C major elements were then fused, using Johnson Matthey Spectrolflux 105, and the raw data corrected using internal software. Synthetic oxide mixtures, international standard rocks, and internal controls were used to make the standard calibrations. Calibration standards were primary International Reference Materials USGS series (USA) and NIM series (South Africa). Precision is taken as 1% for elements in abundance of greater than 5% by weight, and 5% for elements in abundance less than 5%.. Standard

calibrations use BCR2, NIM-P, NIM-D, W-2, NIM-S, GSP-2, NIM-N, NIM-G, PCC1, BHVO2, AGV2, G2 DTS1.

Pressed pellets of the central sample from each site were used to identify trace elements. The pressed pellets were first analysed using a Moviol solution binder. Following this, standardization was carried out using International Reference Materials USGS series (USA) and NIM series (South Africa). Precision was based on counting time and was taken as 5% for elements in abundance greater than 100 ppm, and 10% for elements in abundance between 10 and 100 ppm. The instrument used was the Philips PW2404 x-ray spectrometer.

This allows for the identification of any margin of error created using the handheld scanner and ensured more precise results. The study also compared the sediment surface samples of each site to the water samples. This allows for a greater understanding of the interactions taking place within the lake.

Dot Density Maps

To easily represent the spatial distribution of the trace element concentrations across each site, dot density maps were produced. The points where sediment samples were taken were projected onto ArcMaps, using the conventional geographical coordinate system WSG 1984 and projected coordinate WGS 1984 UTM Zone 35s.

Sediment Quality Standard

There are some basic sediment quality guidelines that can be found in the literature. The main source of such guidelines is MacDonald *et al.* (2000; Table 3.3). MacDonald *et al.* (2000) collate several differing sediment quality guidelines to

establish a consensus of two types of guidelines, threshold effect concentrations (TEC) and probable effect concentrations (PEC). TECs are values in which there is no threat by trace element contamination, whereas PEC, are concentrations that are relatively high and would provide an influence on the local environment. The SQG does not cover every trace element and only include As, Cd, Cr, Cu, Ni, Pb, and Zn

Table 3.3: SQL for TEC and PEC (in PPM) for specific trace elements as set out by MacDonald et al. (2000)

Trace Element	TEC	PEC
As	9.79	33
Cd	0.94	4.98
Cr	43.4	111
Cu	31.6	146
Ni	35.8	128
Pb	227	48.6
Zn	121	459

GeoAccumulation Index

To identify the levels of trace element contamination in each sediment sampled, after analysis, the GeoAccumulation Index (*Igeo*) was applied. *Igeo*, first proposed by Müller (1981), is a calculation that aids in identifying the level of probable pollution of trace elements in sediments (Ruiz, 2001; Roychoudury and Starke, 2006; Barbieri, 2016). Furthermore, *Igeo* is an indicator that is used to assess the concentrations of anthropogenic contaminant deposition in sediments. *Igeo* is calculated according to the normalisation of the trace element concentration, in the sediment, to the concentrations of the natural background levels of that trace element (Müller, 1981: Ruiz, 2001; Roychoudury and Starke, 2006; Barbieri, 2016). The method to identify *Igeo* was done according to the procedure undertaken by Müller (1981), Ruiz (2001), Roychoudury and Starke (2006), and Barbieri (2016) and is as follows:

$$Igeo = \log_2 \frac{C_n}{1.5 \times B_n},$$

Where C_n represents the value of the trace element concentration in the sample, B_n is the natural geochemical background value for that trace element in the area, and 1.5 represent a constant which takes into account any possible form of variation (Müller, 1981: Ruiz, 2001; Roychoudury and Starke, 2006; Barbieri, 2016). The background values for the study area were based on the average values of each trace element in shales and sandstones taken from Wronkiewicz and Condie (1987) and Turekian (1972). Each site's background value was determined based on the underlying local geological background. According to Muller's (1979) original index, there are 7 classifications to identify the rate of pollution in the sediments, zero (unpolluted) to six (extremely polluted) (Table 3.4).

Table 3.4: The Classification of the *Igeo* used to identify levels of pollution in each sediment sample

Igeo	Level of Pollution	Colour
Igeo ≤ 0	Uncontaminated	
0 < *Igeo* < 1	Very Low	
1 < *Igeo* < 2	Low	
2 < *Igeo* < 3	Moderate	
3 < *Igeo* < 4	High	
4 < *Igeo* < 5	Heavy	
Igeo ≥ 5	Extreme	

3.3.4. Water Sampling

Sample Collection and Preparation

Very little to no information was available on the water chemistry of the various lakes and dams across the Benoni area. Thus, there was no information based on the epilimnion and hypolimnion of each study area. Sampling was done using a similar

sampler to the van Dorn water sampler, which allows for water samples to be taken at selected depths within the water column (Oberholster *et al.,* 2010). The two water samples came from the central point at each site. When taking samples, the van Dorn sampler was cleaned out three times with water from the bottom of the lake surface to ensure there is no cross-contamination. The fourth sample was used to wash and fill a 500ml water bottle. Surface water samples were done by washing and filling a 500ml water bottle with the water from the surface. Before these bottles were filled in the field, they were rinsed with deionised water three times. This was done to minimise any form of cross contamination.

In addition, *in situ* measurements such as temperature, conductivity, dissolved oxygen (DO) and pH of the water at both the surface and bottom were taken. These physical characteristics are closely related to various trace elements (Tutu *et al.,* 2008), and can aid in the mobilisation of such metals.

The YSI multi-parameter probe was used to identify physical water characteristics at two points in the water column. In order to use the YSI one needs to calibrate the probes for pH, conductivity and DO. The calibration of the pH probe can be done in any order. The two point calibration was first done using a pH 7 buffer solution, followed by a pH 4 buffer solution. Following this, a conductivity calibration was done using a standard solution of 1413 µS/cm. Calibrating for dissolved oxygen was done at each individual site.

Once samples were taken, they were filtered through two different filter sizes, 1.2 µm and 0.45 µm. These samples were then transferred into two smaller 100 ml bottles, which were washed with deionised water three times, and then once with

filtered sample water. Once again this was done to avoid any forms of cross-contamination. One 100 ml bottle of 0.45 µm filtered water was used for analysis using ICP-OES.

Analysis – YSI

Using the YSI multi-parameter probe, the following physical characteristics were identified: temperature, dissolved oxygen (DO), conductivity, and pH. These characteristics were compared to the South African Water Quality Guidelines (SAWQG) for both the domestic and ecosystem ranges, as well as the WHO drinking water guidelines (Table 2.1).

Analysis ICP-OES

The inductively coupled plasma optical emission spectroscopy or ICP-OES was used to analyse the water samples from each site. ICP-OES is a method of trace element analysis that uses the emission spectra of a sample to identify the type and concentrations of elements within the sample. The process involves light being emitted from a 3-5 mm high region of plasma, which is focussed into an entrance slit of a polychromator or monochromator to monitor emissions from different trace elements (Olesik, 1991). ICP-OES is different from other methods such as inductively coupled plasma mass spectroscopy ICP-MS as it uses a collection of photons which makes it non-intrusive and the emission intensities are strongly dependent on the fraction of the excited ions (Olesik, 1991). Although ICP-MS has lower detection limits, the nature of the samples was thought to not require such detection, thus ICP-OES was used. The main benefit of using ICP-OES for this research was that it was more affordable than ICP-MS. The concentrations of the

same elements that were identified in the surface sediments, As, Cu, Co, Fe, Mn, Ni, Pb and Zn, were analysed for in water samples. The water samples were analysed according to the following method provided by the Wits Chemistry Lab.

First samples were filtered using a 0.22µm syringe filter to remove any further possible particles. They were then diluted (by a factor of 5, then 10, based on the element concentrations) with 5% HNO_3^+ and de-ionised H_2O used as the final matrix. Argon (Ar) was used as the monitor line. The samples were then analysed at the calibration range of 0- 2ppm. Independent quality control checks were also used in house. The following parameters were also used:

- Coolant Flow: 14 l/min
- Nebulizer Flow: 1 l/min
- Nebulizer Flow: 1 l/min
- Plasma Power: 1250 W
- Optic Temperature: 28 – 32°C
- OSC. Exhaust: 155 – 320 Imp/s

3.4. Statistical Analysis

Once samples were taken for both water and sediment of each site, and the data identified through ICP-OES and XRF respectively, statistical analysis was done using XLStat on Microsoft Excel and R. The statistical analysis was done in order to identify the distribution of trace elements within each site, and the overall distribution of individual trace elements across all the sites in the Benoni area. The analysis was also done in order to identify the relevance of distance of each site from the collection of tailings dams found near the centre of the City. The main way in which this was achieved was through principal component analysis (PCA). PCA is

a type of multivariate technique that analyses a data table, that contains descriptions of observations described by multiple inter-correlated quantitative dependent variables (Abdi and Williams, 2014; Lopez-Paz *et al.,* 2014). PCA can be used to identify a pattern of similarity of the observations and variables, by displaying them as points on a matrix (Abdi and Williams, 2014; Lopez-Paz *et al.,* 2014). Thus, PCA was used to identify the similarities of multiple sites together in order to understand the distribution of trace elements. Following this, a simple correlation was done to identify the relationships between the trace elements identified in each individual sample (see Table 3.2). Identifying the relationships between the trace elements allowed for the further identification of the sources of such trace elements. A pairwise comparison was also be conducted using analysis of variance (ANOVA). Analysis of variance, similar to a *t-test*, was done when comparing more than two sample sites to each other to see if there are any significant differences between the means (Burt *et al.,* 2009; van Emden, 2009).

3.5. Limitations and Setbacks

3.5.1. Fieldwork Duration

With any form of research, there are various limitations that one comes across and this research was no different. The first limitation experienced was trying to gain access to the various study sites. Most of the sites were either run by a conservancy or only had accessible points through private property, for example accessing Amata Pan required the permission of the L&P Springs manufacturing plant and the accessing of Korsman Pan required the permission of the conservancy. The difficulty in accessing these sites led to a delay at the start and within the fieldwork period.

The accessibility of one site was nearly impossible and thus this site was dropped from the study. Once access was granted for each site, the next limitation experienced during this research was finding fieldwork assistants to help with the fieldwork. Due to scheduling issues, and the fact that some sites were only accessible during the week, the fieldwork process was drawn out over a few months, longer than what had been intended. Delays in the fieldwork process were further enforced by the breaking of the shear pin for the boat motor. This led to further set back as a new shear pin needed to be sourced. Once this was completed the research finally continued and was completed on the 30th October 2017. When the fieldwork was being completed, various limitations were experienced collecting actual data.

3.5.2. Data Collection

There were various limitations that occurred with the collection of data. The main limitations were associated with the mapping of the depths of the site. Not the entire site, that is to say, the edges of various sites could be mapped. This is due to the sites either being surrounded by private properties or just unsafe in terms of personal security, as was the case with Civic Lake and Kleinfontein Dam. Most of the sites also contains a large amount and variety of plant life within them. The excessive plant growth made it difficult to manoeuvre the boat and also influenced the results of the depth when using the echo sounder. This was predominantly when the depth of the water exceeded 1 metre, so the measuring plank could not be used. Plant life provided a possible influence on the echo sounder and thus was one of the many limitations of working with it and mapping the bathymetry of each site. Another limitation associated with the bathymetry was the echo sounder measurements. The echo sounder only records depth to the nearest decimal place (0.1m) and thus gave

more averaged, and less detailed, depths of each site. Collecting of sediment samples was also time-consuming as the sediment grab would often get caught on stones and or any other form of rubbish found at the bottom of each thus making it difficult to collect sediment samples. Other than this the data collection processes were relatively smooth and straight forward.

CHAPTER 4: RESULTS

4.1. Introduction

The following chapter expresses the results of the months of fieldwork done at each site during the period of July to October 2017. This chapter will start by explaining the bathymetric maps created using the depths of each site. This will assist in interpreting the data and hydrology later. Following this, the chapter will explain the results acquired by the sediment and water samples. Due to the importance of the sediments, and them making the bulk of the research project, there will be greater detail given to this section of the chapter. The sediment data will be used to understand the spatial distribution of trace elements across the entire region and then across every site. The data will then be used to understand the severity of different trace element pollution in each site, followed by the metals that are closely correlated to each other. Correlation of metals will provide an idea of which suite of metals tend to be found together and could allow for the identification of possible sources of trace element contamination. Furthermore, the chapter will also take a brief look at the water data gathered, to give a basic understanding of the variation in concentrations of physical and chemical water characteristics.

4.2. Bathymetric Maps

The depths of each site were taken during the fieldwork in order to create bathymetric maps that are as detailed as possibly could be. Bathymetry has a whole range of uses, apart from just telling the depths of various water bodies. Bathymetry is useful in understanding hydrological dynamics and possible depositional patterns. It also aids in understanding the variation of trace element concentrations

in each site. The following section describes the results of the bathymetric surveys of the nine sites in their two classifications, pans and dams (See Appendix 1).

4.2.1. The Bathymetry of the Pans

The depths of the sites classified as pans tended to be very shallow, which helps to indicate how water fills such inlets in the region. The smallest, area wise, of the four pans, Amata Pan (Fig. 4.1), contained a maximum possible map depth, that is the depth modelled using kriging, between 1.51m to 1.8m below the surface of the pan, and a maximum measurable depth, that is the depth measured using the sonar during fieldwork, of 1.7m (See Appendix 1). There was a gradual increase in depth towards the centre of the pan from each side, with the deepest points being towards the southeast corner of the site. Compared to this, the depths of Bullfrog Pan (Fig. 4.2) and the Sandpan (Fig. 4.3.) were relatively shallow. The deepest measured point of the Bullfrog Pan was approximately 1.2m below the surface (Fig 4.2; (See Appendix 1), while the deepest map depth was up to 0.96m. The deepest points once again also seemed to be more concentrated towards the southeast part of the pan, with the shallowest parts being towards the northern reaches of the site.

Sandpan was even shallower than Bullfrog pan, with the deepest measured point being about 1.1m (See Appendix 1) below the surface and the deepest map area being between 0.81 and 1.0 m. This area was mainly concentrated in a small point towards the northeast reaches of the site (Fig. 4.3). The rest of the pan was relatively shallow and quite flat, with predominant depths between 0.41m to 0.6m below the surface of the site. The Sandpan was the only site that was so shallow it contained two islands in the northern parts, off the centre, of the site.

In comparison to the Sandpan and Bullfrog Pan, the deepest of the four sites was Korsman's Pan (Fig. 4.4). The deepest measurable point at this site was 1.6m (See Appendix 1) below the surface, with the deepest mapped region being between 1.81m and 2m. There is a gradual increase in depth from the northern reaches of the pan towards the southern parts. There were also various spots along across the pan that contained depths between 1.41m to 1.60m below the surface of the site (Fig 4.4). The deepest points of the pans, however, are still not as deep as some of the shallower dams.

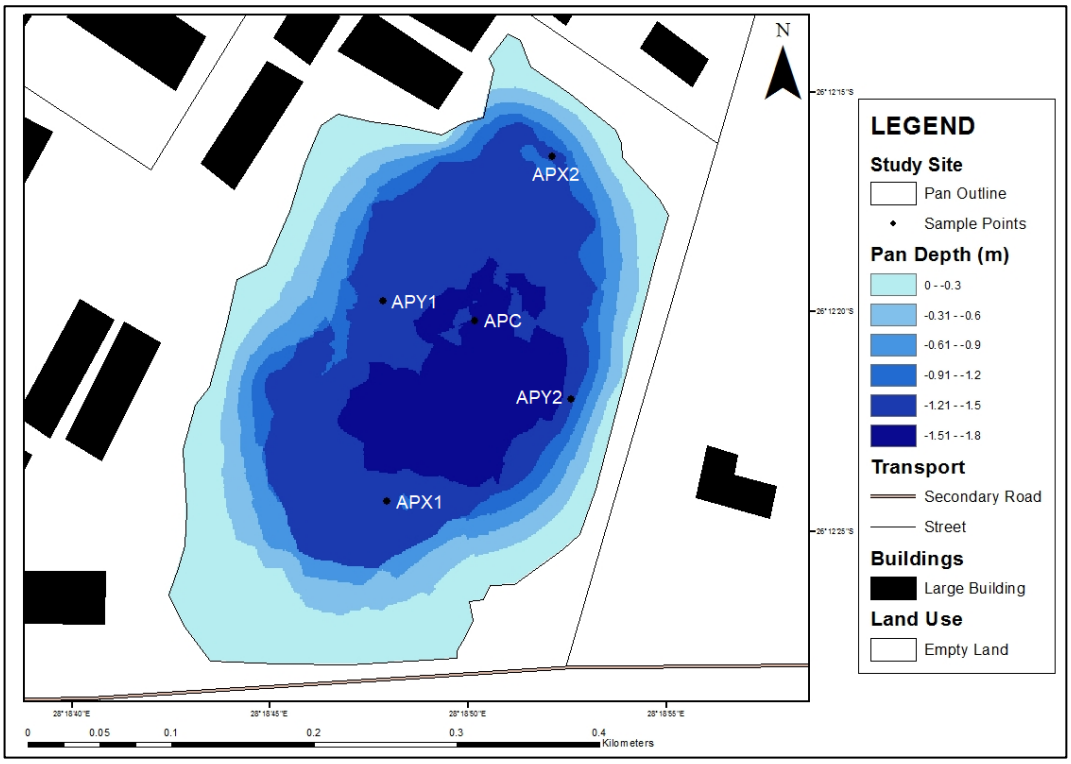


Figure 4.1: Bathymetric Map of Amata Pan

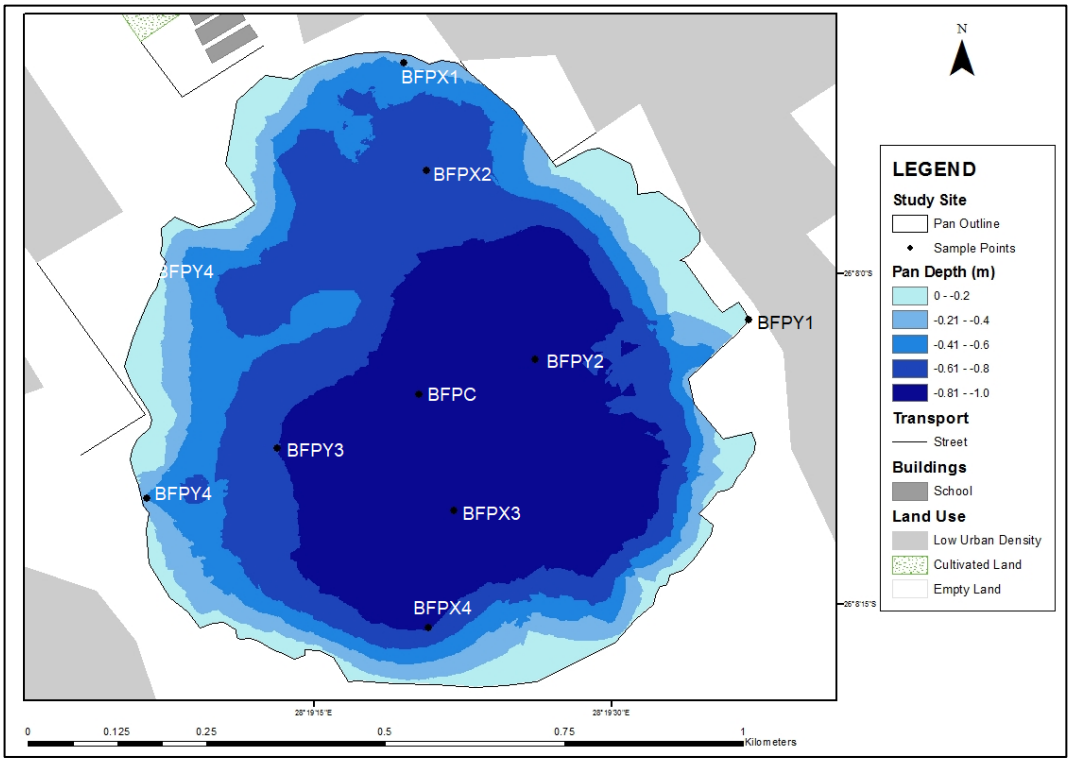


Figure 4.2: Bathymetric Map of Bullfrog Pan

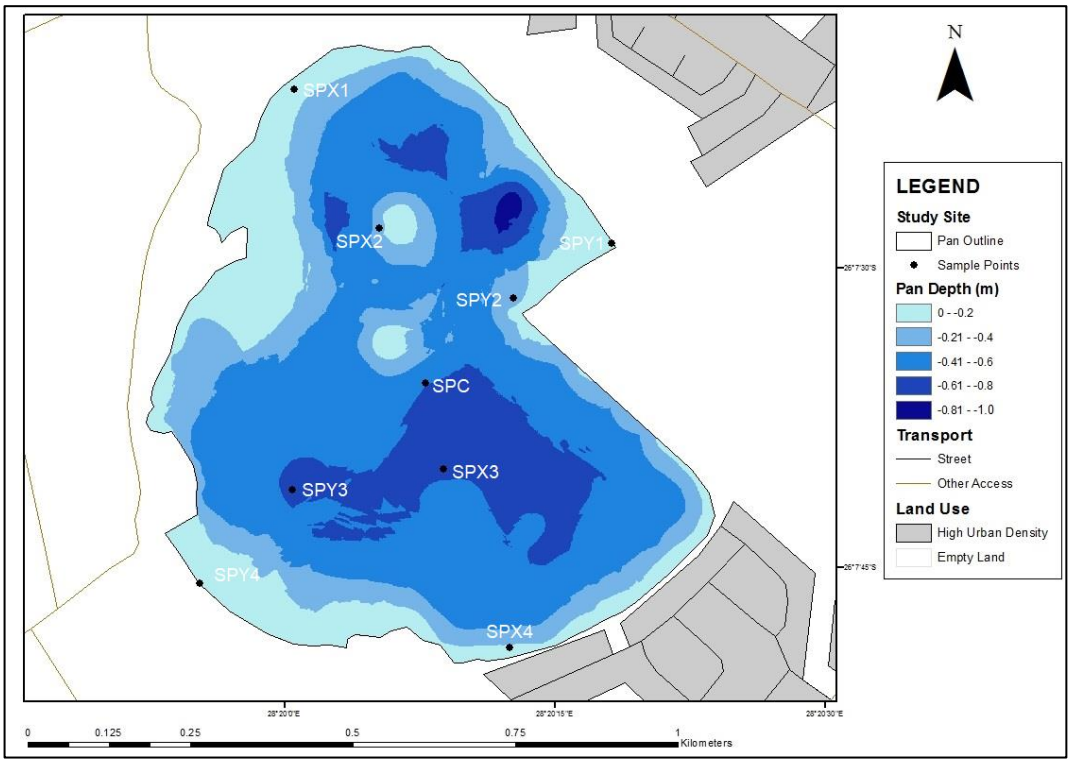


Figure 4.3: Bathymetric Map of Sandpan

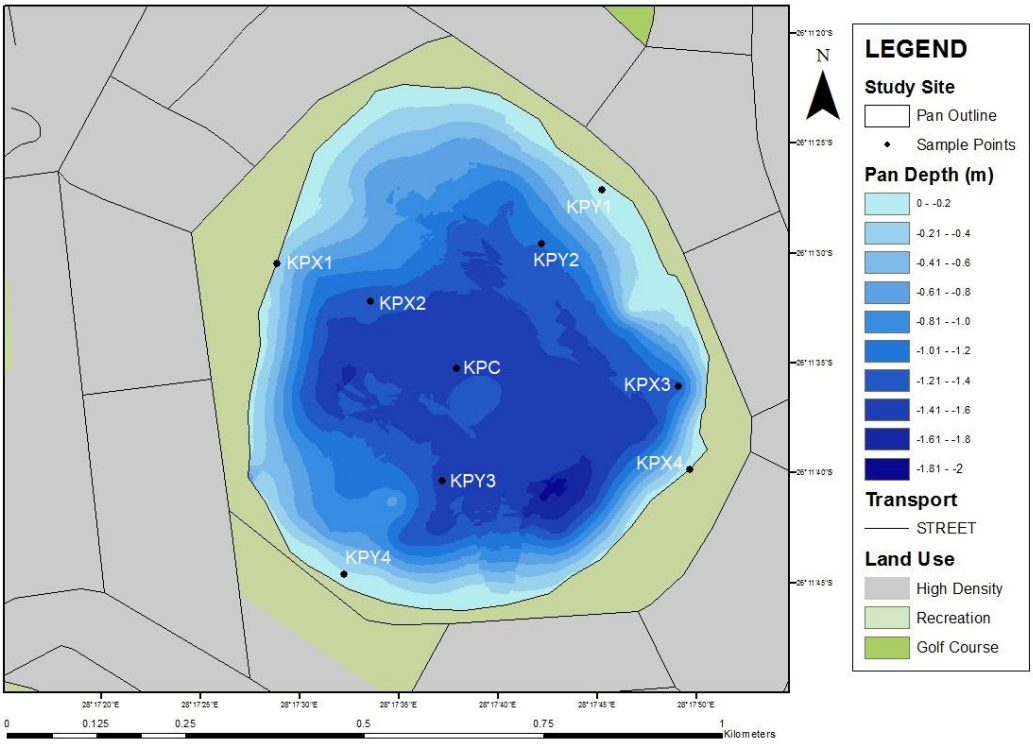


Figure 4.4: Bathymetric Map of Korsman Pan

4.2.2. The Bathymetry of the Dams

There are five sites that were classified as dams in this study, and each site is relatively deep, with the site that is generally the shallowest still being slightly deeper than the deepest pan. This site is Civic Lake (Fig 4.5), which also happens to be the smallest dam covered in this research. The site shows a gradual increase in depth from the western to the eastern side of the dam, with a sharp decrease towards the eastern bank. The deepest measured point of this site is approximately 2.4m (See Appendix 1) below the surface, while the deepest area seen on the bathymetric image is between 2.01m and 2.5m below the surface (Fig 4.5). Along the northern and southern sides of the dam, one can also see steep increases in depth towards the centre of this site.

Following this, van Ryn Dam is the next shallowest dam within this research (Fig. 4.6). The deepest area of the site was between 3.01m and 3.5m (Fig. 4.6), which is consistent with the deepest point measured of 3.3m (See Appendix 1) below the surface. The shallowest depth (0 to 0.5m) can be identified towards the northern reaches of the site where a river enters the dam. There is a gradual increase in depths from the northern reaches of the site towards the south-eastern part where the dam wall can be found. The edges of the dam contain steep increases in depth towards the centre of the site.

Following van Ryn Dam, the next deepest dam was Kleinfontein Dam (Fig 4.7). The site contained a maximum depth measured of 5.3m (See Appendix 1), with the maximum possible depth, according to the bathymetric map being 5.5m below the surface (Fig 4.7). The site also contained a gradual increase from west to east across the site, with a steep decrease in depth towards the eastern bank, which happens to be along a major mine dump. The site also contains steep increases in depth, along the northern and southern banks.

Middle Lake, which the most elongated of all the sites, had a maximum measured depth during field work of approximately 5.6m (See Appendix 1) below the surface and the deepest area of the map being between 6.01m to 6.5m (Fig 4.8). The site contained a gradual increase in depth from the western reaches of the site towards the eastern reaches where the dam wall can be found. Approximately halfway across, however, there was some variation in the depths, with the deepest point, not being right against the dam wall (Fig. 4.8). The site also contained steep increases in depths along the northern and southern borders of the site.

The site with the greatest maximum depth measured, 6.1m (See Appendix 1) below the surface, was Homestead Dam. Compared to this the deepest area on the Homestead Dam map is between 6.01m and 6.5m (Fig 4.9). There are gradual increases in depth from the river inlets, towards the centre of the site and then further towards the dam wall. The site also contained a more irregular bathymetry pattern, with the centre containing various depths that were not necessarily uniform. By looking at the structure of the depths of each site, one can fully comprehend the spatial distribution of trace elements within the site

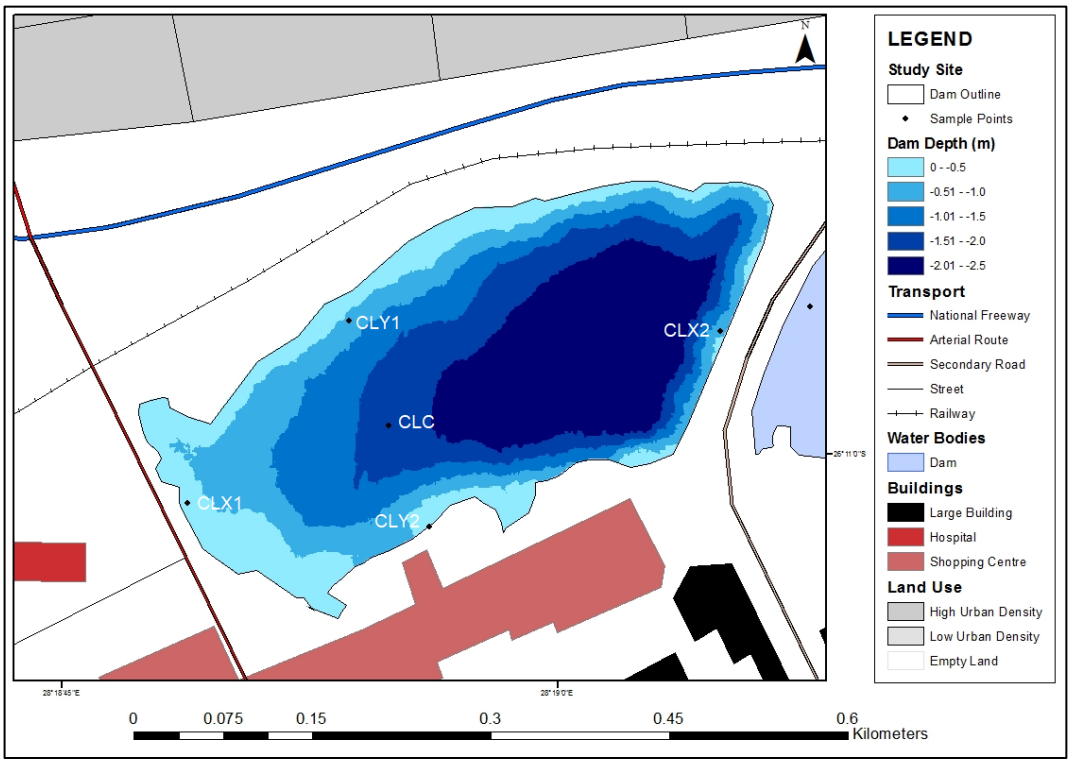


Figure 4.5: Bathymetric Map of Civic Lake

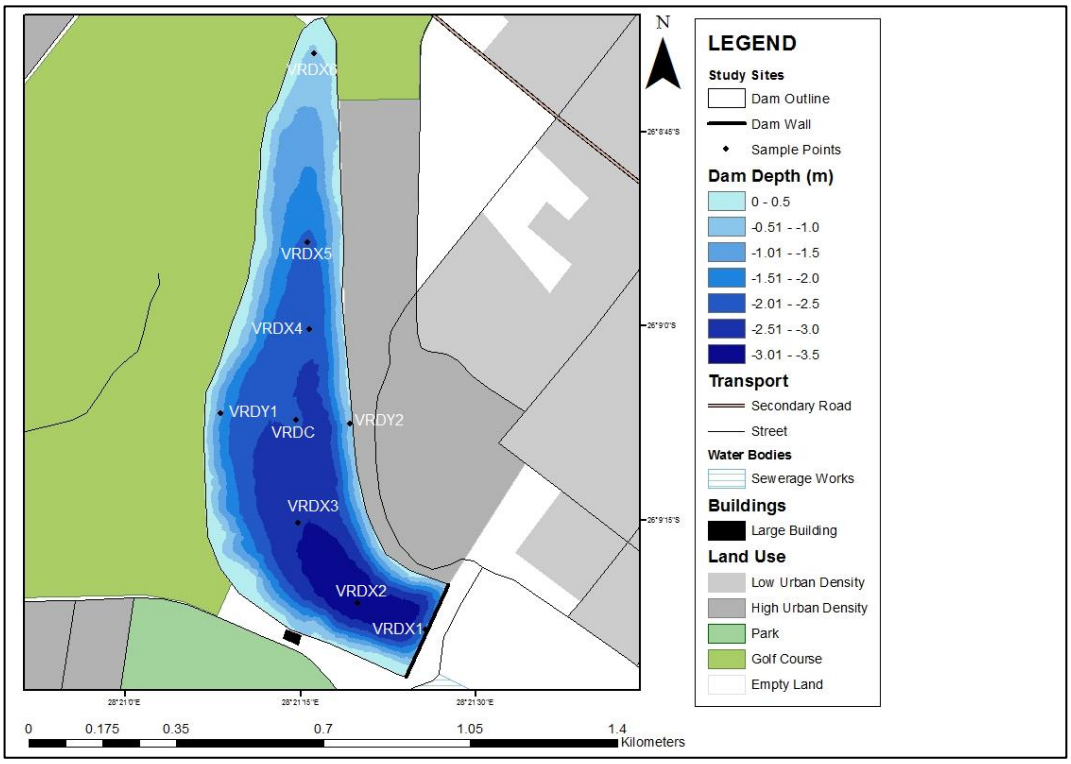


Figure 4.6: Bathymetric Map of van Ryn Dam

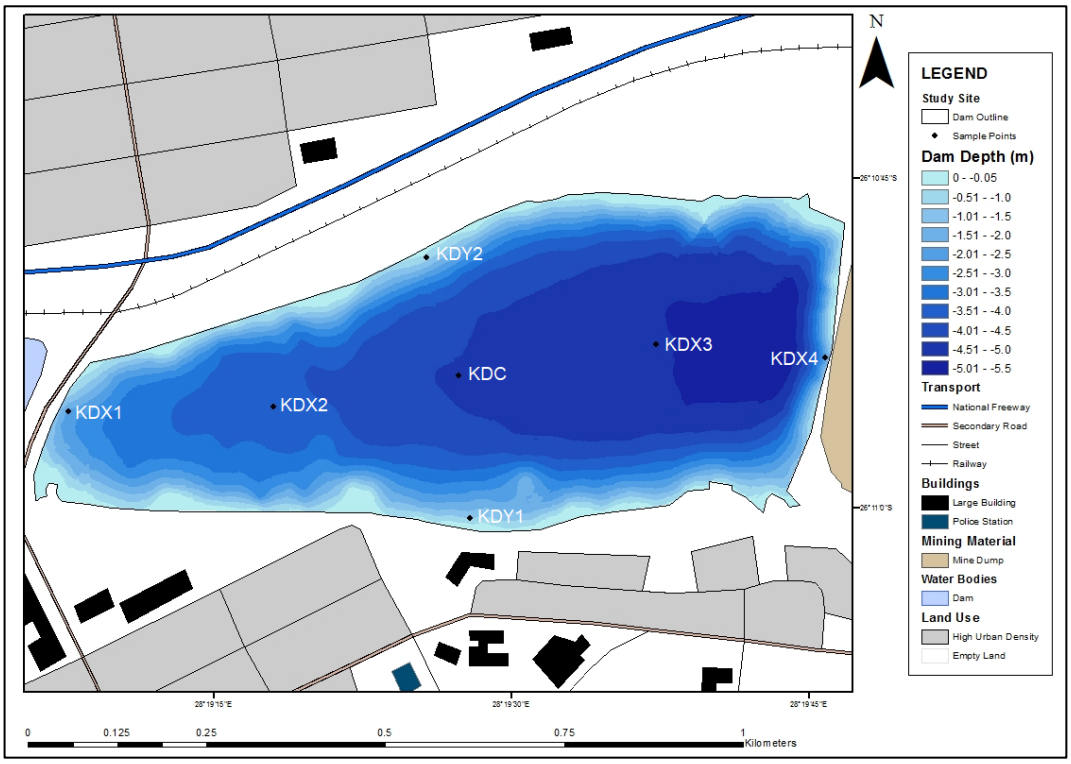


Figure 4.7: Bathymetric Map of Kleinfontein Dam

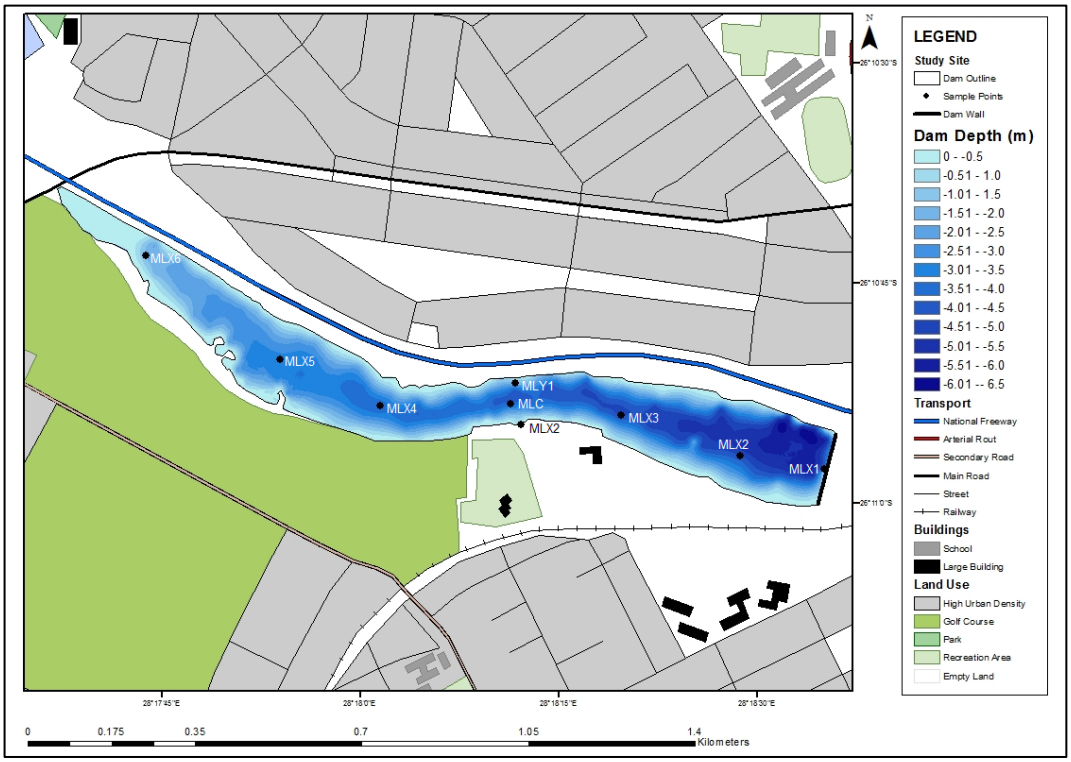


Figure 4.8: Bathymetric Map of Middle Lake

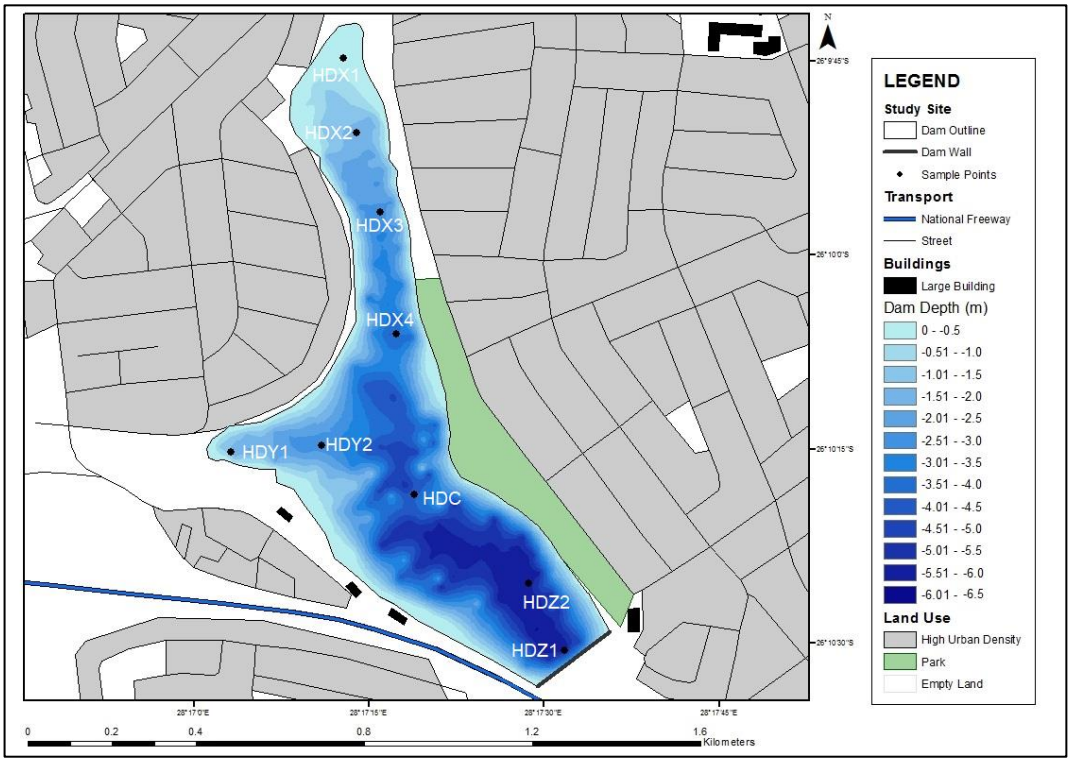


Figure 4.9: Bathymetric Map of Homestead Dam

4.2.3. The Volume of Each Dam

Table 4.1 expresses the varying volumes of each site, based on the max depth using bathymetric data, and average surface area measured in Google Earth. The site with the largest volume is Homestead Dam (2 950 279.74 m^3), and the smallest is Amata Pan (182 623.84 m^3).

Table 4.1: Average Volumes of each site based on Bathymetric Depths

Site	Max Depth (m)	Average Surface Area (m^2)	Volume (m^3)
Korsmans Pan	2	359 289	718 578
Amata Pan	1.8	101 458	182 624
Bullfrog Pan	1	576 505	576 505
Sandpan	1	544 990	544 990
Homestead Dam	6.5	453 889	2 950 280
Middle Lake	6.5	224 654	1 460 250
Civic Lake	2.5	104 051	260 126
Kleinfontein Dam	5.5	381 476	2 098 119
van Ryn Dam	3.5	418 494	1 464 728

4.3. Wind Rose Diagrams

Two wind rose diagrams were created, to identify the predominant wind direction and speed for a 20-year period (Fig 4.10) and the year of the study 2017 (Fig 4.11). The data from the two diagrams were used to give an understanding of the wind dynamics in the region and help provide some evidence as to if the trace elements could have originated from tailings dams and mine dumps in the Benoni City region. The predominant wind direction for the region over the 20-year period was from the north, with the wind speed ranging from 4 to 8 m/s (Fig. 4.10). Other dominant wind directions include north-west, east, and south south-west.

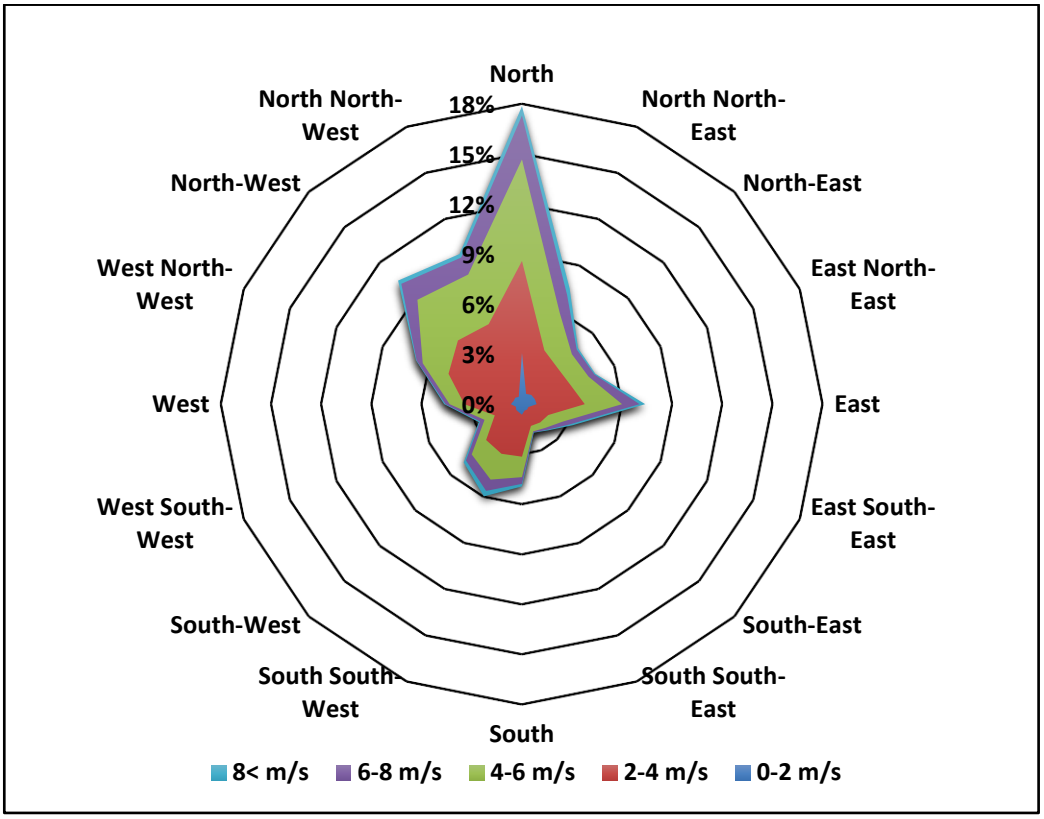


Figure 4.10: Wind rose diagram comparing the average wind speed to the average direction for a 20-year period (1997 - 2017)

A wind rose diagram for the year of sampling was created (Fig 4.11). The diagram expresses a similar distribution of predominant wind direction as figure 4.10, but a slightly different predominant wind speed. It is important to note that different wind directions can be characterised with multiple wind speeds and vice versa. The predominant wind speed range, during 2017, came from a northerly direction and was 4-6 m/s. The greatest wind speed range coming from the west to west north-west direction is 2-4 m/s. There have been some days within the year where the wind came from an easterly and southerly direction, in which the wind speeds were between 4-6 m/s and 2-4 m/s respectively. The wind direction and speed helped indicate if there is a likelihood of contaminants coming from the tailing dams and mine dumps in the middle of the city region.

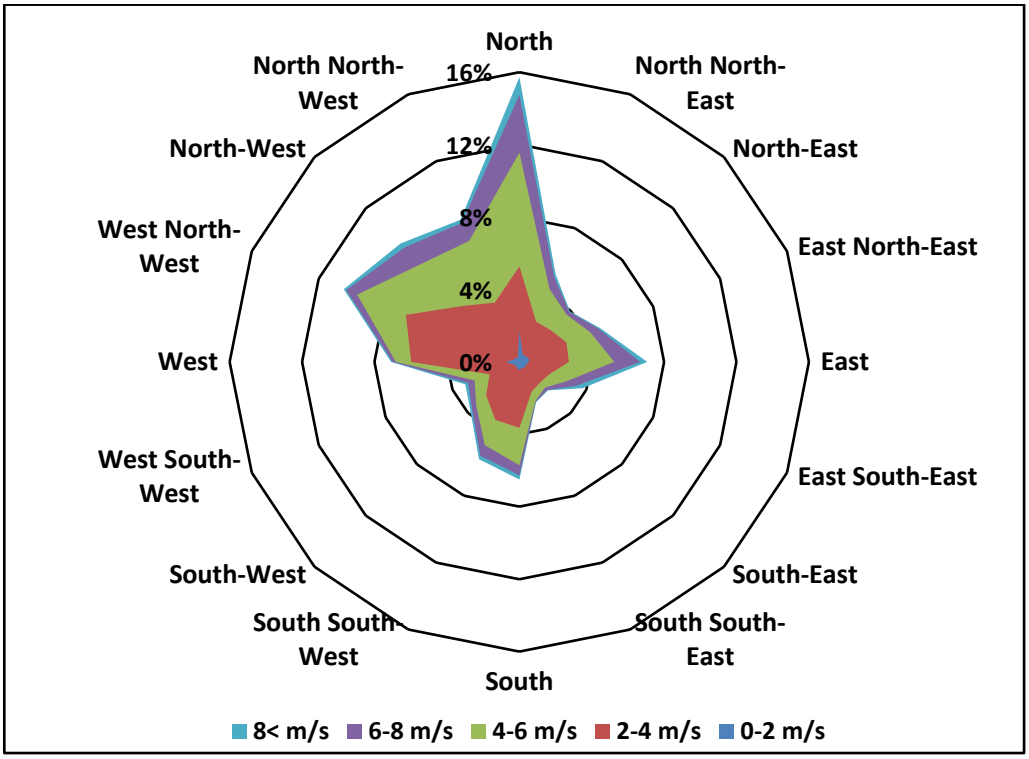


Figure 4.11: Wind rose diagram comparing the average wind speed and direction for 2017

4.4. Results of Water Analysis

Data were collected by taking water samples in the field and using the YSI multiparameter probe to identify physical water characteristics. The water samples were further analysed using ICP-OES to identify various chemical characteristics. Once this was identified, the data from each site were compared to each other and the water quality standards provided by the SAWQG and the WHO drinking water guidelines. Water data were acquired to give an understanding of the basic water conditions of each site, and not for a fully comprehensive study. This is beyond the scope of this research project and could possibly be done in the future.

4.4.1. Physical Characteristics

Physical water characteristic data were collected when in the field using the YSI multiparameter probe. This helped identify data for temperature (°C), DO (% and mg/L), conductivity (µS/cm), and pH (Table 4.2). Understanding physical characteristics can give a good understanding of the chemical characteristics of the water at each site.

The first characteristic to note is temperature (Table 4.2). The temperature of the water at each site varied slightly when compared to each other. The sites with the greatest temperature were Civic Lake, van Ryn Dam and Amata Pan. This was due mainly to the fact that the data taken at these three sites was for September/October when the seasons in the region change and get warmer. It is notable that the temperature at each site was greatest at the surface than at the bottom of the water column, indicating some thermal stratification, with the greatest difference in temperature being at Korsman Pan (12.9°C and 10.7°C). In comparison to the temperature data, the DO data were less uniform.

There were various issues with the DO probe on the YSI, when in the field. The values for the DO was constantly greater than 100% and even though this is possible (the DO can actually be greater than 100%, up to about 20% more) the DO managed to reach higher than 200% at two sites at the top of the water column (Table 4.2), compared to lower than 100% at the bottom of the water column (Bullfrog and Amata Pans). Therefore, this means that the data is most likely unreliable even if it does express a difference between the top and the bottom of the water column at

each individual site. The data for the conductivity, however, suggested no problems and expressed a greater range across all sites.

Conductivity is the measure of the ability of water to pass electrical flow. It is also closely related to salinity and thus can give a good indication of the salt concentrations in the water (Table 4.2). The sites with the greatest conductivity values were Bullfrog (2572 µS/cm at the surface and 2492µS/cm at depth) and Sandpan (2416µS/cm at the surface and 2401µS/cm at depth). These values indicate the two sites are highly saline, most likely due to evaporative action. These two sites, as well as Korsman Pan, were the only sites that had greater conductivity values at the surface of the water column (Table 4.2). The rest of the sites expressed an increase in conductivity towards the bottom of the water column. The conductivities of the four pans were comparatively higher than the five dams, which were all below 500 µS/cm.

All the sites had a relatively high pH value that ranged from 6.8 to 9.22 (Table 4.2). The sites that were more alkaline than the rest, were, once again, Bullfrog Pan (9.22 and 9.19) and Sandpan (8.7 and 8.55), as well as Amata Pan (9.15 and 7.12) and van Ryn Dam (8.45 and 6.96). Each site had relatively higher pH values at the surface compared to the bottom of the water column. with the greatest difference being at Amata Pan.

Table 4.2: Physical characteristics identified at the surface and depth of each site, with the YSI multi-parameter probes (S = surface; D = depth)

Site	Date	Sample Depth (m)	Temp °C		DO(%)		DO (mg/L)		Cond (µS/cm)		pH	
			Surface	*Depth*	*Surface*	*Depth*	*Surface*	*Depth*	*Surface*	*Depth*	*Surface*	*Depth*
Amata Pan	30/10/2017	1.5	17.3	16.3	254.2	21.6	20.18	1.75	557	580	9.15	7.12
Korsman Pan	21/7/2017	1.5	12.9	10.7	103	75.5	9.12	6.92	740	698	8.02	7.9
Bullfrog Pan	5/8/2017	0.92	15	14.4	207.7	98.9	17.18	8.23	2572	2492	9.22	9.19
Sandpan	10/8/2017	0.66	14.7	14.2	97.9	88.6	8.16	8.55	2416	2401	8.7	8.55
Homestead Dam	24/08/2017	4.1	12	11.4	111.5	111.7	9.91	10.03	243.3	250.2	7.6	7.43
Middle Lake	7/8/2017	4	13.7	12.5	123.9	24	10.75	2.12	247.1	287.9	8.2	7.18
Civic Lake	30/10/2017	1.7	20.2	19.1	107	11.9	8.09	0.92	297.5	364.1	7.91	6.88
Kleinfontein Dam	1/9/2017	4.6	14.6	14.2	113.5	66.7	9.49	5.65	352.6	358.9	7.48	7.19
van Ryn Dam	26/10/2017	2.6	20.9	20.5	98.8	2.1	7.3	0.16	232.6	317	8.45	6.96

4.4.2. Chemical Characteristics

The water samples were analysed to identify various metal concentrations within the water column. The main trace elements, As, Cu, Cr, Fe, Mn, Ni, Pb, and Zn were analysed in each sample, but due to the detection limits of the ICP-OES (1mg/L), they were undetectable. The ICP-OES was able to identify concentrations of other elements such as Ca, Mg, K, Na, S, and Si (Table 4.3).

The samples with greatest concentrations of Ca (Table 4.3) came from Korsman Pan (2242.2 mg/L at the surface and 1983.3mg/L at the bottom) and Amata Pan (2129.4 mg/L at the surface and 2366.6mg/L at the bottom). There was also a difference between the surface samples and the bottom samples at all the sites, with Korsman Pan, Bullfrog Pan, Middle Lake and Kleinfontein Dam having greater concentrations of Ca at the surface, and the rest of the sites containing greater concentrations at the depth (Table 4.3). The dam with the greatest concentrations of Ca was Kleinfontein Dam. The greatest concentrations of K were identified at very different sites.

The samples with the greatest concentrations of K came from the Bullfrog Pan (6584.9mg/L at the surface and 6644.4mg/L at the bottom of the pan) (Table 4.3). Then next sites to contain the greatest concentrations of the K was Sandpan (1704.65mg/L at the surface and 1702.35mg/L at the bottom of the pan), followed by Korsman's Pan (1362.2mg/L at the surface and 1209.15mg/L at the bottom of the pan). Compared to these sites, the K concentrations at each dam was below 100mg/l. Surface samples with greater concentrations of K than the bottom samples came from Korsman Pan, Amata Pan, Sandpan, Civic Lake, and Kleinfontein Dam.

Table 4.3: The concentrations, identified with ICP-OES, of various chemical characteristics for the surface and depth samples at each site. These were the only trace elements identified using this method.

Site	Date	Sample Depth (m)	Ca (ppm)		K (ppm)		Mg (ppm)		Na (ppm)		S (ppm)		Si (ppm)		Sr (ppm)	
			Surface	*Depth*	*Surface*	*Depth*	*Surface*	*Depth*	*Surface*	*Depth*	*Surface*	*Depth*	*Surface*	*Depth*	*Surface*	*Depth*
Amata Pan	30/10/2017	1.5	2129.40	2366.60	127.10	122.28	167.18	164.10	0.28	0.30	3068.65	3100.35	< 0.008	0.22	0.27	0.29
Korsman Pan	21/7/2017	1.5	2242.20	1983.30	1362.20	1209.15	1614.30	1618.75	0.43	0.42	3296.75	2965.75	1.29	1.31	0.29	0.28
Bullfrog Pan	5/8/2017	0.92	1276.75	1190.85	6584.90	6644.45	3279.50	3332.85	12.44	13.23	48.60	54.87	1.81	2.21	0.33	0.33
Sandpan	10/8/2017	0.66	658.25	913.50	1704.65	1702.35	139.10	142.96	33.40	34.04	4068.55	4272.75	67.74	73.76	0.19	0.19
Homestead Dam	24/08/2017	4.1	1288.30	1310.95	22.67	23.10	600.35	601.20	0.06	0.07	1461.80	1497.30	2.13	2.12	0.15	0.15
Middle Lake	7/8/2017	4	1386.95	1269.70	22.93	23.37	553.05	574.00	0.06	0.07	1519.60	1475.15	2.12	2.18	0.15	0.16
Civic Lake	30/10/2017	1.7	1059.65	1110.55	54.08	50.48	126.53	124.69	0.12	0.12	198.75	195.29	0.22	0.22	0.14	0.15
Kleinfontein Dam	1/9/2017	4.6	1740.60	1425.35	64.58	62.76	144.70	144.70	0.14	0.14	2410.30	2410.30	29.73	29.73	0.20	0.20
van Ryn Dam	26/10/2017	2.6	185.67	555.98	50.19	50.60	81.61	79.81	0.09	0.08	151.91	156.66	0.33	0.48	0.11	0.13

In comparison sites such as Bullfrog Pan, Homestead Dam, Middle Lake, and van Ryn Dam contained greater K concentrations in the samples from the bottom of the water column (Table 4.3).

Large Mg concentrations were found in the samples that came from the Bullfrog Pan (3279.5mg/L at the surface and 3332.85mg/L at the bottom), followed by Korsman Pan (1614.3 mg/L at the surface and 1618.75 mg/L at the bottom). Concentrations of Mg were relatively low in samples that came from all the sites considered as dams (Table 4.3). At the majority of the sites, except for Sandpan, Civic Lake and van Ryn Dam, the greater concentrations of Mg came from samples taken at the bottom of the water column.

Compared to this, there were large concentrations of Na identified in samples from the Sandpan (33.4mg/L at the surface and 34.04mg/L at the bottom) and Bullfrog Pan (12.435mg/L at the surface and 13.225mg/L at the bottom). Notably, all concentrations of Na at every site were below 50mg/L (Table 4.3). Concentrations of S at the majority of the sites were well above 1000mg/L (Table 4.3). The only sites that had lower values of S were Bullfrog Pan, Civic Lake and van Ryn Dam (Table 4.3). The samples with the largest concentrations of S came from Sandpan (4068.55mg/L at the surface and 4272.75mg/L at the bottom), Amata Pan (3296.75mg/L at the surface and 2965.75mg/L at the bottom) and Korsman Pan (3068.65mg/L at the surface and 3100.35mg/L at the bottom). The dam with the largest concentrations of S was Kleinfontein Dam (2410.3 mg/L at the surface and 2410.3 mg/L at the bottom), which is the only site with no difference between the surface and bottom samples and the closest to the mine dumps. Only two sites

contained S concentrations that were greater towards the bottom of the water column; Homestead Dam and Bullfrog Pan (Table 4.3).

The highest concentration of Si (Table 4.3), once again, came from samples taken at Sandpan (67.74mg/L at the surface and 73.76 mg/L at the bottom). The site with the next greatest concentrations of Si was Kleinfontein Dam (29.73 at both the surface and the bottom of the water column). The remaining sites all contained samples with Si concentrations well below 10mg/L (Table 4.3).

4.4.3. Comparisons to Water Quality Standards

The results from the *in situ* water monitoring and the water samples were compared to standards for water quality provided by the SAWQG and the WHO. These standards only provided information on temperatures, the pH, DO, K, Mg, and Na. There was no information available for the other characteristics.

The Ecosystem range for water quality, provided by the SAWQG, indicates that the temperature of a natural system should not exceed 10% more than the daily average for that area. There is insufficient data regarding the temperatures of the day in which samples were taken, thus the standard could not be applied. The DO range for ecosystems, according to the SAWQG, is between 80 and 120 %. Four sites, Amata Pan, Middle Lake, and van Ryn Dam contained DO levels at the bottom of the water column that were below 80%/L (Table 4.2). Once again, it should be noted that issues with DO probe were persistent and thus these data are unreliable. There were three different ranges, 6-8, 6-8, and 6.5-8, provided for the pH of water by the various guidelines. According to the ecosystem range, by the SAWQG the pH of a natural system should not be below six and greater than eight, these values coincide

with the WHO guidelines of 6.5-8. None of the sites had a pH value below, but the two measuring points at Bullfrog Pan (9.22 at the surface and 9.19 at the depth) and the surface point at Amata Pan (9.15) were above nine, making them more alkaline than the rest of the sites (Table 4.2).

For water chemistry, only K, Mg, and Na were compared to the water quality guidelines. The average range of K concentrations in the water samples should be between 0-50mg/L. There is considerable K pollution at most sites, as all the samples contained concentrations of K greater than 50mg/L (Table 4.3). The sites with the greatest levels of pollution were the pans, Korsman Pan, Bullfrog Pan and Sandpan. Only two sites did not contain some form of K pollution and they were Middle Lake and Homestead Dam. The average range of Mg concentrations on water systems is 0-30mg/L. There was considerable Mg pollution at every site this time, with all the samples containing Mg concentrations greater than 30mg/L the concentrations at Bullfrog Pan were 100x greater than the recommended range (Table 4.3). The next highest was identified at Korsman Pan, followed by Homestead Dam, then Middle Lake. For Na, there were two recommended ranges, one by the SAWQG and the other by the WHO. The SAWQG suggests that Na concentrations should be between 0-100mg/L whereas the WHO suggests the maximum should be 200mg/L. None of the sites contained Na concentrations higher than any of the two ranges, SAWQG and the WHO, and therefore none of the sites contained any Na pollution (Table 4.3).

4.5. XRF Analysis

A statistical analysis of the handheld XRF data was done in order to check the accuracy of the method employed. This has been done in two ways, the first is correlating the sample data to the error means of each trace element. This allows to identify the accuracy of the data within the machine, and whether it is usable for further analysis. Furthermore, the handheld XRF sample data was correlated against the conventional lab XRF. This was done to check the accuracy of the data provided by the handheld data, against a machine that has higher accuracy. The reason for doing this is due to the large number of samples that required analysing and the lack of funds needed to analyse all of them on a conventional lab XRF, while the handheld XRF was freely available for personal use.

4.5.1. Average Trace Element Concentrations across each Site.

The average trace element concentrations from each site varied considerably, with the high concentrations coming from the dams and Amata Pan. (Table 4.4). The raw data used to identify the means of individual trace elements concentrations can be found in the appendix (Appendix 2).

Table 4.4: Average trace metal concentrations of each site in ppm

Site	As	Cu	Fe	Mn	Ni	Pb	Zn	Ca	S	K	Ti	V	Cr	Th	U
Amata Pan	247	1177	247638	4755	271	2396	20160	10710	4464	4731	3138	113	1382	8	2
Korsman Pan	11	84	22804	533	3	75	385	18682	2059	7677	3841	97	306	9	5
Bullfrog Pan	9	53	27991	926	7	51	197	30430	916	15921	3182	92	206	15	13
Sandpan	3	38	24045	534	6	32	84	11084	236	19068	3193	96	225	18	18
Homestead Dam	20	106	79711	1824	33	151	550	5539	1136	5350	4465	153	474	6	9
Middle Lake	32	103	63343	1601	45	188	550	6594	2778	4989	4447	150	447	11	12
Civic Lake	33	149	56824	1500	28	268	1151	6364	1896	5900	4474	131	502	11	12
Kleinfontein Dam	55	196	58191	1072	82	437	2386	7905	3130	6002	4196	127	482	13	14
van Ryn Dam	12	82	43454	398	19	63	252	4464	649	9973	3769	112	277	25	18

4.5.2. Handheld XRF Error Correlation

Statistical analysis between the means of the sample data and the margin of error for each trace element was undertaken (Table 4.5). Both significant difference and correlation were done to determine the level of confidence needed to use the data. A strong positive correlation indicates stronger confidence in the data than a negative one. The significant difference for all trace element data was lower than the alpha value of 0.05, indicating a significant difference between them. The data for Th and U both expressed very low negative correlations, indicating little to no relationship between the sample data and the error data. Compared to this there were intermediate to strong positive correlations for the rest of the trace elements. Therefore, there is very little confidence in using the data for Th and U, but high confidence when using the data for the rest of the trace elements analysed.

Table 4.5: The Correlation of the Sample means versus the Error mean to identify the accuracy of the Handheld XRF data

Trace Element	Sample Mean	Error Mean	Difference	P-Value	Correlation Value
As	36.338	6.244	30.094	0.004	0.869
Ca	11715.919	124.285	11591.634	< 0.0001	0.880
Cr	425.506	14.636	410.871	< 0.0001	0.941
Cu	171.724	11.401	160.322	< 0.0001	0.979
Fe	60306.769	244.519	60062.250	< 0.0001	0.980
K	9323.702	159.121	9164.581	< 0.0001	0.730
Mn	1283.292	55.131	1228.160	< 0.0001	0.977
Ni	43.399	17.926	25.473	0.019	0.671
Pb	301.926	7.904	294.022	0.000	0.980
S	1741.900	190.089	1551.811	< 0.0001	0.869
Th	13.514	3.409	10.105	< 0.0001	-0.178
Ti	3852.296	67.128	3785.168	< 0.0001	0.497
U	11.912	4.191	7.721	< 0.0001	-0.061
V	118.463	19.636	98.826	< 0.0001	0.749
Zn	1991.589	19.494	1972.095	0.005	0.983

4.5.3. Conventional XRF Correlation

A similar procedure was conducted when comparing the data from the conventional XRF and the handheld XRF (Table 4.6). The complete dataset was too large and therefore included in the appendices (Appendix 3) for completeness with only selected data shown here. The reason for doing this is to identify the confidence levels of using the handheld XRF as the main data source. Firstly, the R-value was calculated to identify how closely correlated the two data sets were. The correlation was conducted between data for each trace element, except for As and S which could not be analysed using the conventional lab XRF. Doing this allows for the identification of which trace element values one is more confident using. A high positive or negative R-value represents a strong correlation between the two data sets. Compared to this low positive R-value represents a weak to no correlation between the data. (Table 4.6). A positive correlation between the two would indicate that both datasets have the same trend, and thus provide a higher level of confidence than that of a weak or a negative correlation.

None of the trace element data from the handheld and conventional XRFs were negatively correlated together, but Th did show a very low positive R-value. This could indicate that there is not much of a relationship between the two datasets, therefore making it less reliable than the others. Compared to this, all the other trace elements had R-values greater than 0.9, with only U and V being 0.774 and 0.879 respectively. Overall, there is a high level of confidence for using the handheld data.

Table 4.6: The correlation and significant difference of the Conventional XRF means for each trace elements versus the Handheld means to identify the similarity and subsequent accuracy of the Handheld XRF Data

Trace Element	Mean		Difference	R-value	R-Squared Value	P-value
	Conventional	Handheld				
As	-	-	-	-	-	-
Ca	13317.262	14007.447	-690.185	0.998	0.997	0.060
Cr	443.117	514.436	-71.319	0.997	0.994	< 0.0001
Cu	164.444	199.353	-34.909	0.997	0.994	0.002
Fe	53529.939	76788.569	-23258.630	0.991	0.983	0.034
K	11585.163	9807.788	1777.375	0.999	0.998	0.008
Mn	1385.418	1888.124	-502.707	0.974	0.950	0.056
Ni	110.972	60.590	50.382	0.985	0.970	< 0.0001
Pb	360.618	429.240	-68.622	0.998	0.996	0.023
S	-	-	-	-	-	-
Th	10.666	18.849	-8.183	0.108	0.012	0.026
Ti	4163.250	4132.090	31.160	0.934	0.871	0.700
U	1.152	14.560	-13.408	0.774	0.600	< 0.0001
V	90.132	138.702	-48.570	0.879	0.772	< 0.0001
Zn	2279.587	2747.000	-467.413	0.998	0.997	0.052

4.6. Sediment Results

Sediment data were analysed using the following statistical methods:

- Correlation matrix to identify which trace elements are more likely to occur together;
- Principle Component Analysis (PCA), to identify the spatial distribution of trace elements within sites and across the entire region and
- ANOVA to further characterise the spatial distribution of trace elements across the entire region.

The data were also compared to the *Igeo* to identify the level of pollution at each sample point.

4.6.1. Understanding Trace Element Distribution across Benoni

PCA was undertaken, using the average concentrations of each trace element, to identify which sites are being strongly driven by the various trace elements analysed using XRF. A square root transformation was done on the samples measured in ppm. The transformation was done in order to down-weight the more dominant elements. This transformation was coded in R. A further PCA was done to understand the overall relation of trace elements to samples across the entire study area. PCA was also conducted on each individual site to understand patterns in the distribution of trace elements with each site. This allows for an understanding of the regional distribution and the within site distribution.

The PCA (Fig 4.12) shows that axis one is mainly being driven by Amata Pan and differs from all the other sites with regards to the main trace elements tested for (As, Cu, Fe, Mn, Ni, Pb, and Zn), with the main driver being Fe. Axis 2 further shows the difference between the sites that are dams versus the sites that are pans. Dams are mainly to the top of the graph and seem to be driven by Ti, with a PCA 1 between -5 and 5, and a PCA 2 between 0 and -10. Compared to these, the other three pans (Korsman Pan, Sandpan, and Bullfrog Pan) are being driven by elements such as Ca and K, which could be due to their increased evaporative concentration. The difference between dams and pan could be as a result of differences between windblown versus surface runoff sources of contamination.

The PCA for the site averages is similar in distribution to the PCA graph for the distribution of trace elements in each individual sediment sample (Fig 4.13). A great number of the samples are clustered together in the top left corner of the PCA (Fig

4.13). Fe is driving both samples, APY 1 and 2, with principal component (PC) 1 between 12.5 and 27.5, while PC 2 is between -1 and -4. Compared to this Zn is driving samples APC, APX1, and APX2 with a PC1 between 5 and 10 and a PC2 between -0.5 and 0.

Over the entire area, samples, KPC, KPY3, KPX3, BFPC, BFPX2, BFPX4, BFPY1, and BFPY3 are being driven strongly by Ca with a PC 1 between -5 and 0 and a PC 2 between -12.5 and -5. Compared to this K is driving the following samples, BFPY1, BFPX3, KPY2, KPX2, SPC, SPY2, SPX2, and SPY3, with PC 1 between -5 and 0 and PC 2 between -5 and 0. The remainder of the sites are all clustered at the top of the PCA plot. Although the above samples are being driven by certain trace elements across the entire area, many are also being driven by others across the local site. A deeper look into PCAs of each site shows differences in driving factors across the study site compared to the greater study area.

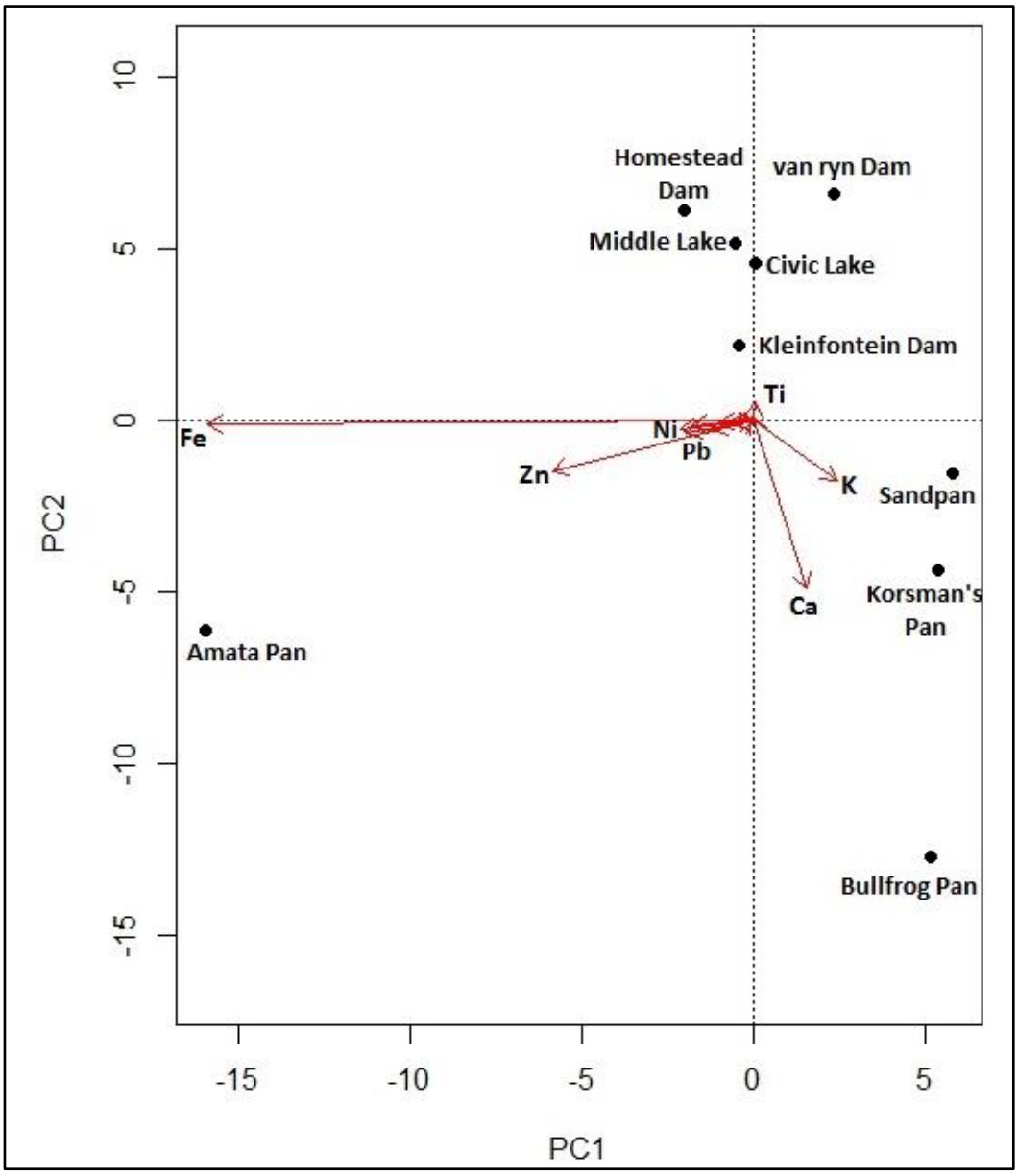


Figure 4.12: The relationship between the individual sites and the main trace elements (site mean values) found within them

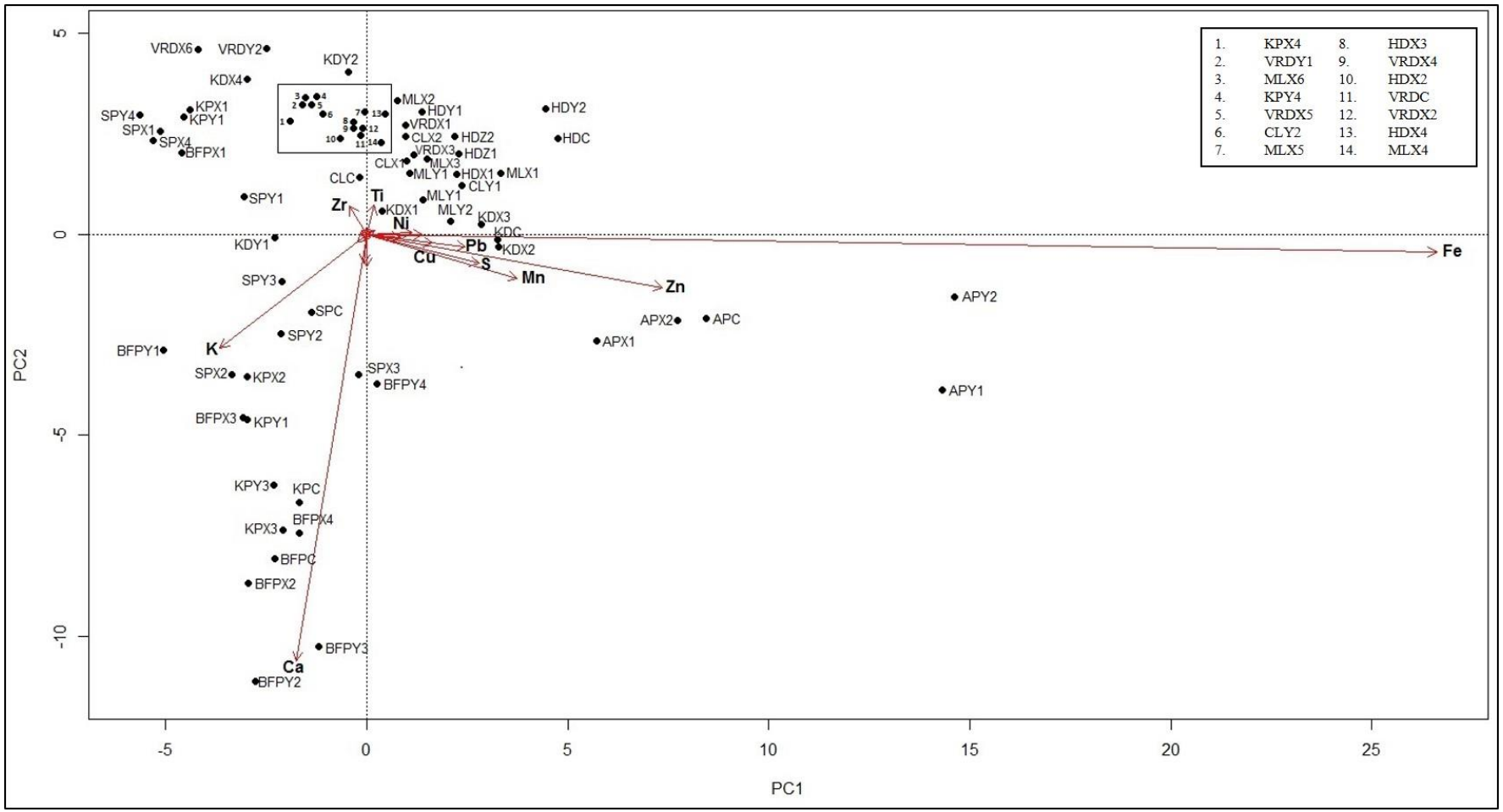


Figure 4.13: The PCA expressing the relationship of individual samples across the entire research area

Pan Sites

A deeper look at each individual site allows one to identify the particular drivers within it. A closer look at Amata Pan (Fig. 4.14a) shows that although Fe is driving sample APY 1 and 2 when looking across the entire area, it is only driving APY 2 in the actual site. Individual study sites have different interactions taking place and thus different drivers will be identified. At Bullfrog Pan (Fig. 4.14b), Mn, Ca, and S are driving samples BFPY3, BFPY2, BFPC, and BFPX2, with a PC 1 between -10 and 0, and PC 2 between -7.5 and -5.0. Compared to this the main driver of these samples across the entire region is just Ca (Fig. 4.14b). This shows that these samples are not only similar to each other but similar to samples from other sites, with respect to Ca. Samples from sites that constitute pans are shown mainly to be driven by the more common trace elements across the entire region. Once again, a closer look also shows the difference within each site.

At Sandpan (Fig. 4.14c), there was a large variation in the distribution of samples across the plot, with the most notable relationship being shown between SPY2 and, Ca and Mn. Compared to this SPC, SPX3 and SPY3 are being driven by both Fe and K, which is slightly different to what is represented in the PCA plot for the entire study area, which expressed these three samples as only being driven by K. The PCA plot for the last of the four pans, Korsman Pan (Fig. 4.15a), expressed a similar distribution of samples being driven by the same trace elements as the PCA plot for the entire area. The main difference was with sample KPC,

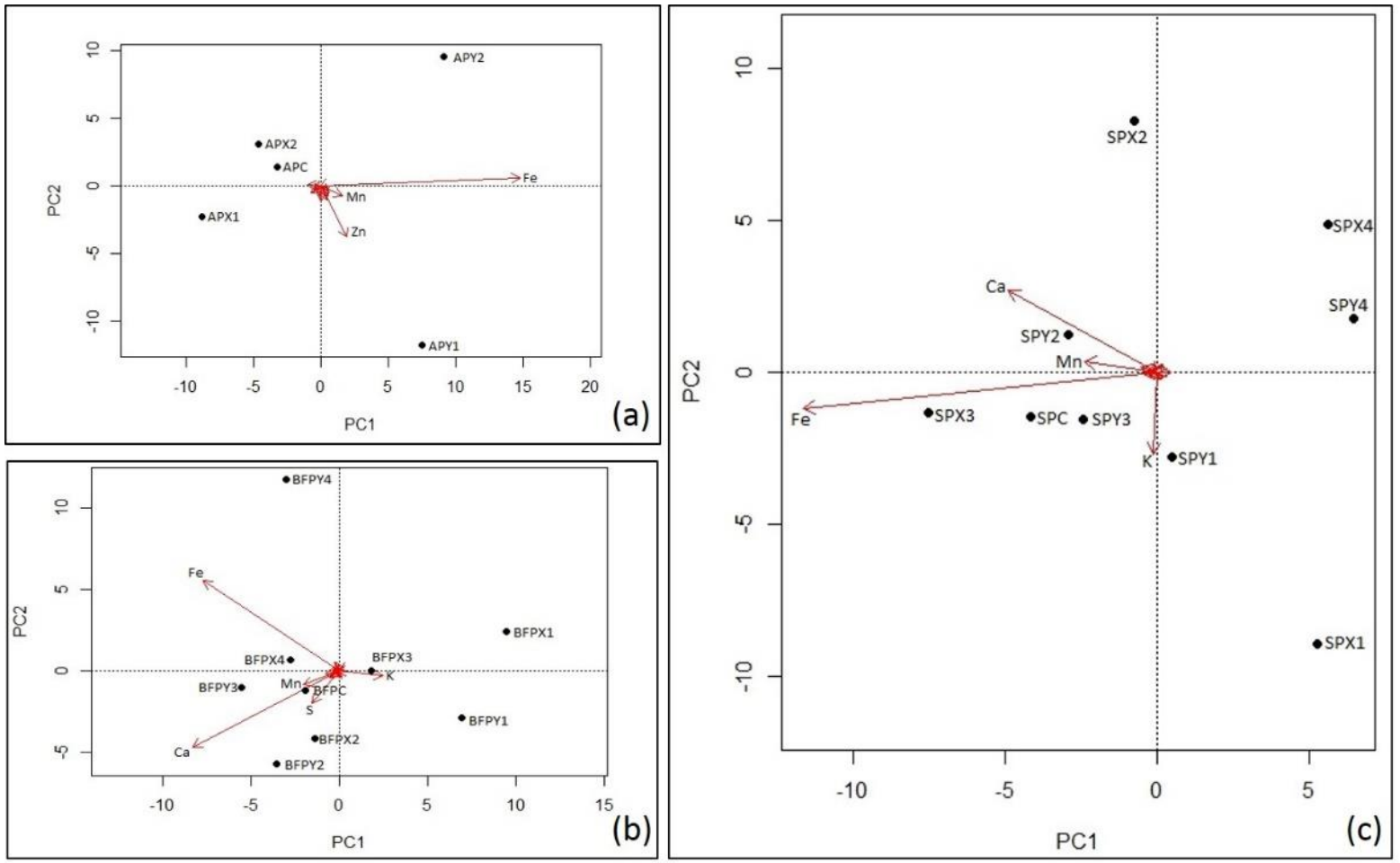


Figure 4.14: PCA expressing the relationship of samples and trace elements within selected sites (a. Amata Pan; b. Bullfrog Pan; c. Sandpan)

which in the local site plot was being driven by slightly more by Fe, with a PC 1 of -4 and -6, and PC 2 between -1 and -6 (Fig. 4.15a). The distributions of the samples from the dams were slightly different from those from the pans. Most of these samples were clustered to the top left of the plot in the overall study area PCA plot.

Dam Sites

There are differences that can be identified when comparing the PCA plots for each individual site that are classified as a dam (Fig. 4.15) and the PCA plot for the entire study area (Fig. 4.13). A closer look at the area plot shows that the majority, if not all, of the samples taken from dams, were clustered together and being driven by Pb, Ti and Zirconium (Zr). This difference is evident for samples HDY1 (Fig 4.15b), MLY1, MLY2, MLX3 (Fig 4.15c) KDX2, KDY3 (Fig 4.15e), VRDX2, VRDX3, and VRDX1 (Fig 4.15f) which are being driven by both Ca and Mn in the individual site plots but are mainly being driven by Zr and Ti in the overall study area plot (Fig 4.13). The same differences can be seen for CLX2 (Fig. 4.15d), KDX3 (Fig. 4.15e), VRDC, and VRDX4 (Fig. 4.15f), which are being driven by K in their individual plots but not across the entire area plot.

The spatial individual PCAs gave a better understanding of the spatial distribution of trace elements within each site, while a PCA for the average concentrations of pollutants at each site provided an understanding of the spatial distribution across the entire region. To provide further detail on the spatial distribution and to identify which sites are either significantly different or not significantly different from each other, ANOVA tests were undertaken.

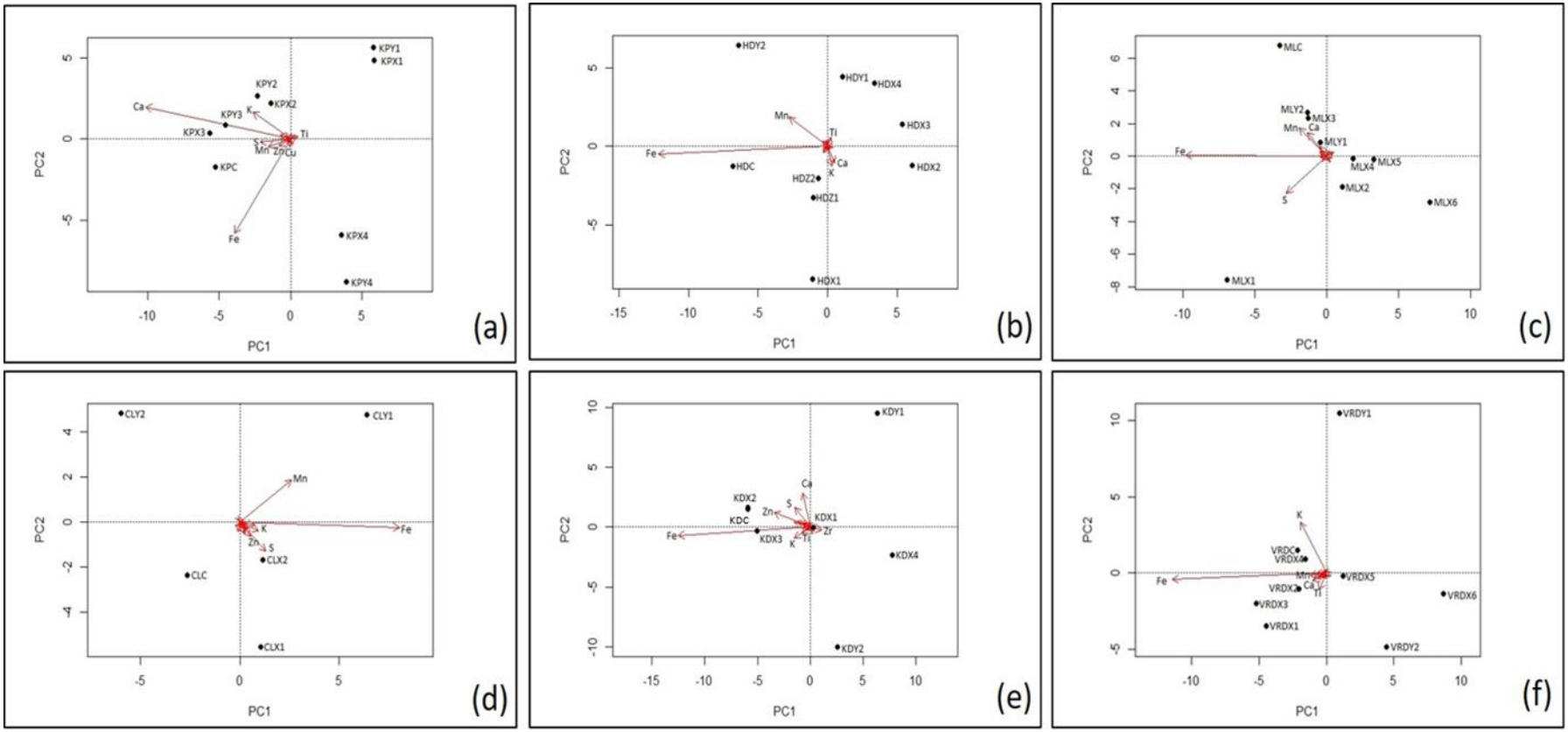


Figure 4.15: PCA expressing the relationship of samples and trace metals within selected sites
(a. Korsman Pan; b. Homestead Dam; c. Middle Lake; d. Civic Lake; e. Kleinfontein Dam; f. van Ryn Dam)

4.6.2. Representing Trace Element Distribution at each Site

Various dot density maps were produced to better visualise the spatial distribution of the seven main trace elements analysed in the research (As, Cu, Fe, Mn, Ni, Pb, and Zn). The maps showed that the pans (Fig 4.16 - 4.19). contained similar spatial patterns to each other but different to that of the dams (Figs 4.20 - 4.24). For Amata Pan (Fig 4.16), one sample point (APY1) contained predominantly greater trace element concentrations for all the trace elements except Fe. The other four sampling points contained relatively similar concentrations for each trace element. The spatial pattern was slightly different at the other three pans, where multiple samples contained varying concentrations of each trace element. The spatial patterns for concentrations of varying trace elements at Korsman Pan (Fig 4.17), Bullfrog Pan (Fig 4.18) and Sandpan (Fig 4.19) expressed a more scattered and irregular distribution.

At the same time the dams also contained a similar predominant spatial pattern, with the greatest concentrations being identified towards the middle of the site, the deepest sample points and the dam wall at each site. For most of the sites, except Civic Lake (Fig 4.22)., the greater trace element concentrations were identified in the samples along the x-axis,. The only other exception to this pattern was the distribution of As in Middle Lake.

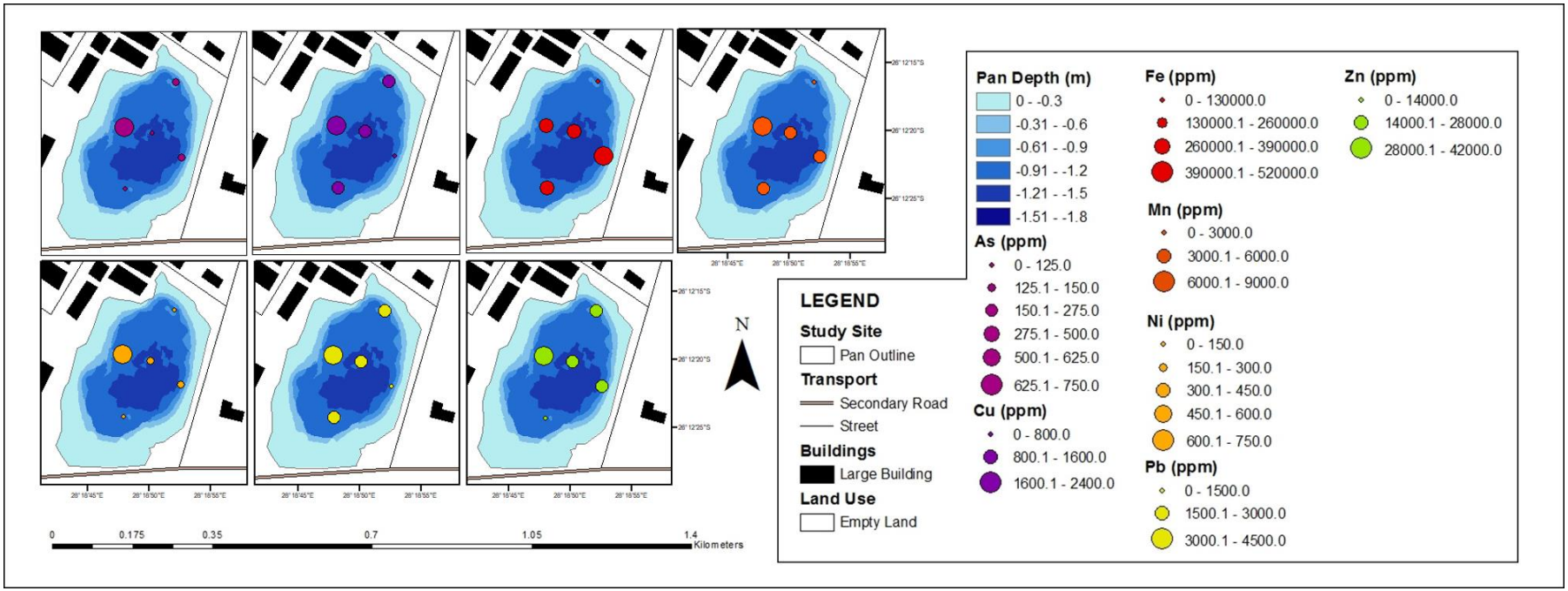


Figure 4.16: Spatial distribution of 7 trace metal concentrations across Amata Pan

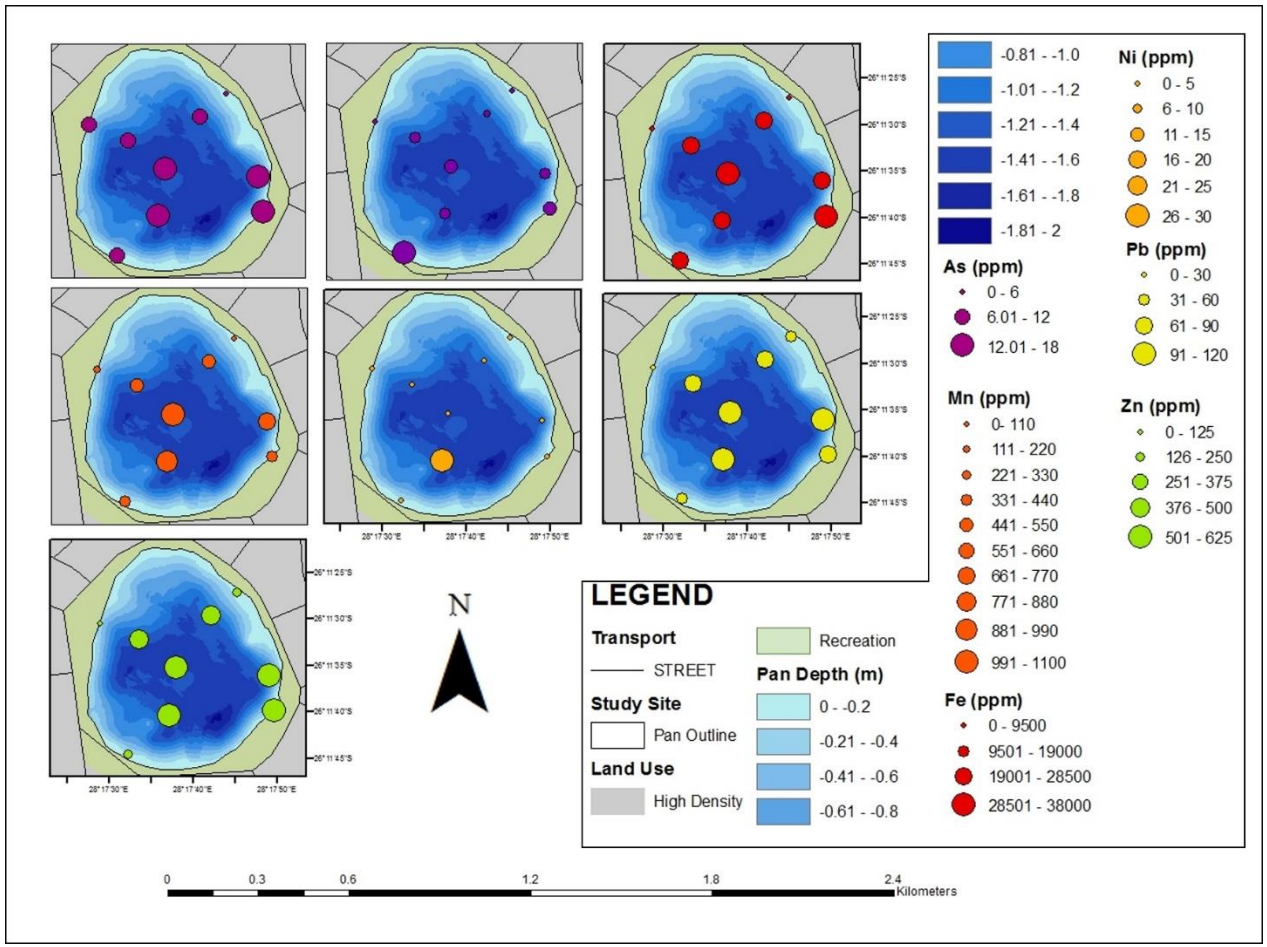


Figure 4.17: Spatial distribution of 7 trace metal concentrations across Korsman Pan

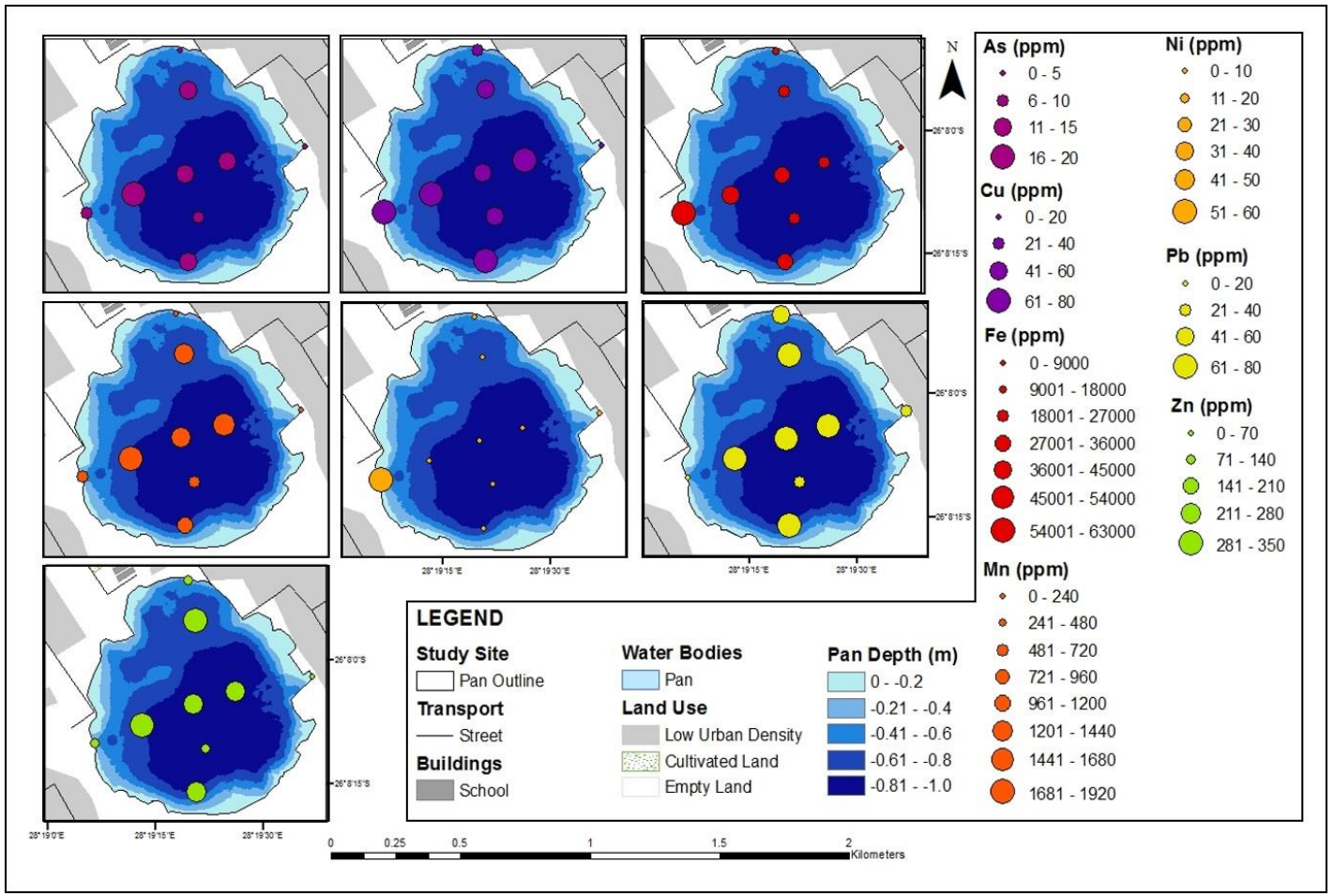


Figure 4.18: Spatial distribution of 7 trace metal concentrations across Bullfrog Pan

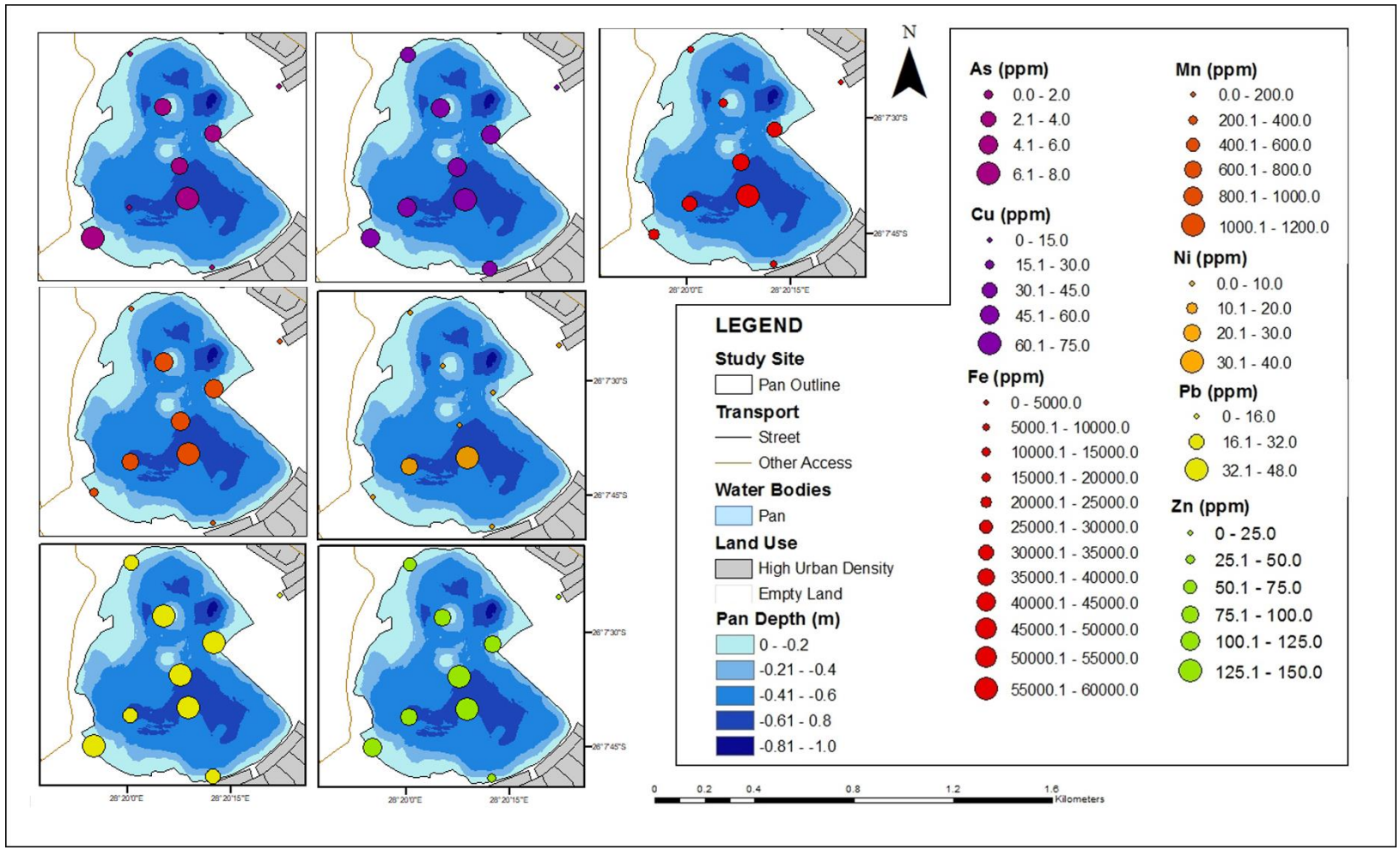


Figure 4.19: Spatial distribution of 7 trace metal concentrations across Sandpan

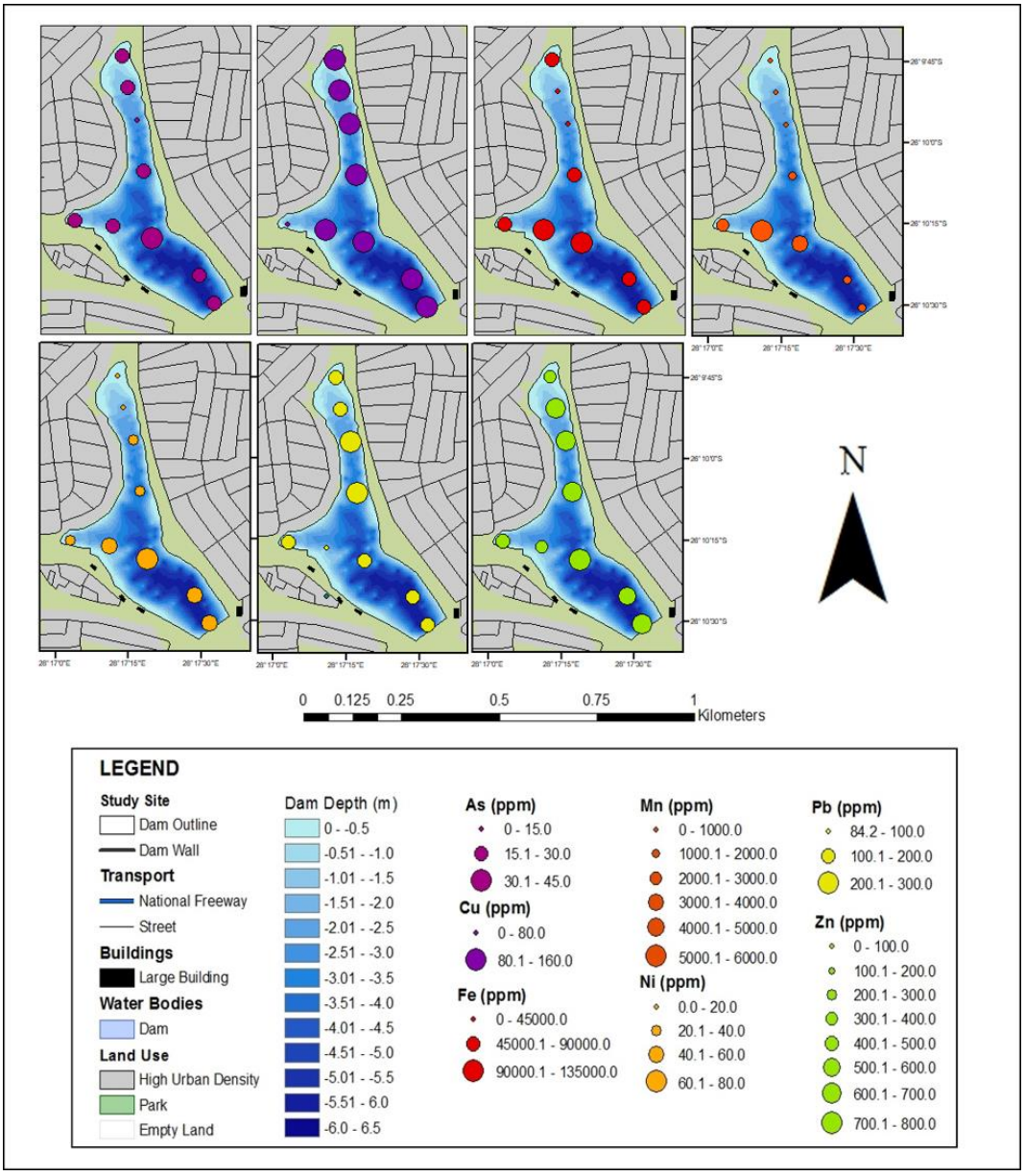


Figure 4.20: Spatial distribution of 7 trace metal concentrations across Homestead Dam

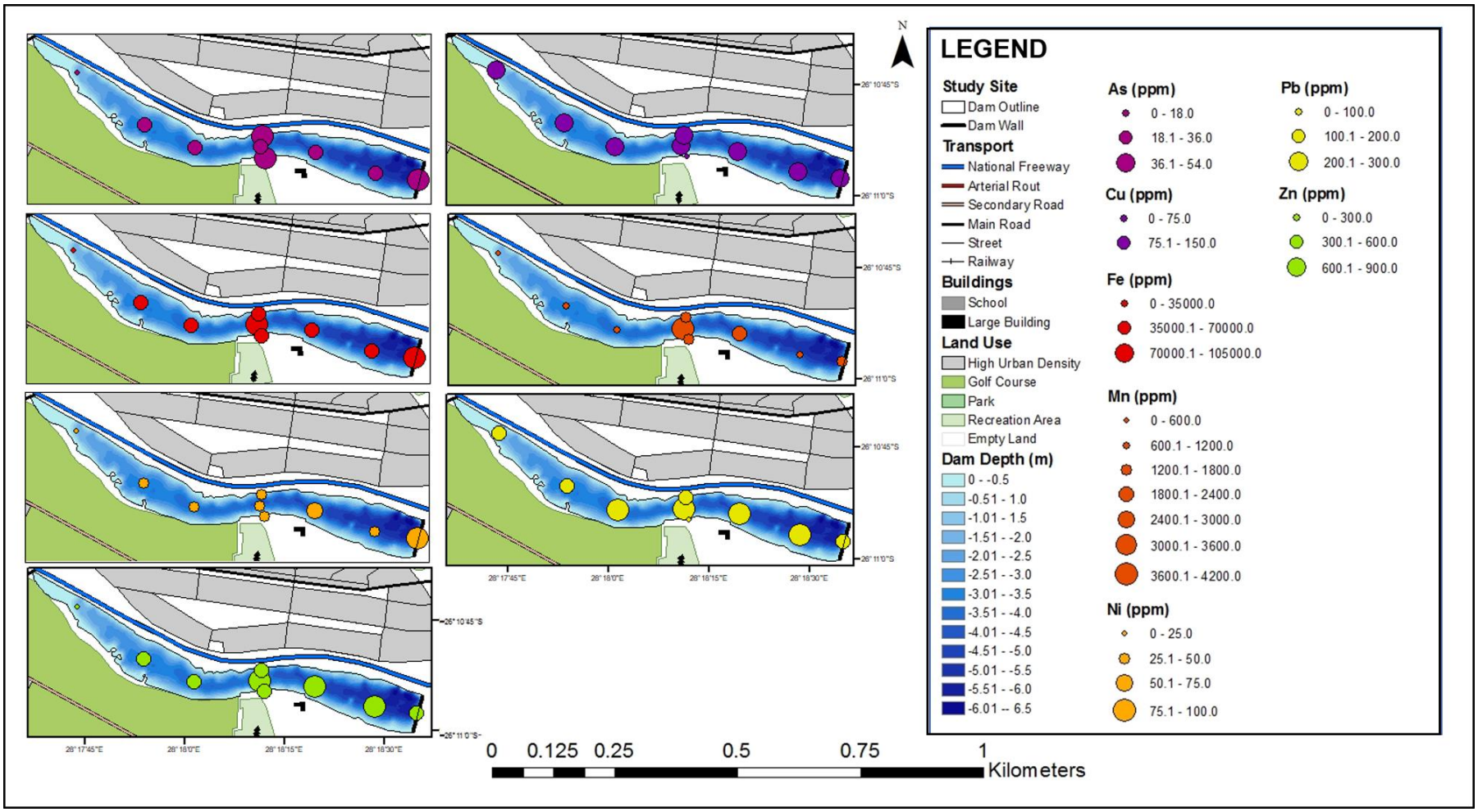


Figure 4.21: Spatial distribution of 7 trace metal concentrations across Middle Lake

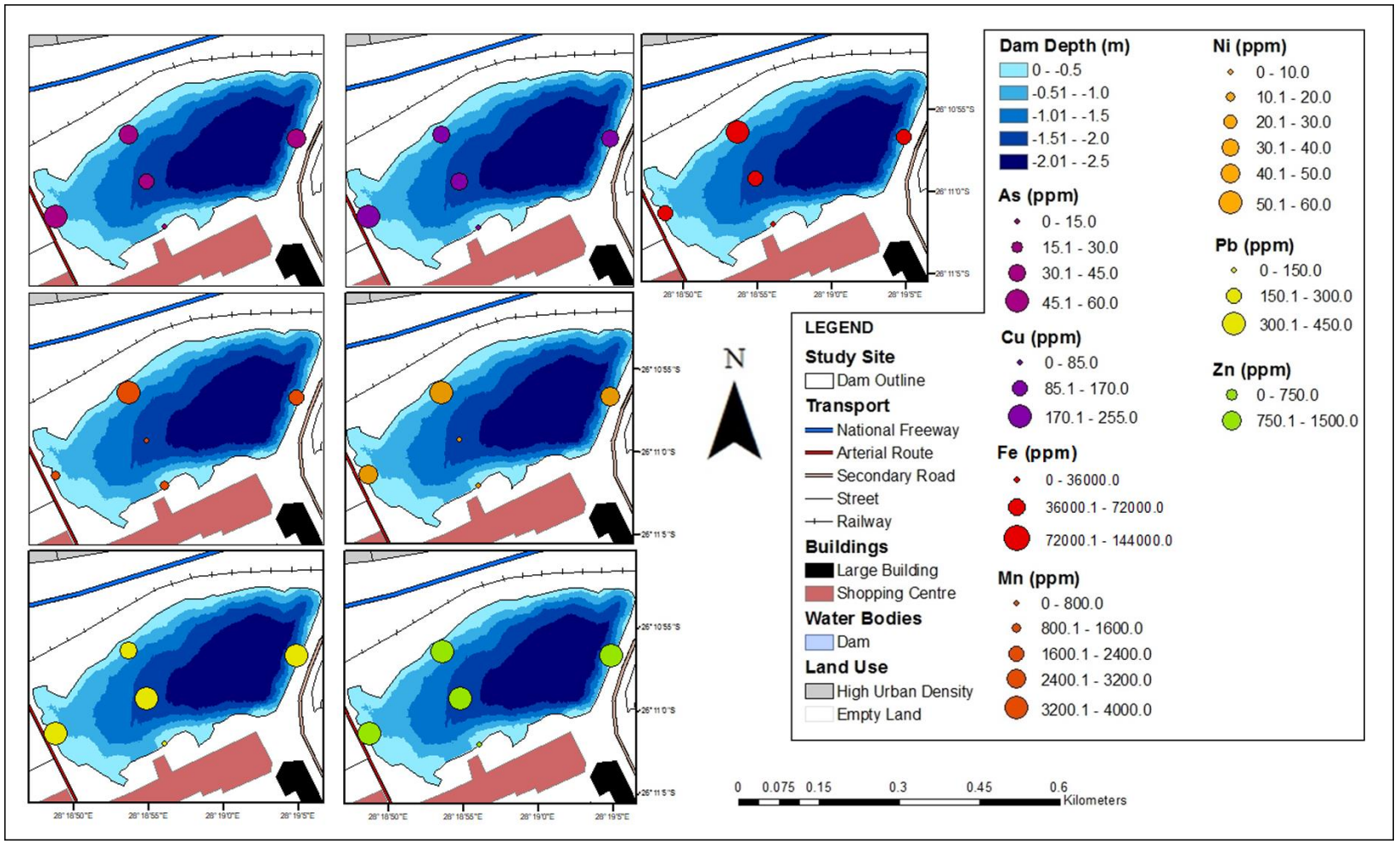


Figure 4.22: Spatial distribution of 7 trace metal concentrations across Civic Lake

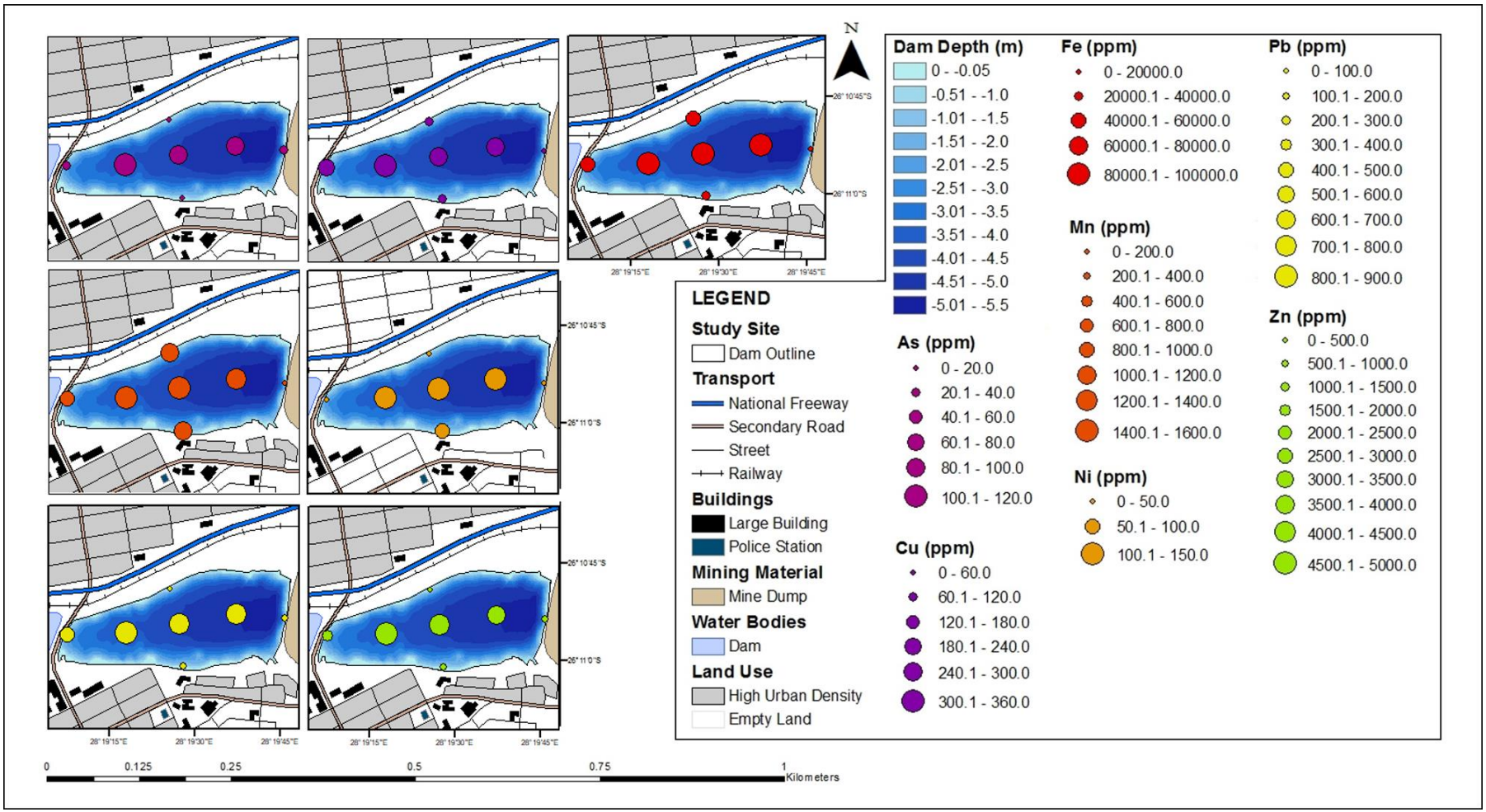


Figure 4.23: Spatial distribution of 7 trace metal concentrations across Kleinfontein Dam

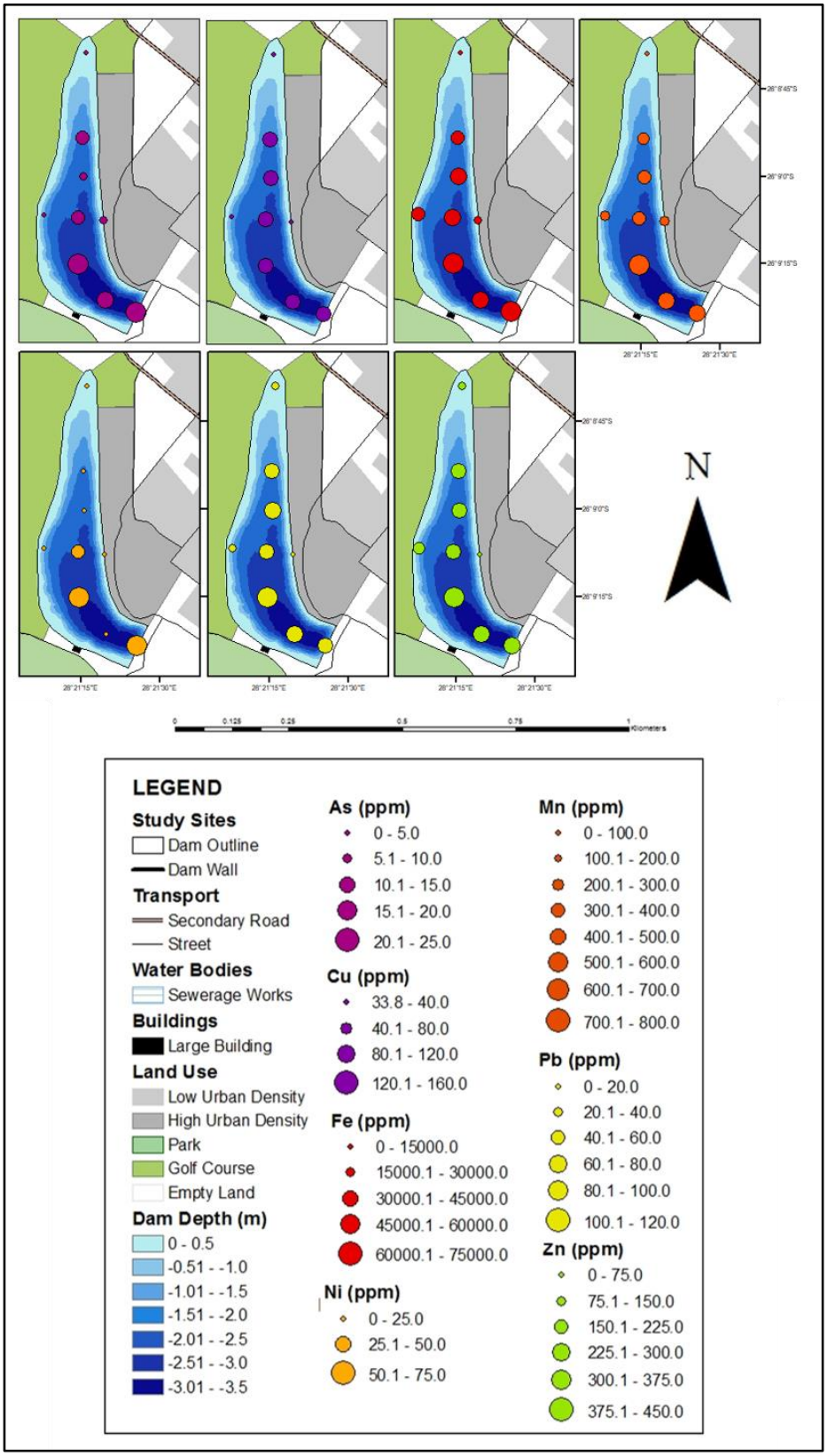


Figure 4.24: Spatial distribution of 7 trace metal concentrations across van Ryn Dam

4.6.3. Understanding Trace Element Distribution across the Region

The ANOVA was run for the means of each trace element from each site, to identify if there were any statistical differences or similarities between the various sites. Identifying the difference and similarities can give a greater understanding of the variation of trace elements across the entire region.

The ANOVA for the means of four trace elements, As (Fig. 4.25a), Cu (Fig. 4.25b), Ni (Fig. 4.25c), and Zn (Fig 4.25d), expressed very similar graphs, with two groups created, A and B. Only one site fell within group A, for all four trace elements, that site was Amata Pan. Therefore, it can be assumed that Amata Pan is statistically significantly different to all the other sites, for As, Cu, Ni, and Zn. Amata Pan also contained the greatest average concentrations for the mentioned trace elements.

Compared to this, the ANOVA for Ca was very different, with Bullfrog Pan having the greatest average compared to the other sites (Fig 4.26). The ANOVA created four groups for Ca (A, AB, BC, and C). These groups show that Bullfrog Pan, A, and Korsman Pan, AB, are not significantly different, but Bullfrog Pan is significantly different from every other site. Two sites, Homestead Dam and van Ryn Dam, both fell into group C, which makes them not significantly different to each other and all the sites in Group BC (Sandpan, Amata Pan, Kleinfontein Dam, Middle Lake, and Civic Lake), but significantly different to Korsman Pan. The sites that fall within groups AB and BC are also considered to not be significantly different from each other. The ANOVA also

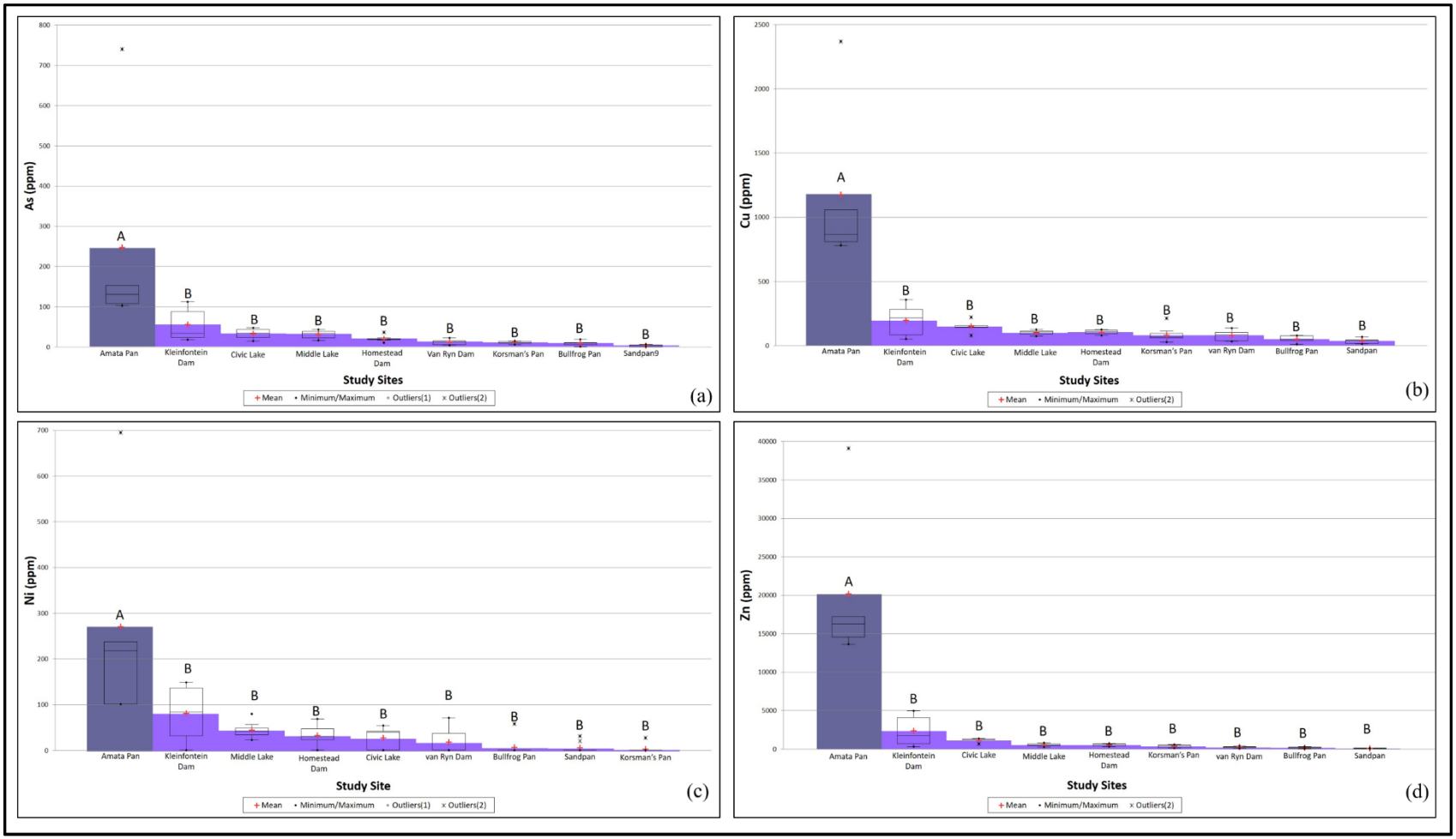


Figure 4.25: The ANOVA plot comparing each site to each other based on mean As (a), Cu (b), Ni (c), and Zn (d) concentrations.

represent an interesting pattern with a slight separation between pans and dams, with pans containing higher Ca concentration compared to dams, but some slight overlap between the two types of sites.

Five groups, A, B, BC, CD, and D were created when the ANOVA was run on the Cr means for each site (Fig. 4.27). Once again Amata Pan was the only site in group A, thus making it statistically significantly different from the other sites. Three sites, Civic Lake, Kleinfontein Dam, and Homestead Dam, all fall within group B and are not significantly different to each other or Middle lake, group BC, but significantly different to the sites that fall within groups CD and D. Korsman Pan, which falls within grouping CD, is not significantly different to the sites within groupings BC, which includes Middle Lake, and D, which includes van Ryn Dam, Sandpan and Bullfrog Pan (Fig. 4.27).

The ANOVA for the means of Fe (Fig. 4.28) for each site created four groups, A, B, BC, and C. Amata Pan contained the highest average concentrations of Fe, compared to all the other sites and thus the only site to fall into group A. this makes Amata Pan statistically different to each other site. Homestead Dam was the only site to be in group B, making it statistically different from the sites in grouping A, Amata Pan, and C, which includes Korsman Pan and Sandpan. The remaining five sites were all grouped in BC, making them not significantly different to Homestead Dam, Korsman Pan and Sandpan, but significantly different to Amata Pan (Fig. 4.28).

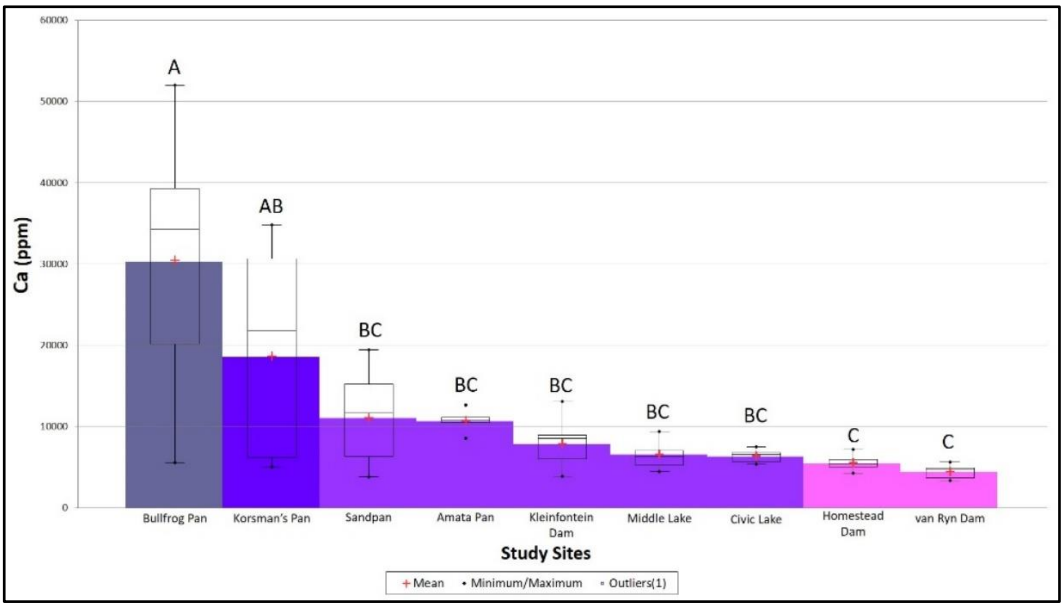


Figure 4.26: The ANOVA plot comparing each site to each other based on mean Ca concentrations.

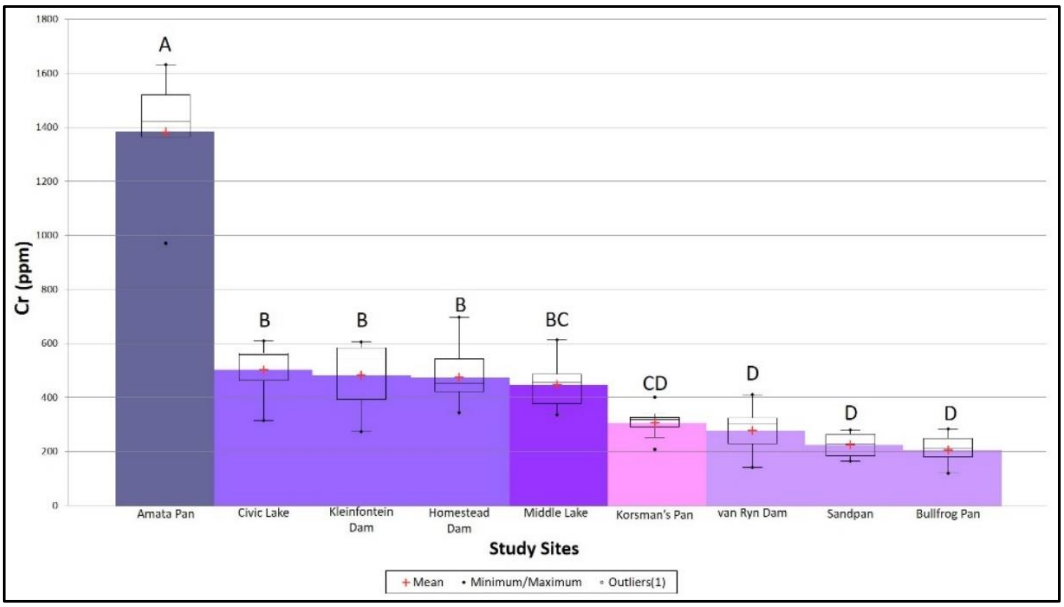


Figure 4.27: The ANOVA plot comparing each site to each other based on mean Cr concentrations.

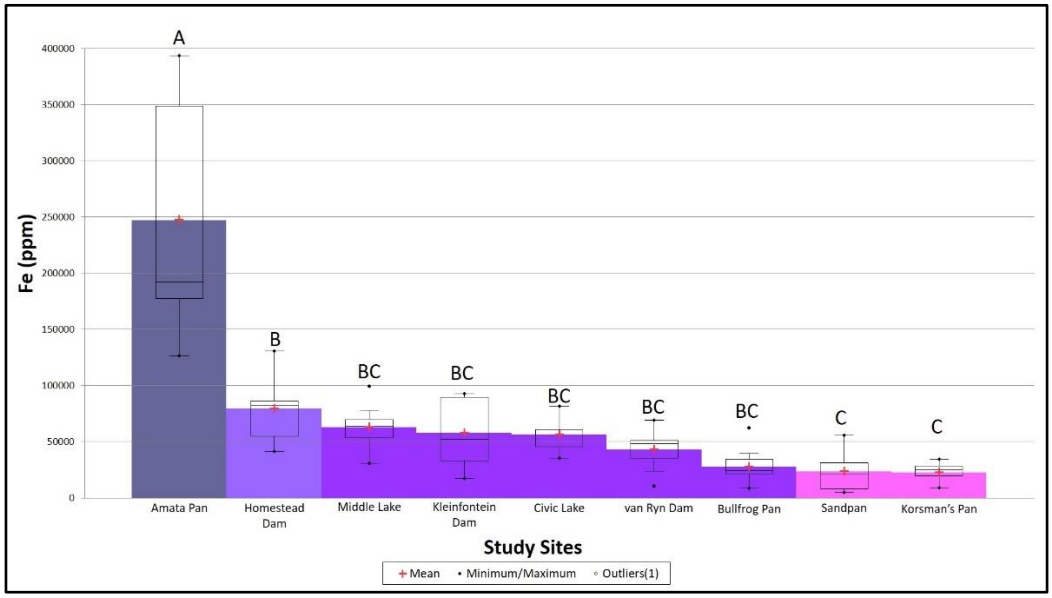


Figure 4.28: The ANOVA plot comparing each site to each other based on mean Fe concentrations.

Once again four groups, A, B, BC, and C, were identified in the ANOVA run on the K means of all sites (Fig. 4.29). There were two sites that fell within group A, Sandpan and Bullfrog Pan, one site in group B, van Ryn Dam, and three sites each in groups BC, which includes Korsman Pan, Kleinfontein Dam, and Civic Lake, and C, which includes Homestead Dam, Middle Lake and Amata Pan. Therefore, it could be said that Bullfrog Pan and Sandpan are significantly different from all the other sites while being not being significantly different from each other. van Ryn Dam, being in group B is still not significantly different to the sites that fell within group BC, while significantly different to the site that fell within groups A and C (Fig. 4.29).

The ANOVA conducted on the means for Mn for each site also produced four groups, A, B, BC, and C. Amata Pan (group A), Homestead Dam (group B), and van Ryn Dam (group C), are all significantly different to each other (Fig. 4.30). The remaining sites, Middle Lake, Civic Lake, Kleinfontein Dam, Bullfrog Pan,

Sandpan and Korsman Pan, which fall in groups BC, are all not significantly different to each other, as well as Homestead Dam and van Ryn Dam. It is noted that there was a decrease in the means, from upstream to downstream, for the four sites that fall on the same river gradient.

Once again, the ANOVA for Pb expressed four groups with similar sites in each group (Fig. 4.31). Amata Pan, A, was the outlier of all the means and was significantly different from the remaining groups. Kleinfontein Dam, B, and Sandpan, C, although significantly different to each other were not significantly different to all the sites that fell within group BC. Compared to ANOVA for Mn, there was an increase in means, from upstream to downstream, in the sites that fell on the same river gradient.

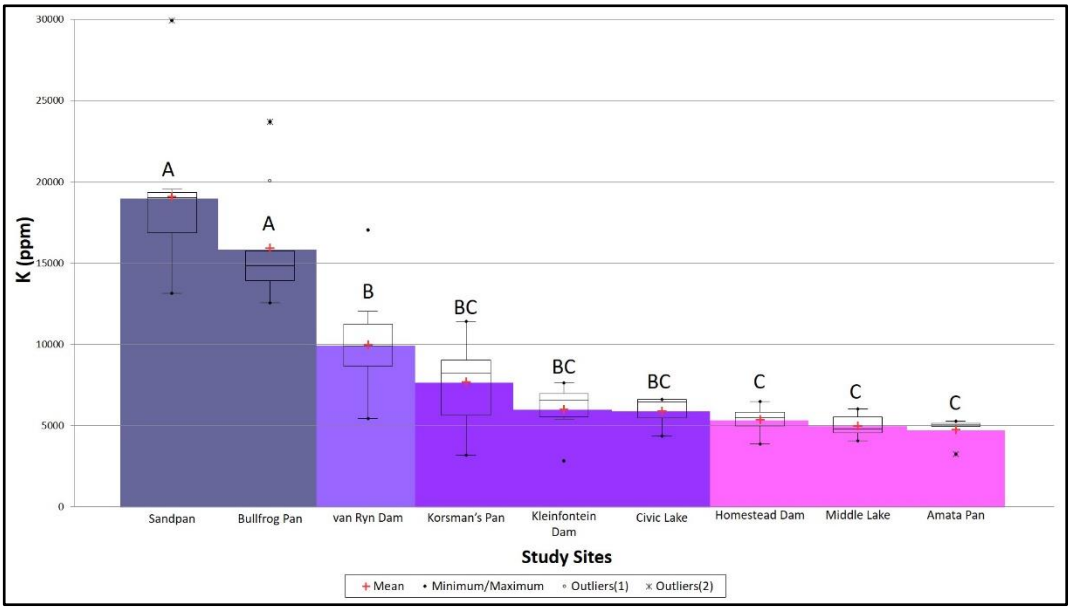


Figure 4.29: The ANOVA plot comparing each site to each other based on mean K concentrations.

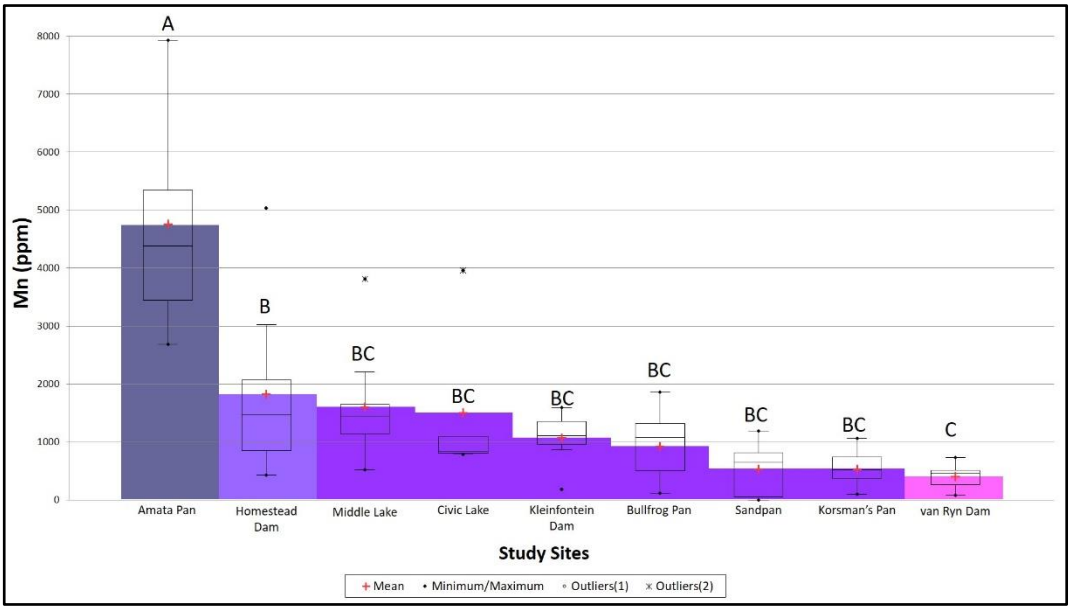


Figure 4.30: The ANOVA plot comparing each site to each other based on mean Mn concentrations.

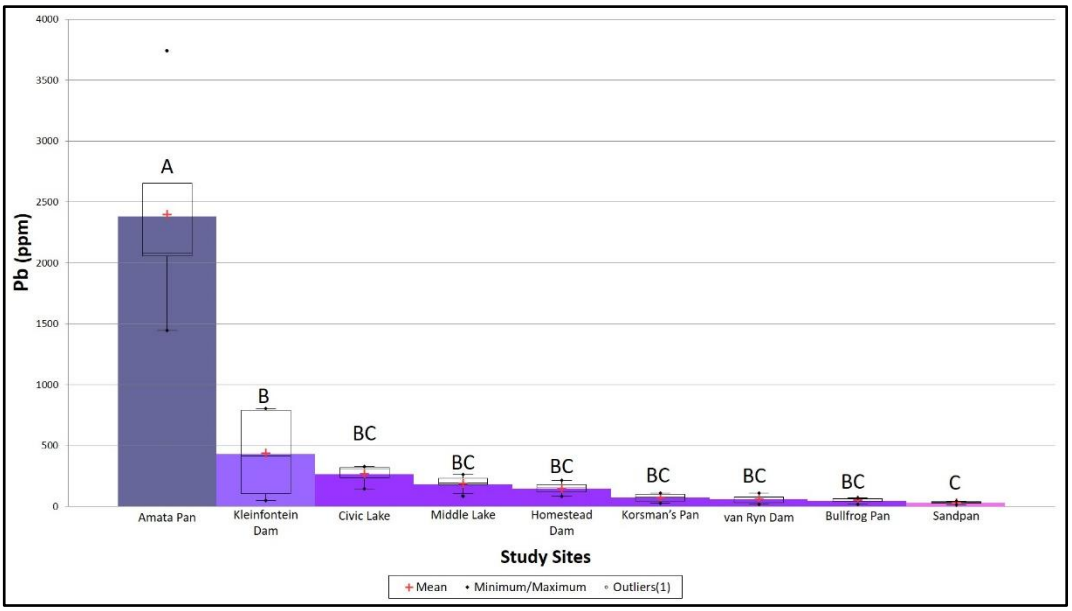


Figure 4.31: The ANOVA plot comparing each site to each other based on mean Pb concentrations.

Six groups, A, AB, BC, BCD, CD, and D were identified in the ANOVA of the S means of each site (Fig. 4.32). Amata Pan, A, is not significantly different to Kleinfontein Dam and Middle Lake (AB) but different from all the other sites. Civic Lake, however, fell into group BCD, making it the only site to not be significantly different to majority of the sites, that is, all the sites that fell within AB, BC, CD and D. One site fell within group BC and D each; these two sites include Korsman Pan and Sandpan respectively, and both sites are therefore significantly different to each other. The sites (Homestead Dam, Bullfrog Pan, and van Ryn Dam) that fall within group CD are significantly different from the three sites that fall within groups A and AB.

Only three groups, A, AB, and B were produced by the ANOVA run on the Ti means of each site (Fig. 4.33). Korsman Pan and van Ryn Dam, were the only two sites that fell within group AB, which means they are both not significantly different to each other and every other site. Sandpan, Bullfrog Pan, and Amata Pan make up group B, which are significantly different to Civic Lake, Homestead Dam, Middle Lake, and Kleinfontein Dam, which make up group A. There is a significant difference of means between the pans versus the dams.

The last ANOVA to be produced was for the V means of each site (Fig. 4.34). The ANOVA for the V means produced five categories, A, AB, ABC, BC, and C. Homestead Dam (group A) was significantly different to the sites that fell within categories BC (van Ryn Dam) and C (Korsman Pan, Sandpan and Bullfrog Pan). Three sites, group ABC, were not significantly different to all the other sites; these three sites include Civic Lake, Kleinfontein Dam and Amata Pan. There was also a

decrease in the mean concentrations for V, from upstream to downstream, within the sites that fell along the same river gradient.

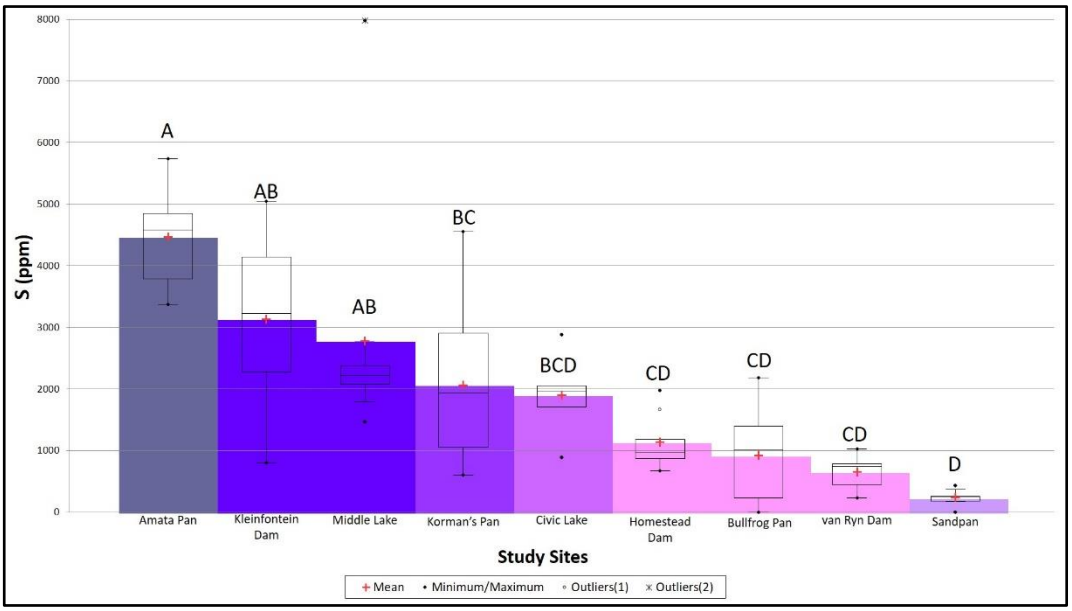


Figure 4.32: The ANOVA plot comparing each site to each other based on mean S concentrations.

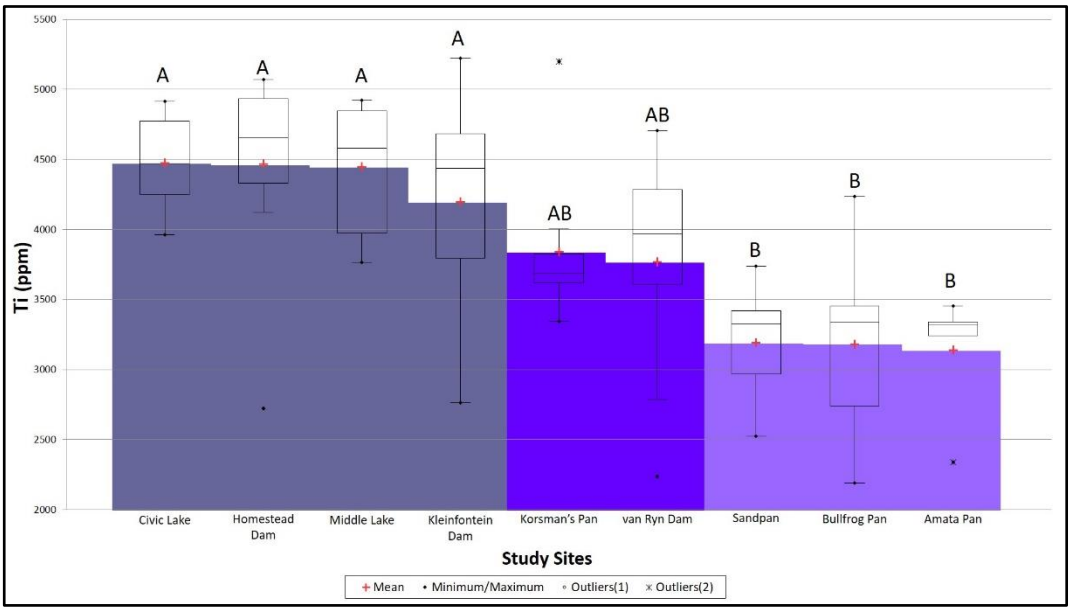


Figure 4.33: The ANOVA plot comparing each site to each other based on mean Ti concentrations

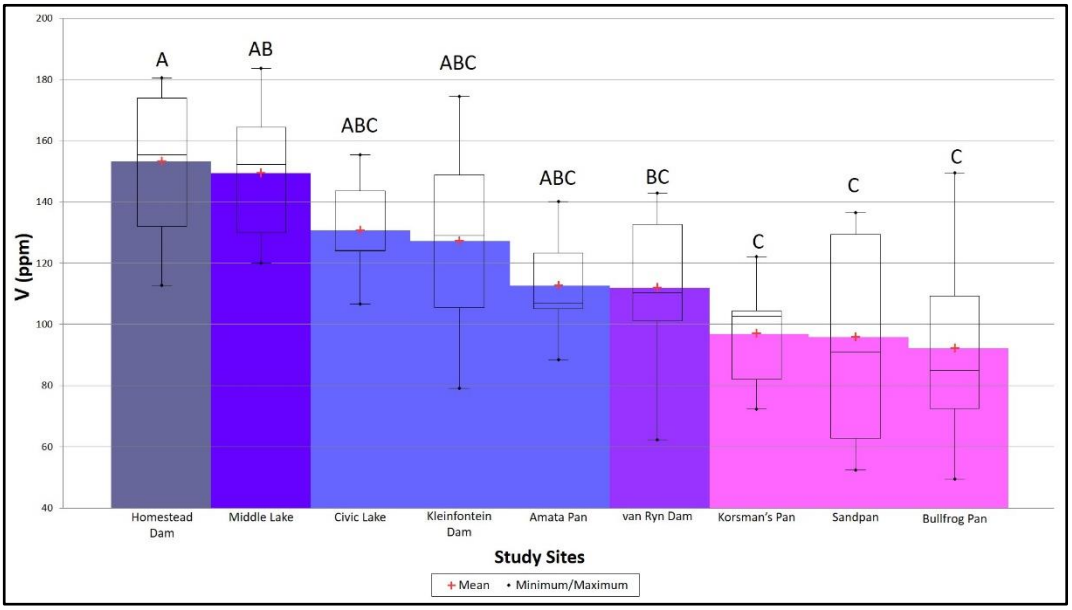


Figure 4.34: The ANOVA plot comparing each site to each other based on mean V concentrations

The ANOVA is a good way to see what is happening in the sediments of each site, across the entire area. It allowed for the identification of the difference between mean trace element concentrations in sediments at each site.

4.6.4. Relationships between varying Trace Elements

A correlation matrix was created to understand which trace elements were closely related to each other and which ones were not. In this case, a strong positive correlation meant that there was a relationship between the two metals, and subsequently they both either always occurred together or increased together. Comparatively, a negative correlation meant that there was the opposite form of relationship between the two metals. In this case, a negative correlation meant that when one trace element increased, then the other decreased, and vice versa. The correlation will aid in identifying which trace elements occur together and further what types of suite of trace elements exist in each individual site. Identifying suites

of pollutants that occur together will be used to further identify the possible anthropogenic or natural sources of trace elements to each individual site. A correlation matrix was conducted for the entire study area, as well as each site. This would give a good understanding of the main sources of trace elements to the entire region, as well as identify the direct local sources of each site. The same forms of contamination may not influence all the sites.

Across the entire region, a strong to an extremely strong positive correlation between As, Cr, Cu, Fe, Mn, Ni, Pb, S, and Zn could be identified (Fig. 4.35). There was also a moderate positive correlation between Ti and V across the entire region. These positive correlations indicate that these metals are heavily related and when one tends to increase then so do the others. This also suggests the possibility of a common source of trace elements across all the sites in the area. This strong correlation does not necessarily occur in each site, and only gives a general understanding as to what is happening over the area.

Each individual site is susceptible to some form of direct local sources of trace elements, and thus it is important to take account of the possible variation that might arise. Once again identifying which trace elements are related to each other at each site, allows for the identification of the possible sources of trace elements and to identify if each site is uniformly impacted across the entire area.

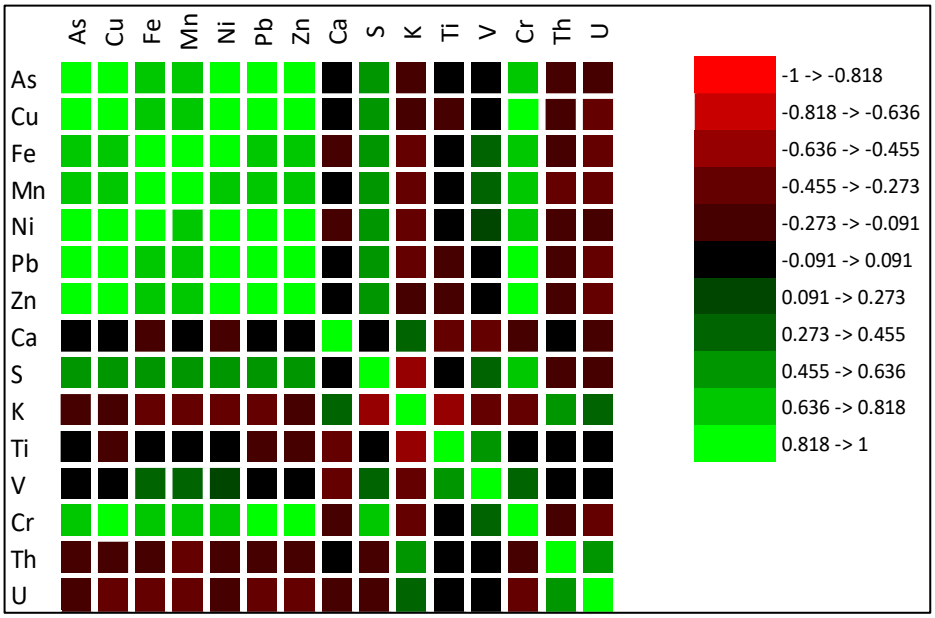


Figure 4.35: An image representation of the correlations matric for trace element concentrations from sediment samples across the entire region

Trace Elements in Pans

At Amata Pan, Fe had a strong negative correlation with Ca, K, Ti, V, and Cr (Fig. 4.36a). This indicates that an increase in Fe concentration can be associated with a decrease in concentrations of Ca, Cr, K, Ti, and V. Mn and V were also negatively correlated. Compared to this As, Cu, Mn, Ni, Pb, S, and Zn were all positively correlated to each other. There was also a strong positive correlation between Fe, Mn and Ni. All the trace elements and ions that had a strong negative correlation with Fe contained a strong positive correlation between each other.

There were slight differences in which trace elements were correlated at Bullfrog Pan (Fig. 4.36b). A strong positive correlation was identified between As, Cu, Mn, Pb, Zn, Ca, S and Cr. Cu was also strongly correlated with Fe, Ti, and V, while Fe was positively correlated with Ni, V, and Cr. Compared to the overall area, where Pb and Ni were positively correlated, at this site they were negatively correlated

(4.36b). At Bullfrog Pan, K was negatively correlated to every other trace element, with a strong correlation between As, Ca, Cr, Cu, Fe, Mn, S, V, and Zn. This negative correlation between K and all the other trace elements is similar, although not as strong, to what is taking place across the entire area

At Korsman Pan there was once again very little variation in trace elements that were positively correlated with each other (Fig. 4.36c). The following trace elements, As, Fe, Mn, Pb, V, and Zn, were strongly correlated to each other, while Fe and Cu were also strongly correlated. One of the main differences to the overall study area was that at this site K was not negatively correlated to every other trace element. At Korsman, K had a strong positive correlation with Ca, Mn and Pb. The only strong negative correlation at Korsman Pan was between Ti and Pb, and Ti and S (Fig 4.36c). The last of the four pans, Sandpan, had a very different correlation matrix to the other pans and the overall study area.

Once again at the Sandpan (Fig 4.36d), there was a strong positive correlation between As, Cu, Fe, Mn, Zn, and Ca. Fe and Ni were both strongly positively correlated to each other, whereas Ni had a strong negative correlation with S. The main difference at this site was the strong correlation of V and Cr with Cu, Fe, Mn, Pb, S, and, Zn. This expresses a major difference to the correlation matrix for the entire area, where V was strongly correlated with Ti. This provides significant evidence of something different taking place at this site. The difference in matrices across the pans can also be seen in those for the dams.

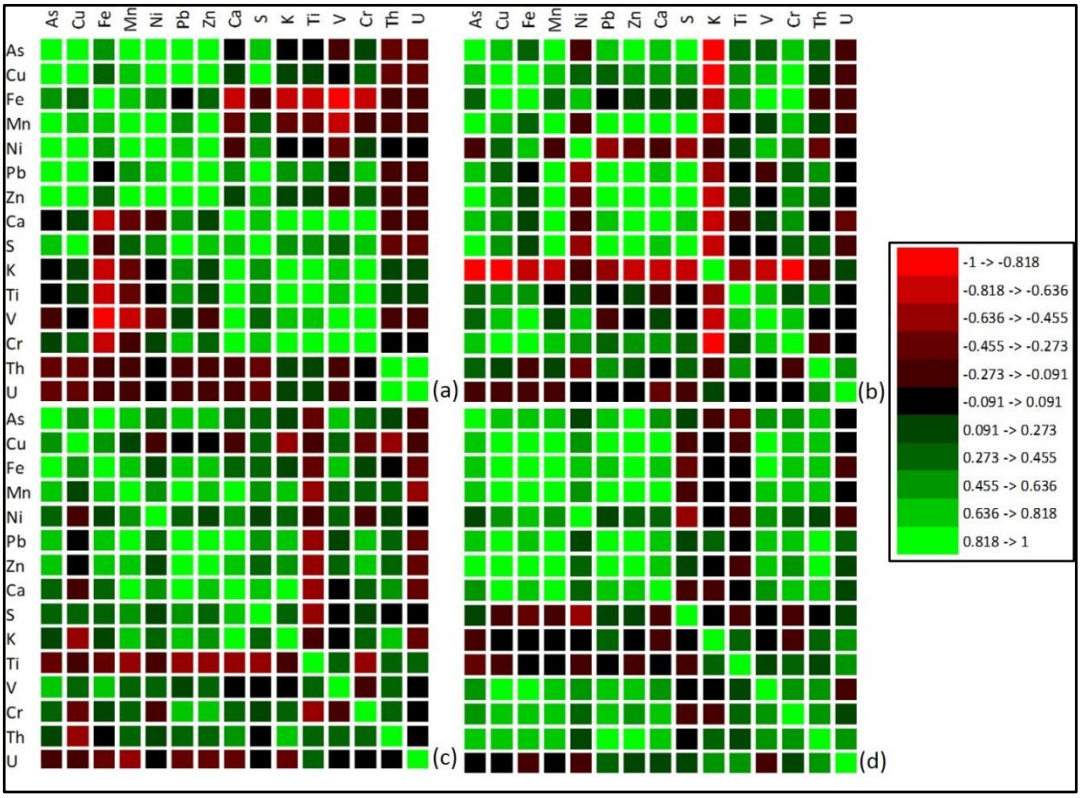


Figure 4.36: An image representation of multiple correlation matrices for trace element concentrations from across the four pans (a. Amata Pan; b. Bullfrog Pan; c. Korsman Pan; d. Sandpan)

Trace Element in Dams

There were five dams studied for this research and each one had a particularly different correlation matrix to the other, with some expressing similarities to the correlation matrix for the entire area. The first dam to be looked at is Homestead Dam (Fig. 4.38a). At Homestead there was a strong positive correlation between As, Cu, Fe, and Ni, while Cu and Fe were also strongly correlated with K and V. The only strong negatively correlated trace elements were Mn, Pb, Ca and K. Compared to this the correlation matrix of Middle Lake is slightly different, which is unusual considering the sites fall along the same river gradient.

At Middle Lake (Fig 4.37b), As had a strong positive correlation with Fe and Cr only, but strong negative correlation with Ti. Compared to this Fe was strongly correlated with As, Ni, S, V and Cr but also negatively correlated with Ti. There was also a strong positive correlation between Cu, Mn, Zn, K, and V. The next dam along this gradient once again contained a very different correlation matrix to the sites that came before it.

At Civic Lake there was a strong positive correlation between As and Cu, Fe, Ni, Zn, S, V, and Cr (Fig 4.37c). Fe and Ni also had a strong positive correlation with Mn. There was a positive correlation between Pb, and Cu, Zn, S, K, Ti and Cr, with the correlation with other AMD trace elements not being strongly correlated. Across the entire river gradient that the three sites mentioned follow, there appears to be a pattern of a relationship between As, Fe, and Ni, with a positive relationship with S, V, and Cr at both Civic and Middle Lake.

The last site to fall along the river gradient is Kleinfontein Dam (Fig. 4.37d). The data is expected to support strong trace element influence from mine dumps, as this site falls right on the edge of a major mine dump. Once again at this site there was no strong negative correlation between any of the trace elements but once again at this site there was a strong positive correlation between As, Cu, Fe, Mn, Ni, Pb, Zn, S, K, and V. There was also a strong positive correlation of Cr with Cu, Fe, Pb, Zn, K, Ti, and V. Ti was also strongly correlated with Fe, Mn, and V.

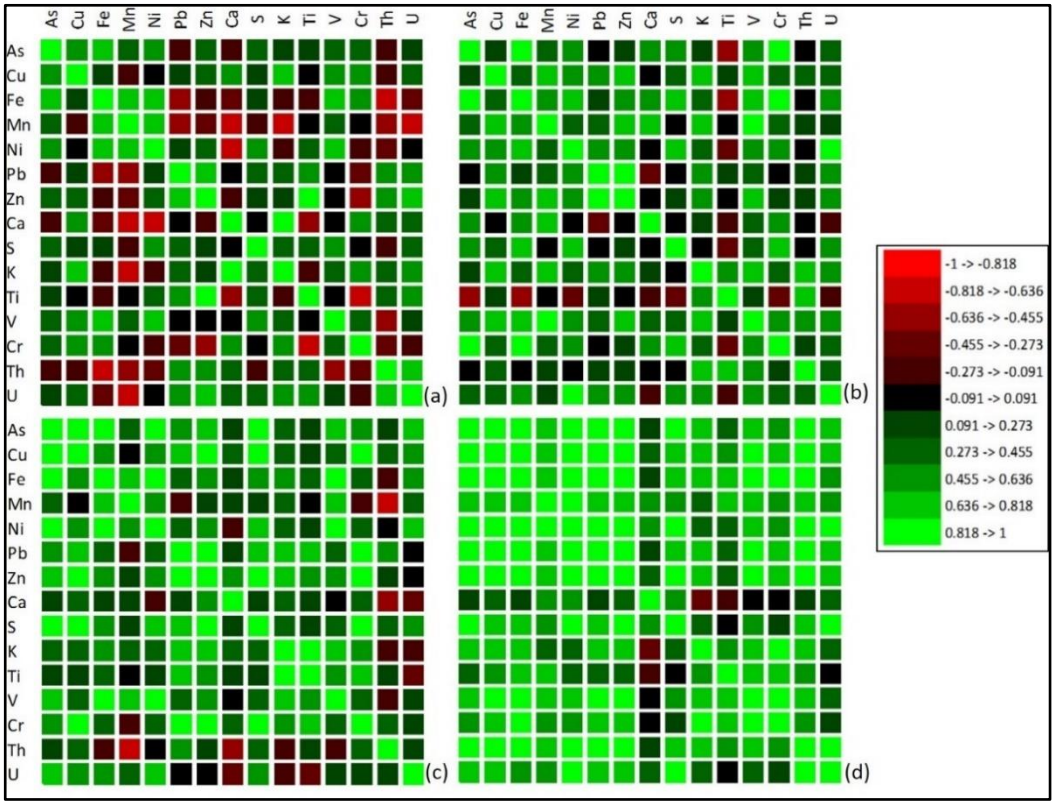


Figure 4.37: Image representation of the correlation matrix done for the relationship between trace elements analysed from various sediment samples for the four dams that fall along the same river gradient
(a. Homestead Dam; b. Middle Lake; c. Civic Lake; d. Kleinfontein Dam)

Across all four sites along the river gradient, there is a pattern of correlation that appears to emerge, with weaker positive correlations between trace elements occurring at Homestead Dam, and a stronger positive correlation between trace elements occurring at Kleinfontein Dam. Overall the strength of the correlation amongst trace elements such as As, Cu, Fe, Mn, Ni, Pb, and Zn, as well as ions such as Ca and S, tend to increase towards the bottom of the gradient. This could suggest that two possible processes are taking place, the homogenization of trace elements, thus reducing spatial variability or the effect of local sources. It could also indicate the possible overwhelming influence of the mine dump situated right at Kleinfontein Dam influencing the samples at the site.

The fifth and only dam not along the same river gradient was van Ryn Dam (Fig 4.38). Once again, this site did not have any trace elements that had a strong negative correlation with each other. Once again at this site, there were strong positive correlations between As, Cu, Fe, Mn, Ni, Pb, Zn, Ca, S, V, and Cr. V also had a strong positive correlation with Ti. Identifying the relationship between the trace elements identified in this study allows us to identify the possible sources to not only the entire area but to each site. In order to identify the level of pollution at each site, *Igeo* was applied to each trace element for each sample.

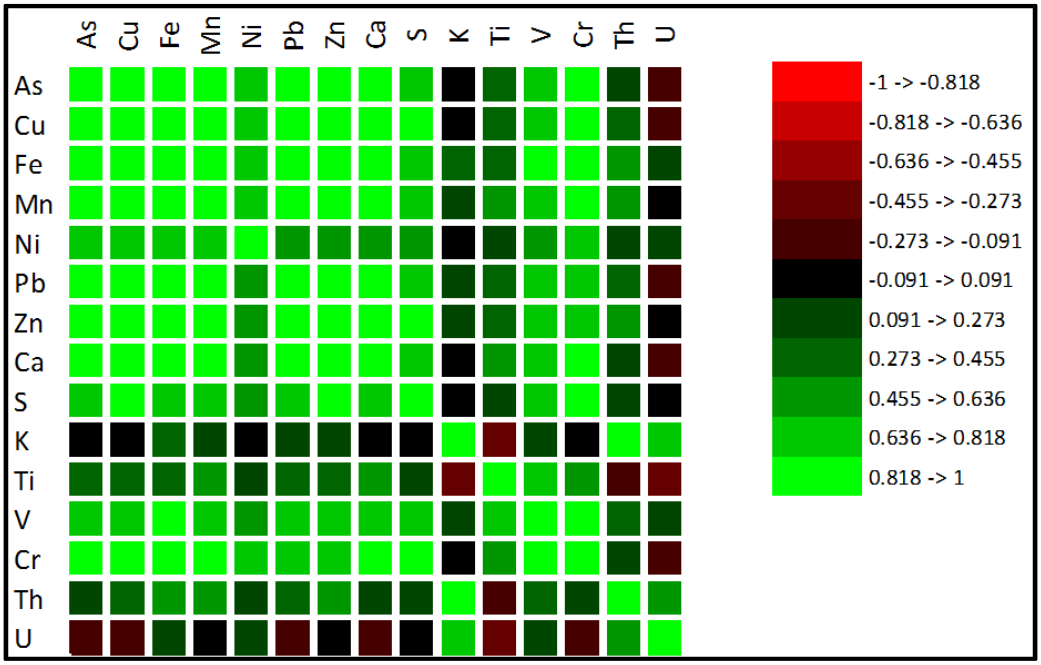


Figure 4.38: Image representation of the correlation matrix for the relationship between trace elements identified in sediments at van Ryn Dam

4.6.5. Trace Element Pollution and Toxicity

Sediment Quality Guidelines

The average trace element concentrations (Table 4.4) from each site were compared to the SQG where applicable. Of the seven trace elements recognised by the SQG

(Table 3.4), five (As, Cr, Cu, Pb, and Zn) were identified to be well over their respective PEC values at particulate sites. When compared to the SQG, average As concentrations at both Amata Pan and Kleinfontein Dam were above the PEC values. Average Cu concentrations at Amata Pan, Civic Lake, and Kleinfontein Dam were also identified to be above the recommended SQG PEC. For Amata Pan, Homestead Dam, Middle Lake, Civic Lake and Kleinfontein the average concentrations for Pb and Zn were well above the recommended SQG PEC, while all the sites in the region contained average concentrations of Cr that were well above the recommended PECs recommended by MacDonald *et al.* (2000).

GeoAccumulation Index

The *Igeo* was calculated to identify any forms of trace element pollution; this was done by comparing the trace element concentrations identified in the samples to the average background value for each trace element. The index was applied to each sample for the following trace elements; As, Co, Cr, Cu, Fe, K, Mn, Ni, Pb, S, Th, Ti, V, U, and Zn. All sites, except the Sandpan, contained some form of Zn contamination, with the two most contaminated sites being Amata Pan and Kleinfontein Dam (Table 4.6 – Table 4.8). Individually each pan expressed various forms of trace element contamination.

Compared to the other sites, Korsman Pan only contained very low levels of Ca, Pb, and Zn contamination (Table 4.7). All samples contained Ca, Pb, and Zn pollution. The samples that contained the most forms of contamination were KPX3 and KPY3. Other forms of contamination found in this site include Cu, S, and Ti. All samples contained moderate to high levels of Ti pollution.

Amata Pan came across as the most contaminated pan. Across the entire site, sediments were extremely polluted with both, Pb and Zn, with sample APY1 containing the highest concentrations. Following this, sample APY1 was also extremely contaminated with both, As and Cu. Several samples were contained high forms of Cu contamination, as well as containing low to moderate levels of As, Cr, Fe, Mn, and Ni contamination (Table 4.7). Once again, every sample contained a level of Ti pollution, one sample expressed a low level of contamination, while the rest all expressed moderate levels of contamination.

Contamination at Bullfrog Pan was not nearly as severe as Amata Pan. Contamination varied between samples, with five samples containing some form of Pb pollution and/or Zn pollution. The rest of the samples either contained very low levels of contaminations or were uncontaminated with trace elements. Moderate levels of Ti contamination can be identified across the entire site, with very low to low levels of Th being identified as well.

The fourth pan, Sandpan, also contained very little evidence of trace element pollution (Table 4.7). The only notable form of contamination was moderate levels of Ti pollution. Once again, this site also contained Cr, Pb, and Th pollution, although not as high as the other sites. The Sandpan was the only site that did not contain some form of Zn contamination. The natural pans, apart from Amata, were not found to contain any levels of pollution above moderately contaminated (Table 4.7). This could possibly be due to their locations relative to the mine tailings dams and the lack of surface water sources. Compared to this the sites classified as dams

were comparatively slightly more polluted, the only exception to this being Amata Pan.

Comparatively, slightly greater levels of trace element contamination could be found in the dams (Table 4.8), when compared to the pans (Table 4.7). All the dams contained the same types of trace element contaminants, while Middle Lake and Kleinfontein Dam contained some form of S contamination. Four of the five dams studied in this research were found to be situated along the same river system and thus there was expected to be a slight gradient in the trace element contamination of the sites.

The first site along this gradient was Homestead Dam (Table 4.8). All samples at this site contained very low levels of Ca and Cu contamination. High levels of Pb contamination were identified in six of the nine samples, with the other three expressing moderate levels. The site contained moderate to high levels of Ti pollution as well. Following this, the site also contained low to moderate levels of Zn contamination. The least contaminated sample at this site was HDY2, which only contained Ca, Cu, Pb, Ti, and Zn, contamination.

The next site along the river gradient is Middle Lake (Table 4.8). The entire site contained very low levels of As, Ca, and Cu contamination while the greatest forms of trace element pollution came in the form of Pb and Ti, followed by Zn. This site contained an increase in Pb pollution, with seven samples being highly polluted, and two samples being moderately polluted (Table 4.8). Across Middle Lake, moderate to high levels of Ti contamination can also be identified. The number of samples that contained moderate Zn contaminations dropped to four in this site

when compared to Homestead Dam. This, however, does not mean there is an overall decrease across all four sites along the gradient. Only one sample, MLC, contained some form of S contamination. The next site to fall along the river gradient was Civil Lake (Table 4.8). At this site, a considerable increase in Pb and Zn contamination was noted in the samples, with the range being from moderate to high levels of trace element contamination, Followed by moderate levels of Ti pollution (Table 4.8). Low levels of Cu were identified, followed by very low levels of Ca pollution across the majority of the lake.

The last site along the river gradient and the one that is situated on the very edge of one of the larger mine dumps in the area is Kleinfontein Dam (Table 4.9). This site contained more varied levels of Pb and Zn pollution. Three samples (KDC, KDX2, and KDX3), from Kleinfontein dam, contained extreme levels of Pb pollution, followed by KDX1 which was heavily polluted with Pb contamination. Samples KDC and KDX3 were also heavily contaminated with Zn while KDX1 contained high levels of Zn contamination. The site also contained moderate levels of As, Ca, Cu, and Ti contamination. The increase in trace element pollution at all four dams, represents a gradient of contamination, starting at Homestead and increasing towards Kleinfontein Dam.

The final dam in this study, van Ryn Dam (Table 4.9), expressed low levels of trace element contamination, and thus was considered one of the more unpolluted sites. Only two samples from the site contained high levels of Ti pollution. Of all the dams, van Ryn contained the lowest levels of Pb contamination (from very low to

moderate). Other forms of contaminations, which were all very low, include As, Ca, Cu, and Zn.

Table 4.7: The Igeo values, based on the trace element concentrations identified in each individual sample for all the sites considered as pans. The Igeo values are subsequently colour coded to easily identify pollution extremes and to contrast with unpolluted samples (The key to the colour coding can be identified in Table 3.3

Site	Sample	Igeo														
		As[1]	Ca[2]	Cr[2]	Cu[1]	Fe[2]	K[2]	Mn[2]	Ni[2]	Pb[2]	S[1]	Th[2]	Ti[2]	U[2]	V[2]	Zn[1]
Korsmans	KPC	-0.50	2.85	-1.81	0.53	-2.35	-0.80	-2.69	-10.09	2.62	-0.73	0.64	2.70	-2.58	-1.12	2.02
	KPX1	-1.70	0.51	-1.83	-1.26	-4.19	-1.82	-6.05	-10.09	1.26	-1.77	-0.48	2.64	0.98	-1.63	0.31
	KPX2	-1.05	2.33	-1.84	-0.17	-3.08	-1.24	-3.66	-10.09	2.17	-1.02	0.06	2.62	-2.58	-1.45	1.47
	KPX3	-0.51	3.01	-1.97	0.05	-2.55	-0.92	-2.85	-4.32	2.52	-0.31	0.40	2.62	0.93	-0.94	1.85
	KPX4	-0.76	0.62	-2.47	1.65	-2.62	-2.65	-4.21	-10.09	1.31	-0.29	-1.29	2.67	0.86	-1.11	0.32
	KPY1	-1.36	0.52	-2.18	-1.21	-4.23	-1.32	-5.84	-10.09	0.65	-2.56	0.71	3.14	1.54	-1.13	-0.31
	KPY2	-1.00	2.56	-1.93	-0.01	-3.07	-1.28	-3.71	-10.09	2.27	-0.90	0.01	2.56	0.95	-1.52	1.61
	KPY3	-0.52	2.82	-1.51	0.11	-2.73	-1.14	-3.21	-10.09	2.61	0.34	0.49	2.50	1.41	-1.30	1.89
	KPY4	-0.37	0.22	-1.75	0.78	-2.27	-2.10	-4.16	-10.09	2.17	-2.58	0.10	2.76	0.89	-0.88	1.93
Amata Pan	APC	2.47	1.27	0.25	3.59	0.21	-1.98	-0.65	-1.20	6.88	0.07	2.26	2.50	1.67	-1.07	6.84
	APX1	2.75	1.54	0.51	3.97	-0.40	-1.92	-1.35	-2.43	7.23	0.43	-4.04	2.55	-2.58	-0.68	6.92
	APX2	2.40	1.36	0.32	3.68	0.09	-1.96	-0.99	-2.43	6.86	0.35	-4.04	2.49	-2.58	-0.87	6.58
	APY1	5.25	1.32	0.41	5.13	1.07	-2.01	0.21	0.35	7.72	0.67	-4.04	2.46	-2.58	-1.10	8.10
	APY2	2.97	0.98	-0.24	3.53	1.24	-2.63	-0.36	-1.33	6.35	-0.10	-4.04	1.98	-2.58	-1.35	6.67
Bullfrog Pan	BFPC	-0.95	3.06	-2.49	-0.38	-2.53	-0.34	-2.49	-10.09	1.82	-1.84	1.35	2.52	2.99	-1.04	0.72
	BFPX1	-2.05	0.35	-3.20	-1.34	-4.03	0.01	-5.87	-10.09	1.18	-3.99	1.40	2.55	3.67	-1.64	-0.34
	BFPX2	-0.76	3.18	-2.20	-0.50	-2.92	-0.43	-2.38	-10.09	2.04	-1.37	0.71	2.21	3.03	-1.63	1.01
	BFPX3	-1.57	2.42	-2.66	-0.68	-2.96	-0.38	-3.46	-10.09	1.15	-2.45	0.77	2.50	-2.58	-1.40	-0.11
	BFPX4	-0.48	2.98	-2.42	0.24	-2.27	-0.60	-2.67	-10.09	1.88	-1.28	1.30	2.84	-2.58	-1.00	0.90
	BFPY1	-5.29	1.95	-3.27	-2.41	-4.27	0.25	-5.47	-10.09	0.56	-4.42	0.01	1.89	-2.58	-2.18	-1.21
	BFPY2	-0.82	3.59	-2.28	-0.16	-2.78	-0.52	-2.23	-10.09	1.95	-1.68	0.86	2.17	1.20	-1.49	0.87
	BFPY3	-0.05	3.43	-2.21	0.18	-2.07	-0.67	-1.89	-10.09	1.95	-0.72	0.83	2.37	1.45	-1.16	1.23
	BFPY4	-1.61	2.22	-2.01	0.21	-1.42	-0.50	-3.76	-3.23	0.15	-12.81	0.24	2.59	2.27	-0.59	-0.78
Sandpan	SPC	-1.96	1.62	-2.03	-0.22	-2.09	-0.07	-3.08	-10.09	1.31	-3.28	1.44	2.53	2.51	-0.73	-0.12
	SPX1	-5.29	-0.20	-2.64	-2.01	-4.38	0.59	-7.00	-10.09	0.81	-3.94	1.17	2.57	3.37	-1.84	-1.48
	SPX2	-2.02	2.17	-2.11	-0.62	-3.12	-0.24	-2.98	-10.09	1.13	-3.80	1.53	2.41	3.41	-1.51	-0.53
	SPX3	-1.57	2.02	-2.09	0.00	-1.58	-0.06	-2.53	-4.12	1.21	-12.81	1.51	2.33	2.18	-0.80	-0.07
	SPX4	-5.29	0.55	-2.81	-2.15	-4.78	-0.60	-6.94	-10.09	-0.13	-4.05	-0.25	2.10	-2.58	-2.10	-2.39
	SPY1	-1.54	0.74	-2.67	-0.73	-2.96	-0.09	-4.20	-10.09	0.99	-3.07	1.39	2.20	2.47	-1.31	-0.31
	SPY2	-2.14	1.81	-2.25	-0.58	-2.42	-0.04	-3.07	-10.09	1.14	-4.33	1.51	2.53	2.25	-0.87	-0.65
	SPY3	-5.29	1.43	-2.36	-0.72	-2.42	-0.03	-3.41	-4.72	0.71	-3.80	0.89	2.49	2.31	-0.72	-0.87
	SPY4	-5.29	0.25	-2.32	-2.19	-5.07	-0.32	-13.74	-10.09	-0.15	-4.41	0.46	2.66	2.74	-2.06	-2.52

1 = Background data based on values from Turekian (1974) 2=Background data based on values from Wronkiewicz and Condie (1987)

Table 4.8: The *Igeo* values, based on the trace element concentrations identified in each individual sample for three sites considered as dams, Homestead Dam, Middle Lake, and Civic Lake. The *Igeo* values are subsequently colour coded to easily identify pollution extremes and to contrast with unpolluted samples (The key to the colour coding can be identified in Table 3.3)

Site	Sample	Igeo														
		As[1]	Ca[2]	Cr[2]	Cu[1]	Fe[2]	K[2]	Mn[2]	Ni[2]	Pb[2]	S[1]	Th[2]	Ti[2]	U[2]	V[2]	Zn[1]
Homestead Dam	HDC	0.90	0.20	-1.05	0.84	-0.35	-1.86	-1.18	-2.98	3.11	-1.61	-0.35	3.08	1.98	-0.36	2.37
	HDX1	-0.05	0.73	-0.71	0.83	-0.94	-1.62	-3.00	-10.09	2.73	-2.43	-0.76	2.20	0.86	-0.53	1.14
	HDX2	0.02	0.56	-1.44	0.69	-2.00	-1.78	-4.01	-10.09	3.01	-2.06	0.65	3.10	2.32	-0.77	2.22
	HDX3	-0.92	0.36	-1.74	0.49	-1.89	-1.87	-3.25	-4.15	3.51	-1.93	0.54	3.06	2.19	-0.61	2.25
	HDX4	-0.12	0.22	-1.72	0.58	-1.61	-2.00	-2.16	-4.19	3.61	-1.90	0.06	2.98	0.94	-0.77	2.13
	HDY1	-0.01	0.22	-1.28	0.22	-1.28	-2.30	-1.73	-4.53	2.55	-1.63	-0.69	2.80	0.64	-0.99	1.50
	HDY2	-0.16	-0.02	-1.37	0.46	-0.43	-2.37	-0.45	-3.37	2.25	-2.17	-4.04	2.87	-2.58	-0.39	1.39
	HDZ1	0.11	0.46	-1.08	0.70	-0.98	-1.64	-2.22	-3.53	3.35	-0.87	-0.35	2.97	1.87	-0.32	1.84
	HDZ2	0.22	0.33	-1.33	0.90	-1.02	-1.82	-2.42	-3.65	3.22	-1.11	-4.04	3.00	1.88	-0.37	2.17
Middle Lake	MLC	0.79	1.04	-1.23	0.91	-1.09	-1.75	-0.85	-3.48	3.75	-0.60	0.54	2.99	1.79	-0.29	2.51
	MLX1	1.15	0.59	-0.90	0.77	-0.74	-2.06	-2.13	-2.78	3.42	1.15	0.21	2.71	2.61	-0.45	2.07
	MLX2	0.68	0.05	-1.74	0.52	-1.52	-2.14	-2.60	-3.70	3.89	-0.78	-0.35	2.75	2.13	-0.76	2.26
	MLX3	0.87	0.55	-1.33	0.79	-1.27	-1.85	-1.63	-3.26	3.57	-0.69	0.75	2.94	2.63	-0.37	2.33
	MLX4	0.20	0.51	-1.60	0.37	-1.64	-1.88	-2.58	-3.57	3.72	-0.70	0.82	3.04	2.32	-0.56	1.99
	MLX5	0.03	0.28	-1.60	0.66	-1.80	-2.10	-2.90	-3.74	3.46	-1.30	0.25	2.96	1.49	-0.91	1.74
	MLX6	-0.22	0.28	-1.77	0.43	-2.43	-2.29	-3.72	-4.55	2.60	-1.01	0.40	3.06	1.15	-0.80	1.06
	MLY1	1.01	0.70	-1.03	0.69	-1.39	-1.73	-2.05	-3.97	3.34	-0.37	1.04	3.04	2.08	-0.49	1.70
	MLY2	1.11	1.11	-1.26	0.12	-1.26	-2.30	-2.24	-4.14	2.22	-0.79	-0.37	2.67	1.40	-0.79	1.25
Civic Lake	CLC	0.25	0.79	-1.03	1.08	-1.87	-1.59	-3.12	-10.09	4.14	-1.08	0.34	3.02	1.01	-0.86	3.20
	CLX1	1.31	0.60	-0.91	1.72	-1.46	-1.86	-3.09	-3.77	4.21	-0.32	0.60	2.85	2.45	-0.86	3.26
	CLX2	0.83	0.30	-1.02	1.11	-1.45	-1.63	-2.64	-3.68	4.18	-0.88	0.69	3.06	2.07	-0.65	3.04
	CLY1	1.16	0.64	-1.31	1.20	-1.03	-1.59	-0.79	-3.33	3.73	-0.81	0.09	2.92	2.21	-0.53	3.08
	CLY2	-0.39	0.40	-1.86	0.26	-2.24	-2.19	-3.02	-10.09	3.04	-2.03	0.41	2.75	1.94	-1.07	2.30

1 = Background data based on values from Turekian (1974); 2=Background data based on values from Wronkiewicz and Condie (1987)

Table 4.9: The Igeo values, based on the trace element concentrations identified in each individual sample for two sites considered as dams, Kleinfontein Dam and van Ryn Dam. The Igeo values are subsequently colour coded to easily identify pollution extremes and to contrast with unpolluted samples (The key to the colour coding can be identified in Table 3.3)

Site	Sample	Igeo														
		As[1]	Ca[2]	Cr[2]	Cu[1]	Fe[2]	K[2]	Mn[2]	Ni[2]	Pb[2]	S[1]	Th[2]	Ti[2]	U[2]	V[2]	Zn[1]
Kleinfontein Dam	KDC	2.25	0.98	-1.08	2.13	-0.84	-1.51	-2.27	-1.87	5.47	0.49	1.01	2.91	2.38	-0.37	4.93
	KDX1	0.52	1.04	-0.92	1.69	-1.67	-1.60	-2.98	-3.76	4.55	-0.83	0.05	2.82	1.52	-0.80	3.63
	KDX2	2.53	1.04	-0.99	2.41	-0.85	-1.52	-2.11	-1.97	5.50	0.25	1.22	2.98	2.54	-0.58	5.12
	KDX3	2.10	0.86	-0.95	2.03	-0.94	-1.39	-2.41	-2.04	5.50	0.16	1.41	3.00	2.69	-0.61	4.77
	KDX4	0.80	-0.05	-1.92	-0.39	-3.26	-1.88	-5.21	-10.09	2.62	-0.52	-0.26	2.23	1.98	-1.51	1.94
	KDY1	-0.04	1.60	-2.06	0.61	-2.93	-2.81	-2.64	-2.70	2.55	-0.16	0.21	2.54	2.24	-1.39	2.60
	KDY2	-0.08	-0.17	-1.25	0.04	-1.92	-1.82	-2.71	-4.53	1.45	-2.16	0.10	3.14	1.34	-0.84	1.09
van Ryn Dam	VRDC	-0.53	0.18	-1.83	0.42	-1.71	-0.73	-3.85	-3.85	2.11	-2.21	1.81	2.88	3.59	-0.73	1.00
	VRDX1	0.13	0.16	-1.48	0.90	-1.34	-1.20	-3.74	-2.94	1.97	-1.82	1.43	2.61	2.45	-0.79	1.17
	VRDX2	-0.33	0.17	-1.82	0.63	-1.70	-1.01	-3.67	-10.09	2.18	-2.08	1.77	2.75	2.00	-1.03	1.16
	VRDX3	0.21	0.38	-1.68	1.01	-1.26	-0.94	-3.23	-3.32	2.64	-2.29	1.94	2.86	2.24	-0.76	1.60
	VRDX4	-1.08	0.14	-1.93	0.36	-1.78	-0.83	-3.92	-10.09	2.19	-2.24	1.83	2.84	2.21	-0.65	0.99
	VRDX5	-0.59	0.04	-2.18	0.34	-2.24	-1.10	-4.42	-10.09	2.11	-2.42	1.54	2.68	2.26	-1.15	0.89
	VRDX6	-2.13	-0.23	-3.02	-0.79	-3.97	-1.76	-6.47	-10.09	0.61	-3.01	0.05	2.24	2.06	-1.85	-0.19
	VRDY1	-2.03	-0.38	-2.81	-0.77	-2.23	-0.23	-4.70	-10.09	0.75	-3.42	2.36	1.92	3.50	-1.30	0.24
	VRDY2	-1.68	-0.23	-2.32	-1.00	-2.79	-1.88	-5.06	-10.09	0.05	-3.98	0.49	2.99	1.99	-1.14	-1.02

1 = Background data based on values from Turekian (1974); 2=Background data based on values from Wronkiewicz and Condie (1987)

CHAPTER 5:

DISCUSSION

5.1. Introduction

The results clearly express a spatial distribution of certain trace elements within each site and across the entire region, with some showing increased amounts greater than expected natural concentrations. The chapter will, therefore, look at how these trace elements are spatially distributed across the entire region and how they are distributed within each site. Identifying the regional distribution of trace elements can aid in identifying if the tailings dams and mine dumps, towards the centre of the city, have an influence on the trace element concentrations at each site. Looking into internal distribution at each site also allows for the identification of localised sources of trace elements compared to regional sources, especially for the dam reservoirs which have inflow and outflow points. Following this, an in-depth look at the relationships between each individual trace element will be done in order to identify what the possible sources are at each site and across the entire regions. Lastly, the chapter will identify the possible environmental effects of the trace element contamination at each site.

5.2. The Spatial Distribution of Contaminants in Water across Benoni

Water samples were taken at both the top and bottom of the water column. Both physical, *in situ,* and chemical water measurements were taken. The in situ characteristics include temperature, DO, conductivity and pH, while samples taken at each site were analysed using ICP-OES to identify any possible major ions in the water. The data from the water was only used to give a bigger understanding of the

pollution levels of the water within the site. A further study could possibly be conducted to do a more in-depth analysis of the water quality at each site, especially with the identification of trace element concentrations at each site.

5.2.1. *In Situ* Water Characteristics

There is no relevant data on water quality for each site currently available, so most data are based on when the samples were taken. During the research, it was assumed that there was a general problem with DO probe in the YSI during certain dates of fieldwork, at certain sites. DO values that tended to be greater than 120% occurred at Amata Pan, Bullfrog Pan, and Homestead Dam. Some sites contained relatively high DO values at the surface but extremely low values at depth, with differences being greater than 50%. These sites included Middle Lake, Kleinfontein Dam, Civic Lake, van Ryn Dam and Amata Pan. All sites, except Homestead, contained greater DO values at the surface compared to the bottom of the water column. The difference in DO levels between the top and bottom of the water column are generally expected, but the magnitude of these differences is larger than expected. Such a great difference could indicate that the deoxygenated zone may be geochemically active, compared to the oxygenated zone. The level at which this zone is active could be determined with further research

Conductivity levels generally tended to be below 1000µS/cm at seven of the nine sites. Two sites, Bullfrog Pan and Sandpan, contained values well above 2000µS/cm, but fell within the expected value of conductivity for endorheic wetlands in South Africa (de Klerk *et al.,* 2016), but considerably higher than a study conducted by Burger *et al.* (2019). The conductivity values at both Bullfrog

Pan (2572 µS/cm at the surface and 2492µS/cm at depth) and Sandpan (2416µS/cm at the surface and 2401µS/cm at depth) indicate the two sites are somewhat saline (van Niekerk *et al*., 2009). The two sites, Bullfrog Pan (9.22 and 9.19) and Sandpan (8.7 and 8.55), also contained the greatest pH values compared to all the other sites, which were around the same values as identified by Burger *et al.*(2019). These values were also well above the SAWQG and WHO drinking water guidelines. A further hydrological study of the two sites could provide a better understanding of their water regimes.

5.2.2. The Chemical Characteristics

The concentrations of seven elements, Ca, K, Mg, Na, S, Si, and Sr were detected by the ICP-OES, while the trace element concentrations were below the limit of detection from the machine. The seven elements had varying concentrations across all the sites, with varying sites containing the highest concentrations of each. All concentrations of Ca across the entire region were extremely high when compared to the SAWQG. The most polluted of the sites include Korsman Pan, Amata Pan, and Kleinfontein Dam. The levels of Ca, along with Mg and K arise from various combinations of salts, that can be found in both sediments and water across the world (Chhabra, 2017).

Bullfrog Pan contained the greatest concentrations of K and Mg, both of which were considerably higher than the recommendations set out by the SAWQG, as well as the greatest concentration of Sr. The greatest concentrations of Na, S, and Si were found at Sandpan, which is only a few metres away from Bullfrog Pan. Both sites contained elements that are generally indicative of various forms of salts.

Concentrations of elements associated with salts at Bullfrog Pan and Sandpan fell within the expected concentrations for endorheic wetlands in South Africa (de Klerk *et al.,* 2016), but were also considerably higher than the study conducted by Burger *et al.* (2019). These concentrations could be caused by either human input or the natural hydrological regime, *i.e.* precipitation and evaporation into the site. For the natural pans, the varying changes in precipitation and evaporation may be the lead cause of increased salinity. Another source of such elements may be through the underlying geology of the two pans, Sandpan and Bullfrog pan, which, according to Fig 1.3 is composed of felsic rocks, which consist of both feldspar and silicon. Feldspar, usually consisting of minerals such as albite ($NaAlSi_3O_{8)}$, orthoclase ($KAlSi_3O_{8)}$, and anorthite ($CaAl_2Si_2O_{8)}$, may be the main source of Ca, K, and Na to the water column, via mixing and mobilisation (Taylor and Brown, 1979; Krbetschek *et al.,* 2002).

5.3. The Spatial Distribution of Trace Elements across Benoni

One of the main objectives of this research was to identify the spatial distribution of trace elements within surface sediments of pans and dams across Benoni, as well as the spatial distribution across the entire region. This first section will look at the spatial distribution of trace elements within each pan and dam; followed by the distribution across the entire Benoni region.

Bathymetric maps were created for all the sites used to conduct the research. These maps were done to ensure that sediment sampling covered the full range of available depths. The depths of each site, especially the pans, are not fixed, as water levels may vary seasonally and over longer periods of time. The depths and subsequent

volumes of each site aid in creating a good understanding of the possible distribution of trace elements across each site.

The concentrations of sediments at each is related to the volume and depths of each site. Increasing depth is characteristically associated with greater concentrations of contaminants compared to shallower parts. This could be due to a process known as sediment focussing. Sediment focussing takes place when the effects of gravity and currents on lateral movement may result in greater accumulations of varying trace elements at greater depths (Davis and Ford. 1985; Blais and Kalff, 1995; Yang *et al.*, 2002; Morales-Marin *et al.*, 2018). While faster accumulation may dilute the contaminant concentration, focussing of contaminated inputs (e.g. windblown dust) may act to increases concentrations. Trace element distribution would also likely be affected by varying accumulation rates at each site, as well as wetting and drying of the endorheic wetland systems (Duthie, 1999; de Klerk *et al.*, 2016; de Necker *et al.*, 2016; Yapiyev *et al.*, 2017).

5.3.1. The Distribution of Trace Elements within each Pan

The distribution within each site will differ slightly due to varying forms of sources and entry points, as well as varying sedimentary and hydrological dynamics of the systems. The distribution of trace elements at Amata Pan varies considerably, with two sample points expressing the main concentrations of various trace elements, compared to the other three sample points. SampleAPY1 was identified to contain the largest concentrations of Mn and Zn, while both samples, APY1 and APY2 were identified to contain the main concentrations of Fe. This distribution may be due to

the shallowness of the overall site, therefore limiting the amount of sediment focussing that could take place.

The distribution of trace elements within Bullfrog Pan is considerably different from that of Amata Pan and expressed a greater variability of samples containing large concentrations of individual ions and trace elements. Samples BFPX3 and BFPY1 contained the greatest concentrations of K compared to the other samples across the site. The greatest concentrations of Fe were found to be in samples BFPX4 and BFPY4 which could both be found towards the south and eastern parts of the pan. The greatest concentrations of Ca, Mn, and S can be found in samples BFPC, BFPX2, BFPY2, and BFPY3, which is the central part of the site, thus it can be said that these three trace elements are concentrated in the centre of the site. The greatest concentrations of K were identified in BFPX3 to the south of the centre of the site.

In comparison to the distribution at Bullfrog Pan, the distribution of trace elements at the Sandpan were slightly different. The greatest concentrations of Fe were identified in samples SPX3, followed by SPC and then SPY3. Thus, showing a greater concentration of Fe to the centre and south of the centre of the site. This also coincides with the deep plateau of the shallow site. The greatest concentrations of Ca and Mn were identified in SPY 2, north of the centre of the site. The greatest concentrations of K were identified in sample SPY1, which was towards the western end of the site. The distribution of trace elements in the site is mainly evenly distributed apart from the ones already mentioned. The distribution of Korsman's Pan also differed slightly from the others.

As expected with all pans the highest concentrations of trace elements in Korsman Pan were identified in samples from the centre of the site. The highest concentrations of trace elements such as Cu, Fe, Mn, S, and Zn, can be found at the centre of the site (Sample KPC). The greatest concentrations of Ca were identified in samples KPX3 and KPY3. The greatest concentrations of K can be identified in samples KPX2, KPY2, and KPY3, which were all in the middle of the site towards the northwest. The outliers, with the lowest concentrations of trace elements, were samples KPX1, KPX4, KPY1, and KPY4, all which were taken along the edges of the site, mainly surrounded by reeds and other various water plants.

The distribution of trace elements at the site Korsman Pan, Sandpan and Bullfrog Pan, express slightly similar patterns of distribution that could be explained by two possible processes taking place. The one possibility is that the overall waterbody in each site is constantly shrinking, through evaporation and filling up, via precipitation, that after the shrinking event there is a concentration of trace elements in the deeper part of the pans. The other possible reasons could be the remobilization of trace elements in both oxic and anoxic sediments (Vidal-Durà *et al.*, 2018). Sediment focussing is most likely not solely taking place at all four sites, as most of the greater concentrations were identified at varying depths. The lack of sediment focussing could be due to the sites relatively flat and shallow depths.

5.3.2. The Distribution of Trace Elements within each Dam

The pattern of trace element distribution in the sites constituting dams is expected to differ from the pans for the main reason that these systems are more dynamic with points of surface inflow and outflow at each site. The spatial pattern of trace

elements for van Ryn Dam will be discussed first as it is the only dam that is situated by itself, with less complex hydrological influence than the other four sites. Once this had been achieved, the pattern of distribution of the four dams along the same gradient will be explored followed by an overall pattern of trace element distribution along the entire gradient.

van Ryn is situated to the north of the city centre, and the concentration of tailings dams in Benoni. The site used to be a part of the van Ryn Gold Mine but is now wedged between the luxurious Ebotse Golf Estate. The greatest concentrations of K were identified in samples VRDY1, VRDC, VRDX3 and VRDX4. Samples VRDX3, VRDC, VRDX1, and VRDX2 contained the greatest amounts of Ca, Mn, as well as the greatest concentrations of Fe. The samples containing the greatest concentrations of trace elements were situated towards the centre of the dam and at the deepest points of the site. The three outliers were all in shallow waters and thus contained many varying plant species.

The first (most upstream) site to be found along the same river gradient is Homestead Dam. This site was one of the biggest sites covered in the research, with two inflow points and one single outflow point towards the southeast of the Dam. The largest concentration of Fe was identified in sample HDC which is considered to be roughly the centre of the site. The greatest concentrations of Mn were identified in sample HDY2, which was towards the west of the site, near the second inflow point into the site. Samples HDZ 1 and 2 contained the largest concentrations of Ca and K. both sampling points were situated closest to the dam wall and the

only outflow point of the actual site. These two points were also closest to the freeway that runs along the southern end of the site.

The next site to fall along the same river gradient was Middle Lake. The distribution of trace elements at this site were slightly different, with the largest concentration of Fe and S being at MLX1 which was towards the end of the site near the dam wall. The greatest concentrations of Ca came from samples MLY1, MLX3, and MLX2 respectively, while the largest concentrations of Mn were identified in the same samples but the largest being in MLX3, then MLY1 and MLX2. This is similar to Homestead Dam, in the fact that the greatest concentrations of various trace elements were found closer to the dam wall of that site and some of the deepest points of the site. It should be noted that there is a connection between the two dams, with the outflow point of Homestead Dam connecting to the inflow point of Middle Lake. The outflow of Middle Lake subsequently then runs into Civic Lake.

The main outliers at this site were probably CLY 2 and CLC. This may be because Civic Lake is the smallest dam analysed in this research. the greatest concentrations of Fe and Mn could be found in sample CLY1, which was to the north of the site. Sample CLX 2 contained the greatest concentrations of K, S, and Zn. It also contained the next greatest concentrations of Fe and Mn within the site. This sample happened to be situated towards the east of the site, near the outflow point and along the eastern bank, which is situated along the main road into the CBD.

The last site to fall along the river gradient was Kleinfontein Dam. The dam, which is situated right next to a mine dump, expresses a very different distribution to each other site along the gradient. The greatest concentrations of most trace elements

were identified further away from the eastern bank and subsequent outflow point of the site. The greatest concentrations of Fe, S, and Zn were identified in samples KDC, KDX3, and KDX2, respectively. These three samples were all towards the centre of the site, similar to the spatial pattern of the pans in the region. The greatest concentrations of Ca were identified in samples KDX2, KDX1, KDC, and KDX3 respectively, while at the same time KDX3 also contained the greatest concentrations of K and Ti. There seems to be a relationship between the depth of the site and the concentrations of trace elements, with the greatest concentrations being towards the deepest parts of the site and the lowest being towards the edges, even if there are substantial concentrations at KDX 1.

The distribution of trace elements across all four sites needs to be considered as it adds to the greater understanding of the spatial distribution across the entire region. An increase in trace element concentrations, from upstream to downstream, along the gradient is expected. The average concentrations appear to differ for individual trace elements from the top of the gradient (Homestead Dam) to the bottom of the gradient (Kleinfontein Dam). The average concentrations of trace elements such as As, Cu, Pb, and Zn appear to increase with the change in the gradient from Homestead Dam to Kleinfontein Dam. This could indicate the possibility of the upstream sites acting as contaminant sources to the sites downstream. Comparatively, there was an overall decrease in concentrations of Mn and V from Homestead Dam to Kleinfontein Dam. Average concentrations of Ca, Cr, Ni, S, and Ti were all varied from site to site, with the largest concentrations being at Kleinfontein Dam, while both Fe and K concentrations decreased from Homestead

then slightly increased at Kleinfontein Dam. The overall highest average concentrations of the two trace elements were found at Homestead Dam.

These slight differences in concentrations could possibly be due to many varying factors but are probably best understood with regards to the hydrological influences of each site. Homestead Dam which is found at the top of the river gradient has two river inflow points, of which both could be contributing trace elements from their flow, that is to say, that atmospheric fallout is not the only possible contributor to trace element concentrations at this site. The general increase in the majority of trace elements towards the bottom of the gradient is expected, especially as Kleinfontein Dam is situated right next to a massive mine dump. Overall the increased concentrations towards deeper sampling points at all five sites is most likely due the sediment focussing..

5.3.3. Spatial Distribution Across the Entire Area

The spatial distribution of trace elements across the entire area was hypothesized to increase in concentrations towards the tailings' dams and mine dumps to the centre of the city. Although this may be the case for some sites, they may not be the main source. The largest concentrations of trace elements As, Cr, Cu, Fe, Mn, Ni, Pb, S, and Zn, were identified in Amata Pan. The concentrations for these trace elements were significantly different from every other site in the area. In comparison there was no significant difference in As, Cr, Cu, Ni, and Zn concentrations across the remaining eight sites. The concentrations of As, Cu, Ni, and Zn also expressed an increase towards the collection of tailings dams and mine

dumps in the centre of the city. This distribution is further supported by the PCA (Fig 4.15).

Concentrations of Cr were relatively significantly different from each other with sites, van Ryn Dam, Bullfrog Pan and Sandpan, which are further north and upwind of the tailings dams and mine dumps, containing the lowest concentrations. The smallest concentrations of Fe were identified in three sites that were relatively far from the centre of the city. These sites were Bullfrog Pan, Sandpan, and Korsman Pan respectively.

Compared to this, the greatest concentrations of Ca and K ions could be found within Korsman Pan, Bullfrog Pan and Sandpan. For both Sandpan and Bullfrog Pan, the mean concentrations of Ca and K were significantly different from all the other sites, possibly due to extreme evaporation of the pans and/or atmospheric fallout. The identification of Ca and K can give greater evidence to whether the pans are open or closed systems, as there is no existing information as to whether any of them are fed by underground water, and as for now, it is only assumed that each pan is fed via rainfall during the summer rainfall seasons.

Overall, the main distribution and concentrations of trace elements such as, As, Cu, Fe, Mn, Ni, Pb, and Zn, in the region, were identified at Amata Pan.

5.4. The Level of Trace Element Contamination in Sediments across Benoni

The description of the spatial distribution of trace elements across the Benoni region, will not necessarily give an indication to the level of pollution across that

same region. In order to identify the level of trace element contamination in sediments across the region, a basic *Igeo* was undertaken. The *Igeo* was done based on the average natural background values for the local geology identified in Wronkiewicz and Condie (1987) and average background values for sandstones in Turekian (1972). This next section will discuss the level of pollution at each site in order to give an overall understanding of the level of pollution across the entire region. This will also aid in identifying possible sources of trace element contamination across the region.

5.4.1. Contamination in the Pans

The most contaminated site within the region was Amata Pan. The site contained varying concentrations of Zn > Pb > Cu > As > Ti > Fe > S > Cr pollution. The most considerable amount of pollution came in the form of Zn and Pb, which could be considered extremely high according to the *Igeo* rating. This is also supported by the ANOVA that was done which identified Amata Pan in a different group to every other site, for almost every trace element looked at. At the same time, Amata Pan was the only site that contained some level of Fe, S, and Cr contamination, even if it were minimal or almost negligible. The site contains a mix of contaminants that would be associated with mine tailings and dumps (Yacoub *et al.*¸ 2013; Park and Allaby, 2017), as well as probable local dumping. The level of contamination at this site is perhaps the most interesting, as it is a natural pan that is considerably polluted even when compared to the built dams in the region.

In comparison to this site, all the other pans, Korsman Pan (Ti > Pb > Zn > Cu), Bullfrog Pans (Ti > Pb > Zn), and Sandpan (Ti > Zn > Pb) were relatively

unpolluted. Like every other site in the area, all three of the pans contained some levels of Pb and Ti contamination according to the *Igeo*., with the Sandpan containing the lowest concentrations of Pb and the lowest indication of Pb contamination. A plausible reason for the lack of pollution at this site, is most likely the location of the site, which is not surrounded by any form of industry, and it is north and subsequently upwind of the tailings dams and mine dumps. A similar reasoning could be used for the Bullfrog Pan. The lack of trace element contamination could be mainly due to its location northwest of the tailings and mine dumps. Further detail into the possible sources of trace elements at each site will be discussed later.

It is safe to assume that, barring Amata Pan, there is relatively little trace element contamination at the pans within the region. There are many possible reasons for this, with the most likely being their location within the region, with regards to wind direction, distance from tailings dams and general location. The sites are also relatively less contaminated than the dams studied in the region.

5.4.2. Contamination in the Dams

Five dams were monitored, each with relatively different levels of trace element contamination. Four of the dams, which are situated along the same river, expressed, although not statistically significant, a gradient in trace element concentrations from the top to the bottom. The first site, Homestead Dam, mainly contained Pb > Ti > Zn > Cu > As pollution but generally expressed the lowest levels of contamination along the gradient. Following this the greatest levels of contamination at Middle Lake was Pb > Ti > Zn > As > Cu. The greatest levels of

contamination at Civic Lake and Kleinfontein Dam were Pb > Zn > Ti > Cu > As and Pb > Zn >Ti > Cu > As respectively.

The gradient of these sites has a major influence on the distribution of such trace elements within them. Since each site is connected there is an expected gradient in trace element contamination to be found within this area of Benoni. For trace elements such as Pb and Zn, there was an increase in contamination from the dam at the top of the river gradient (Homestead Dam) to the dam at the bottom (Kleinfontein Dam). The increase in contamination of As, Pb, and Zn also corresponds with the location of the site relative to the tailings dams and mine dumps in the area, with the greatest levels of contamination naturally being right next to the large mine dumps.

The last dam that was studied was van Ryn Dam. The levels of pollution at the site were lower in comparison to all the other dam reservoirs. The same types of trace elements proved a similar issue at this site (Ti > Pb > Zn > Cu). van Ryn Dam was the only site where Ti proved to have the greatest concentration of these elements. The results of the concentrations of this site are more variable since the site falls next to a former tailings dam that no longer exists in the area. The overall distribution of contamination across the region could give a better picture of the level of contamination and the influence of the tailing's dams and dumps in the centre of the city.

5.4.3. Contamination Across the Entire Region

Overall, if there were any influence by the mine dumps and tailings dams in the region, the general trend of trace element contamination across the entire region

needs to be identified. The level of specific forms of trace element contamination at each site, related to their location and the predominant wind direction identified in the wind-rose data may aid in identifying if the tailings dams in the region are a source of trace element contamination in the area. Across the entire region, the main form of trace element contamination was in the form of Ca, Pb, Ti, and Zn pollution. This evidence of contamination is similar to that found in a study by Roychoudhury and Starke (2006) on the Blesbokspruit, further east of Benoni. Roychudhury and Starke (2006) identified similar forms of trace element contamination in the river, with the highest levels of pollution coming from samples close to the tailings dam.

There was also some form of As and Cu pollution found across the region, although not at every site. As concentrations increased to the south of the area, with the main concentrations coming from dam reservoirs. A similar pattern of Cu contamination can be seen across the area. Generally, most sites seemed to contain some form of contamination of trace elements associated with gold mine tailings dams and dumps. With every form of contamination, there appears to be some form of a decrease in contamination with distance from the centre of the tailings dams and mine dumps. The only exception to this is that of Amata Pan, which is considered the most polluted site in the area. The level of contamination across the region also appears to be related slightly with the predominant wind speed and direction in the area.

The majority of the sites with the greatest levels of pollution tended to be downwind of the tailings dams and mine dumps, with the Amata Pan falling downwind of the tailings dams and mine dumps, in a north to north-west direction identified in the

wind-rose for both the 20 years period and 2017 (Fig 4.10 and 4.11). The other sites that also fell within the direction of a predominant wind direction include Korsman Pan, the four dams along the same river gradient, and van Ryn Dam. Korsman Pan and the five sites along the river gradient fell downwind of the tailings dams and mine dumps, within a generally easterly direction, while van Ryn fell within a less dominant general south to south-south-westerly direction. Overall there is generally some form of sediment contamination related to trace elements across the entire region

5.5. The Possible Sources of Trace Elements Across Benoni

The main objective of this research is to identify if a series of tailings dams and mine dumps, situated in the centre of the City of Benoni, have contributed to trace element concentrations at various dams and pans across the area. With the study area being an urban area, however, the tailings dams and mine dumps are not the only possible sources of trace elements across the entire region, and each individual site is influenced by their own immediate local environment.

The most polluted site within the region and the one that generally tends to contain the greatest concentrations of trace elements was Amata Pan. Sampling at the site expressed strong positive correlations between trace elements such as As, Cu, Mn, Ni, Pb, Zn, as well as Fe, Mn and Ni. The site is situated on the edge of an industrial zone with a large spring manufacturing company along its northern and western borders and is located south (downwind) of the tailings dams and mine dumps. The increase in concentrations of As, Cu, Fe, Mn, Ni, Pb, Zn, and S could possibly represent a form of anthropogenic influence. The site is possibly at risk of

contamination via exhaust fumes of trucks (Lee and von Lehmden, 1973; Herman and Neumann-Mahltau, 1985; Islam *et al.*, 2014; Pan and Wang, 2015) that park along the northern border and, as anecdotal evidence suggests, the constant oil spillages that previously took place at the factory. Oil may contain elements such as those that are positively correlated (As, Cu, Fe, Mn, Ni, Pb, S, V, Zn,) to each other and constant runoff into the pan could be responsible for the build-up of the various trace elements at the site (Islam *et al.*, 2014; Pan and Wang, 2015; Howard *et al.*, 2016; Väänänen *et al.*, 2018). The site may also be influenced by tailings dams and mine dumps to the north, as elements such as Fe, S, As, Pb and Ni which are commonly associated with tailings and mine dumps, were correlated with each other (Jung et al. 2005; Roychoudury and Starke, 2006). The extent as to how much influence the local tailings dams and mine dumps have is unknown and further research will need to be done to identify this.

In comparison to this, the other pans expressed very different forms of trace element contamination and thus must have different local sources to those of Amata Pan. All three pans, Korsman Pan, Bullfrog Pan, and Sandpan, are situated in middle-class suburbs with the Bullfrog Pan and Sandpan being situated at the edge of former agricultural holdings. All three sites contain very little sources of trace elements. Apart from the possibility of wastewater effluent and household runoff, elevated levels of Ca at this site may be due to the association of Ca with various salts (Chhabra, 2017). The possible source of these salts may be from the underlying geology which contains mainly felsic rocks which are rich in Ca (Roychoudhury and Starke, 2006; Kleinhans and van Rooy, 2016), or via windblown sources. This

may be further exacerbated by constant wetting and drying of the two pans, which are situated on surficial geology consisting predominantly of felsic rock (Fig 1.3).

The most likely source of elevated levels of trace elements, such as Pb and Ti, may be from atmospheric fallout in the area. Atmospheric fallout may include general pollution from the region, coal combustion or the incorporation of substances from the tailings dams and mine dumps, picked up by the wind, into the atmosphere. Due to the general location of the two sites, the influence of the tailings dams and mine dumps seems unlikely. Both Bullfrog Pan and Sandpan are further north and upwind of any predominant wind direction and mine dump sources. The source of Cu, Pb, Ti, and Zn concentrations, which were above natural background levels, maybe from the collections of mine dumps in the city centre. Korsman Pan falls downwind of a general easterly wind direction and is only a few kilometres away from the central location of previous mining activity. Another probability is groundwater recharge. There is the possibility that the three pans, Korsman, Bullfrog and Sandpan, are fed with some form of underground water, which is common due to the various dolomites and limestones (Roychoudhury and Starke, 2006; Kleinhans and van Rooy, 2016) in the region, but this may only be definitive with further research of the regional geohydrology.

Like Amata Pan and unlike the other three natural pans, the several dams in the region also contained elevated levels of trace elements such as As, Ca, Cu, Pb, Ti, and Zn, as well as the odd sample containing extremely low levels of S contamination. The sources of these contaminants to each dam tends to be relatively similar to each other. Both, Homestead Dam and Middle Lake are affected by

various stream inputs, which could both provide sources of trace elements. The two sites can also be found along the N12 national freeway, which is likely to provide sources of trace elements, via exhaust fumes, tarmac and various other materials (Lee and von Lehmden, 1973; Herman and Neumann-Mahltau, 1985; Islam *et al.*, 2014; Alyazichi *et al.*, 2015; Väänänen *et al.*, 2018). The freeway may also explain why there tends to be greater concentrations of trace elements towards the southern part of Homestead dam, and the varying concentrations along Middle Lake. The possible evidence for this comes from the strong positive correlation of trace elements such as Zn and Pb, which are generally associated with trace elements from vehicles and roads (Huang *et al.*, 1994).

Further down the river gradient is Civic Lake, which is situated between two major roads into the CBD, a mall and train track, all providing potential sources for trace elements, via urban stormwater runoff (Lee and von Lehmden, 1973; Herman and Neumann-Mahltau, 1985; Islam *et al.*, 2014; Alyazichi *et al.*, 2015; Väänänen *et al.*, 2018). The site is also downriver of two other dams that release water to the two dams further downstream. Once again Civic Lake also contained elevated levels of As, Ca, Cu, Pb, Ti, and Zn. All these trace elements were positively correlated with each other, suggesting that they possibly came from similar sources. The same could be said for Kleinfontein Dam, with the only difference being its proximity to a large mine dump and the overall collection of mine dumps and tailings dams. There is also a strong positive correlation between various trace elements, As, Cu, Fe, Mn, Ni, Pb, U, and Zn, associated with gold mine tailings and dumps (Coetzee *et al.*, 2002; Jung *et al.*, 2005; Roychoudhury and Starke, 2006; Tutu *et al.*, 2008; Humphries *et al*., 2017).

Along the entire river gradient, there is an increase in trace element contamination, suggesting an accumulation of sediments towards the bottom of the gradient. The sites are also upwind of a generally easterly wind direction that can transport various sediments. These four sites are therefore influenced by not only each other but multiple other sources such as the tailings dams, the freeways that run alongside two of them and train lines.

The sources of trace elements to van Ryn Dam is slightly different from that of the other four dam reservoirs. van Ryn Dam is situated in between an up-market golf estate, next to the former van Ryn gold mine. It is plausible that the very little form of contamination is based on historical deposits from the former mine dump that used to be situated there. This would explain the lower levels of contamination at the site, and the strong positive correlation of varying trace elements such as As, Cu, Fe, Mn, Ni, Pb, Ti, and Zn. The site is also situated north of the collection of the mine tailings and dumps and is in the path of a reasonable south south-westerly to southerly wind direction, thus indicating a possible influence of the mine tailings and dumps. The site is also a dam and thus has very dynamic water and sediment regimes, suggesting that trace elements are possibly flushed away with less accumulation taking place in the sediment.

The movement of substances within each site varies considerably, but the main difference comes from the type of site. Movement within pans differs considerably compared to dams. This is possibly due to the more closed system typical of natural pans in this region (McCarthy *et al.*, 2007; de Klerk *et al.*, 2016). The only possible movement of materials out of each site may be due to wind after desiccation has

taken place. Compared to this, dams are more dynamic with the movement of water and sediment in and out of each site, via surface flows. There would especially be more of an influence of each dam, along the same river gradient, on each other, as each site would supply sediment and water to the sites further downstream. The four dams along the same river gradient are influenced by multiple sources of pollutants. This is unfortunately a limitation to all the sites across the region. Urban areas will always provide a great number of sources.

Overall across the entire region, there are very similar sources of the trace element accumulation at each site, although most of the general trace elements such as Fe, Mn, and Ni, fall within natural background values, the rest like As, Cu, Pb, Ti, and Zn, pose a significant problem. Possible common sources of trace elements across the entire region include atmospheric fallout, urban runoff, via domestic wastewater or industrial wastewater, and the underlying geology. There does appear to be some form of influence by the collection of tailings and mine dumps in the region, but the extent of this influence is difficult to determine, due to the many varying sources of trace elements that can be found in an urban area.

5.6. The Influence of Gold Mine Tailings' Dams and Dumps

There appears to be a form of influence by the various gold mine tailings dams and dumps on the various sites in the region. The level of influence at each site differs with their location relative to the tailings and mine dumps, and the predominant wind direction. Evidence for the influence of said tailings and dumps comes from the concentrations of trace elements mainly associated with the Witwatersrand Region. The main trace elements associated with gold mines tailings and dumps

include As, Cr, Co, Cu, Fe, Hg, Mn, Ni, Pb, U, V, and Zn (Coetzee *et al.*, 2002; Jung *et al.*, 2005; Roychoudhury and Starke, 2006; Tutu *et al.*, 2008; Kossof *et al.*, 2014; Humphries *et al*., 2017). Of all of these trace elements, only Co and Hg were not analysed for in the results. Identifying concentrations and level of pollution for the remaining trace elements may help indicate the level of influence at each site and create a picture of the spatial distribution, across the entire region. The spatial distribution across the area will determine if there is an increase or decrease from the central group of tailings dams and mine dumps in the Benoni area.

Across the entire region, there were increased concentrations of As, Cu, Pb, U and Zn (Table 4.3 and 4.4), five of the 12 of the trace elements commonly associated with gold mining. The only sites to not contain increased levels of As and Cu were Bullfrog Pan and Sandpan. These sites also contained the lowest levels of Pb, U, and Zn pollution. The possibility of this being their location from the tailings dams and mine dumps. The two pans can be found upwind of the subsequent sources, in a predominantly northerly wind direction. Therefore, there is a minimal amount of influence on these two sites by the central tailings dams and mine dumps in the region. The next site to contain the lowest concentrations and levels of Cu, Pb, U, and Zn was van Ryn Dam. The site, which is also north and upwind of the tailings dams and mine dumps, contained very low to low levels of contamination for the five trace elements and was uncontaminated with As, Cr, Fe, Mn, Ni, and V.

The most polluted site in the region and the one that was furthest away from the central tailings dams and mine dumps was Amata Pan. The site was considerably contaminated with trace elements such as As, Cr, Cu, Fe, Pb, S, Ti, and U. Of these

trace elements six of them (As, Cr, Cu, Fe, Pb, and Zn) can be associated with gold mining. The possibility of a strong influence by the tailings dams and mine dumps is there and is even supported by the location of the site being downwind of the tailings sources of the region (Fig. 4.10 and 4.11) but is obscured by the fact that the site also falls within an industrial area and next to a springs manufacturing company. Therefore, it is assumed that the majority of the contamination comes from the immediate surroundings of the site, then the entire region.

In comparison to Amata Pan, Korsman Pan only contains low to very low levels of Cu, Pb, U and Zn contamination. The site is relatively closer to the central tailings dams and mine dumps, compared to Bullfrog Pan, Sandpan, van Ryn Dam, and Amata Pan. The site is also a more closed system, located in the middle of an upmarket suburb, eastwards and downwind of the central tailings dams and mine dumps. Due to its general location, the site is not susceptible to many sources of trace elements, with the only possible source being from atmospheric fallout. Therefore, with its location relative to the predominant wind direction, the most likely source of trace elements at this site would come from the tailings dams and mine dumps.

The last four sites, Homestead Dam, Middle Lake, Civic Lake, and Kleinfontein Dam fall on the same river gradient and express contamination of the same trace elements, As, Cu, Pb, U, and Zn. The location of the four sites, to the east and downwind of the tailings dams and mine dumps, indicates an increased likelihood of contamination coming from those tailings dams and dumps. This is especially true of Kleinfontein Dam. There was a general increase down the gradient in the

level of contamination of As, Cu, Pb, U, and Zn, with Kleinfontein Dam, the only site situated right next to a mine dump, containing the greatest levels of contamination of the four sites. The site also contained very low levels of S contamination, which is commonly associated with gold mining (Coetzee *et al.*, 2002; Jung *et al.*, 2005; Roychoudhury and Starke, 2006; Tutu *et al.*, 2008; Humphries *et al*., 2017).

Overall there appears to be an influence of tailings dams and mine dumps in contaminating the sites within the region, with sites that tend to be downwind of predominant wind directions containing greater levels of trace element contamination. Apart from Amata Pan, there also appears to be an increase in trace element contamination towards the tailings dams and mine dumps. That is, the sites closer to the collection of tailings dams and mine dumps contain the greater levels of contamination. The only exception to this is Amata Pan, and this is due to the multiple sources of trace element contamination the site experiences. The current contamination at each site poses a possible risk on the local environment and many flora and fauna species that inhabit each site.

5.7. The Possible Environmental Impacts

The elevated levels of As, Cu, Pb, Ti and Zn pose possible environmental impacts to the nine sites that were monitored. This is especially true of the pans which act as havens for various plant, bird, and fish species. There is a possibility that these trace elements could become bioavailable and move through the food chain of these sites (Väänänen *et al.*, 2018). The possible trace element that is toxic to species at all the sites monitored was Cr, while concentrations of Pb were well above PEC

values for all sites except Sandpan. Levels of As and Cu were above PEC values, at Amata Pan, Civic Lake, and Kleinfontein Dam. Toxic levels of Zn could also be identified at Amata Pan, Homestead Dam, Middle Lake, Civic Lake and Kleinfontein Dam. The extent to which these trace elements affect the varying plants, birds and fish species is based on their bioavailability, and redox potential (Costello *et al.*, 2015, Anawar *et al.*, 2018), which could be better determined in further research. Toxicity of trace elements such as As, Cu, Pb, and Zn have varying effects of different species of plants, fish, and birds.

Trace element interaction between sediments and various fish and bird species would not necessarily be direct. Trace elements from mining tend to have a lower solubility and stronger affinity for the solid phase, and thus are more likely to be removed from the water column via precipitation and sorption (Besser *et al.*, 2015; de Castro-Català *et al.*, 2016; Anawar *et al.*, 2018). However, some sediments may contain high concentrations of metals associated with precipitates and suspended particles, thus leading to benthic organisms, especially macroinvertebrates, being exposed to increased metal concentrations and the associated toxic effects (Besser *et al.*, 2015). These toxic effects could lead to a decrease in benthic invertebrate productivity and the removal of metal-sensitive taxa (Canfield *et al.*, 1994; Besser *et al.*, 2015; Väänänen *et al.*, 2018). Through benthic invertebrates, metals are transferred through the food chain into fish and various bird species, as well as humans.

Both As and Pb are especially harmful to various animal species and human health. Pb is considered to cause neurotoxicity, nephrotoxicity (kidney toxicity), and many

other adverse health effects, such as immune, cardiovascular, renal, gastrointestinal and endocrine issues (Munyangane *et al.*, 2016; La Colla *et al.*, 2017). As is also extremely harmful and can cause shortness of breath, a rise in skin lesions, as well as being the cause of various cancers such as skin, bladder, and lung cancer (Kavcar *et al.* 2009; Munyangane *et al.*, 2016). Overall there is a complex relationship that takes place between the sources, exposure, and possible toxicity of trace elements, and may vary with individual metals, varying organisms and specific characteristics of each site (Väänänen *et al.*, 2018).

6. CONCLUSIONS

6.1. Introduction

The aim of this research was to identify the spatial distribution of trace element contaminants in lakes, dams and pans across Benoni. In order to do the research, there were four objectives that were designed to help answer the overall research question: What is the spatial distribution of trace elements contaminants associated with AMD in lakes, pans and dams in Benoni, Gauteng? The four objectives aimed to understand the spatial distribution of trace element contaminants in the sediments and waters of lakes, dams and pans, across Benoni, as well as understand the depth of each site. No similar studies have previously been published in this area.

6.2. Objective 1: To identify the deepest sections of the dams and pans to take sediment and limnological samples and to map each lake/dam/pan.

The first objective of this research was to identify the deepest sections of each site across the region. This was done by undertaking a bathymetric assessment. During field research, depths across each site were taken. Kriging analysis was done, using ArcGIS, to produce the individual bathymetric maps for each site. A common pattern in lake depths was identified for the sites based on their type, pans or dam. The pans tended to all have a deeper middle area, with a shallow gradient going towards the edge of the pans. The pan with the deepest measured point was Amata Pan (1.7m), followed by Korsman Pan (1.6m). The maximum measured depths at both Bullfrog Pan and Sandpan were 1.2m and 1.1m respectively.

In comparison, the sites classified as dams were considerably deeper. All the dams contained similar bathymetries with the water depth being shallow near the entrance of the dam, and getting gradually deeper towards the wall, with the depth right by the wall being slightly less shallow, possibly due to sediment build up along the wall. The dam with the greatest measured depth was Homestead Dam (6.1m) followed by Middle Lake (5.6m). The greatest measured depths at Kleinfontein Dam, van Ryn Dam, and Civic Lake were 5.3m, 3.3m, and 2.4m respectively. Understanding the depths of each site, gave a greater understanding of both the sediment and hydrological dynamics of each individual site. This also aided in maximizing the points at which to take samples.

6.3. Objective 2: To identify the spatial patterns in water chemistry, associated with AMD contamination, of lakes/pans/dams.

The second objective of the research study was to identify any spatial patterns in water chemistry. A complete spatial pattern of water chemistry was not possible, due to lack of funding and resources, but physico-chemical characteristics, using the YSI multi-parameter probe, and two water samples, one at the surface and one at depth, were taken at each site, to give a basic understanding of the water quality within each site. The physico-chemical characteristics monitored for include temperature, dissolved oxygen, conductivity, and pH.

The data for the DO was considered to be unusable for three of the nine sites, due to the DO probe being damaged. Conductivity for each site was relatively high with the greatest measurements coming from Bullfrog Pan (2572µS/cm at the surface

and 2492µS/cm at depth) and Sandpan (2416µS/cm at the surface and 2401µS/cm at depth). The possible reasoning for this could be due to extreme evaporation of the individual sites. For six of the nine sites, the pH was above 8, with Bullfrog Pan and Amata Pan both having a pH above 9. The pH values for those six sites were above the recommended ranges set out by various water quality guidelines. The samples, taken from each site, were filtered and analysed using ICP-OES. The results for specific trace elements were inconclusive and tended it to be below the detection limit of the ICP-OES. The only conclusive results were identified for the following: Ca, K, Mg, Na, S, Si, and Sr.

The greatest concentrations of Ca were identified at Korsman Pan and Amata Pan. There was also a difference between the surface samples and the bottom samples at all the sites, with Korsman Pan, Bullfrog Pan, Middle Lake and Kleinfontein Dam having greater concentrations of Ca at the surface, and the rest of the sites containing greater concentrations at the depth. The samples with the greatest concentrations of K came from Bullfrog Pan, followed by Sandpan, then by Korsman Pan. Large Mg concentrations were found in the samples that came from Bullfrog Pan, followed by Korsman Pan. Lower concentrations of Mg were identified in sites classified as dams.

Compared to this, there were large concentrations of Na identified in samples from Sandpan and Bullfrog Pan. Notably, all concentrations of Na at every site were below 50mg/L. The samples with the largest concentrations of S came from Sandpan, Amata Pan, and Korsman Pan. The highest concentration of Si, once again, came from samples taken at Sandpan. The site with the next greatest

concentrations of Si was Kleinfontein Dam. Once the concentrations of the chemical characteristics and the data provided by the physical characteristics were obtained, they were then compared to various standards for water quality, provided by SAWQG and the WHO.

For the water chemistry, only K, Mg, and Na were provided for and thus compared to the water quality guidelines. The concentrations of K and Mg were well above their recommended environmental guidelines, while the concentrations of Na at each site were below the recommended guideline ranges. The possible cause of such contamination may be due to human input, underlying geology or the natural hydrological regime. The main contaminants in the region tend to be ions associated with salts. This differs considerably for the sediments of the at each site.

6.4. Objective 3: To determine the spatial variation, of contaminants associated with AMD, in surface sediments, within lakes/pans/dams.

PCA was used to determine the relationship between the trace elements and the sites within the area. It gave a basic understanding of which samples contain the greatest concentrations of trace elements compared to the others. PCA was also used to identify the general distribution of trace elements within each site. The spatial patterns of trace elements in the sediments of each site were similar, based on the type of site they fell under, pan or dam. The spatial distributions of Amata Pan, Korsman Pan, Bullfrog Pan, and Sandpan were very similar, with the greatest concentrations of trace elements being found in samples towards the centre of the site. These four sites were also similar in that they were categorised as pans. For

Amata Pan, the greatest concentrations of Zn, Mn, and Fe were identified at sample point APY1, closest to the springs factory. Sample KPC at, Korsman pan contained the greatest concentrations of Cu, Fe, Mn, an Zn, while the central sample point at Bullfrog Pan, BFPC, contained the greatest concentrations of S and Mn. The greatest concentration of Fe at Sandpan was identified in sample points SPX3, SPC, and SPY3. At all four sites, the lowest concentrations of trace elements tended to always be towards the edges of the site.

The sites characterised as dams also contained similar spatial distribution patterns to each other. The greatest concentrations of trace elements at Homestead Dam, Middle Lake, Civic Lake, Kleinfontein Dam, and van Ryn Dam, were all identified in samples from the centre of the site towards the dam wall. For samples HDY2, and HDC, which were more in the middle of Homestead Dam, the greatest trace element concentrations were for Mn and Fe. A similar distribution took place at both Kleinfontein Dam and van Ryn Dam, with samples KDX2, KDC, KDX3, and VRDX2, VRDX3, VRDC, and VRDX4 respectively, containing the greatest concentrations of Fe and Mn. The sample point CLX2 which was closer towards the outflow point of Civic Lake contained the greatest concentrations of trace elements such as Fe, Mn, and Zn.

To better visualise such spatial patterns, dot density maps were also created. These maps expressed similar patterns to the PCA graphs for the majority of the sites. The dot density maps showed that the majority of the pans shared similar spatial patterns for various trace element concentrations. Compared to this the dams, except for Civic all expressed similar patterns to each other, with the greatest trace element

concentrations being identified at the deepest points. The XRF data were further analysed using ANOVA, to identify the significant differences of average trace element concentrations at each site.

6.5. Objective 4: To establish the difference between lakes/pans/dams' trace element concentrations

The ANOVA was used to identify the main difference in average trace element concentrations of each site. ANOVA was used to give a more comprehensive understanding of the spatial distribution of contaminants across the entire area. The main purpose of this was to also give greater importance as to whether the tailings dams and mine dumps had a significant impact on the trace element concentrations in the sites across Benoni. A significant difference in average As, Cr, Cu, Fe, Mn, Ni, Pb, S, and Zn concentrations were identified specifically for Amata Pan when compared to the remaining sites. There was a no significant difference between the remaining eight sites for average concentrations of As, Cu, Ni, and Zn. In comparison, the greatest concentrations of minerals such as Ca and K ions were identified in Korsman Pan, Bullfrog Pan, and Sandpan.

Further analysis of the spatial distribution of trace elements across the area, came from developing an understanding of the spatial distribution of trace elements along the four dams, Homestead Dam, Middle Lake, Civic Lake, and Kleinfontein lake, which fell along the same river gradient. It was identified that there was a slight increase of concentrations from the upstream of the gradient, at Homestead Dam, to downstream, at Kleinfontein Dam, for trace elements such as As, Cu, Pb, and Zn, while a decrease in Mn and V were also identified. Determining the distribution

along the same river gradient aided understanding the greater spatial distribution across the entire area.

Determining the spatial distribution of trace elements across Benoni was closely linked to the influence of several tailings dams and mine dumps identified towards the city centre. Through analysis of the varying trace element concentrations across all nine sites, it was established, that, barring Amata Pan, concentrations of trace elements associated with gold mining tended to increase closer towards the tailings dams and mine dumps. However, in considering this, it was also taken into account the various other local sources, identified within urban areas, that could impact trace element concentrations across the entire region. One site, Amata Pan, was possibly more influenced by more immediate sources of trace element contamination, than the other sites. At this site, it was established, according to anecdotal evidence, that the local springs manufacturing industry which was found along the northern banks of the pan, used to regularly allow seepage of oil, a major source of trace elements, into the site.

6.6. Recommendations

The main focus of this research study was to identify the spatial distribution of trace element contaminants associated with gold mining in lakes, dams, and pans across the city of Benoni. However, there is more that could have been accomplished given more time and resources. Further research should look at the extent to which the trace elements identified in this research affects the various benthic, plants, fish, and bird species found at all the sites. This is especially crucial for the four pans which act as natural habitats for many bird species. A better understanding of the

effect these trace elements have on local food chains is extremely important. Better research into the trace element concentrations of the water column could be done, with further research possibly developing a more in-depth look across each site, as well as using more sensitive analytical methods such as ICP-MS. Importantly, it would be interesting to see further studies looking at the possible effect that these trace element concentrations have on the local community who interact with some of the various dams for recreational purposes. Furthermore, future research could look at the impact the removal of the tailings dams and mine dumps have on the same sites, drawing a comparison to what has already taken place.

6.7. Synthesis

From the beginning, this research set out to create a comprehensive understanding of the spatial distribution of trace element contaminants in lakes, dams, and pans across the Benoni City region, something that had never been done before. In order to understand the spatial distribution of trace elements across the entire region, one would need to develop an understanding of the local distribution of trace elements at each site. This was done by the collection and analysis of multiple sediment samples from each individual site. These samples were used to understand the spatial distribution of trace elements within each site, which then aided in understanding the greater distribution of trace elements across the City of Benoni. Based on the spatial distribution, the research aimed to identify if there was any influence of a collection of tailings dams and mine dumps towards the city centre. The level of influence of such tailings dams and mine dumps was determined to decrease the further away the site was. Their influence on specific sites was also

based on the predominant wind directions within the region. Therefore, it can be stated that there is some form of influence by these tailings dams and mine dumps in the majority of sites within the Benoni city region. Furthermore, the difference in concentration of trace elements, and therefore contamination of pans versus dams in the area, with the latter being more contaminated than the former, is important to understand. These differences highlight the importance of local direct contamination to individual sites, as some sites, for example, Homestead Dam compared to Sandpan, tended to be more contaminated based on local sources than others. Through further research, the impact these trace elements have on the local environment could be determined.

REFERENCE LIST

References

Abdi, H. and Williams, L.J., 2010. Principal component analysis. *Wiley interdisciplinary reviews: computational statistics*, *2*(4), 433-459.

Abiye, T.A., 2014. Mine water footprint in the Johannesburg area, South Africa: an analysis based on existing and measured data. *South African Journal of Geology*, *117*(1), pp.87-96.

Agangi, A., Hofmann, A., Rollion-Bard, C., Marin-Carbonne, J., Cavalazzi, B., Large, R. and Meffre, S., 2015. Gold accumulation in the Archaean Witwatersrand Basin, South Africa—Evidence from concentrically laminated pyrite. *Earth-science reviews*, *140*, 27-53.

Akcil, A. and Koldas, S., 2006. Acid Mine Drainage (AMD): causes, treatment and case studies. *Journal of Cleaner Production*, *14*(12), 1139-1145.

Alamdar, A., Eqani, S.A.M.A.S., Hanif, N., Ali, S.M., Fasola, M., Bokhari, H., Katsoyiannis, I.A. and Shen, H., 2017. Human exposure to trace metals and arsenic via consumption of fish from river Chenab, Pakistan and associated health risks. *Chemosphere*, *168*, 1004-1012.

Allinson, G., Zhang, P., Bui, A., Allinson, M., Rose, G., Marshall, S. and Pettigrove, V., 2015. Pesticide and trace metal occurrence and aquatic benchmark exceedances in surface waters and sediments of urban wetlands and retention ponds in Melbourne, Australia. *Environmental Science and Pollution Research*, *22*(13), pp.10214-10226.

Alyazichi, Y.M., Jones, B.G. and McLean, E., 2015. Source identification and assessment of sediment contamination of trace metals in Kogarah Bay, NSW, Australia. *Environmental Monitoring and Assessment*, *187*(2), 20.

Anawar, H.M., Rengel, Z., Damon, P. and Tibbett, M., 2018. Arsenic-phosphorus interactions in the soil-plant-microbe system: Dynamics of uptake, suppression and toxicity to plants. *Environmental Pollution*, *233*, 1003-1012.

Andes, L.C. and Cox, A.L., 2017. Rectilinear inverse distance weighting methodology for bathymetric cross-section interpolation along the Mississippi River. *Journal of Hydrologic Engineering*, *22*(7), 04017014.

Ashton, P.J. and Schoeman, F.R., 1983. Limnological studies on the Pretoria Salt Pan, a hypersaline maar lake. *Hydrobiologia*, *99*(1), 61-73.

Bain, R.E., Gundry, S.W., Wright, J.A., Yang, H., Pedley, S. and Bartram, J.K., 2012. Accounting for water quality in monitoring access to safe drinking-water as part of the Millennium Development Goals: lessons from five countries. *Bulletin of the World Health Organization*, 90, 228-235.

Barbieri, M., 2016. The importance of enrichment factor (EF) and geoaccumulation index (Igeo) to evaluate the soil contamination. *J Geol Geophys*, *5*(237),2.

Bello-Pineda, J. and Hernández-Stefanoni, J.L., 2007. Comparing the performance of two spatial interpolation methods for creating a digital bathymetric model of the Yucatan submerged platform. *Pan-American Journal of Aquatic Sciences*, *2*(3), 247-254.

Benson, N.U., Anake, W.U., Essien, J.P., Enyong, P. and Olajire, A.A., 2017. Distribution and risk assessment of trace metals in Leptodius exarata, surface water and sediments from Douglas Creek in the Qua Iboe Estuary. *Journal of Taibah University For Science*, *11*(3), 434-449.

Besser, J.M., Brumbaugh, W.G. and Ingersoll, C.G., 2015. Characterizing toxicity of metal-contaminated sediments from mining areas. *Applied Geochemistry*, *57*, 73-84.

Blais, J.M. and Kalff, J., 1995. The influence of lake morphometry on sediment focusing. *Limnology and Oceanography*, 40(3), 582-588.

Blight, G.E., 2007. Wind erosion of tailings dams and mitigation of the dust nuisance. *Journal of the Southern African Institute of Mining and Metallurgy*, *107*(2), 99-107.

Blott, S.J. and Pye, K., 2012. Particle size scales and classification of sediment types based on particle size distributions: Review and recommended procedures. *Sedimentology*, *59*(7), 2071-2096.

Bruker, 20178. The Final face of: fussed vs pressed pellets.

Available from: www.bruker-axs.com (Date Accessed: 6/04/2018)

Burger, M., van Vuren, J.H.J., de Wet, L. and Nel, A., 2019. A comparison of water quality and macroinvertebrate community structure in endorheic depression wetlands and a salt pan in the Gauteng province, South Africa. *Environmental Monitoring and Assessment*, 191(1), 14.

Burt, J.E., Barber, G.M. and Rigby, D.L., 2009. *Elementary statistics for geographers*. Guilford Press, New York.

Burton Jr, G.A., 2002. Sediment quality criteria in use around the world. *Limnology*, 3(2), 65-76.

Canfield, T.J., Kemble, N.E., Brumbaugh, W.G., Dwyer, F.J., Ingersoll, C.G. and Fairchild, J.F., 1994. Use of benthic invertebrate community structure and the sediment quality triad to evaluate metal-contaminated sediment in the upper Clark Fork River, Montana. *Environmental Toxicology and Chemistry*, *13*(12), 1999-2012.

Chhabra, R., 2017. *Soil salinity and water quality*. Routledge.

Coetzee, H., Wade, P. and Winde, F., 2002. Reliance on existing wetlands for pollution control around the Witwatersrand gold/uranium mines of South Africa-Are they sufficient?. In *Uranium in the Aquatic Environment: Proceedings of the International Conference Uranium Mining and Hydrogeology III and the International Mine Water Association Symposium Freiberg, Germany* (59-64). Springer Berlin Heidelberg.

Combi, T., Pintado-Herrera, M.G., Lara-Martin, P.A., Miserocchi, S., Langone, L. and Guerra, R., 2016. Distribution and fate of legacy and emerging contaminants along the Adriatic Sea: a comparative study. *Environmental Pollution*, 218, 1055-1064.

Costello, D.M., Hammerschmidt, C.R. and Burton, G.A., 2015. Copper sediment toxicity and partitioning during oxidation in a flow-through flume. *Environmental Science & Technology*, *49*(11), 6926-6933.

Coward, M.P., Spencer, R.M. and Spencer, C.E., 1995. Development of the Witwatersrand Basin, South Africa. *Geological Society, London, Special Publications*, *95*(1), 243-269.

Curtarelli, M., Leão, J., Ogashawara, I., Lorenzzetti, J. and Stech, J., 2015. Assessment of spatial interpolation methods to map the bathymetry of an Amazonian hydroelectric reservoir to aid in decision making for water management. *ISPRS International Journal of Geo-Information*, *4*(1), 220-235.

Davis, M.B. and Ford, M.S., 1982. Sediment focusing in Mirror Lake, New Hampshire. *Limnology and Oceanography*, 27(1), 137-150.

de Castro-Català, N., Kuzmanovic, M., Roig, N., Sierra, J., Ginebreda, A., Barceló, D., Pérez, S., Petrovic, M., Picó, Y., Schuhmacher, M. and Muñoz, I., 2016. Ecotoxicity of sediments in rivers: Invertebrate community, toxicity bioassays and the toxic unit approach as complementary assessment tools. *Science of the Total Environment*, *540*, 297-306.

de Klerk, A.R., De Klerk, L.P., Chamier, J. and Wepener, V., 2012. Seasonal variations of water and sediment quality parameters in endorheic reed pans on the Mpumalanga Highveld. *Water SA*, *38*(5), 663-672.

de Klerk, A.R., de Klerk, L.P., Oberholster, P.J., Ashton, P.J., Dini, J.A. and Holness, S.D., 2016. *A review of depressional wetlands (pans) in South Africa, including a water quality classification system*. Water Research Comission Report No 2230/1/16, Gezina, South Africa.

de Necker, L., Ferreira, M., van Vuren, J.H.J. and Malherbe, W., 2016. Aquatic invertebrate community structure of selected endorheic wetlands (pans) in South Africa. *Inland Waters*, 6(3), 303-313.

[a]Department of Water Affairs and Forestry, South Africa (DWAF), 1996. *South African Water Quality Guidelines. Vol. 7: Aquatic Ecosystems.* Department of Water Affairs and Forestry, Pretoria, South Africa.

[b]Department of Water Affairs and Forestry, South Africa (DWAF), 1996. *South African Water Quality Guidelines. Vol. 8: Field Guide.* Department of Water Affairs and Forestry, Pretoria, South Africa.

du Toit, A.L., 1927. *The geology of South Africa*. Oliver and Boyd, Edinburgh.

Durand, J.F., 2012. The impact of gold mining on the Witwatersrand on the rivers and karst system of Gauteng and North West Province, South Africa. *Journal of African Earth Sciences*, 68,24-43

Duthie A, editor. 1999. Ecoregional typing for wetland ecosystems. Resource directed measures for water resource protection: wetland ecosystems. Department of Water Affairs and Forestry, South Africa.

Dyson, L.L., 2015. A heavy rainfall sounding climatology over Gauteng, South Africa, using self-organising maps. *Climate dynamics*, *45*(11-12), 3051-3065.

Dyson, L.L., Van Heerden, J. and Sumner, P.D., 2015. A baseline climatology of sounding-derived parameters associated with heavy rainfall over Gauteng, South Africa. *International Journal of Climatology*, *35*(1), 114-127.

Edokpayi, J., Odiyo, J., Popoola, O. and Msagati, T., 2016. Assessment of trace metals contamination of surface water and sediment: A case study of Mvudi River, South Africa. *Sustainability*, *8*(2), 135.

Fanelli, R.M. and Lautz, L.K., 2008. Patterns of water, heat, and solute flux through streambeds around small dams. *Groundwater*, *46*(5), 671-687.

Ferreira, M., Wepener, V. and Van Vuren, J.H.J., 2012. Aquatic invertebrate communities of perennial pans in Mpumalanga, South Africa: a diversity and functional approach. *African Invertebrates*, *53*(2), 751-768.

Ferreira, I.O., Rodrigues, D.D., Santos, G.R.D. and Rosa, L.M.F., 2017. In bathymetric surfaces: IDW or kriging?. *Boletim de Ciências Geodésicas*, *23*(3), pp.493-508.

Förstner, U. and Wittmann, G.T.W., 1976. Metal accumulations in acidic waters from gold mines in South Africa. *Geoforum*, *7*(1), 41-49.

Foster, L., Malherbe, W., Ferreira, M. and Van Vuren, J.H.J., 2015. Macroinvertebrate variation in endorheic depression wetlands in North West

and Mpumalanga provinces, South Africa. *African Journal of Aquatic Science*, 40(3), 287-297.

Galloway, J.N., Thornton, J.D., Norton, S.A., Volchok, H.L. and McLean, R.A., 1982. Trace metals in atmospheric deposition: a review and assessment. *Atmospheric Environment*, 16(7), 1677-1700.

Geldenhuys, J.N., 1982. Classification of the pans of the western Orange Free State according to vegetation structure with reference to avifaunal communities. *South African Journal of Wildlife Research, 12*(2), 55-62.

Gewurtz, S.B., Shen, L., Helm, P.A., Waltho, J., Reiner, E.J., Painter, S., Brindle, I.D. and Marvin, C.H., 2008. Spatial distributions of legacy contaminants in sediments of Lakes Huron and Superior. *Journal of Great Lakes Research*, 34(1), 153-168.

Gordon, A.K. and Muller W.J., 2010. *Developing sediment quality guidelines for south Africa phase 1: Identification of international best practice and applications for South Africa to develop a research and implementation framework*. Water Research Commission Report No. KV 242/10, Gezina.

Grundling P., Linström A., Grobler R. and Engelbrecht, J., 2003. The Tevredenpan peatland complex of the Mpumalanga Lakes District. In: *International mire conservation group.* Couwenberg, J. and Joosten, H. (2007) Newsletter Issue 2007/3.

Hanif, N., Eqani, S.A.M.A.S., Ali, S.M., Cincinelli, A., Ali, N., Katsoyiannis, I.A., Tanveer, Z.I. and Bokhari, H., 2016. Geo-accumulation and enrichment

of trace metals in sediments and their associated risks in the Chenab River, Pakistan. *Journal of Geochemical Exploration*, 165, 62-70.

Harding, W.R., 2015. Living with eutrophication in South Africa: a review of realities and challenges. *Transactions of the Royal Society of South Africa*, 70(2), 155-171.

Hart, R.C. and Appleton, C.C., 1997. A limnological synopsis of Bhangazi south, a dystrophic coastal lake in the greater St Lucia Wetland Park (KwaZulu-Natal), with comments on its conservation value. *Southern African Journal of Aquatic Science*, *23*(2), 34-54.

Haydar, S., Arshad, M. and Aziz, J.A., 2016. Evaluation of drinking water quality in urban areas of Pakistan: A case study of Southern Lahore. *Pakistan Journal of Engineering and Applied Sciences*.

Hermann, R. and Neumann-Mahlkau, P., 1985. The mobility of zinc, cadmium, copper, lead, iron and arsenic in ground water as a function of redox potential and pH. *Science of the Total Environment*, *43*(1-2), 1-12.

Howard, I.C., Azuatola, O.D. and Abiodun, I.K., 2017. Investigation on impacts of artisanal refining of crude oil on river bed sediments. *Our Nature*, *15*(1-2), 34-43.

Huang, X., Olmez, I., Aras, N.K. and Gordon, G.E., 1994. Emissions of trace elements from motor vehicles: potential marker elements and source composition profile. *Atmospheric Environment*, *28*(8), 1385-1391.

Hui, W., Lina, S., Zhe, L. and Qing, L., 2017. Spatial Distribution and Seasonal Variations of Heavy Metal Contami-nation in Surface Waters of Liaohe River, Northeast China. *Chinese Geographical Science 27*(1), pp.52-62.

Humphries, M.S., McCarthy, T.S. and Pillay, L., 2017. Attenuation of pollution arising from acid mine drainage by a natural wetland on the Witwatersrand. *South African Journal of Science*, *113*(1-2), 1-9.

Hutchinson, G.E., Pickford, G.E., and Schuurman, J.F.M., 1932. A contribution to the hydrobiology of pans and inland waters of South Africa. *Archiv fur Hydrobiologie,* 24**,** 1-154.

Islam, M.S., Han, S., AHMED, M.K. and Masunaga, S., 2014. Assessment of trace metal contamination in water and sediment of some rivers in Bangladesh. *Journal of Water and Environment Technology*, *12*(2), 109-121.

Islam, M.S., Ahmed, M.K., Raknuzzaman, M., Habibullah-Al-Mamun, M. and Islam, M.K., 2015. Heavy metal pollution in surface water and sediment: a preliminary assessment of an urban river in a developing country. *Ecological Indicators*, *48*, 282-291.

Jansson, R., Nilsson, C. and Renöfält, B., 2000. Fragmentation of riparian floras in rivers with multiple dams. *Ecology*, *81*(4),899-903.

Jung, H.B., Yun, S.T., Mayer, B., Kim, S.O., Park, S.S. and Lee, P.K., 2005. Transport and sediment–water partitioning of trace metals in acid mine

drainage: an example from the abandoned Kwangyang Au–Ag mine area, South Korea. *Environmental Geology*, *48*(4-5), 437-449.

Kargar, M., Clark, O.G., Hendershot, W.H., Jutras, P. and Prasher, S.O., 2015. Immobilization of trace metals in contaminated urban soil amended with compost and biochar. *Water, Air, & Soil Pollution*, *226*(6), 191.

Kavcar, P., Sofuoglu, A. and Sofuoglu, S.C., 2009. A health risk assessment for exposure to trace metals via drinking water ingestion pathway. *International Journal of Hygiene and Environmental Health*, *212*(2), 216-227.

Kleinhans, I. and Van Rooy, J.L., 2016. Guidelines for sinkhole and subsidence rehabilitation based on generic geological models of a dolomite environment on the East Rand, South Africa. *Journal of African Earth Sciences*, *117*, 86-101.

Kossoff, D., Hudson-Edwards, K.A., Dubbin, W.E. and Alfredsson, M.A., 2011. Incongruent weathering of Cd and Zn from mine tailings: a column leaching study. *Chemical Geology*, *281*(1-2), 52-71.

[a]Kossoff, D., Hudson-Edwards, K.A., Dubbin, W.E. and Alfredsson, M., 2012. Major and trace metal mobility during weathering of mine tailings: implications for floodplain soils. *Applied Geochemistry*, *27*(3), 562-576.

[b]Kossoff, D., Hudson-Edwards, K.A., Dubbin, W.E., Alfredsson, M. and Geraki, T., 2012. Cycling of As, P, Pb and Sb during weathering of mine tailings: implications for fluvial environments. *Mineralogical Magazine*, *76*(5), 1209-1228.

Kossoff, D., Dubbin, W.E., Alfredsson, M., Edwards, S.J., Macklin, M.G. and Hudson-Edwards, K.A., 2014. Mine tailings dams: characteristics, failure, environmental impacts, and remediation. *Applied Geochemistry*, *51*, 229-245.

Krbetschek, M.R., Götze, J., Irmer, G., Rieser, U. and Trautmann, T., 2002. The red luminescence emission of feldspar and its wavelength dependence on K, Na, Ca–composition. *Mineralogy and Petrology*, *76*(3-4), 167-177.

Kříbek, B., Majer, V., Pašava, J., Kamona, F., Mapani, B., Keder, J. and Ettler, V., 2014. Contamination of soils with dust fallout from the tailings dam at the Rosh Pinah area, Namibia: Regional assessment, dust dispersion modelling and environmental consequences. *Journal of Geochemical Exploration*, *144*, 391-408.

Large, R.R., Danyushevsky, L., Hollit, C., Maslennikov, V., Meffre, S., Gilbert, S., Bull, S., Scott, R., Emsbo, P., Thomas, H. and Singh, B., 2009. Gold and trace element zonation in pyrite using a laser imaging technique: implications for the timing of gold in orogenic and Carlin-style sediment-hosted deposits. *Economic Geology*, *104*(5), 635-668

La Colla, N.S., Botté, S.E., Oliva, A.L. and Marcovecchio, J.E., 2017. Tracing Cr, Pb, Fe and Mn occurrence in the Bahía Blanca estuary through commercial fish species. *Chemosphere*, *175*, 286-293.

Lee Jr, R.E. and Von Lehmden, D.J., 1973. Trace metal pollution in the environment. *Journal of the Air Pollution Control Association*, *23*(10), 853-857.

Legleiter, C.J., Kyriakidis, P.C., McDonald, R.R. and Nelson, J.M., 2011. Effects of uncertain topographic input data on two-dimensional flow modelling in a gravel-bed river. *Water Resources Research*, *47*(3), 1-24.

Lehner, B., Liermann, C.R., Revenga, C., Vörösmarty, C., Fekete, B., Crouzet, P., Döll, P., Endejan, M., Frenken, K., Magome, J. and Nilsson, C., 2011. High-resolution mapping of the world's reservoirs and dams for sustainable river-flow management. *Frontiers in Ecology and the Environment*, *9*(9), 494-502.

Leistner, O.A., 1967. The plant geology of the southern Kalahari. *Memoirs of the Botanical Survey of South Africa,* 38**,** 1-172.

Lessard, J.L. and Hayes, D.B., 2003. Effects of elevated water temperature on fish and macroinvertebrate communities below small dams. *River Research and Applications*, *19*(7), 721-732.

Le Roux, J.J., Newby, T.S. and Sumner, P.D., 2007. Monitoring soil erosion in South Africa at a regional scale: review and recommendations. *South African Journal of Science*, *103*(7-8), 329-335.

Le Roux, J.J., Morgenthal, T.L., Malherbe, J., Pretorius, D.J. and Sumner, P.D., 2008. Water erosion prediction at a national scale for South Africa. *Water SA*, *34*(3), 305-314.

Le Roux, J.J. and Sumner, P.D., 2012. Factors controlling gully development: comparing continuous and discontinuous gullies. *Land Degradation & Development*, *23*(5), 440-449.

Linos, A., Petralias, A., Christophi, C.A., Christoforidou, E., Kouroutou, P., Stoltidis, M., Veloudaki, A., Tzala, E., Makris, K.C. and Karagas, M.R., 2011. Oral ingestion of hexavalent chromium through drinking water and cancer mortality in an industrial area of Greece-An ecological study. *Environmental Health*, *10*(1), 50.

Liu, S., Wang, C., Yang, J. and Zhao, Q., 2014. Assessing the heavy metal contamination of soils in the water-level fluctuation zone upstream and downstream of the Manwan Dam, Lancang River. *Journal of Soils and Sediments*, *14*(6), 1147-1157.

Long, E.R. and Morgan, L.G., 1990. The potential for biological effects of sediments-sorbed contaminants tested in the National Status and Trends Program. National Oceanic and Atmospheric Administration.

Lopez-Paz, D., Sra, S., Smola, A., Ghahramani, Z. and Schölkopf, B., 2014. Randomized nonlinear component analysis. In *International Conference on Machine Learning*, 1359-1367.

MacDonald, D.D., Ingersoll, C.G. and Berger, T.A., 2000. Development and evaluation of consensus-based sediment quality guidelines for freshwater ecosystems. Archives of Environmental Contamination and Toxicology, 39(1), 20-31.

Mantel, S.K., Hughes, D.A. and Muller, N.W., 2010. Ecological impacts of small dams on South African rivers Part 1: drivers of change-water quantity and quality. *Water Sa*, *36*(3), 351-360.

Marchand, E.A. and Dinkelman, I., 2006. Minerals and mine drainage. *Water Environment Research*, *78*(10), 1654-1698.

McCarthy, T.S., 2011. The impact of acid mine drainage in South Africa. *South African Journal of Science*, *107*(5-6), 01-07.

McCarthy, T.S. and Humphries, M.S., 2013. Contamination of the water supply to the town of Carolina, Mpumalanga, January 2012. *South African Journal of Science*, *109*(9-10), 01-10.

Morales-Marin, L.A., French, J.R., Burningham, H. and Battarbee, R.W., 2018. Three-dimensional hydrodynamic and sediment transport modeling to test the sediment focusing hypothesis in upland lakes. *Limnology and Oceanography*, 63(S1), S156-S176.

Moreno-Amich, R. and Garcia-Berthou, E., 1989. A new bathymetric map based on echo-sounding and morphometrical characterization of the Lake of Banyoles (NE-Spain). *Hydrobiologia*, *185*(1), 83-90.

Muller, G., 1979. Schwermetalle in den sedimenten des Rheins-VeraÈnderungenseit. Umschau 79: 778–783.

Munyangane, P., Mouri, H. and Kramers, J., 2016. Assessment of some potential harmful trace elements (PHTEs) in the borehole water of Greater Giyani,

Limpopo Province, South Africa: possible implications for human health. *Environmental Geochemistry and Health*, 1-19.

Mustajärvi, L., Eek, E., Cornelissen, G., Eriksson-Wiklund, A.K., Undeman, E. and Sobek, A., 2017. In situ benthic flow-through chambers to determine sediment-to-water fluxes of legacy hydrophobic organic contaminants. *Environmental Pollution*, 231, 854-862.

Naicker, K., Cukrowska, E. and McCarthy, T.S., 2003. Acid mine drainage arising from gold mining activity in Johannesburg, South Africa and environs. *Environmental Pollution*, *122*(1), 29-40.

**National GeoSpatial Institute

Ncube, E.J. and Schutte, C.F., 2005. The occurrence of fluoride in South African groundwater: A water quality and health problem. *Water SA*, *31*(1), 35-40.

Nolakana, P., Siad, A. and Solomon, H., 2017. Evaluation of groundwater suitability for domestic and irrigational purposes in newcastle, kwazulu-natal, south africa. visnyk of taras shevchenko national university of kyiv-geology, (1), 76-84.

Norrish, K. and Hutton, J. T. 1969. An accurate X-ray spectrographic method for the analysis of geologic samples. Geochemica et Cosmochimica Acta 33, 431-454.

Nwaila, G., Frimmel, H.E. and Minter, W.E., 2017. Provenance and Geochemical Variations in Shales of the Mesoarchean Witwatersrand Supergroup. *The Journal of Geology*, *125*(4), 399-422.

Pan, Y.P. and Wang, Y.S., 2015. Atmospheric wet and dry deposition of trace elements at 10 sites in Northern China. *Atmospheric Chemistry and Physics*, *15*(2), pp.951-972.

Park, C. and Allaby, M., 2017. *A Dictionary of Environment and Conservation, 3rd edition*. Oxford University Press, Oxford.

Persaud, D., Jaagumagi, R. and Hayton, A., 1993. Guidelines for the protection and management of aquatic sediment quality in Ontario. Water Resources Branch, Ontario Ministry of the Environment, Toronto, 27

Oberholster, P.J., 2010: The current status of water quality in South Africa – A Review/ In: CSIR. *A CSIR Perspective on Water in South Africa* – 2010. CSIR Report No. CSIR/NRE/PW/IR/2011/0012/A, 8-17.

Oberholster, P.J. and Ashton, P.J., 2008. State of the nation report: An overview of the current status of water quality and eutrophication in South African rivers and reservoirs. *Parliamentary Grant Deliverable. Pretoria: Council for Scientific and Industrial Research (CSIR).*

Oberholster, P.J., Myburgh, J.G., Ashton, P.J. and Botha, A.M., 2010. Responses of phytoplankton upon exposure to a mixture of acid mine drainage and high levels of nutrient pollution in Lake Loskop, South Africa. *Ecotoxicology and Environmental Safety*, *73*(3), 326-335.

Oelofse, S.H.H., Hobbs, P.J., Rascher, J. and Cobbing, J.E., 2007, December. The pollution and destruction threat of gold mining waste on the Witwatersrand: A West Rand case study. In *10th International Symposium on Environmental Issues and Waste management in Energy and Mineral Production (SWEMP, 2007), Bangkok* (pp. 11-13).

Olesik, J.W., 1991. Elemental analysis using ICP-OES and ICP/MS. *Analytical Chemistry*, *63*(1), pp.12A-21A.

Olsen, M., Fjeld, E. and Lydersen, E., 2019. The influence of a submerged meadow on uptake and trophic transfer of legacy mercury from contaminated sediment in the food web in a brackish Norwegian fjord. *Science of The Total Environment*, 654, 209-217.

Palamuleni, L. and Akoth, M., 2015. Physico-chemical and microbial analysis of selected borehole water in Mahikeng, South Africa. *International journal of environmental research and public health*, *12*(8), 8619-8630.

Paul, M.J. and Meyer, J.L., 2001. Streams in the urban landscape. *Annual review of Ecology and Systematics*, 32, 333-365.

Richter, T.O., Van der Gaast, S., Koster, B., Vaars, A., Gieles, R., de Stigter, H.C., De Haas, H. and van Weering, T.C., 2006. The Avaatech XRF Core Scanner: technical description and applications to NE Atlantic sediments. *Geological Society, London, Special Publications*, *267*(1), 39-50.

Robb, L.J. and Meyer, F.M., 1995. The Witwatersrand Basin, South Africa: geological framework and mineralization processes. *Ore Geology Reviews*, *10*(2), 67-94.

Rösner, T. and van Schalkwyk, A., 2002. The environmental impact of gold mine tailings footprints in the Johannesburg region, South Africa. *Bulletin of Engineering Geology and the Environment*, *59*(2), 137-148.

Roychoudhury, A.N. and Starke, M.F., 2006. Partitioning and mobility of trace metals in the Blesbokspruit: Impact assessment of dewatering of mine waters in the East Rand, South Africa. *Applied Geochemistry*, *21*(6), 1044-1063.

Ruiz, F., 2001. Trace metals in estuarine sediments from the southwestern Spanish coast. *Marine Pollution Bulletin*, *42*(6), 481-489.

Seaman, M.T., Ashton, P.J. and Williams, W.D. 1991. Inland salt waters of southern Africa. *Hydrobiologia*, 210, 75-91.

Seutloali, K.E. and Beckedahl, H.R., 2015. Understanding the factors influencing rill erosion on roadcuts in the south eastern region of South Africa. *Solid Earth*, *6*(2), 633.

***South African Weather Service (1997 – 2017)

Stanley, E.H., Luebke, M.A., Doyle, M.W. and Marshall, D.W., 2002. Short-term changes in channel form and macroinvertebrate communities following low-head dam removal. *Journal of the North American Benthological Society*, 21(1), 172-187.

Taylor, M. and Brown Jr, G.E., 1979. Structure of mineral glasses—I. The feldspar glasses NaAlSi3O8, KAlSi3O8, CaAl2Si2O8.*Geochimica et Cosmochimica Acta*, *43*(1), 61-75.

Turekian, K.K., 1972. *Chemistry of the Earth. Holt,* Rinehart and Winston, New York.

Turton, A., Schultz, C., Buckle, H., Kgomongoe, M., Malungani, T. and Drackner, M., 2006. Gold, scorched earth and water: the hydropolitics of Johannesburg. *Water Resources Development*, *22*(2), 313-335.

Tutu, H., McCarthy, T.S. and Cukrowska, E., 2008. The chemical characteristics of acid mine drainage with particular reference to sources, distribution and remediation: The Witwatersrand Basin, South Africa as a case study. *Applied Geochemistry*, *23*(12), 3666-3684.

Umemura, T. and Wako, Y., 2006. Pathogenesis of osteomalacia in itai-itai disease. *Journal of Toxicologic Pathology*, *19*(2), 69-74.

Väänänen, K., Leppänen, M.T., Chen, X. and Akkanen, J., 2018. Metal bioavailability in ecological risk assessment of freshwater ecosystems: From science to environmental management. *Ecotoxicology and Environmental Safety*, *147*, 430-446.

van Emden, H., 2009. *Statistics for terrified biologists*. Blackwell Publishers, Oxford

van Niekerk, H., Silberbauer, M.J. and Hohls, B.C., 2009. Monitoring programme revision highlights long-term salinity changes in selected South African rivers and the value of comprehensive long-term data sets. *Environmental Monitoring and Assessment*, 154(1-4), 401-411.

Varol, M., 2013. Dissolved heavy metal concentrations of the Kralkızı, Dicle and Batman dam reservoirs in the Tigris River basin, Turkey. *Chemosphere*, *93*(6), 954-962.

Vidal-Durà, A., Burke, I.T., Stewart, D.I. and Mortimer, R.J., 2018. Reoxidation of estuarine sediments during simulated resuspension events: Effects on nutrient and trace metal mobilisation.*Estuarine, Coastal and Shelf Science*, *207*, .40-55.

Wang, H., Sun, L., Liu, Z. and Luo, Q., 2017. Spatial distribution and seasonal variations of heavy metal contamination in surface waters of Liaohe River, Northeast China. *Chinese Geographical Science*, *27*(1), 52-62.

Weltje, G.J. and Tjallingii, R., 2008. Calibration of XRF core scanners for quantitative geochemical logging of sediment cores: theory and application. *Earth and Planetary Science Letters*, *274*(3), 423-438.

World Commission on Dams, 2000. *Dams and development: A new framework for decision-making: The report of the world commission on dams*. Earthscan, London.

World Health Organisation (WHO), 2011. Guidelines for drinking-water quality. *WHO chronicle*, *38*(4), 104-8.

Wronkiewicz, D.J. and Condie, K.C., 1990. Geochemistry and mineralogy of sediments from the Ventersdorp and Transvaal Supergroups, South Africa: cratonic evolution during the early Proterozoic. *Geochimica et Cosmochimica Acta*, *54*(2), 343-354.

Yacoub, C., Blazquez, N., Pérez-Foguet, A. and Miralles, N., 2013. Spatial and temporal trace metal distribution of a Peruvian basin: recognizing trace metal sources and assessing the potential risk. *Environmental Monitoring and Assessment*, *185*(10), 7961-7978.

Yang, H., Rose, N.L., Battarbee, R.W. and Boyle, J.F., 2002. Mercury and lead budgets for Lochnagar, a Scottish mountain lake and its catchment. *Environmental Science & Technology*, 36(7), pp.1383-1388.

Yapiyev, V., Sagintayev, Z., Inglezakis, V., Samarkhanov, K. and Verhoef, A., 2017. Essentials of endorheic basins and lakes: a review in the context of current and future water resource management and mitigation activities in Central Asia. *Water*, 9(10), 798.

Yetman, C.A., 2018. What you need to know about Bullfrogs. Endangered Wildlife Trust. Available from: https://www.ewt.org.za/TAP/pdf/Bullfrog%20booklet.pdf (Accessed 2019)

Available from:(Accessed 2019)

YSI Incorporated 2009. *YSI professional plus: user manual*. United States of America. YSI Incorporated.

Available from:

https://www.ysi.com/File%20Library/Documents/Manuals/605596-YSI-ProPlus-User-Manual-RevD.pdf (Accessed 2018)

Zaaboub, N., Martins, M.V.A., Dhib, A., Béjaoui, B., Galgani, F., El Bour, M. and Aleya, L., 2015. Accumulation of trace metals in sediments in a Mediterranean Lagoon: usefulness of metal sediment fractionation and elutriate toxicity assessment. *Environmental Pollution*, *207*, 226-237.

.

APPENDICES

APPENDIX 1: The Initial Measured Depth Data used to Create the Bathymetric Maps

Table A1: Depth Measurements for Korsman Pan

Sample	Lat	Long	Depth (m)	Sample	Lat	Long	Depth (m)	Sample	Lat	Long	Depth (m)	Sample	Lat	Long	Depth (m)
KPX1	-26.19089	28.29581	0.1	35	-26.19389	28.29164	1.1	103	-26.19372	28.29725	0.1	169	-26.1913	28.29653	0
KPX2	-26.19158	28.29497	1.2	26	-26.19444	28.29244	1.1	106	-26.19239	28.29625	0.09	168	-26.1946	28.29071	0
KPX3	-26.19458	28.29361	1.5	21	-26.19533	28.29294	1.1	86	-26.19314	28.29100	0.09	167	-26.195	28.29646	0
KPX4	-26.19578	28.29225	0.17	63	-26.18983	28.29508	1	115	-26.18958	28.29303	0.08	166	-26.1911	28.29101	0
KPC	-26.19317	28.29381	1.5	60	-26.19181	28.29550	1	108	-26.19133	28.29611	0.08	165	-26.1932	28.29746	0
KPY1	-26.19186	28.29127	0.23	41	-26.19192	28.29297	1	107	-26.19194	28.29675	0.08	164	-26.1929	28.29071	0
KPY2	-26.19233	28.29258	1.4	39	-26.19200	28.29208	1	85	-26.19289	28.29106	0.08	163	-26.1961	28.29516	0
KPY3	-26.19336	28.29692	1.3	27	-26.19472	28.29211	1	113	-26.18961	28.29394	0.07	162	-26.1894	28.29291	0
KPY4	-26.19442	28.29708	0.09	24	-26.19472	28.29294	1	101	-26.19514	28.29628	0.07	161	-26.1917	28.29685	0
44	-26.19286	28.29447	1.6	3	-26.19203	28.29186	1	116	-26.18983	28.29250	0.06	160	-26.1943	28.29066	0
49	-26.19381	28.29614	1.5	69	-26.19072	28.29433	0.9	112	-26.18975	28.29442	0.06	159	-26.1953	28.29653	0
48	-26.19342	28.29572	1.5	66	-26.19108	28.29486	0.9	111	-26.19000	28.29492	0.06	158	-26.1906	28.29127	0
47	-26.19333	28.29525	1.5	40	-26.19186	28.29250	0.9	96	-26.19589	28.29272	0.06	157	-26.1935	28.2975	0
45	-26.19294	28.29447	1.5	28	-26.19506	28.29222	0.9	84	-26.19247	28.29103	0.06	156	-26.1926	28.29084	0
43	-26.19250	28.29411	1.5	22	-26.19492	28.29303	0.9	118	-26.19044	28.29178	0.05	155	-26.1962	28.29472	0
19	-26.19522	28.29358	1.5	91	-26.19458	28.29092	0.8	109	-26.19103	28.29592	0.05	154	-26.1894	28.29294	0
18	-26.19461	28.29381	1.5	70	-26.19061	28.29428	0.8	104	-26.19300	28.29731	0.04	153	-26.1902	28.29539	0
17	-26.19450	28.29442	1.5	65	-26.19108	28.29506	0.8	100	-26.19556	28.29589	0.04	152	-26.1958	28.29186	0
16	-26.19519	28.29528	1.5	34	-26.19419	28.29158	0.8	117	-26.19014	28.29214	0.03	151	-26.191	28.29637	0
15	-26.19497	28.29550	1.5	30	-26.19500	28.29186	0.8	102	-26.19481	28.29656	0.03	150	-26.1949	28.29091	0
14	-26.19481	28.29572	1.5	29	-26.19525	28.29206	0.8	95	-26.19556	28.29183	0.03	149	-26.195	28.29673	0
13	-26.19453	28.29583	1.5	80	-26.19083	28.29258	0.7	114	-26.18961	28.29347	0.02	148	-26.1915	28.29087	0
11	-26.19383	28.29536	1.5	79	-26.19069	28.29281	0.7	199	-26.1895	28.29426	0	147	-26.1929	28.29742	0
10	-26.19381	28.29483	1.5	72	-26.19031	28.29397	0.7	198	-26.1897	28.29477	0	146	-26.1932	28.29062	0
7	-26.19300	28.29311	1.5	71	-26.19044	28.29417	0.7	197	-26.1961	28.29301	0	145	-26.196	28.29555	0
6	-26.19278	28.29275	1.5	33	-26.19442	28.29156	0.7	196	-26.1904	28.29575	0	144	-26.1895	28.29257	0
51	-26.19383	28.29664	1.4	23	-26.19483	28.29294	0.7	195	-26.1956	28.29159	0	143	-26.1897	28.29476	0
50	-26.19406	28.29644	1.4	2	-26.19194	28.29161	0.68	194	-26.1946	28.29713	0	142	-26.19	28.29523	0
46	-26.19306	28.29486	1.4	74	-26.19025	28.29378	0.6	193	-26.1917	28.29092	0	141	-26.1959	28.29229	0
42	-26.19219	28.29344	1.4	73	-26.19028	28.29394	0.6	192	-26.1919	28.297	0	140	-26.1908	28.29619	0
38	-26.19258	28.29197	1.4	64	-26.19111	28.29525	0.6	191	-26.1941	28.2906	0	139	-26.1952	28.29107	0
37	-26.19311	28.29186	1.4	31	-26.19506	28.29161	0.6	190	-26.1955	28.29635	0	138	-26.1949	28.29695	0
12	-26.19433	28.29606	1.4	1	-26.19186	28.29147	0.53	189	-26.1902	28.29165	0	137	-26.1909	28.29132	0
9	-26.19375	28.29422	1.4	78	-26.19036	28.29294	0.5	188	-26.1939	28.29751	0	136	-26.1926	28.29725	0
5	-26.19253	28.29236	1.4	75	-26.19019	28.29347	0.5	187	-26.1922	28.29081	0	135	-26.1935	28.2906	0
52	-26.19350	28.29664	1.3	32	-26.19489	28.29136	0.42	186	-26.1962	28.29418	0	134	-26.1957	28.29586	0
36	-26.19353	28.29167	1.3	81	-26.19106	28.29233	0.4	185	-26.1893	28.29328	0	133	-26.1897	28.29221	0
20	-26.19533	28.29308	1.3	77	-26.19017	28.29317	0.4	184	-26.1896	28.29451	0	132	-26.1944	28.29733	0
8	-26.19344	28.29403	1.3	76	-26.19011	28.29342	0.36	183	-26.1898	28.29483	0	131	-26.1921	28.29057	0
4	-26.19247	28.29253	1.3	82	-26.19122	28.29211	0.33	182	-26.1961	28.29264	0	130	-26.1962	28.29333	0
67	-26.19106	28.29458	1.2	83	-26.19133	28.29186	0.26	181	-26.1906	28.29594	0	129	-26.1894	28.29391	0
62	-26.19164	28.29472	1.2	92	-26.19461	28.29103	0.24	180	-26.1954	28.29135	0	128	-26.18969	28.29436	0
61	-26.19178	28.29522	1.2	90	-26.19428	28.29097	0.23	179	-26.1947	28.29689	0	127	-26.19178	28.29664	0
57	-26.19233	28.29572	1.2	89	-26.19428	28.29092	0.17	178	-26.1914	28.29121	0	126	-26.19197	28.29686	0
56	-26.19256	28.29586	1.2	105	-26.19300	28.29725	0.15	177	-26.1923	28.29713	0	125	-26.19214	28.29697	0
54	-26.19300	28.29639	1.2	99	-26.19578	28.29544	0.15	176	-26.1938	28.29054	0	124	-26.19225	28.29703	0
53	-26.19325	28.29667	1.2	93	-26.19489	28.29114	0.15	175	-26.1955	28.29633	0	123	-26.19394	28.29722	0
25	-26.19453	28.29253	1.2	110	-26.19036	28.29517	0.13	174	-26.19	28.29186	0	122	-26.19622	28.29394	0
68	-26.19086	28.29439	1.1	98	-26.19600	28.29514	0.13	173	-26.1941	28.29745	0	121	-26.19550	28.29150	0
59	-26.19203	28.29558	1.1	94	-26.19508	28.29125	0.12	172	-26.1924	28.2907	0	120	-26.19419	28.29733	0
58	-26.19222	28.29567	1.1	88	-26.19378	28.29089	0.12	171	-26.1963	28.29368	0	97	-26.19603	28.29406	0
55	-26.19269	28.29619	1.1	87	-26.19353	28.29092	0.11	170	-26.1894	28.29357	0				

Table A2: Depth Measurements for Amata Pan

Sample	Lat	Long	Depth (m)	Sample	Lat	Long	Depth (m)	Sample	Lat	Long	Depth (m)	Sample	Lat	Long	Depth (m)
x1	-26.20459	28.31441	1.3	87	-26.20559	28.31410	1.5	125	-26.20480	28.31411	1.3	179	-26.2072	28.31182	0
x2	-26.20678	28.31328	1.3	88	-26.20551	28.31390	1.5	126	-26.20487	28.31427	1.3	180	-26.2071	28.31186	0
c	-26.20563	28.31388	1.5	89	-26.20543	28.31369	1.5	127	-26.20493	28.31441	1.3	181	-26.2069	28.31188	0
y1	-26.20551	28.31324	1.2	95	-26.20534	28.31385	1.5	128	-26.20499	28.31456	1.3	182	-26.2068	28.31187	0
y2	-26.20612	28.31456	1.3	96	-26.20540	28.31404	1.5	129	-26.20492	28.31456	1.3	183	-26.2065	28.31187	0
65	-26.20610	28.31443	1.7	97	-26.20547	28.31421	1.5	130	-26.20483	28.31444	1.3	184	-26.2062	28.31193	0
18	-26.20652	28.31326	1.6	98	-26.20555	28.31439	1.5	131	-26.20473	28.31426	1.3	185	-26.2062	28.31193	0
31	-26.20654	28.31339	1.6	101	-26.20542	28.31438	1.5	132	-26.20466	28.31414	1.3	186	-26.2061	28.31202	0
32	-26.20660	28.31351	1.6	102	-26.20533	28.31422	1.5	133	-26.20460	28.31402	1.3	187	-26.2061	28.31202	0
33	-26.20652	28.31362	1.6	103	-26.20523	28.31398	1.5	136	-26.20452	28.31408	1.3	188	-26.2061	28.31202	0
34	-26.20648	28.31344	1.6	5	-26.20666	28.31323	1.4	1	-26.20675	28.31336	1.2	189	-26.2061	28.31203	0
35	-26.20637	28.31318	1.6	6	-26.20664	28.31311	1.4	3	-26.20673	28.31340	1.2	190	-26.2059	28.31207	0
36	-26.20629	28.31301	1.6	8	-26.20639	28.31272	1.4	38	-26.20610	28.31287	1.2	191	-26.2057	28.31214	0
40	-26.20614	28.31315	1.6	10	-26.20645	28.31290	1.4	55	-26.20588	28.31299	1.2	192	-26.2054	28.31221	0
41	-26.20620	28.31333	1.6	11	-26.20651	28.31299	1.4	114	-26.20532	28.31466	1.2	193	-26.2054	28.31236	0
42	-26.20627	28.31349	1.6	13	-26.20665	28.31325	1.4	116	-26.20523	28.31461	1.2	194	-26.2049	28.31258	0
44	-26.20641	28.31381	1.6	14	-26.20668	28.31336	1.4	124	-26.20475	28.31396	1.2	195	-26.2046	28.31268	0
45	-26.20648	28.31396	1.6	20	-26.20639	28.31295	1.4	134	-26.20453	28.31393	1.2	196	-26.2044	28.31279	0
50	-26.20629	28.31371	1.6	21	-26.20632	28.31280	1.4	135	-26.20449	28.31398	1.2	197	-26.2043	28.31291	0
51	-26.20613	28.31352	1.6	23	-26.20617	28.31258	1.4	137	-26.20458	28.31420	1.2	198	-26.2044	28.31314	0
52	-26.20607	28.31332	1.6	27	-26.20624	28.31280	1.4	138	-26.20461	28.31429	1.2	199	-26.2044	28.3134	0
59	-26.20604	28.31370	1.6	37	-26.20618	28.31286	1.4	115	-26.20527	28.31469	1.1	200	-26.2045	28.31359	0
60	-26.20609	28.31388	1.6	47	-26.20656	28.31421	1.4	139	-26.20464	28.31438	1.1	201	-26.2058	########	0
61	-26.20612	28.31404	1.6	75	-26.20543	28.31345	1.4	140	-26.20456	28.31423	1.1	202	-26.2065	28.31489	0
62	-26.20619	28.31421	1.6	83	-26.20591	28.31463	1.4	142	-26.2045	28.31364	0	203	-26.2037	28.31403	0
66	-26.20603	28.31430	1.6	84	-26.20582	28.31463	1.4	143	-26.204	28.314	0	204	-26.208	28.31324	0
67	-26.20598	28.31417	1.6	91	-26.20527	28.31332	1.4	144	-26.204	28.31396	0	205	-26.2041	28.31296	0
68	-26.20592	28.31403	1.6	93	-26.20520	28.31343	1.4	145	-26.2038	28.31409	0	206	-26.2074	28.31441	0
78	-26.20565	28.31398	1.6	100	-26.20548	28.31453	1.4	146	-26.2039	28.31418	0	207	-26.2046	28.31522	0
81	-26.20584	28.31440	1.6	106	-26.20496	28.31347	1.4	147	-26.204	28.31425	0	208	-26.2079	28.31178	0
7	-26.20661	28.31304	1.5	110	-26.20502	28.31400	1.4	148	-26.2042	28.31453	0	209	-26.2049	28.31223	0
9	-26.20642	28.31280	1.5	111	-26.20514	28.31428	1.4	149	-26.2044	28.31485	0	210	-26.2071	28.31479	0
12	-26.20659	28.31315	1.5	118	-26.20500	28.31418	1.4	150	-26.2045	28.31489	0	211	-26.2041	28.31481	0
17	-26.20657	28.31340	1.5	141	-26.20447	28.31415	1.4	151	-26.2046	28.3149	0	212	-26.208	28.31238	0
19	-26.20646	28.31311	1.5	2	-26.20674	28.31319	1.3	152	-26.2048	28.31516	0	213	-26.2042	28.31368	0
25	-26.20607	28.31249	1.5	4	-26.20670	28.31335	1.3	153	-26.205	28.31523	0	214	-26.2079	28.31405	0
28	-26.20633	28.31295	1.5	15	-26.20669	28.31340	1.3	154	-26.2052	28.31516	0	215	-26.2052	28.31536	0
29	-26.20641	28.31312	1.5	16	-26.20664	28.31349	1.3	155	-26.2058	28.315	0	216	-26.2073	28.31153	0
30	-26.20648	28.31326	1.5	22	-26.20624	28.31264	1.3	156	-26.2061	28.3149	0	217	-26.2059	28.31512	0
39	-26.20608	28.31302	1.5	24	-26.20613	28.31253	1.3	157	-26.2064	28.31482	0	218	-26.2066	28.3117	0
43	-26.20632	28.31365	1.5	26	-26.20620	28.31268	1.3	158	-26.2067	28.31474	0	219	-26.2053	28.31198	0
46	-26.20654	28.31410	1.5	54	-26.20597	28.31297	1.3	159	-26.207	28.31462	0	220	-26.2068	28.31485	0
48	-26.20651	28.31409	1.5	73	-26.20535	28.31323	1.3	160	-26.2071	28.31451	0	221	-26.2038	28.3145	0
49	-26.20642	28.31391	1.5	74	-26.20538	28.31334	1.3	161	-26.2072	28.31432	0	222	-26.208	28.31277	0
53	-26.20602	28.31313	1.5	90	-26.20534	28.31345	1.3	162	-26.2073	28.31418	0	223	-26.2042	28.31338	0
56	-26.20590	28.31314	1.5	92	-26.20517	28.31330	1.3	163	-26.2073	28.314	0	224	-26.2076	28.31411	0
57	-26.20595	28.31332	1.5	94	-26.20528	28.31365	1.3	164	-26.2074	28.31396	0	225	-26.2049	28.31542	0
58	-26.20600	28.31350	1.5	99	-26.20563	28.31456	1.3	165	-26.2074	28.31386	0	226	-26.2076	28.31158	0
63	-26.20624	28.31435	1.5	104	-26.20510	28.31373	1.3	166	-26.2075	28.31388	0	227	-26.2043	28.31257	0
64	-26.20626	28.31443	1.5	105	-26.20503	28.31356	1.3	167	-26.2076	28.31384	0	228	-26.2074	28.31466	0
69	-26.20586	28.31390	1.5	107	-26.20482	28.31351	1.3	168	-26.2077	28.31378	0	229	-26.2044	28.31508	0
70	-26.20579	28.31377	1.5	108	-26.20488	28.31366	1.3	169	-26.2078	28.31378	0	230	-26.208	28.3121	0
71	-26.20573	28.31364	1.5	109	-26.20496	28.31385	1.3	170	-26.2078	28.31377	0	231	-26.2039	28.31386	0
72	-26.20564	28.31345	1.5	112	-26.20524	28.31445	1.3	171	-26.2078	28.31305	0	232	-26.208	28.31368	0
76	-26.20549	28.31360	1.5	113	-26.20530	28.31458	1.3	172	-26.2078	28.31304	0	233	-26.2056	28.31522	0
77	-26.20557	28.31380	1.5	117	-26.20514	28.31443	1.3	173	-26.2078	28.31253	0	234	-26.207	28.31164	0
79	-26.20572	28.31416	1.5	119	-26.20493	28.31402	1.3	174	-26.2078	28.31252	0	235	-26.2062	28.31502	0
80	-26.20577	28.31427	1.5	120	-26.20482	28.31376	1.3	175	-26.2078	28.31205	0	236	-26.2061	28.31178	0
82	-26.20589	28.31453	1.5	121	-26.20473	28.31360	1.3	176	-26.2076	28.31187	0				
85	-26.20574	28.31450	1.5	122	-26.20465	28.31363	1.3	177	-26.2074	28.31175	0				
86	-26.20566	28.31433	1.5	123	-26.20467	28.31377	1.3	178	-26.2073	28.3118	0				

Table A3: Depth Measurements for Sandpan

Sample	Lat	Long	Depth (m)	Sample	Lat	Long	Depth (m)	Sample	Lat	Long	Depth (m)	Sample	Lat	Long	Depth (m)	Sample	Lat	Long	Depth (m)
x1	-26.122590	28.333360	0.24	78	-26.127557	28.338481	0.61	143	-26.122962	28.336101	0.58	45	-26.130096	28.336694	0.50	93	-26.130074	28.333496	0.18
x2	-26.124510	28.334690	0.54	86	-26.128187	28.336631	0.61	12	-26.128230	28.331990	0.57	55	-26.127939	28.339413	0.50	34	-26.125261	28.334652	0.13
x3	-26.127849	28.335717	0.62	98	-26.128470	28.335336	0.61	16	-26.127850	28.332410	0.57	69	-26.129771	28.335616	0.50	36	-26.125723	28.334610	0.11
x4	-26.130335	28.336769	0.23	102	-26.127252	28.336664	0.61	19	-26.127240	28.333140	0.57	54	-26.128280	28.339549	0.49	91	-26.129892	28.334716	0.09
c	-26.126660	28.335420	0.66	108	-26.126362	28.336096	0.61	27	-26.123066	28.334310	0.57	33	-26.125178	28.334643	0.48	134	-26.123776	28.336250	0.09
y1	-26.124687	28.338270	0.16	122	-26.125557	28.334715	0.61	44	-26.129504	28.336562	0.57	47	-26.130098	28.337328	0.48	145	-26.12467583	28.33830	0
y2	-26.125470	28.336760	0.69	124	-26.125172	28.335136	0.61	57	-26.128335	28.338726	0.57	48	-26.129857	28.337760	0.48	146	-26.13021333	28.3340211	0
y3	-26.128170	28.333390	0.61	139	-26.123875	28.335137	0.61	88	-26.128902	28.335791	0.57	126	-26.124736	28.335592	0.48	147	-26.12463412	28.3322326	0
y4	-26.123720	28.339380	0.25	11	-26.127930	28.332000	0.6	99	-26.128191	28.335643	0.57	8	-26.127310	28.331610	0.47	148	-26.12978011	28.3383083	0
132	-26.124120	28.336763	1.1	18	-26.127500	28.332750	0.6	112	-26.127483	28.334413	0.57	24	-26.122292	28.335039	0.46	149	-26.12235966	28.3334551	0
131	-26.124017	28.336745	0.98	29	-26.123633	28.334294	0.6	119	-26.126809	28.333550	0.57	50	-26.129600	28.338220	0.44	150	-26.13054776	28.3360425	0
81	-26.126857	28.338902	0.84	43	-26.128958	28.336365	0.6	26	-26.122754	28.334646	0.56	144	-26.122953	28.336267	0.44	151	-26.1273968	28.3314019	0
130	-26.123991	28.336722	0.81	62	-26.129351	28.337104	0.60	28	-26.123293	28.334053	0.56	7	-26.127270	28.331300	0.43	152	-26.12781507	28.3395222	0
129	-26.123970	28.336535	0.71	75	-26.128419	28.337483	0.60	39	-26.126896	28.334648	0.56	53	-26.128583	28.339457	0.43	153	-26.12196528	28.335427	0
123	-26.125427	28.334870	0.7	77	-26.127819	28.338160	0.6	64	-26.129853	28.336415	0.56	121	-26.125736	28.334526	0.43	154	-26.13005406	28.3351725	0
128	-26.124011	28.336245	0.67	84	-26.127494	28.337501	0.60	71	-26.129448	28.336100	0.56	51	-26.129334	28.338556	0.42	155	-26.12663571	28.3312754	0
10	-26.127710	28.331900	0.64	85	-26.127804	28.337132	0.60	72	-26.129276	28.336374	0.56	68	-26.129887	28.335448	0.42	156	-26.12907294	28.3392847	0
41	-26.127747	28.335185	0.64	87	-26.128487	28.336259	0.60	79	-26.127358	28.338720	0.56	106	-26.125799	28.336826	0.41	157	-26.12385261	28.3323794	0
101	-26.127554	28.336330	0.64	97	-26.128940	28.334744	0.60	111	-26.127158	28.334906	0.56	90	-26.129616	28.335011	0.40	158	-26.13011323	28.3378432	0
114	-26.127932	28.333608	0.64	100	-26.127755	28.336123	0.60	117	-26.127480	28.333006	0.56	46	-26.130120	28.337247	0.39	159	-26.12948517	28.3319765	0
31	-26.124425	28.334474	0.63	103	-26.126946	28.336946	0.6	118	-26.127199	28.333217	0.56	95	-26.129480	28.334153	0.39	160	-26.12564184	28.3367315	0
32	-26.124991	28.334590	0.63	59	-26.128714	28.338107	0.59	135	-26.123750	28.336125	0.56	49	-26.129787	28.338036	0.37	161	-26.12333017	28.3370435	0
109	-26.126654	28.335697	0.63	74	-26.128732	28.337107	0.59	56	-26.128078	28.339136	0.55	80	-26.126883	28.338851	0.37	162	-26.13020455	28.334764	0
127	-26.124391	28.335932	0.63	83	-26.127211	28.337934	0.59	82	-26.126977	28.338276	0.55	23	-26.122201	28.335131	0.36	163	-26.1253903	28.3319667	0
60	-26.128989	28.337678	0.62	104	-26.126594	28.337289	0.59	105	-26.126338	28.337540	0.55	66	-26.130172	28.335886	0.36	164	-26.12975868	28.3384317	0
107	-26.126014	28.336526	0.62	138	-26.123924	28.335320	0.59	120	-26.126296	28.334003	0.55	133	-26.123764	28.336371	0.34	165	-26.1232445	28.3327637	0
110	-26.126921	28.335309	0.62	17	-26.127780	28.332290	0.58	14	-26.128270	28.332210	0.54	21	-26.122220	28.335656	0.31	166	-26.13046863	28.3367195	0
136	-26.123696	28.335862	0.62	20	-26.126920	28.333720	0.58	52	-26.128882	28.339021	0.54	94	-26.129830	28.333765	0.30	167	-26.12783738	28.3318605	0
137	-26.123754	28.335593	0.62	25	-26.122459	28.334911	0.58	89	-26.129241	28.335378	0.54	5	-26.126290	28.331480	0.29	168	-26.12647578	28.3378375	0
140	-26.123581	28.335396	0.62	37	-26.125898	28.334407	0.58	115	-26.128305	28.332509	0.54	4	-26.126490	28.331540	0.27	169	-26.12206402	28.3345877	0
141	-26.123343	28.335614	0.62	38	-26.126445	28.334488	0.58	9	-26.127520	28.331760	0.53	92	-26.130177	28.334517	0.27	170	-26.13016063	28.3354112	0
142	-26.123122	28.335810	0.62	40	-26.127341	28.334725	0.58	65	-26.130008	28.336094	0.53	6	-26.127010	28.331410	0.26	171	-26.12714176	28.3311544	0
15	-26.128070	28.332570	0.61	42	-26.128299	28.336026	0.58	70	-26.129650	28.335802	0.52	22	-26.122131	28.335436	0.26	172	-26.12846588	28.3398998	0
30	-26.124041	28.334605	0.61	58	-26.128510	28.338438	0.58	96	-26.129240	28.334400	0.52	2	-26.126090	28.331810	0.24	173	-26.12370365	28.3323192	0
61	-26.129179	28.337400	0.61	63	-26.129580	28.336826	0.58	1	-26.125930	28.331930	0.51	125	-26.124939	28.335394	0.24	174	-26.13008264	28.3379181	0
73	-26.129099	28.336602	0.61	113	-26.127684	28.334064	0.58	13	-26.128400	28.332000	0.51	67	-26.130297	28.335686	0.23	175	-26.13015817	28.3331898	0
76	-26.128154	28.337802	0.61	116	-26.127868	28.332722	0.58	35	-26.125389	28.334648	0.51	3	-26.126270	28.331670	0.21	176	-26.12554808	28.3371298	0

Table A3 Continued: Depth Measurements for Sandpan

Sample	Lat	Long	Depth (m)	Sample	Lat	Long	Depth (m)	Sample	Lat	Long	Depth (m)	Sample	Lat	Long	Depth (m)	Sample	Lat	Long	Depth (m)
177	-26.1241	28.337785	0	214	-26.122157	28.3357125	0	251	-26.1301	28.33492	0	289	-26.1243	28.33474	0	326	-26.129	28.33128	0
178	-26.1303	28.333996	0	215	-26.1237374	28.3373835	0	252	-26.1261	28.33152	0	290	-26.1245	28.33502	0	327	-26.1226	28.33257	0
179	-26.1247	28.332256	0	216	-26.1303417	28.3342477	0	253	-26.1255	28.33230	0	291	-26.1246	28.33473	0	328	-26.1299	28.33884	0
180	-26.1299	28.338358	0	217	-26.1251376	28.3321634	0	254	-26.1251	28.33293	0	292	-26.1253	28.33255	0	329	-26.1227	28.337	0
181	-26.1226	28.333189	0	218	-26.1298288	28.338458	0	255	-26.1254	28.33250	0	293	-26.125	28.33244	0	330	-26.1304	28.33489	0
182	-26.1305	28.336269	0	219	-26.122881	28.3328932	0	256	-26.1247	28.33266	0	294	-26.125	28.33262	0	331	-26.1263	28.33104	0
183	-26.1274	28.331516	0	220	-26.130519	28.3364198	0	257	-26.1254	28.33227	0	295	-26.1253	28.33235	0	332	-26.1275	28.33969	0
184	-26.1274	28.339075	0	221	-26.127536	28.3316563	0	258	-26.1249	28.33264	0	296	-26.1253	28.33255	0	333	-26.1244	28.33845	0
185	-26.122	28.335178	0	222	-26.1271012	28.3385845	0	259	-26.1253	28.33282	0	297	-26.1256	28.3374364	0	334	-26.1301	28.33254	0
186	-26.1299	28.335246	0	223	-26.1220617	28.3349203	0	260	-26.1245	28.33258	0	298	-26.1284	28.331502	0	335	-26.1242	28.33176	0
187	-26.1269	28.331194	0	224	-26.1299275	28.335385	0	261	-26.1255	28.33227	0	299	-26.1218	28.333606	0	336	-26.129	28.33991	0
188	-26.1291	28.339404	0	225	-26.1270287	28.3312366	0	262	-26.1251	28.33278	0	300	-26.1303	28.338243	0	337	-26.1216	28.33574	0
189	-26.1238	28.332334	0	226	-26.128731	28.3397796	0	263	-26.1253	28.33269	0	301	-26.1236	28.33789	0	338	-26.1307	28.33624	0
190	-26.13	28.337814	0	227	-26.1237439	28.3324131	0	264	-26.1245	28.33265	0	302	-26.1307	28.333878	0	339	-26.1278	28.3311	0
191	-26.1298	28.332364	0	228	-26.1299755	28.3378647	0	265	-26.1254	28.33232	0	303	-26.1251	28.33154	0	340	-26.1265	28.33839	0
192	-26.1257	28.33685	0	229	-26.1301143	28.3328808	0	266	-26.1247	28.33265	0	304	-26.1283	28.340109	0	341	-26.1249	28.33851	0
193	-26.1227	28.336446	0	230	-26.1255914	28.3369708	0	267	-26.1253	28.33295	0	305	-26.1216	28.334283	0	342	-26.1295	28.33165	0
194	-26.1301	28.334686	0	231	-26.1221892	28.3359027	0	268	-26.1246	28.33239	0	306	-26.1306	28.337379	0	343	-26.1232	28.33231	0
195	-26.1255	28.331771	0	232	-26.1300679	28.3347689	0	269	-26.1247	28.33225	0	307	-26.128	28.331445	0	344	-26.1296	28.33926	0
196	-26.1297	28.338678	0	233	-26.1258862	28.3315858	0	270	-26.1301	28.33403	0	308	-26.1259	28.33743	0	345	-26.1222	28.33663	0
197	-26.1233	28.332749	0	234	-26.1292849	28.3392002	0	271	-26.1302	28.33437	0	309	-26.1254	28.337817	0	346	-26.1304	28.3353	0
198	-26.1304	28.336742	0	235	-26.1234632	28.3326066	0	272	-26.1302	28.33412	0	310	-26.1285	28.331093	0	347	-26.1269	28.33083	0
199	-26.1281	28.331922	0	236	-26.130415	28.3369512	0	273	-26.13	28.33426	0	311	-26.1223	28.332978	0	348	-26.1272	28.33918	0
200	-26.126	28.337171	0	237	-26.1285185	28.3319227	0	274	-26.1301	28.33409	0	312	-26.1301	28.338418	0	349	-26.124	28.33818	0
201	-26.122	28.334215	0	238	-26.1258012	28.3369006	0	275	-26.1301	28.33441	0	313	-26.1232	28.33741	0	350	-26.1305	28.33316	0
202	-26.1302	28.335419	0	239	-26.1221269	28.3338875	0	276	-26.1302	28.33426	0	314	-26.1305	28.33433	0	351	-26.1246	28.33183	0
203	-26.1273	28.331122	0	240	-26.1305489	28.3359114	0	277	-26.1299	28.33406	0	315	-26.1257	28.331279	0	352	-26.1286	28.34028	0
204	-26.1281	28.339771	0	241	-26.1273695	28.3312051	0	278	-26.1301	28.33403	0	316	-26.1279	28.339975	0	353	-26.1216	28.33506	0
205	-26.1239	28.332203	0	242	-26.1278266	28.3395273	0	279	-26.1262	28.33474	0	317	-26.1247	28.338748	0	354	-26.1307	28.33683	0
206	-26.1299	28.338234	0	243	-26.1244332	28.3320524	0	280	-26.126	28.33488	0	318	-26.1298	28.332008	0	355	-26.1282	28.33103	0
207	-26.1303	28.333432	0	244	-26.1297567	28.3381908	0	281	-26.1262	28.33479	0	319	-26.1236	28.331899	0	356	-26.1262	28.33788	0
208	-26.1252	28.337487	0	245	-26.1303448	28.3337275	0	282	-26.1261	28.33470	0	320	-26.1292	28.339492	0				
209	-26.1291	28.33921	0	246	-26.1250119	28.3378261	0	283	-26.1262	28.33489	0	321	-26.1218	28.336208	0				
210	-26.1237	28.332513	0	247	-26.1245309	28.3321361	0	284	-26.1262	28.33474	0	322	-26.1306	28.335834	0				
211	-26.1303	28.337492	0	248	-26.1297212	28.3382577	0	286	-26.1243	28.33496	0	323	-26.1275	28.330836	0				
212	-26.1288	28.331427	0	249	-26.1302137	28.3338669	0	287	-26.1243	28.33510	0	324	-26.1269	28.338704	0				
213	-26.1257	28.336737	0	250	-26.1247442	28.338334	0	288	-26.1246	28.33497	0	325	-26.1251	28.338231	0				

Table A4: Depth Measurements for Bullfrog Pan

Sample	Lat	Long	Depth (m)	Sample	Lat	Long	Depth (m)	Sample	Lat	Long	Depth (m)	Sample	Lat	Long	Depth (m)
BFPX1	-26.1307	28.3220	0.41	53	-26.1311	28.3211	0.56	114	-26.1357	28.3189	0.59	175	-26.1367	28.3246	0.97
BFPX2	-26.1321	28.3223	0.60	54	-26.1310	28.3208	0.64	115	-26.1358	28.3191	0.66	176	-26.1363	28.3243	0.90
BFPX3	-26.1364	28.3227	0.96	55	-26.1310	28.3206	0.47	116	-26.1361	28.3191	0.83	177	-26.1361	28.3239	0.87
BFPX4	-26.1379	28.3224	0.94	56	-26.1312	28.3207	0.62	117	-26.1362	28.3188	0.52	178	-26.1361	28.3233	0.95
BFPC	-26.1349	28.3222	0.92	57	-26.1313	28.3208	0.62	118	-26.1362	28.3185	0.61	179	-26.1357	28.3229	0.96
BFPY1	-26.1339	28.3268	0.27	58	-26.1315	28.3209	0.63	119	-26.1363	28.3190	0.68	180	-26.1353	28.3228	0.91
BFPY2	-26.1345	28.3239	0.79	59	-26.1315	28.3206	0.63	120	-26.1361	28.3194	0.50	181	-26.1349	28.3225	0.96
BFPY3	-26.1356	28.3203	0.88	60	-26.1316	28.3205	0.68	121	-26.1355	28.3205	0.80	182	-26.1347	28.3222	0.94
BFPY4	-26.1363	28.3184	1.20	61	-26.1316	28.3207	0.66	122	-26.1353	28.3205	0.90	183	-26.1345	28.3225	0.99
1	-26.1317	28.3227	0.60	62	-26.1317	28.3208	0.65	123	-26.1351	28.3207	0.90	184	-26.1313	28.3226	0.89
2	-26.1322	28.3220	0.70	63	-26.1317	28.3208	0.67	124	-26.1351	28.3209	0.80	185	-26.1339	28.3226	0.93
3	-26.1319	28.3218	0.70	64	-26.1318	28.3209	0.71	125	-26.1353	28.3212	0.80	186	-26.1340	28.3229	0.91
4	-26.1316	28.3216	0.60	65	-26.1318	28.3207	0.64	126	-26.1353	28.3212	0.80	187	-26.1343	28.3235	0.78
5	-26.1315	28.3213	0.50	66	-26.1317	28.3207	0.65	127	-26.1351	28.3214	0.80	188	-26.1342	28.3240	0.81
6	-26.1317	28.3211	0.50	67	-26.1319	28.3207	0.65	128	-26.1353	28.3215	0.80	189	-26.1341	28.3244	0.74
7	-26.1322	28.3217	0.60	68	-26.1320	28.3208	0.70	129	-26.1355	28.3216	0.90	190	-26.1339	28.3250	0.97
8	-26.1325	28.3218	0.70	69	-26.1320	28.3207	0.66	130	-26.1357	28.3216	0.95	191	-26.1336	28.3248	0.96
9	-26.1325	28.3213	0.70	70	-26.1320	28.3209	0.61	131	-26.1358	28.3213	0.94	192	-26.1331	28.3246	0.85
10	-26.1332	28.3209	0.60	71	-26.1321	28.3209	0.66	132	-26.1360	28.3210	0.90	193	-26.1337	28.3244	0.97
11	-26.1330	28.3206	0.60	72	-26.1321	28.3209	0.65	133	-26.1366	28.3210	0.88	194	-26.1330	28.3243	0.89
12	-26.1337	28.3207	0.60	73	-26.1321	28.3209	0.69	134	-26.1369	28.3211	0.91	195	-26.1328	28.3243	0.88
13	-26.1339	28.3205	0.40	74	-26.1322	28.3208	0.69	135	-26.1374	28.3209	0.89	196	-26.1329	28.3240	1.00
14	-26.1335	28.3199	0.60	75	-26.1321	28.3210	0.54	136	-26.1378	28.3206	0.71	197	-26.1329	28.3236	0.79
15	-26.1334	28.3194	0.50	76	-26.1322	28.3210	0.57	137	-26.1379	28.3210	0.84	198	-26.1325	28.3238	0.84
16	-26.1330	28.3195	0.30	77	-26.1323	28.3211	0.72	138	-26.1380	28.3216	0.94	199	-26.1323	28.3240	0.78
17	-26.1340	28.3198	0.60	78	-26.1323	28.3210	0.64	139	-26.1380	28.3219	0.83	200	-26.1313	28.3236	0.71
18	-26.1344	28.3197	0.50	79	-26.1323	28.3209	0.58	140	-26.1379	28.3223	0.87	201	-26.1320	28.3232	0.68
19	-26.1350	28.3195	0.50	80	-26.1323	28.3208	0.66	141	-26.1377	28.3225	0.97	202	-26.1322	28.3229	0.65
20	-26.1361	28.3196	0.50	81	-26.1323	28.3208	0.66	142	-26.1379	28.3224	0.94	203	-26.1325	28.3227	0.72
21	-26.1364	28.3192	0.60	82	-26.1324	28.3208	0.67	143	-26.1368	28.3227	0.95	204	-26.1327	28.3225	0.76
22	-26.1372	28.3189	0.50	83	-26.1324	28.3207	0.68	144	-26.1365	28.3226	0.97	205	-26.1329	28.3223	0.80
23	-26.1377	28.3192	0.60	84	-26.1325	28.3209	0.61	145	-26.1363	28.3224	0.90	206	-26.1331	28.3182	0
24	-26.1377	28.3198	0.60	85	-26.1327	28.3210	0.74	146	-26.1361	28.3222	0.88	207	-26.1363	28.3269	0
25	-26.1374	28.3201	0.80	86	-26.1330	28.3208	0.71	147	-26.1363	28.3219	0.99	208	-26.1310	28.3245	0
26	-26.1369	28.3205	0.80	87	-26.1330	28.3207	0.68	148	-26.1368	28.3219	1.00	209	-26.1388	28.3209	0
27	-26.1366	28.3208	0.80	88	-26.1330	28.3206	0.84	149	-26.1364	28.3224	0.90	210	-26.1309	28.3202	0
28	-26.1365	28.3205	0.80	89	-26.1329	28.3205	0.70	150	-26.1364	28.3227	0.96	211	-26.1385	28.3250	0
29	-26.1368	28.3210	0.80	90	-26.1327	28.3205	0.69	151	-26.1366	28.3233	0.95	212	-26.1332	28.3269	0
30	-26.1307	28.3223	0.39	91	-26.1331	28.3206	0.67	152	-26.1342	28.3239	0.87	213	-26.1371	28.3182	0
31	-26.1309	28.3224	0.58	92	-26.1335	28.3206	0.68	153	-26.1343	28.3263	0.98	214	-26.1317	28.3194	0
32	-26.1310	28.3227	0.69	93	-26.1335	28.3204	0.58	154	-26.1346	28.3258	0.98	215	-26.1372	28.3263	0
33	-26.1314	28.3226	0.67	94	-26.1335	28.3204	0.62	155	-26.1350	28.3260	0.96	216	-26.1319	28.3258	0
34	-26.1314	28.3222	0.67	95	-26.1336	28.3203	0.79	156	-26.1350	28.3261	0.47	217	-26.1383	28.3193	0
35	-26.1312	28.3220	0.60	96	-26.1336	28.3201	0.69	157	-26.1351	28.3259	0.98	218	-26.1303	28.3215	0
36	-26.1314	28.3225	0.62	97	-26.1337	28.3201	0.79	158	-26.1354	28.3260	0.99	219	-26.1388	28.3233	0
37	-26.1311	28.3223	0.61	98	-26.1338	28.3200	0.78	159	-26.1359	28.3265	0.55	220	-26.1347	28.3271	0
38	-26.1309	28.3220	0.61	99	-26.1337	28.3199	0.82	160	-26.1360	28.3263	0.60	221	-26.1353	28.3179	0
39	-26.1309	28.3220	0.62	100	-26.1336	28.3198	0.75	161	-26.1364	28.3262	0.79	222	-26.1321	28.3189	0
40	-26.1308	28.3219	0.45	101	-26.1335	28.3196	0.66	162	-26.1367	28.3261	0.71	223	-26.1368	28.3266	0
41	-26.1307	28.3219	0.42	102	-26.1334	28.3194	0.67	163	-26.1370	28.3258	0.72	224	-26.1315	28.3253	0
42	-26.1309	28.3218	0.32	103	-26.1332	28.3191	0.64	164	-26.1372	28.3256	0.66	225	-26.1387	28.3197	0
43	-26.1306	28.3217	0.22	104	-26.1331	28.3190	0.61	165	-26.1367	28.3255	0.92	226	-26.1304	28.3210	0
44	-26.1306	28.3217	1.00	105	-26.1330	28.3188	0.52	166	-26.1363	28.3255	0.97	227	-26.1388	28.3238	0
45	-26.1308	28.3216	0.65	106	-26.1328	28.3186	0.13	167	-26.1359	28.3254	0.93	228	-26.1341	28.3271	0
46	-26.1310	28.3217	0.61	107	-26.1333	28.3187	0.43	168	-26.1356	28.3256	0.88	229	-26.1358	28.3180	0
47	-26.1312	28.3217	0.56	108	-26.1335	28.3187	0.44	169	-26.1355	28.3251	0.84	230	-26.1311	28.3202	0
48	-26.1314	28.3218	0.67	109	-26.1338	28.3188	0.39	170	-26.1358	28.3247	0.89	231	-26.1382	28.3254	0
49	-26.1311	28.3216	0.57	110	-26.1344	28.3191	0.53	171	-26.1363	28.3246	0.94	232	-26.1327	28.3266	0
50	-26.1312	28.3215	0.62	111	-26.1348	28.3193	0.55	172	-26.1368	28.3247	0.96	233	-26.1376	28.3184	0
51	-26.1312	28.3213	0.68	112	-26.1351	28.3194	0.59	173	-26.1375	28.3249	0.87	234	-26.1305	28.3228	0
52	-26.1311	28.3212	0.81	113	-26.1354	28.3187	0.64	174	-26.1378	28.3250	0.76	235	-26.1389	28.3220	0

Table A4 Continued: Depth Measurements for Bullfrog Pan

Sample	Lat	Long	Depth (m)	Sample	Lat	Long	Depth (m)	Sample	Lat	Long	Depth (m)
236	-26.1356	28.3271	0	297	-26.1325	28.3251	0	358	-26.1354	28.3185	0
237	-26.1342	28.3179	0	298	-26.1332	28.3186	0	359	-26.1360	28.3266	0
238	-26.1306	28.3235	0	299	-26.1369	28.3262	0	360	-26.1381	28.3207	0
239	-26.1388	28.3214	0	300	-26.1378	28.3194	0	361	-26.1323	28.3253	0
240	-26.1360	28.3271	0	301	-26.1332	28.3259	0	362	-26.1334	28.3186	0
241	-26.1326	28.3185	0	302	-26.1354	28.3184	0	363	-26.1368	28.3263	0
242	-26.1367	28.3267	0	303	-26.1354	28.3264	0	364	-26.1378	28.3195	0
243	-26.1313	28.3249	0	304	-26.1386	28.3234	0	365	-26.1332	28.3257	0
244	-26.1387	28.3202	0	305	-26.1322	28.3239	0	366	-26.1355	28.3183	0
245	-26.1306	28.3204	0	306	-26.1328	28.3191	0	367	-26.1353	28.3263	0
246	-26.1386	28.3245	0	307	-26.1371	28.3259	0	368	-26.1384	28.3240	0
247	-26.1336	28.3271	0	308	-26.1367	28.3184	0	369	-26.1307	28.3227	0
248	-26.1364	28.3181	0	309	-26.1337	28.3263	0	370	-26.1327	28.3188	0
249	-26.1313	28.3202	0	310	-26.1356	28.3186	0	371	-26.1371	28.3259	0
250	-26.1377	28.3260	0	311	-26.1358	28.3268	0	372	-26.1371	28.3185	0
251	-26.1322	28.3262	0	312	-26.1386	28.3213	0	373	-26.1337	28.3263	0
252	-26.1380	28.3188	0	313	-26.1318	28.3247	0	374	-26.1356	28.3185	0
253	-26.1303	28.3221	0	314	-26.1340	28.3183	0	375	-26.1357	28.3268	0
254	-26.1389	28.3227	0	315	-26.1365	28.3263	0	376	-26.1385	28.3214	0
255	-26.1350	28.3270	0	316	-26.1380	28.3199	0	377	-26.1318	28.3246	0
256	-26.1349	28.3179	0	317	-26.1325	28.3259	0	378	-26.1342	28.3182	0
257	-26.1337	28.3180	0	318	-26.1357	28.3183	0	379	-26.1364	28.3262	0
258	-26.1327	28.3260	0	319	-26.1347	28.3260	0	380	-26.1380	28.3200	0
259	-26.1373	28.3256	0	320	-26.1377	28.3253	0	381	-26.1325	28.3258	0
260	-26.1357	28.3182	0	321	-26.1306	28.3213	0	382	-26.1357	28.3183	0
261	-26.1338	28.3267	0	322	-26.1320	28.3195	0	383	-26.1341	28.3267	0
262	-26.1352	28.3184	0	323	-26.1372	28.3257	0	384	-26.1377	28.3254	0
263	-26.1361	28.3264	0	324	-26.1361	28.3183	0	385	-26.1307	28.3209	0
264	-26.1383	28.3205	0	325	-26.1337	28.3263	0	386	-26.1325	28.3199	0
265	-26.1326	28.3250	0	326	-26.1354	28.3185	0	387	-26.1372	28.3258	0
266	-26.1330	28.3186	0	327	-26.1359	28.3267	0	388	-26.1363	28.3184	0
267	-26.1370	28.3261	0	328	-26.1382	28.3209	0	389	-26.1338	28.3263	0
268	-26.1379	28.3192	0	329	-26.1322	28.3253	0	390	-26.1354	28.3186	0
269	-26.1332	28.3259	0	330	-26.1334	28.3186	0	391	-26.1358	28.3266	0
270	-26.1355	28.3185	0	331	-26.1366	28.3263	0	392	-26.1382	28.3211	0
271	-26.1353	28.3269	0	332	-26.1379	28.3197	0	393	-26.1320	28.3252	0
272	-26.1386	28.3231	0	333	-26.1332	28.3257	0	394	-26.1336	28.3185	0
273	-26.1321	28.3240	0	334	-26.1356	28.3183	0	395	-26.1366	28.3264	0
274	-26.1327	28.3196	0	335	-26.1351	28.3261	0	396	-26.1380	28.3197	0
275	-26.1371	28.3258	0	336	-26.1384	28.3243	0	397	-26.1329	28.3261	0
276	-26.1364	28.3185	0	337	-26.1307	28.3225	0	398	-26.1356	28.3183	0
277	-26.1338	28.3263	0	338	-26.1328	28.3186	0	399	-26.1349	28.3260	0
278	-26.1355	28.3186	0	339	-26.1370	28.3260	0	400	-26.1382	28.3247	0
279	-26.1359	28.3267	0	340	-26.1375	28.3188	0	401	-26.1306	28.3221	0
280	-26.1385	28.3212	0	341	-26.1335	28.3262	0	402	-26.1330	28.3186	0
281	-26.1319	28.3250	0	342	-26.1356	28.3185	0	403	-26.1370	28.3260	0
282	-26.1337	28.3184	0	343	-26.1356	28.3269	0	404	-26.1377	28.3190	0
283	-26.1365	28.3264	0	344	-26.1386	28.3219	0	405	-26.1333	28.3260	0
284	-26.1380	28.3197	0	345	-26.1319	28.3244	0	406	-26.1355	28.3185	0
285	-26.1328	28.3261	0	346	-26.1346	28.3181	0	407	-26.1355	28.3269	0
286	-26.1356	28.3183	0	347	-26.1363	28.3263	0	408	-26.1386	28.3225	0
287	-26.1347	28.3259	0	348	-26.1381	28.3202	0	409	-26.1320	28.3241	0
288	-26.1380	28.3250	0	349	-26.1323	28.3256	0	410	-26.1348	28.3182	0
289	-26.1306	28.3217	0	350	-26.1356	28.3182	0	411	-26.1362	28.3263	0
290	-26.1309	28.3204	0	351	-26.1340	28.3268	0	412	-26.1382	28.3203	0
291	-26.1373	28.3257	0	352	-26.1375	28.3255	0	413	-26.1323	28.3256	0
292	-26.1357	28.3182	0	353	-26.1309	28.3204	0	414	-26.1357	28.3182	0
293	-26.1337	28.3267	0	354	-26.1313	28.3207	0	415	-26.1338	28.3268	0
294	-26.1353	28.3185	0	355	-26.1372	28.3257	0	416	-26.1375	28.3255	0
295	-26.1361	28.3266	0	356	-26.1359	28.3182	0	417	-26.1327	28.3260	0
296	-26.1382	28.3207	0	357	-26.1338	28.3265	0	418	-26.1374	28.3256	0

Table A5: Depth Measurements for Homestead Dam

Sample	Lat	Long	Depth (m)	Sample	Lat	Long	Depth (m)	Sample	Lat	Long	Depth (m)	Sample	Lat	Long	Depth (m)
x1	-26.1625	28.2867	0.39	7	-26.1752	28.2915	5.5	101	-26.1721	28.2875	4.1	176	-26.1658	28.2876	2.8
x2	-26.1641	28.2870	1.6	60	-26.1732	28.2901	5.5	150	-26.1685	28.2879	4.1	30	-26.1735	28.2918	2.7
x3	-26.1658	28.2876	2.7	68	-26.1727	28.2904	5.5	9	-26.1746	28.2922	4	83	-26.1719	28.2895	2.7
x4	-26.1684	28.2880	3.8	69	-26.1724	28.2904	5.5	25	-26.1747	28.2906	4	90	-26.1726	28.2872	2.7
c	-26.1719	28.2885	4.1	72	-26.1728	28.2896	5.5	148	-26.1685	28.2884	4	146	-26.1688	28.2876	2.7
y1	-26.1710	28.2841	1.6	82	-26.1721	28.2895	5.5	139	-26.1700	28.2884	3.9	173	-26.1661	28.2876	2.7
y2	-26.1738	28.2863	2.3	19	-26.1740	28.2918	5.4	154	-26.1681	28.2881	3.9	177	-26.1656	28.2879	2.7
z1	-26.1738	28.2912	5.8	22	-26.1747	28.2911	5.4	64	-26.1740	28.2889	3.8	180	-26.1657	28.2871	2.7
z2	-26.1752	28.2921	6.1	45	-26.1732	28.2913	5.4	147	-26.1687	28.2880	3.8	162	-26.1672	28.2880	2.6
13	-26.1749	28.2914	6	86	-26.1725	28.2884	5.4	158	-26.1677	28.2874	3.7	77	-26.1736	28.2880	2.6
21	-26.1745	28.2913	6	93	-26.1717	28.2883	5.4	10	-26.1742	28.2922	3.6	78	-26.1733	28.2883	2.6
41	-26.1740	28.2909	6	66	-26.1734	28.2894	5.3	70	-26.1724	28.2902	3.6	92	-26.1719	28.2880	2.6
8	-26.1750	28.2919	5.9	5	-26.1754	28.2917	5.2	89	-26.1729	28.2876	3.6	183	-26.1652	28.2876	2.6
12	-26.1746	28.2917	5.9	99	-26.1717	28.2879	5.2	134	-26.1705	28.2879	3.6	18	-26.1739	28.2921	2.5
15	-26.1748	28.2913	5.9	58	-26.1728	28.2906	5	153	-26.1681	28.2878	3.6	65	-26.1737	28.2891	2.5
16	-26.1746	28.2916	5.9	98	-26.1716	28.2880	5	155	-26.1681	28.2882	3.6	129	-26.1706	28.2855	2.5
20	-26.1742	28.2915	5.9	108	-26.1711	28.2881	5	157	-26.1678	28.2878	3.6	175	-26.1660	28.2874	2.5
26	-26.1743	28.2909	5.9	71	-26.1726	28.2899	4.9	161	-26.1674	28.2881	3.5	182	-26.1654	28.2873	2.5
32	-26.1737	28.2912	5.9	94	-26.1715	28.2888	4.9	17	-26.1743	28.2918	3.4	187	-26.1655	28.2869	2.5
46	-26.1734	28.2911	5.9	100	-26.1718	28.2877	4.9	23	-26.1750	28.2907	3.4	44	-26.1731	28.2916	2.4
47	-26.1737	28.2908	5.9	109	-26.1710	28.2885	4.9	144	-26.1692	28.2871	3.4	156	-26.1678	28.2881	2.4
27	-26.1741	28.2913	5.8	4	-26.1750	28.2925	4.8	160	-26.1676	28.2879	3.4	179	-26.1656	28.2874	2.4
33	-26.1739	28.2910	5.8	114	-26.1709	28.2877	4.7	6	-26.1755	28.2912	3.3	186	-26.1655	28.2870	2.4
40	-26.1742	28.2906	5.8	140	-26.1698	28.2880	4.7	116	-26.1713	28.2870	3.3	189	-26.1652	28.2872	2.4
42	-26.1736	28.2911	5.8	113	-26.1708	28.2880	4.6	133	-26.1706	28.2874	3.3	190	-26.1650	28.2877	2.4
48	-26.1741	28.2906	5.8	28	-26.1739	28.2916	4.5	149	-26.1684	28.2882	3.3	37	-26.1748	28.2901	2.3
31	-26.1736	28.2915	5.7	43	-26.1733	28.2914	4.5	164	-26.1670	28.2875	3.3	84	-26.1721	28.2891	2.3
53	-26.1737	28.2905	5.7	76	-26.1737	28.2882	4.5	102	-26.1722	28.2872	3.2	111	-26.1707	28.2887	2.3
54	-26.1734	28.2907	5.7	110	-26.1708	28.2889	4.5	151	-26.1684	28.2875	3.2	128	-26.1706	28.2852	2.3
63	-26.1739	28.2892	5.7	135	-26.1705	28.2884	4.5	163	-26.1670	28.2878	3.2	159	-26.1676	28.2876	2.3
67	-26.1731	28.2898	5.7	142	-26.1696	28.2878	4.5	38	-26.1745	28.2901	3.1	172	-26.1661	28.2879	2.3
80	-26.1728	28.2888	5.7	79	-26.1730	28.2885	4.4	50	-26.1744	28.2900	3.1	178	-26.1656	28.2877	2.3
11	-26.1744	28.2919	5.6	112	-26.1708	28.2883	4.4	107	-26.1713	28.2878	3.1	184	-26.1650	28.2875	2.3
34	-26.1742	28.2907	5.6	136	-26.1704	28.2890	4.4	132	-26.1707	28.2868	3.1	185	-26.1652	28.2873	2.3
55	-26.1730	28.2910	5.6	97	-26.1714	28.2884	4.3	165	-26.1668	28.2877	3.1	194	-26.1651	28.2867	2.3
56	-26.1728	28.2911	5.6	115	-26.1710	28.2874	4.3	166	-26.1666	28.2881	3.1	29	-26.1736	28.2918	2.2
59	-26.1731	28.2903	5.6	141	-26.1699	28.2878	4.3	170	-26.1663	28.2878	3.1	167	-26.1665	28.2880	2.2
61	-26.1734	28.2898	5.6	14	-26.1751	28.2912	4.2	130	-26.1709	28.2858	3	181	-26.1655	28.2872	2.2
62	-26.1737	28.2894	5.6	49	-26.1743	28.2903	4.2	169	-26.1664	28.2875	3	188	-26.1653	28.2870	2.2
73	-26.1731	28.2893	5.6	143	-26.1696	28.2873	4.2	174	-26.1661	28.2873	3	192	-26.1649	28.2872	2.2
74	-26.1733	28.2889	5.6	35	-26.1744	28.2905	4.1	171	-26.1662	28.2880	2.9	193	-26.1650	28.2869	2.2
75	-26.1734	28.2886	5.6	39	-26.1744	28.2903	4.1	24	-26.1749	28.2905	2.8	195	-26.1650	28.2868	2.2
81	-26.1725	28.2891	5.6	52	-26.1740	28.2902	4.1	36	-26.1747	28.2903	2.8	196	-26.1649	28.2871	2.2
87	-26.1727	28.2881	5.6	57	-26.1727	28.2909	4.1	131	-26.1708	28.2863	2.8	197	-26.1646	28.2875	2.2
88	-26.1730	28.2878	5.6	85	-26.1724	28.2887	4.1	168	-26.1665	28.2875	2.8	51	-26.1742	28.2900	2.1

Table A5 Continued: Depth Measurements for Homestead Dam

Sample	Lat	Long	Depth (m)	Sample	Lat	Long	Depth (m)	Sample	Lat	Long	Depth (m)	Sample	Lat	Long	Depth (m)
124	-26.1710	28.2846	2.1	215	-26.1632	28.2861	0.7	262	-26.1638	28.2877	0	307	-26.1704	28.2848	0
95	-26.1712	28.2890	2	214	-26.1634	28.2859	0.5	263	-26.1618	28.2871	0	308	-26.1708	28.2836	0
122	-26.1712	28.2852	2	219	-26.1759	28.2914	0	264	-26.1626	28.2860	0	309	-26.1714	28.2848	0
123	-26.1712	28.2852	2	220	-26.1748	28.2932	0	265	-26.1636	28.2859	0	310	-26.1719	28.2858	0
152	-26.1682	28.2875	2	221	-26.1721	28.2907	0	266	-26.1652	28.2863	0	311	-26.1729	28.2866	0
198	-26.1645	28.2873	2	222	-26.1693	28.2889	0	267	-26.1671	28.2871	0	312	-26.1734	28.2870	0
200	-26.1648	28.2866	2	223	-26.1677	28.2885	0	268	-26.1686	28.2868	0	313	-26.1743	28.2884	0
91	-26.1724	28.2874	1.9	224	-26.1642	28.2878	0	269	-26.1703	28.2849	0	314	-26.1748	28.2894	0
103	-26.1723	28.2867	1.9	225	-26.1621	28.2870	0	270	-26.1707	28.2837	0	315	-26.1732	28.2920	0
199	-26.1646	28.2870	1.9	226	-26.1621	28.2865	0	271	-26.1714	28.2845	0	316	-26.1711	28.2894	0
201	-26.1647	28.2864	1.9	227	-26.1636	28.2857	0	272	-26.1716	28.2856	0	317	-26.1690	28.2888	0
125	-26.1707	28.2845	1.7	228	-26.1650	28.2863	0	273	-26.1726	28.2864	0	318	-26.1661	28.2883	0
127	-26.1709	28.2850	1.7	229	-26.1667	28.2870	0	274	-26.1732	28.2870	0	319	-26.1633	28.2876	0
191	-26.1648	28.2874	1.7	230	-26.1685	28.2869	0	275	-26.1741	28.2879	0	320	-26.1620	28.2868	0
203	-26.1643	28.2869	1.7	231	-26.1700	28.2855	0	276	-26.1746	28.2891	0	321	-26.1628	28.2858	0
204	-26.1642	28.2872	1.7	232	-26.1706	28.2838	0	277	-26.1740	28.2926	0	322	-26.1645	28.2859	0
3	-26.1711	28.2842	1.6	233	-26.1712	28.2841	0	278	-26.1716	28.2897	0	323	-26.1656	28.2867	0
126	-26.1707	28.2847	1.6	234	-26.1718	28.2855	0	279	-26.1689	28.2889	0	324	-26.1675	28.2871	0
145	-26.1689	28.2873	1.6	235	-26.1725	28.2863	0	280	-26.1667	28.2884	0	325	-26.1695	28.2862	0
207	-26.1638	28.2873	1.6	236	-26.1732	28.2870	0	281	-26.1636	28.2876	0	326	-26.1703	28.2847	0
117	-26.1715	28.2868	1.5	237	-26.1740	28.2875	0	282	-26.1618	28.2870	0	327	-26.1709	28.2835	0
118	-26.1716	28.2864	1.5	238	-26.1748	28.2892	0	283	-26.1626	28.2860	0	328	-26.1714	28.2849	0
137	-26.1702	28.2891	1.5	239	-26.1744	28.2929	0	284	-26.1643	28.2860	0	329	-26.1719	28.2858	0
205	-26.1640	28.2875	1.5	240	-26.1719	28.2904	0	285	-26.1652	28.2864	0	330	-26.1729	28.2866	0
208	-26.1639	28.2870	1.5	241	-26.1691	28.2889	0	286	-26.1673	28.2871	0	331	-26.1735	28.2870	0
209	-26.1640	28.2867	1.5	242	-26.1673	28.2885	0	287	-26.1690	28.2867	0	332	-26.1744	28.2886	0
120	-26.1714	28.2859	1.4	243	-26.1640	28.2878	0	288	-26.1704	28.2848	0	333	-26.1749	28.2895	0
121	-26.1713	28.2855	1.4	244	-26.1619	28.2870	0	289	-26.1707	28.2837	0	334	-26.1729	28.2917	0
210	-26.1642	28.2864	1.4	245	-26.1622	28.2864	0	290	-26.1714	28.2846	0	335	-26.1706	28.2893	0
96	-26.1713	28.2887	1.3	246	-26.1636	28.2858	0	291	-26.1717	28.2858	0	336	-26.1689	28.2889	0
106	-26.1715	28.2875	1.3	247	-26.1651	28.2863	0	292	-26.1728	28.2865	0	337	-26.1660	28.2882	0
206	-26.1638	28.2875	1.3	248	-26.1669	28.2870	0	293	-26.1734	28.2870	0	338	-26.1632	28.2875	0
1	-26.1707	28.2841	1.2	249	-26.1685	28.2869	0	294	-26.1742	28.2882	0	339	-26.1620	28.2868	0
2	-26.1709	28.2839	1.2	250	-26.1702	28.2852	0	295	-26.1747	28.2892	0	340	-26.1629	28.2857	0
211	-26.1640	28.2862	1.2	251	-26.1707	28.2838	0	296	-26.1737	28.2924	0	341	-26.1645	28.2860	0
217	-26.1634	28.2865	1.2	252	-26.1713	28.2843	0	297	-26.1714	28.2895	0	342	-26.1658	28.2868	0
218	-26.1637	28.2866	1.2	253	-26.1718	28.2856	0	298	-26.1690	28.2889	0	343	-26.1677	28.2871	0
104	-26.1721	28.2867	1.1	254	-26.1725	28.2864	0	299	-26.1664	28.2883	0	344	-26.1697	28.2861	0
138	-26.1700	28.2888	1.1	255	-26.1732	28.2870	0	300	-26.1634	28.2875	0	345	-26.1704	28.2845	0
216	-26.1633	28.2863	1.1	256	-26.1741	28.2878	0	301	-26.1619	28.2869	0	346	-26.1711	28.2836	0
105	-26.1717	28.2871	1	257	-26.1747	28.2891	0	302	-26.1627	28.2860	0	347	-26.1714	28.2852	0
202	-26.1645	28.2865	1	258	-26.1744	28.2929	0	303	-26.1643	28.2859	0	348	-26.1721	28.2858	0
119	-26.1714	28.2861	0.9	259	-26.1717	28.2901	0	304	-26.1654	28.2865	0	349	-26.1730	28.2866	0
212	-26.1637	28.2861	0.7	260	-26.1691	28.2890	0	305	-26.1675	28.2871	0	350	-26.1736	28.2871	0
213	-26.1636	28.2859	0.7	261	-26.1670	28.2884	0	306	-26.1693	28.2864	0	351	-26.1744	28.2888	0

Table A5 Continued: Depth Measurements for Homestead Dam

Sample	Lat	Long	Depth (m)	Sample	Lat	Long	Depth (m)	Sample	Lat	Long	Depth (m)	Sample	Lat	Long	Depth (m)
352	-26.1751	28.2897	0	397	-26.1647	28.2862	0	442	-26.1739	28.2875	0	487	-26.1746	28.2884	0
353	-26.1725	28.2914	0	398	-26.1660	28.2869	0	443	-26.1748	28.2893	0	488	-26.1746	28.2934	0
354	-26.1699	28.2892	0	399	-26.1681	28.2871	0	444	-26.1755	28.2904	0	489	-26.1681	28.2867	0
355	-26.1686	28.2888	0	400	-26.1700	28.2858	0	445	-26.1757	28.2909	0	490	-26.1641	28.2880	0
356	-26.1659	28.2882	0	401	-26.1705	28.2840	0	446	-26.1758	28.2910	0	491	-26.1735	28.2865	0
357	-26.1631	28.2874	0	402	-26.1712	28.2837	0	447	-26.1758	28.2912	0	492	-26.1706	28.2896	0
358	-26.1620	28.2867	0	403	-26.1717	28.2852	0	448	-26.1760	28.2916	0	493	-26.1713	28.2834	0
359	-26.1631	28.2857	0	404	-26.1723	28.2861	0	449	-26.1646	28.2856	0	494	-26.1636	28.2852	0
360	-26.1645	28.2861	0	405	-26.1733	28.2867	0	450	-26.1687	28.2891	0	495	-26.1758	28.2907	0
361	-26.1659	28.2868	0	406	-26.1738	28.2873	0	451	-26.1717	28.2849	0	496	-26.1759	28.2919	0
362	-26.1677	28.2871	0	407	-26.1749	28.2892	0	452	-26.1730	28.2921	0	497	-26.1652	28.2860	0
363	-26.1699	28.2858	0	408	-26.1752	28.2899	0	453	-26.1696	28.2858	0	498	-26.1682	28.2889	0
364	-26.1705	28.2843	0	409	-26.1694	28.2891	0	454	-26.1618	28.2874	0	499	-26.1718	28.2852	0
365	-26.1711	28.2836	0	410	-26.1681	28.2886	0	455	-26.1742	28.2875	0	500	-26.1726	28.2918	0
366	-26.1714	28.2852	0	411	-26.1645	28.2878	0	456	-26.1750	28.2933	0	501	-26.1699	28.2853	0
367	-26.1721	28.2859	0	412	-26.1626	28.2871	0	457	-26.1669	28.2867	0	502	-26.1616	28.2873	0
368	-26.1731	28.2866	0	413	-26.1618	28.2867	0	458	-26.1654	28.2883	0	503	-26.1744	28.2879	0
369	-26.1737	28.2871	0	414	-26.1634	28.2855	0	459	-26.1728	28.2863	0	504	-26.1749	28.2936	0
370	-26.1745	28.2889	0	415	-26.1648	28.2861	0	460	-26.1714	28.2900	0	505	-26.1676	28.2868	0
371	-26.1751	28.2897	0	416	-26.1661	28.2869	0	461	-26.1706	28.2835	0	506	-26.1648	28.2882	0
372	-26.1722	28.2910	0	417	-26.1682	28.2871	0	462	-26.1627	28.2856	0	507	-26.1732	28.2864	0
373	-26.1699	28.2892	0	418	-26.1700	28.2857	0	463	-26.1753	28.2897	0	508	-26.1711	28.2897	0
374	-26.1684	28.2887	0	419	-26.1705	28.2840	0	464	-26.1754	28.2926	0	509	-26.1709	28.2833	0
375	-26.1658	28.2882	0	420	-26.1712	28.2838	0	465	-26.1658	28.2865	0	510	-26.1632	28.2854	0
376	-26.1629	28.2873	0	421	-26.1717	28.2853	0	466	-26.1667	28.2886	0	511	-26.1755	28.2902	0
377	-26.1619	28.2868	0	422	-26.1724	28.2862	0	467	-26.1723	28.2859	0	512	-26.1752	28.2931	0
378	-26.1632	28.2857	0	423	-26.1733	28.2868	0	468	-26.1718	28.2907	0	513	-26.1664	28.2867	0
379	-26.1647	28.2862	0	424	-26.1739	28.2874	0	469	-26.1703	28.2840	0	514	-26.1661	28.2886	0
380	-26.1659	28.2868	0	425	-26.1749	28.2894	0	470	-26.1616	28.2863	0	515	-26.1726	28.2861	0
381	-26.1678	28.2870	0	426	-26.1753	28.2902	0	471	-26.1749	28.2887	0	516	-26.1717	28.2904	0
382	-26.1699	28.2857	0	427	-26.1694	28.2891	0	472	-26.1742	28.2931	0	517	-26.1704	28.2840	0
383	-26.1705	28.2841	0	428	-26.1680	28.2886	0	473	-26.1686	28.2865	0	518	-26.1622	28.2858	0
384	-26.1712	28.2836	0	429	-26.1642	28.2878	0	474	-26.1634	28.2878	0	519	-26.1751	28.2892	0
385	-26.1715	28.2852	0	430	-26.1623	28.2870	0	475	-26.1735	28.2868	0	520	-26.1738	28.2928	0
386	-26.1722	28.2860	0	431	-26.1620	28.2865	0	476	-26.1700	28.2895	0	521	-26.1691	28.2862	0
387	-26.1733	28.2866	0	432	-26.1635	28.2856	0	477	-26.1714	28.2839	0	522	-26.1628	28.2875	0
388	-26.1738	28.2872	0	433	-26.1649	28.2862	0	478	-26.1638	28.2855	0	523	-26.1739	28.2870	0
389	-26.1747	28.2890	0	434	-26.1665	28.2870	0	479	-26.1760	28.2911	0	524	-26.1694	28.2893	0
390	-26.1752	28.2897	0	435	-26.1683	28.2870	0	480	-26.1756	28.2924	0	525	-26.1715	28.2846	0
391	-26.1696	28.2892	0	436	-26.1700	28.2857	0	481	-26.1655	28.2863	0	526	-26.1642	28.2857	0
392	-26.1682	28.2887	0	437	-26.1705	28.2840	0	482	-26.1674	28.2887	0	527	-26.1761	28.2915	0
393	-26.1652	28.2880	0	438	-26.1712	28.2839	0	483	-26.1721	28.2855	0	528	-26.1735	28.2924	0
394	-26.1626	28.2872	0	439	-26.1717	28.2855	0	484	-26.1722	28.2913	0	529	-26.1695	28.2858	0
395	-26.1618	28.2868	0	440	-26.1725	28.2862	0	485	-26.1701	28.2848	0	530	-26.1622	28.2873	0
396	-26.1633	28.2856	0	441	-26.1733	28.2869	0	486	-26.1614	28.2867	0	531	-26.1741	28.2872	0

Table A6: Depth Measurements for Middle Lake

Sample	Lat	Long	Depth (m)	Sample	Lat	Long	Depth (m)	Sample	Lat	Long	Depth (m)	Sample	Lat	Long	Depth (m)
MLX1	-26.18269	28.30968	3.5	51	-26.18176	28.30114	4	7	-26.17976	28.29648	2.3	169	-26.18191	28.30282	0
MLX2	-26.18246	28.30790	4.6	54	-26.18171	28.30143	4	8	-26.17960	28.29650	2.3	170	-26.18106	28.30552	0
MLX3	-26.18171	28.30540	4.7	56	-26.18169	28.30181	4	10	-26.17926	28.29658	2.3	171	-26.18035	28.29683	0
MLC	-26.18152	28.30307	4	67	-26.18125	28.30316	4	11	-26.17946	28.29690	2.3	172	-26.17965	28.29777	0
MLX4	-26.18158	28.30033	4	115	-26.18250	28.30776	4	12	-26.17963	28.29717	2.3	173	-26.18223	28.30045	0
MLX5	-26.18073	28.29822	3.2	95	-26.18227	28.30658	3.9	16	-26.18011	28.29672	2.3	174	-26.18119	28.30107	0
MLX6	-26.17877	28.29538	1.6	49	-26.18175	28.30072	3.8	22	-26.18040	28.29714	2.3	175	-26.18097	28.29719	0
MLY1	-26.18112	28.30316	1.3	143	-26.18289	28.30858	3.8	29	-26.18094	28.29732	2.3	176	-26.17813	28.29389	0
MLY2	-26.18192	28.30330	0.75	46	-26.18150	28.30020	3.7	35	-26.18035	28.29860	2.3	177	-26.18314	28.30781	0
125	-26.18230	28.30845	5.6	59	-26.18167	28.30223	3.7	42	-26.18086	28.29985	2.3	178	-26.18162	28.30879	0
133	-26.18232	28.30948	5.6	76	-26.18153	28.30437	3.7	87	-26.18221	28.30694	2.3	179	-26.17931	28.29545	0
141	-26.18268	28.30904	5.6	41	-26.18114	28.29968	3.6	113	-26.18266	28.30741	2.3	180	-26.18098	28.30030	0
126	-26.18205	28.30854	5.5	44	-26.18155	28.29979	3.6	118	-26.18160	28.30808	2.3	181	-26.18138	28.29820	0
137	-26.18251	28.30910	5.5	58	-26.18144	28.30205	3.6	4	-26.17891	28.29611	2.2	182	-26.18098	28.30341	0
138	-26.18222	28.30920	5.5	61	-26.18160	28.30243	3.6	5	-26.17913	28.29626	2.2	183	-26.18062	28.29687	0
139	-26.18208	28.30901	5.5	70	-26.18149	28.30381	3.6	9	-26.17948	28.29648	2.2	184	-26.17900	28.29659	0
140	-26.18236	28.30890	5.5	74	-26.18154	28.30408	3.6	36	-26.18042	28.29893	2.2	185	-26.18191	28.30278	0
120	-26.18228	28.30818	5.4	88	-26.18213	28.30618	3.6	75	-26.18171	28.30425	2.2	186	-26.18107	28.30553	0
130	-26.18195	28.30948	5.3	43	-26.18120	28.29997	3.5	1	-26.17858	28.29557	2	187	-26.18039	28.29682	0
117	-26.18203	28.30792	5.2	78	-26.18103	28.30469	3.5	6	-26.17947	28.29611	2	188	-26.17976	28.29784	0
124	-26.18255	28.30847	5.2	38	-26.18106	28.29891	3.4	15	-26.17993	28.29639	2	189	-26.18225	28.30021	0
127	-26.18176	28.30872	5.2	122	-26.18291	28.30819	3.4	47	-26.18134	28.30058	2	190	-26.18120	28.30108	0
129	-26.18189	28.30921	5.2	132	-26.18236	28.30976	3.4	109	-26.18150	28.30736	1.9	191	-26.18092	28.29714	0
131	-26.18213	28.30973	5.2	135	-26.18297	28.30912	3.4	3	-26.17912	28.29574	1.8	192	-26.17797	28.29375	0
98	-26.18198	28.30681	5.1	40	-26.18135	28.29935	3.3	2	-26.17911	28.29558	1.7	193	-26.18300	28.30743	0
107	-26.18200	28.30719	5.1	52	-26.18151	28.30114	3.3	53	-26.18150	28.30135	1.7	194	-26.18204	28.30989	0
111	-26.18213	28.30745	5.1	33	-26.18109	28.29816	3.2	57	-26.18136	28.30178	1.7	195	-26.17877	28.29502	0
116	-26.18226	28.30780	5.1	34	-26.18071	28.29893	3.2	25	-26.18000	28.29799	1.6	196	-26.18104	28.30052	0
119	-26.18196	28.30813	5.1	62	-26.18134	28.30262	3.2	96	-26.18245	28.30660	1.6	197	-26.18156	28.29809	0
128	-26.18178	28.30894	5.1	100	-26.18149	28.30664	3.2	19	-26.17980	28.29775	1.3	198	-26.18098	28.30478	0
104	-26.18205	28.30693	5	37	-26.18071	28.29891	3.1	101	-26.18131	28.30670	1.3	199	-26.18045	28.29695	0
136	-26.18278	28.30908	5	84	-26.18141	28.30577	3.1	123	-26.18301	28.30870	1.3	200	-26.17944	28.29739	0
94	-26.18190	28.30651	4.9	27	-26.18040	28.29776	3	92	-26.18132	28.30623	1.1	201	-26.18201	28.30225	0
134	-26.18284	28.30947	4.9	28	-26.18069	28.29749	3	145	-26.18219	28.30562	1.1	202	-26.18113	28.30643	0
85	-26.18167	28.30893	4.8	55	-26.18190	28.30160	3	30	-26.18120	28.29750	1	203	-26.18027	28.29650	0
89	-26.18191	28.30612	4.8	105	-26.18250	28.30709	3	31	-26.18150	28.29816	0.8	204	-26.18017	28.29888	0
90	-26.18167	28.30608	4.8	24	-26.18021	28.29770	2.9	146	-26.18336	28.30956	0	205	-26.18170	28.29840	0
99	-26.18173	28.30672	4.8	45	-26.18179	28.29997	2.9	147	-26.17863	28.29484	0	206	-26.18122	28.30130	0
121	-26.18259	28.30823	4.8	50	-26.18200	28.30085	2.9	148	-26.18111	28.30070	0	207	-26.18068	28.29704	0
103	-26.18175	28.30697	4.7	72	-26.18106	28.30405	2.9	149	-26.18153	28.29792	0	208	-26.17748	28.29359	0
110	-26.18158	28.30749	4.7	21	-26.18010	28.29734	2.8	150	-26.18100	28.30523	0	209	-26.18234	28.30563	0
82	-26.18155	28.30529	4.6	60	-26.18175	28.30247	2.8	151	-26.18040	28.29703	0	210	-26.18140	28.30813	0
86	-26.18196	28.30599	4.5	81	-26.18183	28.30515	2.8	152	-26.17946	28.29741	0	211	-26.17950	28.29543	0
91	-26.18153	28.30611	4.5	17	-26.17988	28.29720	2.7	153	-26.18212	28.30212	0	212	-26.18067	28.29991	0
106	-26.18228	28.30707	4.5	23	-26.18036	28.29745	2.7	154	-26.18119	28.30705	0	213	-26.18134	28.29826	0
73	-26.18130	28.30408	4.4	39	-26.18147	28.29900	2.7	155	-26.17999	28.29621	0	214	-26.18121	28.30228	0
79	-26.18129	28.30486	4.4	64	-26.18174	28.30276	2.7	156	-26.18040	28.29933	0	215	-26.18063	28.29705	0
93	-26.18162	28.30643	4.4	65	-26.18164	28.30301	2.7	157	-26.18159	28.29827	0	216	-26.17854	28.29576	0
68	-26.18138	28.30338	4.3	102	-26.18156	28.30691	2.7	158	-26.18120	28.30141	0	217	-26.18181	28.30343	0
77	-26.18123	28.30450	4.3	13	-26.17977	28.29687	2.6	159	-26.18073	28.29719	0	218	-26.18100	28.30541	0
80	-26.18162	28.30498	4.3	26	-26.18036	28.29800	2.6	160	-26.17767	28.29397	0	219	-26.18031	28.29694	0
97	-26.18221	28.30679	4.3	14	-26.17969	28.29663	2.5	161	-26.18199	28.30498	0	220	-26.17954	28.29756	0
112	-26.18239	28.30738	4.3	20	-26.17994	28.29753	2.5	162	-26.18149	28.30839	0	221	-26.18223	28.30134	0
63	-26.18149	28.30279	4.2	32	-26.18137	28.29836	2.5	163	-26.17934	28.29543	0	222	-26.18119	28.30094	0
71	-26.18120	28.30383	4.2	18	-26.17976	28.29742	2.4	164	-26.18077	28.30007	0	223	-26.18122	28.29742	0
142	-26.18287	28.30890	4.2	48	-26.18148	28.30071	2.4	165	-26.18132	28.29820	0	224	-26.17838	28.29419	0
144	-26.18253	28.30795	4.2	69	-26.18168	28.30360	2.4	166	-26.18104	28.30263	0	225	-26.18333	28.30847	0
66	-26.18146	28.30310	4.1	83	-26.18123	28.30550	2.4	167	-26.18065	28.29691	0	226	-26.18180	28.30920	0
108	-26.18172	28.30726	4.1	114	-26.18278	28.30766	2.4	168	-26.17885	28.29635	0	227	-26.17925	28.29533	0

Table A6 Continued: Depth Measurements for Middle Lake

Sample	Lat	Long	Depth (m)	Sample	Lat	Long	Depth (m)	Sample	Lat	Long	Depth (m)	Sample	Lat	Long	Depth (m)
228	-26.18103	28.30043	0	287	-26.17959	28.29760	0	346	-26.18056	28.29712	0	405	-26.18186	28.31011	0
229	-26.18145	28.29820	0	288	-26.18224	28.30075	0	347	-26.17835	28.29535	0	406	-26.17858	28.29424	0
230	-26.18089	28.30446	0	289	-26.18118	28.30100	0	348	-26.18179	28.30364	0	407	-26.18077	28.30072	0
231	-26.18052	28.29684	0	290	-26.18115	28.29741	0	349	-26.18099	28.30539	0	408	-26.18223	28.30291	0
232	-26.17917	28.29692	0	291	-26.17830	28.29404	0	350	-26.18032	28.29698	0	409	-26.18091	28.30682	0
233	-26.18194	28.30260	0	292	-26.18322	28.30816	0	351	-26.17954	28.29755	0	410	-26.18165	28.29774	0
234	-26.18109	28.30573	0	293	-26.18193	28.30971	0	352	-26.18221	28.30158	0	411	-26.17863	28.29636	0
235	-26.18046	28.29677	0	294	-26.17903	28.29519	0	353	-26.18122	28.30093	0	412	-26.18347	28.30787	0
236	-26.17988	28.29804	0	295	-26.18103	28.30051	0	354	-26.18130	28.29749	0	413	-26.18079	28.30535	0
237	-26.18190	28.29902	0	296	-26.18152	28.29819	0	355	-26.17848	28.29432	0	414	-26.18201	28.29858	0
238	-26.18125	28.30119	0	297	-26.18089	28.30461	0	356	-26.18336	28.30870	0	415	-26.17803	28.29517	0
239	-26.18085	28.29702	0	298	-26.18047	28.29685	0	357	-26.18170	28.30904	0	416	-26.18371	28.30912	0
240	-26.17769	28.29355	0	299	-26.17918	28.29693	0	358	-26.17924	28.29541	0	417	-26.18180	28.30974	0
241	-26.18287	28.30703	0	300	-26.18186	28.30258	0	359	-26.18104	28.30037	0	418	-26.17889	28.29470	0
242	-26.18141	28.30771	0	301	-26.18112	28.30615	0	360	-26.18145	28.29820	0	419	-26.18059	28.30028	0
243	-26.17983	28.29600	0	302	-26.18045	28.29669	0	361	-26.18093	28.30414	0	420	-26.18216	28.30351	0
244	-26.18058	28.29972	0	303	-26.17999	28.29826	0	362	-26.18058	28.29685	0	421	-26.18080	28.30612	0
245	-26.18144	28.29832	0	304	-26.18183	28.29883	0	363	-26.17901	28.29661	0	422	-26.18179	28.29802	0
246	-26.18111	28.30184	0	305	-26.18122	28.30118	0	364	-26.18191	28.30270	0	423	-26.17835	28.29579	0
247	-26.18063	28.29722	0	306	-26.18079	28.29699	0	365	-26.18108	28.30553	0	424	-26.18361	28.30850	0
248	-26.17812	28.29485	0	307	-26.17757	28.29349	0	366	-26.18044	28.29681	0	425	-26.18072	28.30486	0
249	-26.18184	28.30404	0	308	-26.18279	28.30678	0	367	-26.17977	28.29785	0	426	-26.18215	28.29907	0
250	-26.18121	28.30083	0	309	-26.18140	28.30789	0	368	-26.18212	28.29986	0	427	-26.17783	28.29482	0
251	-26.18137	28.29765	0	310	-26.17972	28.29582	0	369	-26.18124	28.30114	0	428	-26.18361	28.30966	0
252	-26.17854	28.29458	0	311	-26.18058	28.29972	0	370	-26.18093	28.29711	0	429	-26.17760	28.29438	0
253	-26.18340	28.30914	0	312	-26.18140	28.29828	0	371	-26.17784	28.29364	0	430	-26.18072	28.30420	0
254	-26.18124	28.30078	0	313	-26.18113	28.30200	0	372	-26.18287	28.30724	0	431	-26.18307	28.30982	0
255	-26.18141	28.29771	0	314	-26.18058	28.29721	0	373	-26.18135	28.30749	0	432	-26.17728	28.29369	0
256	-26.17857	28.29470	0	315	-26.17825	28.29513	0	374	-26.17993	28.29611	0	433	-26.18081	28.30296	0
257	-26.18340	28.30935	0	316	-26.18183	28.30382	0	375	-26.18046	28.29944	0	434	-26.18247	28.30036	0
258	-26.17861	28.29478	0	317	-26.18100	28.30523	0	376	-26.18150	28.29833	0	435	-26.18151	28.30896	0
259	-26.18119	28.30072	0	318	-26.18037	28.29701	0	377	-26.18116	28.30167	0	436	-26.17996	28.29553	0
260	-26.18147	28.29783	0	319	-26.17951	28.29747	0	378	-26.18068	28.29726	0	437	-26.18012	28.29931	0
261	-26.18275	28.30970	0	320	-26.18218	28.30187	0	379	-26.17795	28.29453	0	438	-26.18233	28.30467	0
262	-26.17870	28.29497	0	321	-26.18121	28.30089	0	380	-26.18186	28.30443	0	439	-26.18241	28.31000	0
263	-26.18104	28.30064	0	322	-26.18134	28.29759	0	381	-26.18126	28.30738	0	440	-26.17764	28.29321	0
264	-26.18154	28.29799	0	323	-26.17852	28.29446	0	382	-26.17999	28.29620	0	441	-26.18094	28.30222	0
265	-26.18098	28.30506	0	324	-26.18337	28.30882	0	383	-26.18041	28.29934	0	442	-26.18240	28.30150	0
266	-26.18044	28.29701	0	325	-26.18196	28.30984	0	384	-26.18156	28.29829	0	443	-26.18129	28.30815	0
267	-26.17945	28.29740	0	326	-26.17894	28.29509	0	385	-26.18120	28.30141	0	444	-26.18073	28.29655	0
268	-26.18209	28.30223	0	327	-26.18103	28.30051	0	386	-26.18073	28.29726	0	445	-26.17946	28.29800	0
269	-26.18115	28.30670	0	328	-26.18157	28.29815	0	387	-26.17774	28.29411	0	446	-26.18278	28.30596	0
270	-26.18013	28.29635	0	329	-26.18098	28.30477	0	388	-26.18196	28.30480	0	447	-26.18270	28.30992	0
271	-26.18040	28.29932	0	330	-26.18045	28.29690	0	389	-26.18336	28.30980	0	448	-26.17734	28.29335	0
272	-26.18166	28.29828	0	331	-26.17934	28.29717	0	390	-26.17740	28.29394	0	449	-26.18086	28.30249	0
273	-26.18120	28.30140	0	332	-26.18195	28.30229	0	391	-26.18077	28.30355	0	450	-26.18251	28.30105	0
274	-26.18069	28.29711	0	333	-26.18113	28.30642	0	392	-26.18237	28.30002	0	451	-26.18138	28.30863	0
275	-26.17757	28.29377	0	334	-26.18040	28.29664	0	393	-26.18168	28.30937	0	452	-26.18023	28.29608	0
276	-26.18211	28.30501	0	335	-26.18006	28.29859	0	394	-26.17941	28.29503	0	453	-26.17997	28.29886	0
277	-26.18140	28.30813	0	336	-26.18177	28.29863	0	395	-26.18033	28.29987	0	454	-26.18259	28.30536	0
278	-26.17941	28.29542	0	337	-26.18118	28.30124	0	396	-26.18219	28.30413	0	455	-26.18215	28.31008	0
279	-26.18068	28.29992	0	338	-26.18072	28.29699	0	397	-26.18202	28.31011	0	456	-26.17800	28.29343	0
280	-26.18132	28.29824	0	339	-26.17753	28.29349	0	398	-26.17826	28.29373	0	457	-26.18087	28.30163	0
281	-26.18118	28.30238	0	340	-26.18260	28.30623	0	399	-26.18092	28.30122	0	458	-26.18238	28.30194	0
282	-26.18066	28.29699	0	341	-26.18140	28.30791	0	400	-26.18228	28.30253	0	459	-26.18113	28.30768	0
283	-26.17868	28.29602	0	342	-26.17964	28.29566	0	401	-26.18101	28.30722	0	460	-26.18101	28.29688	0
284	-26.18188	28.30306	0	343	-26.18059	28.29973	0	402	-26.18141	28.29730	0	461	-26.17926	28.29764	0
285	-26.18100	28.30542	0	344	-26.18138	28.29827	0	403	-26.17898	28.29699	0	462	-26.18307	28.30665	0
286	-26.18032	28.29687	0	345	-26.18120	28.30214	0	404	-26.18326	28.30726	0				

Table A7: Depth Measurements for Civic Lake

Sample	Lat	Long	Depth (m)	Sample	Lat	Long	Depth (m)	Sample	Lat	Long	Depth (m)	Sample	Lat	Long	Depth (m)
X1	-26.1838	28.3135	0.81	147	-26.1830	28.3168	2.2	120	-26.1833	28.3170	1.9	303	-26.1837	28.3146	1.4
X2	-26.1824	28.3180	1.5	148	-26.1828	28.3168	2.2	158	-26.1819	28.3166	1.9	61	-26.1814	28.3181	1.3
C	-26.1832	28.3152	1.7	150	-26.1825	28.3168	2.2	183	-26.1823	28.3161	1.9	62	-26.1815	28.3180	1.3
Y1	-26.1824	28.3149	0.81	162	-26.1828	28.3166	2.2	198	-26.1825	28.3158	1.9	84	-26.1815	28.3179	1.3
Y2	-26.1839	28.3155	0.81	163	-26.1830	28.3166	2.2	205	-26.1825	28.3157	1.9	218	-26.1835	28.3159	1.3
45	-26.1825	28.3178	2.4	164	-26.1832	28.3167	2.2	206	-26.1827	28.3158	1.9	276	-26.1838	28.3150	1.3
71	-26.1831	28.3175	2.4	170	-26.1831	28.3165	2.2	222	-26.1830	28.3156	1.9	281	-26.1833	28.3146	1.3
76	-26.1827	28.3174	2.4	173	-26.1826	28.3163	2.2	223	-26.1828	28.3155	1.9	297	-26.1836	28.3147	1.3
93	-26.1828	28.3174	2.4	185	-26.1827	28.3162	2.2	234	-26.1832	28.3154	1.9	302	-26.1839	28.3146	1.3
29	-26.1831	28.3176	2.3	186	-26.1830	28.3163	2.2	235	-26.1834	28.3155	1.9	304	-26.1836	28.3145	1.3
30	-26.1830	28.3176	2.3	187	-26.1831	28.3164	2.2	37	-26.1817	28.3182	1.8	40	-26.1814	28.3182	1.2
31	-26.1828	28.3177	2.3	34	-26.1822	28.3180	2.1	58	-26.1816	28.3181	1.8	97	-26.1833	28.3171	1.2
32	-26.1826	28.3178	2.3	35	-26.1820	28.3181	2.1	64	-26.1817	28.3179	1.8	179	-26.1818	28.3160	1.2
46	-26.1829	28.3176	2.3	43	-26.1821	28.3179	2.1	111	-26.1816	28.3173	1.8	180	-26.1819	28.3159	1.2
47	-26.1831	28.3175	2.3	80	-26.1820	28.3177	2.1	132	-26.1816	28.3170	1.8	230	-26.1825	28.3149	1.2
49	-26.1831	28.3174	2.3	89	-26.1819	28.3176	2.1	135	-26.1818	28.3168	1.8	241	-26.1826	28.3148	1.2
50	-26.1829	28.3175	2.3	105	-26.1819	28.3174	2.1	154	-26.1818	28.3167	1.8	285	-26.1829	28.3146	1.2
51	-26.1828	28.3176	2.3	106	-26.1818	28.3174	2.1	176	-26.1821	28.3162	1.8	286	-26.1828	28.3145	1.2
53	-26.1825	28.3177	2.3	118	-26.1831	28.3171	2.1	182	-26.1822	28.3160	1.8	305	-26.1834	28.3145	1.2
69	-26.1827	28.3176	2.3	119	-26.1833	28.3170	2.1	190	-26.1836	28.3165	1.8	313	-26.1839	28.3144	1.2
70	-26.1829	28.3175	2.3	123	-26.1832	28.3169	2.1	224	-26.1826	28.3154	1.8	282	-26.1832	28.3145	1.1
74	-26.1831	28.3173	2.3	130	-26.1820	28.3170	2.1	233	-26.1830	28.3153	1.8	283	-26.1831	28.3144	1.1
75	-26.1829	28.3173	2.3	137	-26.1822	28.3168	2.1	82	-26.1817	28.3178	1.7	284	-26.1830	28.3145	1.1
77	-26.1826	28.3175	2.3	142	-26.1833	28.3170	2.1	108	-26.1815	28.3175	1.7	296	-26.1834	28.3146	1.1
91	-26.1823	28.3175	2.3	145	-26.1833	28.3168	2.1	166	-26.1834	28.3168	1.7	306	-26.1833	28.3143	1.1
92	-26.1826	28.3175	2.3	151	-26.1823	28.3168	2.1	199	-26.1823	28.3158	1.7	307	-26.1832	28.3143	1.1
94	-26.1830	28.3173	2.3	160	-26.1823	28.3166	2.1	232	-26.1828	28.3152	1.7	312	-26.1837	28.3143	1.1
100	-26.1829	28.3171	2.3	161	-26.1825	28.3165	2.1	246	-26.1835	28.3152	1.7	11	-26.1827	28.3179	1
101	-26.1827	28.3171	2.3	169	-26.1833	28.3166	2.1	247	-26.1836	28.3153	1.7	87	-26.1815	28.3177	1
102	-26.1825	28.3172	2.3	171	-26.1829	28.3164	2.1	38	-26.1816	28.3182	1.6	109	-26.1814	28.3174	1
103	-26.1823	28.3172	2.3	172	-26.1828	28.3164	2.1	41	-26.1816	28.3182	1.6	156	-26.1816	28.3166	1
115	-26.1825	28.3172	2.3	184	-26.1825	28.3162	2.1	59	-26.1815	28.3181	1.6	191	-26.1836	28.3164	1
116	-26.1827	28.3172	2.3	188	-26.1833	28.3164	2.1	122	-26.1833	28.3170	1.6	287	-26.1828	28.3144	1
117	-26.1829	28.3171	2.3	193	-26.1833	28.3162	2.1	133	-26.1815	28.3170	1.6	295	-26.1832	28.3145	1
125	-26.1829	28.3169	2.3	194	-26.1831	28.3161	2.1	143	-26.1834	28.3170	1.6	308	-26.1831	28.3141	1
126	-26.1827	28.3169	2.3	195	-26.1829	28.3160	2.1	144	-26.1834	28.3169	1.6	311	-26.1834	28.3141	1
127	-26.1825	28.3169	2.3	196	-26.1828	28.3159	2.1	157	-26.1817	28.3166	1.6	319	-26.1838	28.3142	1
128	-26.1823	28.3170	2.3	208	-26.1829	28.3159	2.1	177	-26.1819	28.3161	1.6	322	-26.1836	28.3140	1
138	-26.1824	28.3168	2.3	209	-26.1831	28.3160	2.1	225	-26.1825	28.3153	1.6	271	-26.1841	28.3150	0.99
139	-26.1827	28.3168	2.3	210	-26.1832	28.3160	2.1	226	-26.1823	28.3152	1.6	270	-26.1842	28.3149	0.98
149	-26.1826	28.3168	2.3	36	-26.1818	28.3181	2	236	-26.1836	28.3155	1.6	324	-26.1835	28.3139	0.98
33	-26.1824	28.3179	2.2	42	-26.1818	28.3180	2	244	-26.1831	28.3150	1.6	289	-26.1828	28.3142	0.97
44	-26.1824	28.3179	2.2	56	-26.1819	28.3180	2	245	-26.1833	28.3151	1.6	309	-26.1831	28.3140	0.96
48	-26.1832	28.3174	2.2	65	-26.1819	28.3178	2	278	-26.1836	28.3149	1.6	321	-26.1837	28.3141	0.95
52	-26.1826	28.3176	2.2	81	-26.1818	28.3178	2	28	-26.1833	28.3175	1.5	250	-26.1840	28.3154	0.94
54	-26.1823	28.3178	2.2	96	-26.1833	28.3171	2	39	-26.1815	28.3183	1.5	267	-26.1843	28.3147	0.94
55	-26.1821	28.3179	2.2	107	-26.1816	28.3174	2	60	-26.1814	28.3181	1.5	249	-26.1839	28.3154	0.93
66	-26.1821	28.3178	2.2	112	-26.1817	28.3173	2	63	-26.1815	28.3180	1.5	272	-26.1841	28.3151	0.93
67	-26.1824	28.3177	2.2	131	-26.1818	28.3170	2	83	-26.1816	28.3178	1.5	13	-26.1829	28.3178	0.91
68	-26.1826	28.3177	2.2	136	-26.1820	28.3168	2	155	-26.1816	28.3167	1.5	23	-26.1834	28.3172	0.9
72	-26.1833	28.3173	2.2	152	-26.1821	28.3168	2	181	-26.1820	28.3159	1.5	269	-26.1842	28.3148	0.9
73	-26.1832	28.3172	2.2	153	-26.1819	28.3168	2	200	-26.1822	28.3157	1.5	310	-26.1832	28.3140	0.9
78	-26.1824	28.3176	2.2	159	-26.1821	28.3166	2	231	-26.1826	28.3151	1.5	323	-26.1836	28.3139	0.9
79	-26.1822	28.3176	2.2	165	-26.1833	28.3167	2	243	-26.1829	28.3150	1.5	336	-26.1834	28.3134	0.9
90	-26.1821	28.3176	2.2	168	-26.1834	28.3166	2	277	-26.1837	28.3149	1.5	341	-26.1838	28.3137	0.9
95	-26.1832	28.3172	2.2	174	-26.1824	28.3163	2	279	-26.1835	28.3148	1.5	273	-26.1840	28.3151	0.89
98	-26.1832	28.3170	2.2	175	-26.1822	28.3162	2	14	-26.1829	28.3177	1.4	288	-26.1828	28.3143	0.89
99	-26.1831	28.3170	2.2	189	-26.1835	28.3165	2	110	-26.1814	28.3174	1.4	339	-26.1836	28.3136	0.89
104	-26.1821	28.3173	2.2	192	-26.1835	28.3163	2	134	-26.1815	28.3168	1.4	2	-26.1814	28.3184	0.87
113	-26.1819	28.3173	2.2	197	-26.1826	28.3159	2	178	-26.1818	28.3161	1.4	325	-26.1833	28.3138	0.87
114	-26.1822	28.3172	2.2	207	-26.1828	28.3159	2	203	-26.1821	28.3158	1.4	274	-26.1840	28.3152	0.86
124	-26.1830	28.3169	2.2	211	-26.1834	28.3161	2	227	-26.1822	28.3152	1.4	275	-26.1840	28.3153	0.86
129	-26.1821	28.3170	2.2	219	-26.1834	28.3158	2	242	-26.1827	28.3149	1.4	326	-26.1832	28.3138	0.86
140	-26.1829	28.3169	2.2	220	-26.1833	28.3157	2	280	-26.1834	28.3147	1.4	331	-26.1832	28.3133	0.86
141	-26.1831	28.3169	2.2	221	-26.1831	28.3156	2	298	-26.1838	28.3148	1.4	332	-26.1832	28.3133	0.85
146	-26.1831	28.3168	2.2	57	-26.1817	28.3180	1.9	299	-26.1840	28.3149	1.4	254	-26.1841	28.3152	0.84

Table A7 Continued: Depth Measurements for Civic Lake

Sample	Lat	Long	Depth (m)	Sample	Lat	Long	Depth (m)	Sample	Lat	Long	Depth (m)	Sample	Lat	Long	Depth (m)	Sample	Lat	Long	Depth (m)
293	-26.1829	28.3142	0.84	239	-26.1837	28.3155	0.54	392	-26.1836	28.3174	0	458	-26.1824	28.3146	0	524	-26.1842	28.3140	0
334	-26.1833	28.3134	0.84	4	-26.1817	28.3183	0.53	393	-26.1827	28.3180	0	459	-26.1823	28.3180	0	525	-26.1844	28.3143	0
337	-26.1835	28.3134	0.83	22	-26.1834	28.3173	0.53	394	-26.1837	28.3132	0	460	-26.1843	28.3139	0	526	-26.1817	28.3183	0
217	-26.1836	28.3159	0.81	24	-26.1834	28.3172	0.53	395	-26.1814	28.3156	0	461	-26.1843	28.3142	0	527	-26.1837	28.3164	0
338	-26.1834	28.3136	0.81	342	-26.1839	28.3138	0.53	396	-26.1839	28.3159	0	462	-26.1818	28.3183	0	528	-26.1832	28.3136	0
340	-26.1837	28.3136	0.81	364	-26.1842	28.3140	0.53	397	-26.1811	28.3186	0	463	-26.1838	28.3164	0	529	-26.1841	28.3150	0
348	-26.1840	28.3139	0.81	85	-26.1814	28.3178	0.5	398	-26.1847	28.3150	0	464	-26.1831	28.3137	0	530	-26.1814	28.3164	0
16	-26.1832	28.3176	0.8	229	-26.1823	28.3150	0.5	399	-26.1829	28.3136	0	465	-26.1842	28.3148	0	531	-26.1833	28.3175	0
17	-26.1833	28.3176	0.8	327	-26.1832	28.3137	0.5	400	-26.1836	28.3171	0	466	-26.1814	28.3165	0	532	-26.1835	28.3134	0
88	-26.1817	28.3177	0.8	1	-26.1824	28.3180	0.49	401	-26.1818	28.3185	0	467	-26.1833	28.3174	0	533	-26.1845	28.3149	0
228	-26.1822	28.3151	0.8	18	-26.1834	28.3175	0.49	402	-26.1844	28.3140	0	468	-26.1834	28.3133	0	534	-26.1813	28.3174	0
251	-26.1840	28.3154	0.8	257	-26.1842	28.3150	0.49	403	-26.1820	28.3148	0	469	-26.1845	28.3149	0	535	-26.1833	28.3170	0
268	-26.1843	28.3148	0.8	367	-26.1842	28.3141	0.46	404	-26.1842	28.3161	0	470	-26.1813	28.3176	0	536	-26.1830	28.3132	0
294	-26.1830	28.3144	0.8	26	-26.1834	28.3173	0.45	405	-26.1811	28.3172	0	471	-26.1834	28.3168	0	537	-26.1837	28.3161	0
301	-26.1840	28.3147	0.8	354	-26.1840	28.3142	0.45	406	-26.1843	28.3149	0	472	-26.1830	28.3133	0	538	-26.1819	28.3151	0
314	-26.1841	28.3146	0.8	363	-26.1842	28.3141	0.44	407	-26.1829	28.3130	0	473	-26.1837	28.3160	0	539	-26.1825	28.3179	0
335	-26.1834	28.3134	0.8	6	-26.1819	28.3182	0.42	408	-26.1835	28.3176	0	474	-26.1817	28.3153	0	540	-26.1841	28.3137	0
253	-26.1841	28.3152	0.79	343	-26.1839	28.3137	0.41	409	-26.1825	28.3181	0	475	-26.1825	28.3179	0	541	-26.1845	28.3146	0
255	-26.1841	28.3151	0.79	167	-26.1835	28.3167	0.4	410	-26.1841	28.3135	0	476	-26.1840	28.3137	0	542	-26.1813	28.3181	0
258	-26.1842	28.3149	0.79	215	-26.1837	28.3161	0.4	411	-26.1816	28.3153	0	477	-26.1845	28.3145	0	543	-26.1836	28.3165	0
261	-26.1844	28.3148	0.78	262	-26.1844	28.3147	0.4	412	-26.1838	28.3160	0	478	-26.1813	28.3183	0	544	-26.1831	28.3133	0
291	-26.1829	28.3141	0.78	328	-26.1832	28.3136	0.4	413	-26.1811	28.3182	0	479	-26.1836	28.3164	0	545	-26.1838	28.3156	0
12	-26.1827	28.3178	0.77	320	-26.1838	28.3141	0.39	414	-26.1845	28.3151	0	480	-26.1831	28.3134	0	546	-26.1815	28.3159	0
212	-26.1837	28.3163	0.76	121	-26.1834	28.3170	0.37	415	-26.1828	28.3134	0	481	-26.1838	28.3156	0	547	-26.1829	28.3177	0
213	-26.1838	28.3163	0.75	347	-26.1839	28.3139	0.37	416	-26.1836	28.3171	0	482	-26.1815	28.3161	0	548	-26.1836	28.3134	0
264	-26.1845	28.3147	0.75	355	-26.1840	28.3141	0.36	417	-26.1818	28.3185	0	483	-26.1830	28.3176	0	549	-26.1844	28.3147	0
238	-26.1838	28.3156	0.74	368	-26.1843	28.3142	0.32	418	-26.1844	28.3141	0	484	-26.1836	28.3133	0	550	-26.1814	28.3169	0
237	-26.1837	28.3156	0.73	359	-26.1841	28.3141	0.29	419	-26.1822	28.3145	0	485	-26.1844	28.3147	0	551	-26.1834	28.3173	0
256	-26.1842	28.3151	0.73	360	-26.1841	28.3140	0.29	420	-26.1840	28.3164	0	486	-26.1814	28.3169	0	552	-26.1832	28.3131	0
265	-26.1844	28.3147	0.73	3	-26.1816	28.3184	0.28	421	-26.1812	28.3168	0	487	-26.1834	28.3172	0	553	-26.1839	28.3161	0
260	-26.1843	28.3148	0.72	357	-26.1841	28.3141	0.26	422	-26.1842	28.3152	0	488	-26.1831	28.3131	0	554	-26.1826	28.3142	0
263	-26.1845	28.3147	0.72	356	-26.1841	28.3141	0.25	423	-26.1830	28.3129	0	489	-26.1838	28.3161	0	555	-26.1820	28.3182	0
292	-26.1829	28.3141	0.72	346	-26.1839	28.3138	0.23	424	-26.1834	28.3178	0	490	-26.1825	28.3144	0	556	-26.1843	28.3140	0
330	-26.1832	28.3134	0.71	86	-26.1815	28.3178	0.22	425	-26.1816	28.3186	0	491	-26.1820	28.3181	0	557	-26.1845	28.3145	0
333	-26.1833	28.3133	0.71	362	-26.1841	28.3140	0.22	426	-26.1846	28.3143	0	492	-26.1843	28.3139	0	558	-26.1814	28.3184	0
204	-26.1823	28.3157	0.7	345	-26.1840	28.3138	0.21	427	-26.1824	28.3143	0	493	-26.1845	28.3144	0	559	-26.1836	28.3164	0
240	-26.1824	28.3147	0.7	353	-26.1840	28.3141	0.21	428	-26.1839	28.3166	0	494	-26.1815	28.3184	0	560	-26.1832	28.3135	0
300	-26.1841	28.3148	0.7	361	-26.1841	28.3140	0.21	429	-26.1842	28.3141	0	495	-26.1837	28.3164	0	561	-26.1839	28.3154	0
19	-26.1834	28.3175	0.69	366	-26.1843	28.3141	0.21	430	-26.1819	28.3182	0	496	-26.1831	28.3136	0	562	-26.1815	28.3163	0
27	-26.1834	28.3174	0.69	350	-26.1841	28.3140	0.16	431	-26.1839	28.3163	0	497	-26.1841	28.3151	0	563	-26.1832	28.3176	0
252	-26.1841	28.3153	0.69	352	-26.1840	28.3141	0.11	432	-26.1830	28.3138	0	498	-26.1814	28.3164	0	564	-26.1835	28.3133	0
344	-26.1840	28.3137	0.69	351	-26.1841	28.3140	0.1	433	-26.1842	28.3147	0	499	-26.1832	28.3176	0	565	-26.1845	28.3147	0
316	-26.1843	28.3145	0.68	358	-26.1841	28.3141	0.1	434	-26.1814	28.3165	0	500	-26.1835	28.3134	0	566	-26.1813	28.3170	0
7	-26.1821	28.3182	0.67	369	-26.1832	28.3179	0	435	-26.1833	28.3174	0	501	-26.1845	28.3148	0	567	-26.1834	28.3172	0
266	-26.1844	28.3147	0.67	370	-26.1832	28.3130	0	436	-26.1834	28.3133	0	502	-26.1813	28.3172	0	568	-26.1830	28.3131	0
290	-26.1828	28.3142	0.67	371	-26.1812	28.3164	0	437	-26.1846	28.3148	0	503	-26.1833	28.3171	0	569	-26.1838	28.3161	0
10	-26.1825	28.3180	0.66	372	-26.1840	28.3155	0	438	-26.1813	28.3177	0	504	-26.1830	28.3131	0	570	-26.1822	28.3148	0
25	-26.1834	28.3172	0.66	373	-26.1816	28.3186	0	439	-26.1834	28.3167	0	505	-26.1838	28.3161	0	571	-26.1824	28.3179	0
259	-26.1843	28.3149	0.65	374	-26.1846	28.3145	0	440	-26.1830	28.3133	0	506	-26.1820	28.3151	0	572	-26.1842	28.3139	0
8	-26.1822	28.3181	0.64	375	-26.1825	28.3141	0	441	-26.1837	28.3159	0	507	-26.1824	28.3179	0	573	-26.1846	28.3148	0
216	-26.1837	28.3160	0.64	376	-26.1837	28.3166	0	442	-26.1816	28.3156	0	508	-26.1842	28.3137	0	574	-26.1813	28.3178	0
315	-26.1843	28.3146	0.64	377	-26.1830	28.3180	0	443	-26.1826	28.3179	0	509	-26.1846	28.3146	0	575	-26.1835	28.3165	0
317	-26.1843	28.3144	0.64	378	-26.1835	28.3131	0	444	-26.1838	28.3135	0	510	-26.1813	28.3179	0	576	-26.1830	28.3133	0
5	-26.1818	28.3183	0.6	379	-26.1813	28.3160	0	445	-26.1845	28.3145	0	511	-26.1835	28.3165	0	577	-26.1837	28.3159	0
15	-26.1831	28.3177	0.6	380	-26.1839	28.3157	0	446	-26.1813	28.3184	0	512	-26.1830	28.3133	0	578	-26.1816	28.3157	0
201	-26.1820	28.3156	0.6	381	-26.1813	28.3187	0	447	-26.1836	28.3164	0	513	-26.1837	28.3157	0	579	-26.1826	28.3178	0
202	-26.1820	28.3156	0.6	382	-26.1847	28.3147	0	448	-26.1831	28.3134	0	514	-26.1815	28.3159	0	580	-26.1838	28.3135	0
214	-26.1837	28.3162	0.6	383	-26.1828	28.3138	0	449	-26.1839	28.3154	0	515	-26.1828	28.3177	0	581	-26.1843	28.3147	0
248	-26.1838	28.3153	0.6	384	-26.1836	28.3169	0	450	-26.1815	28.3162	0	516	-26.1837	28.3134	0	582	-26.1814	28.3166	0
9	-26.1824	28.3180	0.59	385	-26.1822	28.3183	0	451	-26.1830	28.3177	0	517	-26.1843	28.3147	0	583	-26.1834	28.3174	0
318	-26.1841	28.3143	0.59	386	-26.1843	28.3137	0	452	-26.1835	28.3132	0	518	-26.1814	28.3168	0	584	-26.1833	28.3132	0
365	-26.1843	28.3140	0.59	387	-26.1818	28.3151	0	453	-26.1845	28.3147	0	519	-26.1834	28.3173	0	585	-26.1839	28.3162	0
329	-26.1832	28.3135	0.57	388	-26.1840	28.3160	0	454	-26.1813	28.3170	0	520	-26.1833	28.3132	0	586	-26.1828	28.3139	0
349	-26.1841	28.3139	0.57	389	-26.1811	28.3177	0	455	-26.1834	28.3172	0	521	-26.1839	28.3161	0	587	-26.1819	28.3182	0
21	-26.1834	28.3173	0.56	390	-26.1844	28.3150	0	456	-26.1831	28.3131	0	522	-26.1827	28.3141	0	588	-26.1842	28.3141	0
20	-26.1834	28.3174	0.55	391	-26.1828	28.3132	0	457	-26.1838	28.3161	0	523	-26.1819	28.3182	0	589	-26.1842	28.3141	0

Table A8: Depth Measurements for Kleinfontein Dam

Sample	Lat	Long	Depth (m)	Sample	Lat	Long	Depth (m)	Sample	Lat	Long	Depth (m)	Sample	Lat	Long	Depth (m)	Sample	Lat	Long	Depth (m)	Sample	Lat	Long	Depth (m)	Sample	Lat	Long	Depth (m)	Sample	Lat	Long	Depth (m)
X1	-26.1822	28.3187	2.8	316	-26.1813	28.3265	4.9	353	-26.1804	28.3260	4.6	109	-26.1818	28.3230	4.3	148	-26.1826	28.3238	4	50	-26.1814	28.3209	3.6	360	-26.1830	28.3262	3.2	150	-26.1832	28.3237	2.5
X2	-26.1821	28.3216	3.8	317	-26.1811	28.3266	4.9	372	-26.1808	28.3255	4.6	117	-26.1819	28.3229	4.3	284	-26.1826	28.3275	4	59	-26.1824	28.3213	3.6	405	-26.1799	28.3249	3.2	173	-26.1832	28.3242	2.5
C	-26.1817	28.3242	4.6	327	-26.1810	28.3264	4.9	382	-26.1808	28.3253	4.6	124	-26.1816	28.3231	4.3	311	-26.1826	28.3269	4	78	-26.1825	28.3219	3.6	7	-26.1822	28.3193	3.1	21	-26.1816	28.3199	2.4
X3	-26.1813	28.3270	4.9	328	-26.1812	28.3265	4.9	384	-26.1815	28.3253	4.6	126	-26.1823	28.3232	4.3	375	-26.1800	28.3255	4	95	-26.1823	28.3223	3.6	10	-26.1819	28.3197	3.1	45	-26.1832	28.3209	2.4
X4	-26.1814	28.3293	3.2	330	-26.1820	28.3266	4.9	397	-26.1821	28.3249	4.6	134	-26.1822	28.3233	4.3	387	-26.1828	28.3256	4	141	-26.1808	28.3233	3.6	46	-26.1830	28.3210	3.1	113	-26.1830	28.3228	2.4
Y1	-26.1835	28.3244	1.1	340	-26.1823	28.3265	4.9	398	-26.1818	28.3249	4.6	143	-26.1812	28.3235	4.3	410	-26.1803	28.3246	4	161	-26.1808	28.3233	3.6	64	-26.1830	28.3215	3.1	307	-26.1830	28.3273	2.4
Y2	-26.1802	28.3237	0.84	341	-26.1819	28.3264	4.9	400	-26.1813	28.3249	4.6	144	-26.1814	28.3236	4.3	75	-26.1817	28.3217	3.9	164	-26.1807	28.3236	3.6	120	-26.1809	28.3228	3.1	379	-26.1798	28.3253	2.4
239	-26.1813	28.3289	5.3	342	-26.1817	28.3263	4.9	145	-26.1817	28.3236	4.5	160	-26.1811	28.3235	4.3	76	-26.1818	28.3218	3.9	25	-26.1822	28.3202	3.5	246	-26.1799	28.3291	3.1	97	-26.1829	28.3223	2.3
251	-26.1813	28.3287	5.3	356	-26.1813	28.3260	4.9	157	-26.1819	28.3238	4.5	166	-26.1811	28.3239	4.3	87	-26.1819	28.3219	3.9	38	-26.1817	28.3206	3.5	255	-26.1827	28.3282	3.1	153	-26.1833	28.3239	2.3
237	-26.1819	28.3288	5.2	367	-26.1821	28.3257	4.9	158	-26.1815	28.3237	4.5	171	-26.1825	28.3242	4.3	112	-26.1827	28.3229	3.9	65	-26.1829	28.3216	3.5	295	-26.1797	28.3272	3.1	189	-26.1803	28.3241	2.3
238	-26.1816	28.3289	5.2	195	-26.1818	28.3248	4.8	167	-26.1814	28.3239	4.5	179	-26.1826	28.3245	4.3	115	-26.1827	28.3229	3.9	70	-26.1814	28.3214	3.5	310	-26.1829	28.3271	3.1	209	-26.1803	28.3294	2.3
240	-26.1810	28.3290	5.2	260	-26.1823	28.3280	4.8	168	-26.1816	28.3240	4.5	185	-26.1810	28.3239	4.3	132	-26.1828	28.3233	3.9	84	-26.1831	28.3220	3.5	333	-26.1829	28.3269	3.1	233	-26.1829	28.3285	2.3
250	-26.1810	28.3288	5.2	267	-26.1803	28.3280	4.8	169	-26.1822	28.3241	4.5	191	-26.1806	28.3244	4.3	186	-26.1807	28.3238	3.9	324	-26.1798	28.3265	3.5	351	-26.1798	28.3261	3.1	270	-26.1796	28.3283	2.3
262	-26.1817	28.3280	5.2	274	-26.1802	28.3279	4.8	180	-26.1824	28.3244	4.5	243	-26.1802	28.3291	4.3	213	-26.1813	28.3292	3.9	18	-26.1826	28.3201	3.4	417	-26.1829	28.3249	3.1	322	-26.1796	28.3267	2.3
264	-26.1812	28.3280	5.2	292	-26.1804	28.3271	4.8	181	-26.1822	28.3243	4.5	365	-26.1827	28.3259	4.3	259	-26.1826	28.3280	3.9	19	-26.1821	28.3200	3.4	6	-26.1824	28.3191	3	418	-26.1833	28.3249	2.3
241	-26.1808	28.3290	5.1	300	-26.1805	28.3270	4.8	183	-26.1816	28.3241	4.5	403	-26.1804	28.3249	4.3	306	-26.1827	28.3272	3.9	24	-26.1820	28.3202	3.4	14	-26.1830	28.3196	3	392	-26.1833	28.3255	2.2
249	-26.1806	28.3288	5.1	318	-26.1808	28.3266	4.8	196	-26.1821	28.3249	4.5	93	-26.1816	28.3221	4.2	404	-26.1802	28.3250	3.9	26	-26.1826	28.3202	3.4	388	-26.1831	28.3256	3	406	-26.1798	28.3249	2.2
252	-26.1817	28.3285	5.1	331	-26.1823	28.3266	4.8	198	-26.1827	28.3250	4.5	104	-26.1819	28.3225	4.2	56	-26.1817	28.3212	3.8	33	-26.1818	28.3204	3.4	30	-26.1829	28.3204	2.9	2	-26.1826	28.3185	2.1
265	-26.1809	28.3281	5.1	344	-26.1811	28.3262	4.8	254	-26.1824	28.3283	4.5	108	-26.1815	28.3228	4.2	57	-26.1820	28.3213	3.8	41	-26.1825	28.3208	3.4	187	-26.1805	28.3237	2.9	28	-26.1831	28.3202	2.1
278	-26.1817	28.3276	5.1	355	-26.1810	28.3260	4.8	320	-26.1801	28.3266	4.5	110	-26.1821	28.3230	4.2	68	-26.1821	28.3215	3.8	42	-26.1827	28.3208	3.4	281	-26.1827	28.3276	2.9	71	-26.1812	28.3213	2.1
286	-26.1821	28.3274	5.1	357	-26.1817	28.3260	4.8	339	-26.1825	28.3266	4.5	111	-26.1824	28.3230	4.2	74	-26.1815	28.3216	3.8	73	-26.1813	28.3215	3.4	283	-26.1828	28.3276	2.9	90	-26.1811	28.3217	2.1
290	-26.1809	28.3271	5.1	358	-26.1822	28.3260	4.8	347	-26.1803	28.3262	4.5	116	-26.1823	28.3229	4.2	85	-26.1826	28.3220	3.8	101	-26.1829	28.3226	3.4	298	-26.1797	28.3270	2.9	207	-26.1800	28.3294	2.1
242	-26.1805	28.3291	5	368	-26.1818	28.3257	4.8	359	-26.1826	28.3261	4.5	118	-26.1816	28.3229	4.2	91	-26.1811	28.3219	3.8	122	-26.1809	28.3229	3.4	376	-26.1798	28.3255	2.9	334	-26.1831	28.3270	2.1
253	-26.1821	28.3284	5	385	-26.1820	28.3254	4.8	373	-26.1805	28.3255	4.5	137	-26.1813	28.3231	4.2	105	-26.1815	28.3225	3.8	149	-26.1830	28.3238	3.4	8	-26.1818	28.3194	2.8	15	-26.1832	28.3197	2
261	-26.1820	28.3280	5	285	-26.1823	28.3274	4.7	386	-26.1825	28.3255	4.5	147	-26.1823	28.3237	4.2	210	-26.1806	28.3293	3.8	244	-26.1800	28.3292	3.4	83	-26.1833	28.3220	2.8	139	-26.1807	28.3229	2
263	-26.1815	28.3280	5	305	-26.1824	28.3271	4.7	396	-26.1824	28.3251	4.5	156	-26.1822	28.3239	4.2	269	-26.1798	28.3283	3.8	394	-26.1829	28.3254	3.4	337	-26.1830	28.3267	2.8	162	-26.1806	28.3233	2
266	-26.1806	28.3281	5	312	-26.1823	28.3267	4.7	399	-26.1815	28.3249	4.5	165	-26.1809	28.3238	4.2	321	-26.1799	28.3267	3.8	11	-26.1821	28.3197	3.3	37	-26.1814	28.3205	2.7	177	-26.1832	28.3245	2
275	-26.1806	28.3278	5	319	-26.1805	28.3266	4.7	401	-26.1809	28.3249	4.5	273	-26.1799	28.3280	4.2	338	-26.1828	28.3266	3.8	12	-26.1824	28.3197	3.3	44	-26.1831	28.3208	2.7	218	-26.1825	28.3290	2
276	-26.1810	28.3278	5	326	-26.1806	28.3264	4.7	402	-26.1807	28.3249	4.5	294	-26.1799	28.3271	4.2	380	-26.1800	28.3253	3.8	13	-26.1829	28.3196	3.3	61	-26.1831	28.3212	2.7	219	-26.1826	28.3290	2
277	-26.1814	28.3276	5	345	-26.1809	28.3262	4.7	412	-26.1811	28.3246	4.5	332	-26.1826	28.3267	4.2	416	-26.1827	28.3249	3.8	23	-26.1817	28.3201	3.3	96	-26.1826	28.3223	2.7	245	-26.1799	28.3292	2
287	-26.1817	28.3272	5	346	-26.1806	28.3262	4.7	413	-26.1815	28.3246	4.5	348	-26.1800	28.3262	4.2	32	-26.1822	28.3204	3.7	27	-26.1827	28.3202	3.3	106	-26.1812	28.3224	2.7	257	-26.1830	28.3281	2
288	-26.1814	28.3272	5	354	-26.1808	28.3260	4.7	414	-26.1820	28.3247	4.5	94	-26.1819	28.3222	4.1	40	-26.1822	28.3208	3.7	47	-26.1828	28.3210	3.3	131	-26.1830	28.3233	2.7	272	-26.1795	28.3282	2
289	-26.1811	28.3271	5	366	-26.1824	28.3258	4.7	415	-26.1823	28.3248	4.5	102	-26.1827	28.3226	4.1	48	-26.1826	28.3210	3.7	79	-26.1829	28.3219	3.3	208	-26.1801	28.3294	2.7	296	-26.1796	28.3271	2
291	-26.1806	28.3272	5	369	-26.1816	28.3257	4.7	125	-26.1819	28.3231	4.4	103	-26.1824	28.3225	4.1	49	-26.1824	28.3210	3.7	214	-26.1815	28.3292	3.3	212	-26.1810	28.3293	2.7	309	-26.1831	28.3272	2
302	-26.1813	28.3270	5	370	-26.1813	28.3256	4.7	135	-26.1819	28.3233	4.4	119	-26.1812	28.3228	4.1	55	-26.1814	28.3211	3.7	364	-26.1829	28.3260	3.3	393	-26.1831	28.3255	2.7	389	-26.1833	28.3257	2
303	-26.1816	28.3271	5	371	-26.1811	28.3256	4.7	136	-26.1816	28.3232	4.4	123	-26.1813	28.3230	4.1	58	-26.1822	28.3213	3.7	20	-26.1819	28.3199	3.2	409	-26.1800	28.3246	2.7	4	-26.1830	28.3188	1.9
314	-26.1818	28.3266	5	383	-26.1811	28.3253	4.7	146	-26.1820	28.3237	4.4	133	-26.1825	28.3233	4.1	66	-26.1825	28.3215	3.7	43	-26.1829	28.3208	3.2	1	-26.1824	28.3186	2.6	52	-26.1812	28.3209	1.9
329	-26.1816	28.3265	5	63	-26.1833	28.3214	4.6	159	-26.1811	28.3236	4.4	142	-26.1810	28.3234	4.1	67	-26.1823	28.3215	3.7	51	-26.1813	28.3208	3.2	17	-26.1829	28.3201	2.6	151	-26.1834	28.3237	1.9
343	-26.1814	28.3262	5	182	-26.1819	28.3242	4.6	170	-26.1824	28.3242	4.4	155	-26.1825	28.3239	4.1	69	-26.1816	28.3214	3.7	54	-26.1813	28.3211	3.2	34	-26.1816	28.3203	2.6	16	-26.1832	28.3199	1.8
236	-26.1821	28.3288	4.9	192	-26.1810	28.3245	4.6	184	-26.1813	28.3240	4.4	215	-26.1817	28.3292	4.1	88	-26.1816	28.3218	3.7	60	-26.1827	28.3212	3.2	128	-26.1830	28.3232	2.6	29	-26.1832	28.3204	1.8
248	-26.1804	28.3289	4.9	193	-26.1812	28.3246	4.6	268	-26.1800	28.3281	4.4	247	-26.1801	28.3290	4.1	138	-26.1809	28.3230	3.7	154	-26.1830	28.3239	3.2	200	-26.1833	28.3252	2.6	217	-26.1824	28.3290	1.8
279	-26.1822	28.3276	4.9	194	-26.1816	28.3247	4.6	325	-26.1802	28.3264	4.4	352	-26.1801	28.3261	4.1	172	-26.1829	28.3242	3.7	178	-26.1830	28.3245	3.2	204	-26.1798	28.3289	2.6	282	-26.1830	28.3277	1.8
301	-26.1808	28.3270	4.9	197	-26.1824	28.3250	4.6	374	-26.1803	28.3255	4.4	77	-26.1824	28.3219	4	190	-26.1804	28.3242	3.7	211	-26.1808	28.3293	3.2	363	-26.1831	28.3261	2.6	336	-26.1832	28.3268	1.8
304	-26.1820	28.3271	4.9	280	-26.1824	28.3276	4.6	381	-26.1804	28.3253	4.4	86	-26.1823	28.3220	4	235	-26.1824	28.3287	3.7	234	-26.1827	28.3286	3.2	5	-26.1828	28.3190	2.5	361	-26.1832	28.3263	1.8
313	-26.1821	28.3267	4.9	293	-26.1802	28.3271	4.6	395	-26.1827	28.3253	4.4	92	-26.1813	28.3220	4	31	-26.1825	28.3204	3.6	258	-26.1828	28.3280	3.2	80	-26.1831	28.3218	2.5	377	-26.1796	28.3255	1.8
315	-26.1816	28.3265	4.9	299	-26.1801	28.3270	4.6	411	-26.1807	28.3246	4.4	127	-26.1827	28.3232	4	39	-26.1820	28.3207	3.6	349	-26.1797	28.3262	3.2	89	-26.1813	28.3217	2.5	3	-26.1829	28.3185	1.7

Table A8 Continued: Depth Measurements for Kleinfontein Dam

Sample	Lat	Long	Depth (m)	Sample	Lat	Long	Depth (m)	Sample	Lat	Long	Depth (m)	Sample	Lat	Long	Depth (m)	Sample	Lat	Long	Depth (m)	Sample	Lat	Long	Depth (m)	Sample	Lat	Long	Depth (m)	Sample	Lat	Long	Depth (m)
9	-26.1816	28.3196	1.7	36	-26.1813	28.3204	0.9	454	-26.1831	28.3184	0	500	-26.1795	28.3251	0	546	-26.1797	28.3291	0	592	-26.1831	28.3274	0	638	-26.1834	28.3220	0	684	-26.1792	28.3270	0
98	-26.1831	28.3223	1.7	223	-26.1831	28.3288	0.9	455	-26.1831	28.3184	0	501	-26.1795	28.3252	0	547	-26.1797	28.3292	0	593	-26.1832	28.3274	0	639	-26.1834	28.3220	0	685	-26.1835	28.3210	0
129	-26.1832	28.3231	1.7	231	-26.1832	28.3284	0.9	456	-26.1830	28.3183	0	502	-26.1795	28.3253	0	548	-26.1797	28.3293	0	594	-26.1832	28.3273	0	640	-26.1834	28.3214	0	686	-26.1805	28.3224	0
390	-26.1833	28.3256	1.7	99	-26.1834	28.3223	0.8	457	-26.1830	28.3183	0	503	-26.1795	28.3255	0	549	-26.1797	28.3293	0	595	-26.1833	28.3273	0	641	-26.1834	28.3213	0	687	-26.1838	28.3254	0
100	-26.1832	28.3225	1.6	225	-26.1831	28.3286	0.8	458	-26.1830	28.3182	0	504	-26.1794	28.3257	0	550	-26.1798	28.3294	0	596	-26.1833	28.3272	0	642	-26.1834	28.3210	0	688	-26.1810	28.3295	0
121	-26.1808	28.3228	1.6	229	-26.1833	28.3284	0.8	459	-26.1827	28.3183	0	505	-26.1794	28.3258	0	551	-26.1798	28.3294	0	597	-26.1833	28.3269	0	643	-26.1834	28.3209	0	689	-26.1835	28.3180	0
130	-26.1833	28.3233	1.6	205	-26.1798	28.3292	0.6	460	-26.1823	28.3185	0	506	-26.1794	28.3260	0	552	-26.1798	28.3295	0	598	-26.1833	28.3268	0	644	-26.1834	28.3206	0	690	-26.1825	28.3182	0
152	-26.1834	28.3239	1.6	227	-26.1833	28.3284	0.5	461	-26.1819	28.3187	0	507	-26.1794	28.3262	0	553	-26.1798	28.3295	0	599	-26.1833	28.3267	0	645	-26.1834	28.3206	0	691	-26.1820	28.3293	0
174	-26.1834	28.3242	1.6	228	-26.1833	28.3284	0.5	462	-26.1816	28.3190	0	508	-26.1795	28.3263	0	554	-26.1801	28.3295	0	600	-26.1834	28.3264	0	646	-26.1835	28.3206	0	692	-26.1796	28.3243	0
175	-26.1835	28.3243	1.6	226	-26.1834	28.3285	0.4	463	-26.1816	28.3190	0	509	-26.1795	28.3264	0	555	-26.1801	28.3295	0	601	-26.1834	28.3264	0	647	-26.1834	28.3205	0	693	-26.1837	28.3231	0
176	-26.1835	28.3243	1.6	199	-26.1830	28.3251	0.2	464	-26.1815	28.3193	0	510	-26.1795	28.3265	0	556	-26.1804	28.3294	0	602	-26.1834	28.3264	0	648	-26.1834	28.3205	0	694	-26.1810	28.3204	0
206	-26.1798	28.3294	1.6	202	-26.1834	28.3217	0.1	465	-26.1815	28.3196	0	511	-26.1795	28.3266	0	557	-26.1805	28.3294	0	603	-26.1834	28.3263	0	649	-26.1834	28.3204	0	695	-26.1835	28.3277	0
222	-26.1830	28.3288	1.6	203	-26.1797	28.3290	0	466	-26.1815	28.3198	0	512	-26.1795	28.3266	0	558	-26.1805	28.3294	0	604	-26.1834	28.3262	0	650	-26.1834	28.3204	0	696	-26.1791	28.3293	0
297	-26.1796	28.3270	1.6	421	-26.1834	28.3193	0	467	-26.1814	28.3199	0	513	-26.1795	28.3267	0	559	-26.1807	28.3294	0	605	-26.1834	28.3261	0	651	-26.1833	28.3204	0	697	-26.1836	28.3198	0
323	-26.1796	28.3265	1.6	422	-26.1834	28.3190	0	468	-26.1815	28.3200	0	514	-26.1795	28.3268	0	560	-26.1808	28.3294	0	606	-26.1834	28.3260	0	652	-26.1832	28.3203	0	698	-26.1815	28.3188	0
335	-26.1832	28.3270	1.6	423	-26.1833	28.3186	0	469	-26.1815	28.3201	0	515	-26.1795	28.3269	0	561	-26.1809	28.3294	0	607	-26.1834	28.3258	0	653	-26.1832	28.3202	0	699	-26.1832	28.3292	0
350	-26.1796	28.3262	1.6	424	-26.1833	28.3186	0	470	-26.1815	28.3201	0	516	-26.1795	28.3270	0	562	-26.1810	28.3294	0	608	-26.1834	28.3258	0	654	-26.1832	28.3201	0	700	-26.1792	28.3265	0
362	-26.1833	28.3262	1.6	425	-26.1833	28.3186	0	471	-26.1814	28.3201	0	517	-26.1795	28.3271	0	563	-26.1810	28.3294	0	609	-26.1834	28.3257	0	655	-26.1833	28.3200	0	701	-26.1835	28.3214	0
419	-26.1834	28.3248	1.6	426	-26.1832	28.3186	0	472	-26.1814	28.3201	0	518	-26.1795	28.3271	0	564	-26.1811	28.3294	0	610	-26.1834	28.3257	0	656	-26.1834	28.3200	0	702	-26.1806	28.3220	0
62	-26.1833	28.3213	1.5	427	-26.1831	28.3186	0	473	-26.1813	28.3203	0	519	-26.1795	28.3272	0	565	-26.1813	28.3294	0	611	-26.1835	28.3255	0	657	-26.1834	28.3193	0	703	-26.1836	28.3258	0
107	-26.1810	28.3223	1.5	428	-26.1830	28.3186	0	474	-26.1812	28.3205	0	520	-26.1795	28.3273	0	566	-26.1816	28.3293	0	612	-26.1835	28.3255	0	658	-26.1828	28.3181	0	704	-26.1806	28.3296	0
114	-26.1831	28.3229	1.5	429	-26.1830	28.3186	0	475	-26.1812	28.3207	0	521	-26.1794	28.3273	0	567	-26.1819	28.3292	0	613	-26.1836	28.3254	0	659	-26.1818	28.3293	0	705	-26.1837	28.3181	0
163	-26.1804	28.3236	1.5	430	-26.1830	28.3185	0	476	-26.1811	28.3209	0	522	-26.1795	28.3274	0	568	-26.1821	28.3292	0	614	-26.1836	28.3254	0	660	-26.1798	28.3239	0	706	-26.1820	28.3184	0
220	-26.1827	28.3289	1.5	431	-26.1830	28.3185	0	477	-26.1811	28.3210	0	523	-26.1795	28.3274	0	569	-26.1824	28.3291	0	615	-26.1837	28.3251	0	661	-26.1837	28.3236	0	707	-26.1827	28.3292	0
224	-26.1831	28.3287	1.5	432	-26.1830	28.3185	0	478	-26.1811	28.3211	0	524	-26.1794	28.3274	0	570	-26.1832	28.3290	0	616	-26.1837	28.3248	0	662	-26.1811	28.3201	0	708	-26.1793	28.3253	0
256	-26.1830	28.3282	1.5	433	-26.1830	28.3185	0	479	-26.1810	28.3215	0	525	-26.1794	28.3275	0	571	-26.1833	28.3290	0	617	-26.1836	28.3246	0	663	-26.1837	28.3281	0	709	-26.1836	28.3223	0
308	-26.1832	28.3273	1.5	434	-26.1831	28.3185	0	480	-26.1809	28.3219	0	526	-26.1795	28.3275	0	572	-26.1833	28.3289	0	618	-26.1836	28.3245	0	664	-26.1791	28.3287	0	710	-26.1808	28.3213	0
22	-26.1815	28.3201	1.4	435	-26.1831	28.3185	0	481	-26.1808	28.3222	0	527	-26.1795	28.3276	0	573	-26.1833	28.3288	0	619	-26.1836	28.3243	0	665	-26.1836	28.3201	0	711	-26.1835	28.3266	0
140	-26.1806	28.3231	1.4	436	-26.1831	28.3185	0	482	-26.1808	28.3223	0	528	-26.1794	28.3276	0	574	-26.1832	28.3288	0	620	-26.1836	28.3242	0	666	-26.1818	28.3186	0	712	-26.1796	28.3298	0
221	-26.1828	28.3289	1.4	437	-26.1831	28.3185	0	483	-26.1807	28.3226	0	529	-26.1794	28.3277	0	575	-26.1832	28.3287	0	621	-26.1836	28.3241	0	667	-26.1829	28.3292	0	713	-26.1836	28.3186	0
271	-26.1795	28.3284	1.4	438	-26.1832	28.3184	0	484	-26.1807	28.3226	0	530	-26.1794	28.3278	0	576	-26.1832	28.3286	0	622	-26.1836	28.3240	0	668	-26.1792	28.3259	0	714	-26.1813	28.3193	0
391	-26.1834	28.3255	1.4	439	-26.1832	28.3184	0	485	-26.1806	28.3227	0	531	-26.1794	28.3279	0	577	-26.1832	28.3285	0	623	-26.1835	28.3237	0	669	-26.1835	28.3217	0	715	-26.1835	28.3290	0
407	-26.1797	28.3248	1.4	440	-26.1832	28.3184	0	486	-26.1805	28.3227	0	532	-26.1794	28.3280	0	578	-26.1833	28.3285	0	624	-26.1835	28.3236	0	670	-26.1808	28.3217	0	716	-26.1791	28.3277	0
408	-26.1798	28.3246	1.4	441	-26.1833	28.3184	0	487	-26.1802	28.3234	0	533	-26.1794	28.3281	0	579	-26.1833	28.3285	0	625	-26.1835	28.3236	0	671	-26.1836	28.3262	0	717	-26.1835	28.3205	0
35	-26.1814	28.3203	1.3	442	-26.1833	28.3184	0	488	-26.1802	28.3237	0	534	-26.1794	28.3282	0	580	-26.1833	28.3284	0	626	-26.1835	28.3231	0	672	-26.1802	28.3297	0	718	-26.1802	28.3230	0
201	-26.1835	28.3252	1.3	443	-26.1833	28.3184	0	489	-26.1800	28.3239	0	535	-26.1794	28.3283	0	581	-26.1833	28.3284	0	627	-26.1834	28.3230	0	673	-26.1837	28.3182	0	719	-26.1838	28.3248	0
232	-26.1830	28.3284	1.3	444	-26.1833	28.3183	0	490	-26.1798	28.3243	0	536	-26.1794	28.3284	0	582	-26.1833	28.3283	0	628	-26.1834	28.3230	0	674	-26.1823	28.3183	0	720	-26.1813	28.3295	0
53	-26.1812	28.3210	1.2	445	-26.1833	28.3183	0	491	-26.1798	28.3244	0	537	-26.1794	28.3288	0	583	-26.1833	28.3283	0	629	-26.1834	28.3229	0	675	-26.1823	28.3292	0	721	-26.1831	28.3180	0
72	-26.1811	28.3214	1.2	446	-26.1833	28.3183	0	492	-26.1798	28.3244	0	538	-26.1794	28.3289	0	584	-26.1832	28.3282	0	630	-26.1833	28.3229	0	676	-26.1795	28.3247	0	722	-26.1812	28.3198	0
81	-26.1832	28.3218	1.2	447	-26.1833	28.3183	0	493	-26.1797	28.3246	0	539	-26.1794	28.3290	0	585	-26.1831	28.3280	0	631	-26.1832	28.3230	0	677	-26.1836	28.3228	0	723	-26.1836	28.3287	0
82	-26.1833	28.3220	1.2	448	-26.1833	28.3183	0	494	-26.1796	28.3248	0	540	-26.1794	28.3290	0	586	-26.1830	28.3280	0	632	-26.1832	28.3229	0	678	-26.1809	28.3209	0	724	-26.1791	28.3282	0
216	-26.1823	28.3290	1.2	449	-26.1833	28.3183	0	495	-26.1796	28.3249	0	541	-26.1794	28.3291	0	587	-26.1830	28.3279	0	633	-26.1831	28.3227	0	679	-26.1835	28.3271	0	725	-26.1836	28.3202	0
420	-26.1835	28.3248	1.2	450	-26.1832	28.3184	0	496	-26.1796	28.3250	0	542	-26.1794	28.3291	0	588	-26.1830	28.3278	0	634	-26.1831	28.3227	0	680	-26.1792	28.3297	0	726	-26.1799	28.3235	0
378	-26.1796	28.3253	1.1	451	-26.1832	28.3184	0	497	-26.1796	28.3250	0	543	-26.1795	28.3291	0	589	-26.1831	28.3277	0	635	-26.1832	28.3227	0	681	-26.1837	28.3193	0	727	-26.1838	28.3241	0
188	-26.1803	28.3237	1	452	-26.1831	28.3184	0	498	-26.1796	28.3250	0	544	-26.1796	28.3291	0	590	-26.1831	28.3276	0	636	-26.1833	28.3226	0	682	-26.1813	28.3190	0	728	-26.1816	28.3294	0
230	-26.1832	28.3283	1	453	-26.1831	28.3184	0	499	-26.1795	28.3251	0	545	-26.1797	28.3291	0	591	-26.1831	28.3275	0	637	-26.1834	28.3225	0	683	-26.1833	28.3292	0	729	-26.1829	28.3180	0

Table A9: Depth Measurements for van Ryn Dam

Sample	Lat	Long	Depth (m)	Sample	Lat	Long	Depth (m)	Sample	Lat	Long	Depth (m)
x1	-26.1566	28.3571	2.5	531	-26.1547	28.3543	3	373	-26.1512	28.3543	2.6
x2	-26.1560	28.3555	3.3	534	-26.1546	28.3552	3	383	-26.1516	28.3543	2.6
x3	-26.1543	28.3540	2.9	540	-26.1548	28.3553	3	402	-26.1520	28.3541	2.6
x4	-26.1501	28.3543	2.4	546	-26.1554	28.3541	3	414	-26.1523	28.3541	2.6
x5	-26.1483	28.3542	2.1	608	-26.1560	28.3568	3	415	-26.1523	28.3539	2.6
x6	-26.1442	28.3543	0.63	615	-26.1567	28.3562	3	416	-26.1522	28.3537	2.6
C	-26.1521	28.3540	2.6	625	-26.1557	28.3562	3	417	-26.1523	28.3535	2.6
y1	-26.1520	28.3522	1.6	405	-26.1521	28.3547	2.9	434	-26.1526	28.3534	2.6
y2	-26.1521	28.3540	1.3	411	-26.1523	28.3546	2.9	435	-26.1526	28.3536	2.6
627	-26.1562	28.3560	3.3	439	-26.1526	28.3547	2.9	436	-26.1526	28.3539	2.6
638	-26.1560	28.3555	3.3	471	-26.1530	28.3546	2.9	445	-26.1528	28.3549	2.6
639	-26.1559	28.3555	3.3	472	-26.1530	28.3549	2.9	446	-26.1528	28.3547	2.6
640	-26.1557	28.3556	3.3	478	-26.1534	28.3548	2.9	452	-26.1528	28.3533	2.6
641	-26.1555	28.3556	3.3	481	-26.1535	28.3543	2.9	453	-26.1529	28.3531	2.6
645	-26.1555	28.3555	3.3	501	-26.1539	28.3542	2.9	487	-26.1537	28.3530	2.6
479	-26.1535	28.3546	3.2	504	-26.1538	28.3549	2.9	539	-26.1547	28.3555	2.6
542	-26.1550	28.3549	3.2	509	-26.1541	28.3552	2.9	575	-26.1563	28.3573	2.6
545	-26.1553	28.3543	3.2	516	-26.1546	28.3537	2.9	305	-26.1497	28.3545	2.5
555	-26.1558	28.3547	3.2	529	-26.1548	28.3536	2.9	306	-26.1497	28.3543	2.5
556	-26.1556	28.3549	3.2	589	-26.1560	28.3571	2.9	307	-26.1497	28.3542	2.5
558	-26.1553	28.3554	3.2	592	-26.1559	28.3570	2.9	321	-26.1500	28.3544	2.5
586	-26.1566	28.3568	3.2	603	-26.1567	28.3563	2.9	330	-26.1504	28.3543	2.5
587	-26.1564	28.3569	3.2	610	-26.1558	28.3567	2.9	346	-26.1508	28.3541	2.5
594	-26.1563	28.3567	3.2	623	-26.1557	28.3564	2.9	348	-26.1507	28.3547	2.5
595	-26.1566	28.3566	3.2	382	-26.1516	28.3545	2.8	356	-26.1510	28.3542	2.5
605	-26.1564	28.3565	3.2	404	-26.1520	28.3545	2.8	357	-26.1511	28.3539	2.5
612	-26.1562	28.3565	3.2	410	-26.1523	28.3548	2.8	358	-26.1511	28.3538	2.5
613	-26.1564	28.3563	3.2	437	-26.1526	28.3543	2.8	372	-26.1512	28.3541	2.5
620	-26.1564	28.3561	3.2	438	-26.1526	28.3545	2.8	384	-26.1515	28.3541	2.5
626	-26.1560	28.3561	3.2	447	-26.1528	28.3544	2.8	385	-26.1515	28.3538	2.5
628	-26.1564	28.3558	3.2	469	-26.1531	28.3541	2.8	400	-26.1519	28.3535	2.5
636	-26.1564	28.3553	3.2	470	-26.1531	28.3545	2.8	401	-26.1519	28.3538	2.5
637	-26.1562	28.3554	3.2	482	-26.1536	28.3541	2.8	406	-26.1521	28.3549	2.5
644	-26.1554	28.3556	3.2	483	-26.1536	28.3538	2.8	418	-26.1523	28.3533	2.5
646	-26.1557	28.3554	3.2	484	-26.1537	28.3536	2.8	419	-26.1523	28.3531	2.5
647	-26.1560	28.3553	3.2	499	-26.1539	28.3535	2.8	432	-26.1526	28.3528	2.5
648	-26.1562	28.3551	3.2	500	-26.1539	28.3538	2.8	433	-26.1526	28.3531	2.5
511	-26.1543	28.3548	3.1	553	-26.1560	28.3541	2.8	454	-26.1529	28.3530	2.5
513	-26.1544	28.3543	3.1	596	-26.1568	28.3565	2.8	455	-26.1529	28.3528	2.5
532	-26.1547	28.3547	3.1	642	-26.1552	28.3558	2.8	465	-26.1532	28.3528	2.5
533	-26.1546	28.3549	3.1	643	-26.1552	28.3557	2.8	624	-26.1556	28.3563	2.5
541	-26.1549	28.3551	3.1	354	-26.1509	28.3545	2.7	630	-26.1567	28.3556	2.5
543	-26.1551	28.3547	3.1	374	-26.1512	28.3546	2.7	282	-26.1492	28.3544	2.4
544	-26.1552	28.3545	3.1	381	-26.1516	28.3547	2.7	297	-26.1495	28.3544	2.4
554	-26.1559	28.3544	3.1	403	-26.1520	28.3543	2.7	320	-26.1501	28.3541	2.4
557	-26.1554	28.3552	3.1	412	-26.1523	28.3544	2.7	322	-26.1501	28.3546	2.4
585	-26.1568	28.3567	3.1	413	-26.1523	28.3543	2.7	328	-26.1504	28.3546	2.4
588	-26.1562	28.3570	3.1	448	-26.1529	28.3541	2.7	331	-26.1504	28.3542	2.4
593	-26.1561	28.3568	3.1	449	-26.1528	28.3540	2.7	332	-26.1504	28.3540	2.4
604	-26.1566	28.3564	3.1	450	-26.1528	28.3538	2.7	333	-26.1504	28.3537	2.4
606	-26.1563	28.3566	3.1	451	-26.1528	28.3536	2.7	344	-26.1507	28.3537	2.4
607	-26.1561	28.3567	3.1	466	-26.1532	28.3532	2.7	345	-26.1507	28.3539	2.4
611	-26.1560	28.3566	3.1	467	-26.1532	28.3534	2.7	359	-26.1511	28.3536	2.4
614	-26.1566	28.3563	3.1	468	-26.1531	28.3538	2.7	360	-26.1511	28.3534	2.4
619	-26.1566	28.3561	3.1	477	-26.1533	28.3550	2.7	371	-26.1512	28.3537	2.4
621	-26.1562	28.3562	3.1	485	-26.1537	28.3534	2.7	386	-26.1515	28.3536	2.4
622	-26.1559	28.3563	3.1	486	-26.1537	28.3532	2.7	387	-26.1515	28.3534	2.4
629	-26.1565	28.3557	3.1	498	-26.1540	28.3532	2.7	388	-26.1515	28.3533	2.4
649	-26.1563	28.3550	3.1	517	-26.1547	28.3534	2.7	399	-26.1519	28.3531	2.4
480	-26.1535	28.3545	3	547	-26.1556	28.3538	2.7	420	-26.1523	28.3529	2.4
502	-26.1539	28.3544	3	590	-26.1558	28.3572	2.7	440	-26.1525	28.3549	2.4
503	-26.1539	28.3547	3	609	-26.1558	28.3568	2.7	497	-26.1540	28.3529	2.4
512	-26.1543	28.3545	3	635	-26.1566	28.3552	2.7	574	-26.1561	28.3574	2.4
514	-26.1545	28.3542	3	329	-26.1504	28.3545	2.6	616	-26.1568	28.3560	2.4
515	-26.1545	28.3539	3	353	-26.1509	28.3547	2.6	618	-26.1568	28.3559	2.4
530	-26.1548	28.3540	3	355	-26.1510	28.3543	2.6	260	-26.1488	28.3544	2.3

Table A9 Continued: Depth Measurements for van Ryn Dam

Sample	Lat	Long	Depth (m)	Sample	Lat	Long	Depth (m)	Sample	Lat	Long	Depth (m)
261	-26.1487	28.3542	2.3	391	-26.1514	28.3527	2.1	185	-26.1474	28.3544	1.7
275	-26.1489	28.3545	2.3	408	-26.1523	28.3550	2.1	190	-26.1476	28.3545	1.7
281	-26.1492	28.3545	2.3	423	-26.1522	28.3523	2.1	195	-26.1475	28.3540	1.7
283	-26.1492	28.3542	2.3	505	-26.1538	28.3552	2.1	203	-26.1477	28.3538	1.7
284	-26.1492	28.3541	2.3	510	-26.1542	28.3550	2.1	217	-26.1478	28.3538	1.7
295	-26.1495	28.3540	2.3	584	-26.1570	28.3566	2.1	225	-26.1480	28.3537	1.7
296	-26.1495	28.3542	2.3	597	-26.1569	28.3564	2.1	242	-26.1483	28.3537	1.7
298	-26.1495	28.3546	2.3	213	-26.1479	28.3543	2	266	-26.1487	28.3536	1.7
304	-26.1497	28.3547	2.3	214	-26.1479	28.3542	2	271	-26.1489	28.3535	1.7
308	-26.1497	28.3540	2.3	215	-26.1478	28.3541	2	280	-26.1492	28.3547	1.7
309	-26.1497	28.3538	2.3	227	-26.1481	28.3542	2	288	-26.1492	28.3534	1.7
318	-26.1500	28.3537	2.3	228	-26.1481	28.3543	2	292	-26.1494	28.3534	1.7
319	-26.1501	28.3539	2.3	229	-26.1481	28.3545	2	299	-26.1495	28.3547	1.7
334	-26.1505	28.3536	2.3	236	-26.1483	28.3545	2	327	-26.1504	28.3548	1.7
335	-26.1505	28.3535	2.3	240	-26.1483	28.3540	2	352	-26.1509	28.3549	1.7
342	-26.1507	28.3533	2.3	241	-26.1483	28.3538	2	380	-26.1516	28.3549	1.7
343	-26.1507	28.3535	2.3	258	-26.1488	28.3547	2	393	-26.1514	28.3524	1.7
347	-26.1507	28.3544	2.3	264	-26.1487	28.3538	2	407	-26.1521	28.3550	1.7
361	-26.1511	28.3533	2.3	272	-26.1489	28.3536	2	458	-26.1529	28.3522	1.7
362	-26.1511	28.3531	2.3	286	-26.1492	28.3537	2	495	-26.1541	28.3524	1.7
363	-26.1511	28.3530	2.3	293	-26.1494	28.3536	2	508	-26.1541	28.3554	1.7
368	-26.1512	28.3529	2.3	312	-26.1498	28.3534	2	631	-26.1568	28.3555	1.7
369	-26.1512	28.3532	2.3	337	-26.1505	28.3531	2	634	-26.1567	28.3552	1.7
370	-26.1512	28.3535	2.3	367	-26.1511	28.3527	2	140	-26.1468	28.3542	1.6
398	-26.1518	28.3527	2.3	392	-26.1514	28.3525	2	148	-26.1469	28.3541	1.6
409	-26.1523	28.3550	2.3	397	-26.1517	28.3525	2	161	-26.1470	28.3541	1.6
421	-26.1523	28.3527	2.3	489	-26.1538	28.3526	2	162	-26.1470	28.3543	1.6
422	-26.1522	28.3525	2.3	496	-26.1541	28.3526	2	168	-26.1473	28.3544	1.6
488	-26.1538	28.3528	2.3	519	-26.1548	28.3530	2	171	-26.1473	28.3541	1.6
518	-26.1547	28.3532	2.3	527	-26.1549	28.3530	2	172	-26.1473	28.3539	1.6
528	-26.1549	28.3533	2.3	578	-26.1568	28.3570	2	182	-26.1474	28.3539	1.6
535	-26.1545	28.3554	2.3	579	-26.1569	28.3569	2	191	-26.1475	28.3546	1.6
559	-26.1551	28.3557	2.3	580	-26.1571	28.3568	2	196	-26.1475	28.3538	1.6
573	-26.1559	28.3575	2.3	650	-26.1565	28.3548	2	218	-26.1478	28.3537	1.6
576	-26.1564	28.3572	2.3	147	-26.1468	28.3543	1.96	231	-26.1481	28.3546	1.6
591	-26.1557	28.3571	2.3	194	-26.1475	28.3542	1.9	313	-26.1498	28.3532	1.6
602	-26.1569	28.3562	2.3	205	-26.1477	28.3542	1.9	338	-26.1505	28.3530	1.6
237	-26.1483	28.3544	2.2	206	-26.1477	28.3543	1.9	340	-26.1507	28.3529	1.6
238	-26.1483	28.3542	2.2	212	-26.1478	28.3545	1.9	349	-26.1507	28.3548	1.6
250	-26.1485	28.3541	2.2	226	-26.1481	28.3539	1.9	365	-26.1510	28.3527	1.6
251	-26.1485	28.3543	2.2	265	-26.1487	28.3537	1.9	366	-26.1511	28.3526	1.6
252	-26.1485	28.3544	2.2	276	-26.1490	28.3547	1.9	394	-26.1515	28.3523	1.6
259	-26.1488	28.3545	2.2	287	-26.1492	28.3535	1.9	395	-26.1515	28.3522	1.6
273	-26.1489	28.3539	2.2	316	-26.1500	28.3532	1.9	429	-26.1526	28.3520	1.6
274	-26.1489	28.3542	2.2	323	-26.1501	28.3547	1.9	476	-26.1533	28.3552	1.6
285	-26.1492	28.3539	2.2	424	-26.1522	28.3522	1.9	490	-26.1538	28.3524	1.6
310	-26.1497	28.3537	2.2	430	-26.1526	28.3522	1.9	520	-26.1548	28.3528	1.6
336	-26.1505	28.3533	2.2	463	-26.1532	28.3525	1.9	549	-26.1559	28.3535	1.6
341	-26.1507	28.3530	2.2	538	-26.1547	28.3556	1.9	572	-26.1557	28.3575	1.6
389	-26.1515	28.3531	2.2	552	-26.1561	28.3539	1.9	118	-26.1466	28.3540	1.5
390	-26.1515	28.3529	2.2	184	-26.1474	28.3542	1.8	119	-26.1466	28.3542	1.5
431	-26.1526	28.3525	2.2	192	-26.1475	28.3544	1.8	127	-26.1467	28.3543	1.5
456	-26.1529	28.3526	2.2	193	-26.1475	28.3543	1.8	128	-26.1467	28.3542	1.5
457	-26.1529	28.3524	2.2	204	-26.1477	28.3540	1.8	129	-26.1467	28.3541	1.5
464	-26.1532	28.3526	2.2	207	-26.1477	28.3545	1.8	139	-26.1468	28.3540	1.5
473	-26.1530	28.3551	2.2	216	-26.1478	28.3539	1.8	146	-26.1468	28.3545	1.5
548	-26.1557	28.3536	2.2	230	-26.1481	28.3545	1.8	149	-26.1469	28.3540	1.5
239	-26.1483	28.3541	2.1	235	-26.1483	28.3546	1.8	160	-26.1470	28.3540	1.5
249	-26.1485	28.3539	2.1	248	-26.1485	28.3537	1.8	163	-26.1470	28.3545	1.5
262	-26.1487	28.3541	2.1	253	-26.1485	28.3546	1.8	173	-26.1473	28.3537	1.5
263	-26.1487	28.3539	2.1	444	-26.1527	28.3551	1.8	181	-26.1474	28.3537	1.5
294	-26.1495	28.3538	2.1	577	-26.1566	28.3571	1.8	197	-26.1475	28.3537	1.5
311	-26.1498	28.3535	2.1	617	-26.1569	28.3560	1.8	202	-26.1477	28.3536	1.5
317	-26.1500	28.3534	2.1	169	-26.1473	28.3543	1.7	208	-26.1477	28.3546	1.5
364	-26.1510	28.3528	2.1	170	-26.1473	28.3542	1.7	224	-26.1480	28.3536	1.5
375	-26.1512	28.3548	2.1	183	-26.1474	28.3541	1.7	243	-26.1483	28.3536	1.5

Table A9 Continued: Depth Measurements for van Ryn Dam

Sample	Lat	Long	Depth (m)	Sample	Lat	Long	Depth (m)	Sample	Lat	Long	Depth (m)	Sample	Lat	Long	Depth (m)
247	-26.1485	28.3535	1.5	303	-26.1497	28.3548	1.3	290	-26.1493	28.3532	1.1	31	-26.1449	28.3542	0.86
267	-26.1487	28.3534	1.5	425	-26.1522	28.3520	1.3	302	-26.1496	28.3549	1.1	47	-26.1452	28.3538	0.86
315	-26.1500	28.3531	1.5	506	-26.1538	28.3553	1.3	351	-26.1509	28.3549	1.1	24	-26.1447	28.3543	0.85
441	-26.1525	28.3551	1.5	521	-26.1549	28.3526	1.3	492	-26.1538	28.3520	1.1	32	-26.1449	28.3540	0.84
462	-26.1531	28.3521	1.5	551	-26.1561	28.3537	1.3	571	-26.1557	28.3574	1.1	25	-26.1447	28.3545	0.82
494	-26.1541	28.3522	1.5	567	-26.1556	28.3568	1.3	583	-26.1572	28.3565	1.1	23	-26.1447	28.3542	0.81
526	-26.1550	28.3528	1.5	569	-26.1556	28.3571	1.3	656	-26.1566	28.3543	1.1	28	-26.1449	28.3545	0.81
598	-26.1570	28.3563	1.5	570	-26.1557	28.3573	1.3	50	-26.1453	28.3541	1	15	-26.1446	28.3544	0.8
601	-26.1570	28.3562	1.5	581	-26.1572	28.3568	1.3	51	-26.1454	28.3543	1	39	-26.1450	28.3545	0.8
81	-26.1460	28.3541	1.4	600	-26.1571	28.3561	1.3	59	-26.1455	28.3538	1	48	-26.1453	28.3537	0.8
88	-26.1461	28.3542	1.4	632	-26.1569	28.3554	1.3	66	-26.1456	28.3545	1	53	-26.1453	28.3546	0.8
89	-26.1461	28.3540	1.4	63	-26.1457	28.3539	1.2	76	-26.1458	28.3536	1	67	-26.1457	28.3546	0.8
98	-26.1463	28.3541	1.4	64	-26.1457	28.3541	1.2	83	-26.1460	28.3545	1	85	-26.1461	28.3546	0.8
99	-26.1463	28.3542	1.4	71	-26.1458	28.3543	1.2	93	-26.1462	28.3534	1	124	-26.1466	28.3547	0.8
106	-26.1464	28.3543	1.4	74	-26.1459	28.3539	1.2	94	-26.1462	28.3534	1	155	-26.1470	28.3533	0.8
107	-26.1464	28.3542	1.4	79	-26.1460	28.3537	1.2	101	-26.1463	28.3546	1	165	-26.1471	28.3547	0.8
108	-26.1465	28.3541	1.4	82	-26.1460	28.3543	1.2	134	-26.1467	28.3533	1	166	-26.1472	28.3547	0.8
109	-26.1465	28.3539	1.4	91	-26.1462	28.3537	1.2	154	-26.1470	28.3534	1	177	-26.1473	28.3533	0.8
117	-26.1466	28.3539	1.4	95	-26.1463	28.3535	1.2	156	-26.1471	28.3534	1	178	-26.1474	28.3532	0.8
120	-26.1466	28.3543	1.4	100	-26.1463	28.3544	1.2	200	-26.1476	28.3533	1	188	-26.1475	28.3547	0.8
126	-26.1467	28.3545	1.4	112	-26.1465	28.3535	1.2	222	-26.1479	28.3533	1	209	-26.1477	28.3547	0.8
137	-26.1468	28.3537	1.4	113	-26.1465	28.3534	1.2	233	-26.1482	28.3548	1	210	-26.1478	28.3548	0.8
138	-26.1468	28.3539	1.4	133	-26.1467	28.3535	1.2	245	-26.1483	28.3533	1	377	-26.1512	28.3550	0.8
141	-26.1467	28.3544	1.4	153	-26.1469	28.3535	1.2	301	-26.1495	28.3549	1	379	-26.1515	28.3550	0.8
150	-26.1469	28.3539	1.4	157	-26.1470	28.3535	1.2	474	-26.1530	28.3552	1	427	-26.1524	28.3519	0.8
159	-26.1470	28.3538	1.4	164	-26.1470	28.3546	1.2	475	-26.1531	28.3553	1	428	-26.1525	28.3519	0.8
167	-26.1472	28.3546	1.4	223	-26.1480	28.3534	1.2	525	-26.1550	28.3525	1	443	-26.1527	28.3552	0.8
174	-26.1473	28.3536	1.4	232	-26.1481	28.3547	1.2	536	-26.1544	28.3556	1	524	-26.1550	28.3523	0.8
180	-26.1474	28.3536	1.4	244	-26.1483	28.3534	1.2	568	-26.1556	28.3569	1	537	-26.1545	28.3557	0.8
289	-26.1492	28.3533	1.4	269	-26.1488	28.3533	1.2	599	-26.1571	28.3562	1	561	-26.1550	28.3560	0.8
314	-26.1498	28.3531	1.4	270	-26.1489	28.3533	1.2	654	-26.1568	28.3548	1	582	-26.1573	28.3567	0.8
396	-26.1517	28.3521	1.4	291	-26.1494	28.3532	1.2	657	-26.1565	28.3542	1	659	-26.1564	28.3538	0.8
459	-26.1529	28.3521	1.4	300	-26.1495	28.3548	1.2	658	-26.1564	28.3540	1	11	-26.1444	28.3543	0.75
491	-26.1538	28.3521	1.4	324	-26.1501	28.3549	1.2	36	-26.1450	28.3541	0.94	16	-26.1446	28.3542	0.75
651	-26.1567	28.3547	1.4	339	-26.1505	28.3529	1.2	29	-26.1449	28.3544	0.92	41	-26.1451	28.3546	0.7
652	-26.1567	28.3546	1.4	350	-26.1507	28.3549	1.2	30	-26.1449	28.3543	0.92	68	-26.1457	28.3547	0.7
72	-26.1459	28.3542	1.3	378	-26.1514	28.3550	1.2	37	-26.1450	28.3542	0.9	102	-26.1462	28.3547	0.7
73	-26.1459	28.3540	1.3	460	-26.1530	28.3520	1.2	38	-26.1450	28.3544	0.9	103	-26.1463	28.3547	0.7
80	-26.1460	28.3539	1.3	522	-26.1549	28.3524	1.2	42	-26.1452	28.3545	0.9	123	-26.1466	28.3547	0.7
87	-26.1461	28.3543	1.3	550	-26.1561	28.3536	1.2	43	-26.1452	28.3544	0.9	256	-26.1487	28.3548	0.7
90	-26.1462	28.3538	1.3	560	-26.1550	28.3559	1.2	44	-26.1452	28.3543	0.9	325	-26.1501	28.3549	0.7
96	-26.1463	28.3537	1.3	563	-26.1553	28.3562	1.2	45	-26.1452	28.3541	0.9	442	-26.1525	28.3552	0.7
97	-26.1463	28.3539	1.3	564	-26.1554	28.3564	1.2	46	-26.1452	28.3540	0.9	523	-26.1549	28.3522	0.7
105	-26.1464	28.3545	1.3	633	-26.1569	28.3553	1.2	49	-26.1453	28.3539	0.9	562	-26.1551	28.3561	0.7
110	-26.1465	28.3538	1.3	55	-26.1455	28.3545	1.1	52	-26.1453	28.3545	0.9	565	-26.1554	28.3566	0.7
111	-26.1465	28.3536	1.3	56	-26.1455	28.3543	1.1	54	-26.1454	28.3547	0.9	10	-26.1444	28.3542	0.69
115	-26.1466	28.3536	1.3	57	-26.1455	28.3541	1.1	60	-26.1455	28.3536	0.9	17	-26.1446	28.3541	0.69
116	-26.1466	28.3538	1.3	58	-26.1455	28.3539	1.1	61	-26.1456	28.3536	0.9	27	-26.1448	28.3546	0.69
121	-26.1466	28.3545	1.3	65	-26.1456	28.3543	1.1	69	-26.1458	28.3546	0.9	26	-26.1447	28.3546	0.67
130	-26.1467	28.3538	1.3	70	-26.1458	28.3545	1.1	77	-26.1458	28.3535	0.9	14	-26.1445	28.3546	0.66
131	-26.1467	28.3537	1.3	75	-26.1458	28.3537	1.1	84	-26.1460	28.3546	0.9	22	-26.1448	28.3540	0.64
132	-26.1467	28.3536	1.3	78	-26.1459	28.3536	1.1	104	-26.1464	28.3546	0.9	12	-26.1444	28.3545	0.63
136	-26.1468	28.3535	1.3	86	-26.1461	28.3545	1.1	122	-26.1466	28.3546	0.9	6	-26.1442	28.3543	0.62
142	-26.1467	28.3545	1.3	92	-26.1462	28.3535	1.1	143	-26.1467	28.3546	0.9	33	-26.1449	28.3539	0.62
151	-26.1469	28.3538	1.3	114	-26.1465	28.3534	1.1	176	-26.1473	28.3533	0.9	40	-26.1450	28.3546	0.6
152	-26.1469	28.3536	1.3	125	-26.1467	28.3546	1.1	187	-26.1474	28.3547	0.9	493	-26.1539	28.3520	0.6
158	-26.1470	28.3536	1.3	135	-26.1468	28.3534	1.1	221	-26.1478	28.3533	0.9	7	-26.1442	28.3541	0.54
186	-26.1474	28.3546	1.3	145	-26.1468	28.3546	1.1	255	-26.1486	28.3548	0.9	35	-26.1449	28.3538	0.54
189	-26.1475	28.3547	1.3	175	-26.1473	28.3535	1.1	326	-26.1504	28.3549	0.9	5	-26.1441	28.3544	0.52
198	-26.1475	28.3535	1.3	179	-26.1474	28.3534	1.1	376	-26.1511	28.3550	0.9	18	-26.1446	28.3539	0.52
201	-26.1477	28.3534	1.3	199	-26.1475	28.3534	1.1	426	-26.1523	28.3519	0.9	9	-26.1443	28.3540	0.5
219	-26.1478	28.3535	1.3	211	-26.1479	28.3548	1.1	461	-26.1531	28.3520	0.9	21	-26.1448	28.3539	0.5
234	-26.1483	28.3547	1.3	220	-26.1478	28.3534	1.1	507	-26.1539	28.3555	0.9	278	-26.1491	28.3549	0.5
254	-26.1485	28.3547	1.3	246	-26.1484	28.3533	1.1	566	-26.1555	28.3567	0.9	13	-26.1444	28.3547	0.49
257	-26.1488	28.3548	1.3	268	-26.1487	28.3533	1.1	653	-26.1568	28.3549	0.9	2	-26.1441	28.3542	0.47
277	-26.1490	28.3548	1.3	279	-26.1492	28.3549	1.1	655	-26.1566	28.3544	0.9	8	-26.1443	28.3540	0.44

Table A9 Continued: Depth Measurements for van Ryn Dam

Sample	Lat	Long	Depth (m)	Sample	Lat	Long	Depth (m)	Sample	Lat	Long	Depth (m)	Sample	Lat	Long	Depth (m)
3	-26.1439	28.3545	0.43	718	-26.1435	28.3543	0	784	-26.1547	28.3520	0	850	-26.1576	28.3562	0
1	-26.1441	28.3540	0.41	719	-26.1435	28.3542	0	785	-26.1549	28.3521	0	851	-26.1459	28.3530	0
34	-26.1448	28.3538	0.41	720	-26.1436	28.3539	0	786	-26.1552	28.3523	0	852	-26.1479	28.3551	0
4	-26.1440	28.3546	0.4	721	-26.1438	28.3537	0	787	-26.1552	28.3524	0	853	-26.1530	28.3516	0
19	-26.1446	28.3538	0.38	722	-26.1441	28.3538	0	788	-26.1553	28.3525	0	854	-26.1551	28.3566	0
20	-26.1447	28.3538	0.37	723	-26.1444	28.3538	0	789	-26.1553	28.3524	0	855	-26.1490	28.3528	0
660	-26.1564	28.3537	0.3	724	-26.1445	28.3537	0	790	-26.1554	28.3523	0	856	-26.1432	28.3545	0
144	-26.1468	28.3547	0.2	725	-26.1446	28.3537	0	791	-26.1555	28.3523	0	857	-26.1559	28.3521	0
62	-26.1456	28.3537	0.1	726	-26.1448	28.3537	0	792	-26.1556	28.3522	0	858	-26.1560	28.3577	0
661	-26.1576	28.3566	0	727	-26.1450	28.3535	0	793	-26.1557	28.3520	0	859	-26.1475	28.3528	0
662	-26.1575	28.3567	0	728	-26.1452	28.3535	0	794	-26.1557	28.3520	0	860	-26.1452	28.3551	0
663	-26.1574	28.3567	0	729	-26.1452	28.3533	0	795	-26.1558	28.3521	0	861	-26.1547	28.3518	0
664	-26.1570	28.3569	0	730	-26.1454	28.3533	0	796	-26.1557	28.3521	0	862	-26.1526	28.3555	0
665	-26.1566	28.3572	0	731	-26.1455	28.3534	0	797	-26.1556	28.3522	0	863	-26.1512	28.3520	0
666	-26.1561	28.3574	0	732	-26.1458	28.3532	0	798	-26.1556	28.3524	0	864	-26.1445	28.3535	0
667	-26.1557	28.3576	0	733	-26.1461	28.3531	0	799	-26.1555	28.3524	0	865	-26.1566	28.3539	0
668	-26.1556	28.3576	0	734	-26.1463	28.3532	0	800	-26.1554	28.3525	0	866	-26.1573	28.3561	0
669	-26.1555	28.3574	0	735	-26.1464	28.3531	0	801	-26.1554	28.3525	0	867	-26.1457	28.3532	0
670	-26.1555	28.3571	0	736	-26.1465	28.3532	0	802	-26.1555	28.3526	0	868	-26.1488	28.3551	0
671	-26.1555	28.3571	0	737	-26.1467	28.3531	0	803	-26.1555	28.3525	0	869	-26.1527	28.3516	0
672	-26.1554	28.3568	0	738	-26.1469	28.3531	0	804	-26.1556	28.3526	0	870	-26.1553	28.3570	0
673	-26.1553	28.3567	0	739	-26.1471	28.3531	0	805	-26.1557	28.3526	0	871	-26.1486	28.3528	0
674	-26.1553	28.3567	0	740	-26.1471	28.3531	0	806	-26.1557	28.3527	0	872	-26.1436	28.3548	0
675	-26.1553	28.3566	0	741	-26.1474	28.3530	0	807	-26.1558	28.3527	0	873	-26.1558	28.3519	0
676	-26.1551	28.3563	0	742	-26.1476	28.3529	0	808	-26.1558	28.3528	0	874	-26.1566	28.3574	0
677	-26.1550	28.3561	0	743	-26.1477	28.3530	0	809	-26.1559	28.3529	0	875	-26.1471	28.3529	0
678	-26.1548	28.3560	0	744	-26.1479	28.3530	0	810	-26.1560	28.3531	0	876	-26.1458	28.3551	0
679	-26.1546	28.3560	0	745	-26.1480	28.3530	0	811	-26.1562	28.3534	0	877	-26.1545	28.3518	0
680	-26.1545	28.3558	0	746	-26.1481	28.3530	0	812	-26.1563	28.3535	0	878	-26.1533	28.3556	0
681	-26.1541	28.3557	0	747	-26.1482	28.3531	0	813	-26.1563	28.3536	0	879	-26.1509	28.3521	0
682	-26.1538	28.3556	0	748	-26.1484	28.3532	0	814	-26.1564	28.3537	0	880	-26.1442	28.3536	0
683	-26.1538	28.3556	0	749	-26.1484	28.3532	0	815	-26.1563	28.3537	0	881	-26.1564	28.3534	0
684	-26.1535	28.3555	0	750	-26.1486	28.3530	0	816	-26.1566	28.3544	0	882	-26.1572	28.3558	0
685	-26.1534	28.3555	0	751	-26.1490	28.3529	0	817	-26.1567	28.3545	0	883	-26.1454	28.3532	0
686	-26.1531	28.3554	0	752	-26.1495	28.3529	0	818	-26.1567	28.3546	0	884	-26.1497	28.3552	0
687	-26.1528	28.3554	0	753	-26.1500	28.3527	0	819	-26.1567	28.3546	0	885	-26.1525	28.3516	0
688	-26.1524	28.3553	0	754	-26.1505	28.3525	0	820	-26.1568	28.3549	0	886	-26.1554	28.3575	0
689	-26.1522	28.3552	0	755	-26.1512	28.3521	0	821	-26.1569	28.3548	0	887	-26.1484	28.3530	0
690	-26.1517	28.3552	0	756	-26.1516	28.3519	0	822	-26.1570	28.3550	0	888	-26.1439	28.3549	0
691	-26.1514	28.3552	0	757	-26.1518	28.3518	0	823	-26.1569	28.3552	0	889	-26.1555	28.3520	0
692	-26.1511	28.3551	0	758	-26.1519	28.3518	0	824	-26.1570	28.3554	0	890	-26.1574	28.3570	0
693	-26.1507	28.3551	0	759	-26.1521	28.3518	0	825	-26.1570	28.3557	0	891	-26.1468	28.3529	0
694	-26.1503	28.3551	0	760	-26.1522	28.3518	0	826	-26.1571	28.3560	0	892	-26.1465	28.3551	0
695	-26.1500	28.3550	0	761	-26.1523	28.3518	0	827	-26.1572	28.3561	0	893	-26.1541	28.3517	0
696	-26.1497	28.3551	0	762	-26.1524	28.3517	0	828	-26.1572	28.3563	0	894	-26.1538	28.3558	0
697	-26.1494	28.3550	0	763	-26.1526	28.3518	0	829	-26.1573	28.3563	0	895	-26.1505	28.3524	0
698	-26.1492	28.3550	0	764	-26.1528	28.3518	0	830	-26.1573	28.3564	0	896	-26.1438	28.3536	0
699	-26.1490	28.3550	0	765	-26.1530	28.3519	0	831	-26.1574	28.3564	0	897	-26.1561	28.3528	0
700	-26.1488	28.3550	0	766	-26.1530	28.3518	0	832	-26.1576	28.3565	0	898	-26.1578	28.3565	0
701	-26.1485	28.3550	0	767	-26.1531	28.3518	0	833	-26.1576	28.3566	0	899	-26.1462	28.3530	0
702	-26.1483	28.3550	0	768	-26.1533	28.3518	0	834	-26.1570	28.3552	0	900	-26.1474	28.3551	0
703	-26.1477	28.3549	0	769	-26.1534	28.3518	0	835	-26.1452	28.3532	0	901	-26.1533	28.3516	0
704	-26.1474	28.3548	0	770	-26.1536	28.3517	0	836	-26.1503	28.3552	0	902	-26.1547	28.3562	0
705	-26.1471	28.3548	0	771	-26.1537	28.3517	0	837	-26.1522	28.3516	0	903	-26.1496	28.3527	0
706	-26.1471	28.3548	0	772	-26.1537	28.3518	0	838	-26.1555	28.3578	0	904	-26.1433	28.3540	0
707	-26.1468	28.3548	0	773	-26.1538	28.3519	0	839	-26.1482	28.3529	0	905	-26.1558	28.3523	0
708	-26.1464	28.3548	0	774	-26.1539	28.3519	0	840	-26.1444	28.3549	0	906	-26.1556	28.3579	0
709	-26.1454	28.3548	0	775	-26.1540	28.3519	0	841	-26.1553	28.3521	0	907	-26.1479	28.3528	0
710	-26.1453	28.3548	0	776	-26.1540	28.3518	0	842	-26.1578	28.3567	0	908	-26.1448	28.3550	0
711	-26.1449	28.3548	0	777	-26.1541	28.3518	0	843	-26.1466	28.3530	0	909	-26.1550	28.3520	0
712	-26.1444	28.3547	0	778	-26.1542	28.3518	0	844	-26.1470	28.3550	0	910	-26.1517	28.3554	0
713	-26.1442	28.3547	0	779	-26.1543	28.3519	0	845	-26.1536	28.3516	0	911	-26.1515	28.3518	0
714	-26.1442	28.3547	0	780	-26.1544	28.3519	0	846	-26.1543	28.3560	0	912	-26.1449	28.3534	0
715	-26.1437	28.3547	0	781	-26.1545	28.3520	0	847	-26.1500	28.3526	0	913	-26.1569	28.3545	0
716	-26.1434	28.3545	0	782	-26.1546	28.3521	0	848	-26.1435	28.3536	0	914	-26.1509	28.3552	0
717	-26.1435	28.3543	0	783	-26.1546	28.3521	0	849	-26.1558	28.3524	0				

APPENDIX 2: The Initial (Raw) Sediment Data obtained from the Handheld XRF

Table B1: The Raw sediment data from the Handheld XRF for the four pans

Site	Sample	Depth (m)	As (ppm)	As Error	Cu (ppm)	Cu Error	Fe (ppm)	Fe Error	Mn (ppm)	Mn Error	Ni (ppm)	Ni Error	Pb (ppm)	Pb Error	Zn (ppm)	Zn Error
Korsmans	KPC	1.5	13.79	4.33	97.3	9.45	32675.25	180.49	1059.45	48.22	0	19.54	108.84	5.58	578.67	13.7
	KPX1	0.1	6.02	2.7	28.2	6.83	9118.33	87.89	103.8	24.99	0	16.25	42.47	3.48	176.69	7.38
	KPX2	1.2	9.41	3.48	59.87	7.7	19632.45	129.93	542.16	35.47	0	17.07	79.48	4.5	395.7	10.62
	KPX3	1.5	13.73	4.06	69.96	8.48	28329.19	162.46	951.85	44.67	27.33	12.57	101.31	5.21	513.1	12.5
	KPX4	0.17	11.5	2.86	212.12	10.41	27129.85	151.63	370.65	32.62	0	16.77	43.84	3.54	177.95	7.55
	KPY1	0.23	7.59	2.48	29.25	7.09	8868.26	88.75	119.51	25.72	0	16.28	27.69	3.11	114.62	6.41
	KPY2	1.4	9.76	3.73	67.18	8.32	19847.77	135.92	522.77	36.55	0	17.74	85.21	4.83	434.35	11.56
	KPY3	1.3	13.63	4.12	73.05	8.52	25095.46	151.06	738.8	40.7	0	18.34	108.34	5.31	527.05	12.51
	KPY4	0.09	15.1	3.75	116.12	9.34	34542.67	179.79	383.8	35.84	0	18.65	79.48	4.73	543.55	12.9
Amata Pan	APC	1.5	108.12	23.15	810.36	27.26	192271.5	588.4	4378.3	126.95	238.1	25.32	2084.74	30.7	16276.15	94.62
	APX1	1.3	130.86	21.6	1060.51	24.93	126354	395.83	2679.66	85.84	101.64	19.21	2652.86	28.68	17231.4	80.77
	APX2	1.3	102.9	22.26	865.23	26.83	177265.4	547.69	3447.02	112.18	101.58	23.22	2054.9	29.54	13629.78	83.99
	APY1	1.2	740.58	39.77	2368.72	54.29	348817.4	952.2	7930.28	206.21	695.01	42.99	3741.52	49.35	39127.2	176.23
	APY2	1.3	153.15	20.12	781.53	28.16	393479.7	852.75	5339.45	148.81	217.69	29.08	1443.61	26	14536.69	90.76
Bullfrog Pan	BFPC	0.92	10.07	3.68	52.04	9.16	28832.22	178.75	1223.91	52.76	0	20.17	62.7	4.73	234.78	9.71
	BFPX1	0.41	4.71	2.81	26.73	7.44	10190.85	98.28	117.1	26.18	0	17.34	40.14	3.69	112.32	6.61
	BFPX2	0.60	11.48	3.79	47.87	8.75	21946.8	152.48	1316.54	52.49	0	19.25	72.55	4.85	286.72	10.28
	BFPX3	0.96	6.56	2.84	42.21	7.9	21434.86	142.96	622.28	38.62	0	17.77	39.2	3.66	131.89	7.06
	BFPX4	0.94	14	3.94	79.85	10.23	34535.02	201.87	1076.95	52.72	0	21.72	65.32	4.96	265.07	10.59
	BFPY1	0.27	0	3.17	12.66	6.15	8650.91	79.75	154.95	23.84	0	15.15	26.12	2.81	61.68	4.74
	BFPY2	0.79	11.01	3.9	60.31	9.7	24227.25	167.94	1459.6	57.47	0	20.87	68.27	4.98	260.66	10.4
	BFPY3	0.88	18.89	4.11	76.28	10.24	39742.3	217.47	1855.55	64.89	0	21.73	68.58	5.05	333.13	11.73
	BFPY4	1.20	6.4	2.57	77.92	9.83	62356.7	260.05	506.22	43.51	58.06	15.06	19.6	3.23	83.15	6.59
Sandpan	SPC	0.66	5.01	3.17	57.76	9.32	38951.72	207.8	811.09	47.24	0	21.1	43.82	4.15	131.11	7.75
	SPX1	0.24	0	3.62	16.73	6.63	8006.36	82.5	53.52	23.2	0	16.38	31.09	3.21	50.97	4.81
	SPX2	0.54	4.82	3.08	44.06	9.02	19196.02	147.48	868.49	46.96	0	20.09	38.84	4.04	98.9	7.03
	SPX3	0.62	6.56	3.53	67.59	11.21	55640.2	276.22	1186.68	60.89	31.34	17.09	40.88	4.56	135.95	8.88
	SPX4	0.23	0	2.96	15.26	6.46	6036.68	71.79	55.77	22.68	0	16.06	16.16	2.59	27.27	4.07
	SPY1	0.16	6.72	2.74	40.81	7.7	21387.01	140.71	373.6	33.43	0	17.86	35.24	3.52	114.81	6.62
	SPY2	0.69	4.42	2.33	45.17	6.75	31064.08	142.32	815.1	35.68	0	15.54	38.99	3.06	90.89	5.18
	SPY3	0.61	0	3.7	41.06	7.73	31165.46	170.18	645.59	39.64	20.79	12.34	28.98	3.28	77.99	5.78
	SPY4	0.25	0	3	14.78	6.54	4961.25	66.07	0	34.07	0	15.99	15.99	2.67	24.93	4.13

Table B1 Continued: Raw sediment data from the Handheld XRF for the four pans

Site	Sample	Ca (ppm)	Ca Error	S (ppm)	S Error	K (ppm)	K Error	Ti (ppm)	Ti Error	V (ppm)	V Error	Cr (ppm)	Cr Error	Th (ppm)	Th Error	U (ppm)	U Error
Korsmans	KPC	31204.37	206.44	2165.88	198.57	11417.58	182.19	3825.81	65.04	103.66	18.65	326.43	12.96	12.82	2.53	0	5.36
	KPX1	6186.85	72.71	1053.76	110.52	5624.9	98.75	3683.46	46.79	72.41	13.06	320.7	9.59	5.9	1.79	5.93	2.58
	KPX2	21772	160	1778.42	167.01	8418.23	145.92	3636.12	57.79	82.1	16.37	318.83	11.8	8.56	2.07	0	4.27
	KPX3	34779.04	216.99	2901.25	217.76	10542.39	176.16	3620.41	62.92	116.82	18.2	291.79	12.55	10.88	2.34	5.72	3.31
	KPX4	6663.73	93.12	2938.21	200	3177.1	97.49	3767.56	59.17	104.38	16.98	206.76	11.2	3.36	1.79	5.44	2.43
	KPY1	6207.07	74.8	610.95	98.74	8003.89	117.07	5200.06	54.8	102.71	15	251.48	9.12	13.41	2.08	8.72	3.08
	KPY2	25588.38	168.5	1928.18	166.63	8229.68	141.31	3489.57	55.62	78.2	15.74	300.79	11.21	8.29	2.17	5.78	3.12
	KPY3	30680.71	189.71	4551.82	236.45	9038.53	152.51	3345.04	56.08	91.1	16.05	399.98	12.48	11.51	2.33	7.98	3.19
	KPY4	5057.5	88.48	603.45	138.3	4640.9	120.87	4002.84	65.88	122.03	19.12	340.42	13.46	8.83	2.22	5.57	2.87
Amata Pan	APC	10463.18	180.26	3789.14	366.81	5065.58	185.66	3340.65	96.99	106.87	29.63	1363.28	31.57	39.25	8.21	9.57	4.79
	APX1	12601.39	182.62	4844.68	368.03	5273.86	176.05	3453.31	96.43	140.14	29.73	1631.63	31.33	0	10.28	0	5.73
	APX2	11112.89	183.99	4582.42	389.25	5134.14	185.78	3318.21	97.87	123.35	30.19	1422.46	31.91	0	10.61	0	6.64
	APY1	10824.66	163.94	5733.53	374.53	4953.43	162.73	3242.72	88.85	105.03	26.95	1520.33	28.78	0	17.73	0	9.31
	APY2	8547.85	174.58	3368.77	380.13	3228.58	165.64	2336.69	90.47	88.41	28.76	970.28	30.05	0	10.54	0	7.16
Bullfrog Pan	BFPC	36205.19	213.09	1003.98	157.05	15742.91	202.18	3386.69	59.84	109.29	17.4	202.79	11.1	20.97	2.87	23.89	4.88
	BFPX1	5527.99	75.81	227.04	92.96	20076.45	179.24	3454.97	46.66	72.32	13.18	124.67	7.9	21.67	2.56	38.12	4.8
	BFPX2	39298.04	209.37	1391.74	158.5	14825.12	186.32	2741.19	51.79	72.5	14.95	249.04	10.76	13.43	2.53	24.55	4.42
	BFPX3	23181.36	163.21	660.55	132.78	15304.5	187.36	3339.92	55.11	85	15.8	180.62	10.21	14.02	2.34	0	5.78
	BFPX4	34256.65	210.35	1486.49	173.79	13132.4	189.02	4233.67	65.21	112.04	18.47	213.47	11.39	20.2	2.95	0	6.92
	BFPY1	16746.15	120.61	168.58	95.18	23670.54	193.71	2191.64	39.19	49.43	11.38	118.76	7.69	8.26	1.89	0	5.86
	BFPY2	52010.22	242.78	1125.92	154.41	13921.74	185.05	2664.29	52.81	79.83	15.32	234.86	10.66	14.94	2.72	6.9	4.45
	BFPY3	46524.94	256.36	2182.47	207.6	12542.96	196.74	3061.75	61.88	100.87	18.07	247.78	12.46	14.64	2.79	8.22	4.36
	BFPY4	20120.98	187.89	< LOD	230.53	14076.12	221.47	3564.82	69.6	149.51	20.8	282.92	14.31	9.73	2.55	14.51	4.77
Sandpan	SPC	13349.24	140.22	371.13	137.79	19006.68	225.74	3417.89	61.98	135.63	18.47	279.86	12.4	22.31	2.89	17.09	4.71
	SPX1	3768.27	68.63	234.6	96.75	29916.4	211.23	3516.57	46.32	62.75	13.05	182.85	8.19	18.56	2.33	30.99	4.59
	SPX2	19456	139.13	258.89	105	16845.97	180.11	3130.29	49.32	79.01	14.12	264.02	9.86	23.75	2.89	31.93	4.99
	SPX3	17555.42	163.72	< LOD	203.6	19157.07	234.4	2967.1	62.66	129.35	18.98	267.87	12.61	23.35	3.34	13.61	5.35
	SPX4	6352.97	73.25	218	81.5	13143.56	139.22	2523.08	38.52	52.48	11.01	163.31	7.75	6.92	1.8	0	4.65
	SPY1	7241.58	97.43	429.24	120.74	18686.11	201.37	2704.11	50.41	90.81	14.99	179.68	10.08	21.6	2.55	16.58	4.28
	SPY2	15229.95	131.38	179.3	114.3	19358.54	201.39	3409.07	54.75	123.21	16.18	240.26	10.55	23.43	2.2	14.25	3.46
	SPY3	11653.97	135.07	259.29	137.17	19530.78	233.17	3325.07	62.43	136.54	18.71	222.99	12.19	15.19	2.36	14.92	3.98
	SPY4	5144.98	66	169.65	78.63	15970.88	147.33	3739.33	43.4	53.85	11.91	228.09	8.01	11.32	2.01	20.11	3.66

Table B2: Raw sediment data from the Handheld XRF for the five dams

Site	Sample	Depth (m)	As (ppm)	As Error	Cu (ppm)	Cu Error	Fe (ppm)	Fe Error	Mn (ppm)	Mn Error	Ni (ppm)	Ni Error	Pb (ppm)	Pb Error	Zn (ppm)	Zn Error
Homestead Dam	HDC	4.1	36.45	6.46	120.74	13.09	130912.1	438.61	3019.51	94.8	69.13	19.27	152.65	7.95	734.95	18.82
	HDX1	0.39	18.88	5.07	120.3	11.36	86470.29	325.84	853.79	56.26	0	23.32	117.42	6.43	314.04	11.66
	HDX2	1.6	19.79	4.97	109.06	9.87	41629.99	206.07	425.43	38.98	0	19.86	142.22	6.36	666.08	14.86
	HDX3	2.7	10.33	5.57	94.54	9.5	44744.57	212.28	720.02	44.04	30.89	13.44	201.93	7.4	680.12	14.87
	HDX4	3.8	17.98	6.05	101.22	10.12	54662.64	243.38	1532.36	58.98	30.02	14.33	215.98	7.91	622.87	14.83
	HDY1	1.6	19.41	4.65	78.4	9.88	68429.06	278.56	2071.82	68.84	23.62	14.81	103.72	5.84	402.84	12.45
	HDY2	2.3	17.45	4.71	92.54	11.6	123746.2	408.89	5029.72	110.01	52.93	17.85	84.17	5.89	374.66	13.23
	HDZ1	5.8	20.99	5.9	109.31	10.91	84532.41	315.14	1476.2	63.34	47.43	15.84	180.56	7.61	510.28	14.14
	HDZ2	6.1	22.67	5.68	125.91	11.19	82274.18	309.39	1284.34	60.01	43.42	15.7	164.8	7.26	640.04	15.62
Middle Lake	MLC	4	33.61	6.94	127	11.63	78087.81	310.5	3812.14	91.48	48.87	15.94	238.72	8.86	812.46	17.96
	MLX1	3.5	43.18	6.59	114.71	11.75	99388.84	356.81	1569.63	69	79.53	17	189.09	8.13	597.31	15.89
	MLX2	4.6	31.15	6.06	96.87	9.12	58086.09	225.94	1131.56	48.33	41.98	13.02	262.03	7.8	684.93	13.98
	MLX3	4.7	35.75	6.26	117.06	10.62	69168.67	276.21	2209.78	69.14	57.19	14.77	210.19	7.89	717.73	16.02
	MLX4	4	22.35	5.99	87.27	9.26	53293.14	228.61	1148.52	50.94	45.88	13.53	232.59	7.8	564.32	13.47
	MLX5	3.2	19.88	5.79	106.76	10.18	47917.82	227.17	915.9	49.34	40.97	14.42	194.13	7.51	477.44	13.08
	MLX6	1.6	16.69	4.3	91.22	9.22	30947.56	173.89	521.92	38.65	23.35	13.02	107.13	5.47	296.25	10.03
	MLY1	1.3	39.25	6.1	108.8	10.84	63600.43	272.55	1652.14	64.3	34.88	15.3	178.85	7.56	463.92	13.51
	MLY2	0.75	42.05	4.98	73.16	10.8	69594.62	298.15	1447.71	64.66	31.01	16.44	82.24	5.65	338.02	12.33
Civic Lake	CLC	0.81	23.17	7	142.9	10.61	45632	217.59	790.94	46.72	0	20.41	311.71	9.2	1310.54	20.67
	CLX1	1.5	48.27	8.33	222.44	14.38	60620.79	280.86	804.88	55.41	40.01	17.18	328.28	10.59	1362.15	23.71
	CLX2	1.7	34.56	7.61	146.18	11.57	61004.01	265.14	1096.06	55.74	42.53	15.41	321.08	9.85	1174.26	20.7
	CLY1	0.81	43.63	7.14	154.71	12.73	81628.77	322.47	3962.26	94.79	54.53	16.86	235.1	8.94	1204.59	22.05
	CLY2	0.81	14.92	4.64	80.67	8.74	35232.85	177.69	844.21	42.8	0	18.46	146.02	6.02	702.24	14.25
Kleinfontein Dam	KDC	4.6	92.59	10.34	295.59	12.95	92777.17	286.88	1423.72	55.33	149.21	15.78	783.46	13.3	4358.59	34.52
	KDX1	2.8	28.04	7.91	217.05	12	52181.04	229.83	869.12	48.31	40.47	14.19	414.08	10.41	1770.22	23.66
	KDX2	3.8	112.31	13.7	359.1	18	92500.32	371.37	1589.09	74.45	139.51	20.45	802.99	17.46	4958.18	47.7
	KDX3	4.9	83.76	12.78	275.21	15.44	86560.64	341.08	1285.46	65.44	133.33	18.66	799.89	16.54	3898.96	40.2
	KDX4	3.2	33.95	4.46	51.38	8.04	17423.57	127.55	184.73	29.2	0	17.69	108.6	5.36	546.16	12.87
	KDY1	1.1	18.96	4.47	103.33	10.13	21877.06	152.74	1103.31	49.68	84.12	14.72	103.44	5.64	863.53	17.08
	KDY2	0.84	18.49	3.61	69.24	9.62	44020.61	221.63	1048.15	52.58	23.71	14.49	48.42	4.33	303.02	10.91
van Ryn Dam	VRDC	2.6	13.51	4.03	90.49	10.07	50957.39	237.23	474.06	42.14	38	14.48	76.52	5.14	285.75	10.59
	VRDX1	2.5	21.27	3.54	126.06	9.85	65910.37	235.21	513.72	39.29	71.41	14.01	69.11	4.31	319.93	9.8
	VRDX2	3.3	15.51	4.3	104.58	10.97	51089.75	246.83	538.88	45.25	0	23.02	80.37	5.44	317.85	11.57
	VRDX3	2.9	22.49	4.31	136.11	10.5	69281.66	249.2	731.59	44.11	54.84	14.45	110.11	5.41	432.89	11.56
	VRDX4	2.4	9.22	4.06	86.37	10.1	48452.09	233.11	453.89	41.97	0	21.76	80.63	5.28	282.63	10.61
	VRDX5	2.1	12.91	4.05	85.27	10.1	35305.92	199.45	320.04	37.64	0	21.65	76.52	5.17	264.29	10.35
	VRDX6	0.63	4.44	2.56	38.98	8.26	10629.2	103.87	77.3	26.05	0	18.76	27.06	3.29	124.72	7.18
	VRDY1	1.6	4.76	2.81	39.54	8.62	35437.88	195.01	263.99	35.12	0	19.98	29.82	3.71	168.81	8.33
	VRDY2	1.3	6.08	2.28	33.82	7.5	24018.26	148.7	204.87	30.16	0	17.95	18.34	2.84	70.11	5.57

Table B2 Continued: Raw sediment data from the Handheld XRF for the five dams

Site	Sample	Ca (ppm)	Ca Error	S (ppm)	S Error	K (ppm)	K Error	Ti (ppm)	Ti Error	V (ppm)	V Error	Cr (ppm)	Cr Error	Th (ppm)	Th Error	U (ppm)	U Error
Homestead Dam	HDC	4981.29	113.78	1177.23	221.05	5496.6	165.79	4989.38	92.22	175.4	27.1	550.02	20.18	6.43	3.44	11.82	4.26
	HDX1	7173.26	122.28	666.94	176.8	6463.54	163.42	2721.06	68.04	155.46	21.43	696.24	19.59	4.86	2.77	5.45	3.41
	HDX2	6370.47	101.14	865.67	154.93	5819.92	136.85	5069.6	74.51	132.01	21.15	422.08	14.62	12.86	2.65	15.02	3.53
	HDX3	5571.15	97.7	942.01	162.83	5439.18	136.19	4932.3	75.35	147.23	21.63	342.95	14.3	11.99	2.75	13.69	3.4
	HDX4	5037.35	95.94	965.71	169.77	4982.93	134.73	4655.21	76.03	131.71	21.9	347.73	14.83	8.56	2.83	5.74	3.35
	HDY1	5047.56	99.95	1164.87	186.55	4059.58	129.16	4119.85	75.54	112.78	21.9	470.91	16.74	5.09	2.55	4.66	3.09
	HDY2	4258.1	103.58	802.66	199.16	3850	140.31	4331.23	85.28	170.98	25.48	441.15	18.69	0	4.42	0	4.95
	HDZ1	5958.63	118.06	1975.4	240.66	6400.78	170.07	4635.81	86.55	180.53	25.73	542.06	19.22	6.46	2.93	10.94	3.74
	HDZ2	5452	112.55	1664.62	227.08	5638.17	160.08	4733.86	86.79	173.92	25.64	453.07	18.21	0	4.17	11.03	3.72
Middle Lake	MLC	8923.68	136.48	2376.21	246.21	5914.99	160.31	4680.4	83.56	183.58	24.74	486.45	18.06	11.97	3.27	10.41	3.85
	MLX1	6529.23	123.77	7977.61	407.82	4770.66	152.75	3876.18	82.58	164.42	25.01	612.49	20.29	9.49	3.22	18.34	3.92
	MLX2	4470.53	91.22	2101.29	210.53	4534.76	129.77	3974.39	71.23	132.91	20.91	341.65	14.79	6.45	2.59	13.13	3.02
	MLX3	6337	115.67	2227.52	237.35	5515.88	153.39	4523.9	81.43	174.33	24.13	454.13	17.56	13.82	3.03	18.58	3.68
	MLX4	6180.68	107.86	2211.39	220.72	5404.85	143.4	4851.06	78.82	152.2	22.8	376.25	15.59	14.53	2.87	14.95	3.36
	MLX5	5244.42	93.65	1460.63	179.4	4635.65	125.76	4579.63	72.34	119.99	20.68	377.64	14.44	9.79	2.77	8.43	3.28
	MLX6	5252.86	83.74	1793.43	167.45	4074.96	107.05	4923.26	66.33	128.8	18.72	336.1	12.43	10.87	2.39	6.68	2.99
	MLY1	7032.56	114.31	2777.78	238.26	6004.39	149.92	4846.3	80.38	159.79	23.44	558.8	17.33	16.93	3.13	12.66	3.76
	MLY2	9373.05	125.83	2078.29	208.27	4048.54	123.94	3764.57	69.12	129.86	20.32	476.35	15.86	6.36	2.71	7.92	3.52
Civic Lake	CLC	7466.01	113.16	1704.86	194.89	6605.56	150.51	4773.35	76.27	124.04	21.83	558.86	16.56	10.38	2.99	6.03	3.28
	CLX1	6559.06	95.29	2883.72	202.55	5479.98	123.62	4250.51	64.66	124.09	18.55	608.71	14.79	12.47	3.53	16.39	4.03
	CLX2	5328.02	100.29	1957.4	208.68	6458.22	152.32	4913.86	79.23	143.55	22.84	564.88	17.05	13.24	3.32	12.6	3.73
	CLY1	6754.12	113.94	2051.58	218.61	6602.28	157.62	4471.93	79.22	155.4	23.34	462.26	16.54	8.75	3.25	13.87	4.05
	CLY2	5712.57	88.94	881.83	139.96	4356.38	112.33	3962.57	63.07	106.74	18.14	314.46	12.43	10.89	2.4	11.55	2.89
Kleinfontein Dam	KDC	8554.78	130.3	5049.67	312.19	6989.23	166.68	4435.96	81.53	174.45	24.3	540.89	17.93	16.61	3.81	15.66	3.52
	KDX1	8878.89	121.85	2031.07	204.3	6558.72	149.6	4157.1	73.3	129.03	21.44	605.4	16.83	8.49	3.15	8.59	3.39
	KDX2	8919.03	132.2	4278.01	290.11	6968.63	165.66	4651.48	82.76	150.21	24.2	574.15	17.95	19.16	5.04	17.49	4.69
	KDX3	7865.86	130.72	4009.06	296.96	7608.07	179.53	4715.77	85.87	147.26	25.05	592.62	19.08	21.89	4.81	19.34	4.46
	KDX4	4189.88	67.01	2511.64	162.58	5408.69	105.75	2764.08	45.38	79.07	13.18	302.63	10.33	6.87	2.13	11.85	2.8
	KDY1	13084.91	115.88	3224.27	185.96	2832.05	85.53	3430.51	52.99	85.57	15.16	273.9	10.46	9.53	2.41	14.17	3.04
	KDY2	3838.15	79.18	803.06	146.52	5646.05	130.84	5220.34	72.81	125.47	20.48	482.05	14.67	8.79	2.46	7.62	3.43
van Ryn Dam	VRDC	4919.28	97.78	778.8	163.42	12030.96	196.78	4338.68	72.77	135.4	21.15	321.34	14.23	28.9	3.2	36.07	5.21
	VRDX1	4827.48	85.58	1023.01	151.81	8668.72	152.33	3609.98	60.77	130.39	17.97	409.98	13.42	22.12	2.63	16.36	3.84
	VRDX2	4871.82	90.54	852.69	152.69	9862.82	169.33	3969.23	66.25	110.25	19.14	323.53	13.24	28.07	3.28	11.97	4.7
	VRDX3	5619.69	77.46	735.92	119.92	10380.19	139.28	4284.65	55.23	132.75	16.02	356.26	10.86	31.49	3.07	14.19	4.38
	VRDX4	4773.3	92.49	762.37	154.21	11229.28	183.52	4218.37	69.09	142.9	20.18	300.88	13.4	29.26	3.23	13.86	4.79
	VRDX5	4440.24	79.9	674.63	130	9264.06	151.78	3772.55	59.25	101.13	17.02	251.35	11.35	23.88	2.99	14.38	4.34
	VRDX6	3693.69	55.94	448.26	84.38	5881.69	96.42	2787.16	39.66	62.26	11.25	140.56	7.54	8.52	2.04	12.48	3.2
	VRDY1	3337.08	77.58	337.35	125.46	17015.55	205.35	2235.88	51.09	91.13	15.67	162.57	10.69	42.07	3.44	33.99	6.03
	VRDY2	3689.02	70.26	228.11	105.29	5422.8	116.76	4707.18	62.2	102.22	17.32	228.61	10.93	11.55	2.11	11.95	3.18

APPENDIX 3: Handheld XRF Data compared to the Conventional XRF Data

Table C1: Initial Data used to compare the Handheld XRF to the Conventional XRF

Sample	Cr		Cu		Fe		Mn		Ni		Pb		Zn	
	Conv	Hand	Conv	Hand	Conv	Hand	Conv	Hand	Conv	Hand	Conv	Hand	Conv	Hand
KPC	279.99	326.43	88.3	97.3	33153.12	32675.25	1161.686	1059.45	67.27	0.5	97.28	108.84	495.42	578.67
APC	1374.61	1363.28	713.46	810.36	109391.3	192271.47	2555.708	4378.3	273.11	238.1	1845.58	2084.74	14229.19	16276.15
BFPC	149.38	202.79	39.43	52.04	22871.46	28832.22	1084.24	1223.91	35.49	0.5	47.38	62.7	151.98	234.78
SPC	204.56	279.86	41.39	57.76	33013.24	38951.72	774.457	811.09	56.02	0.5	35.96	43.82	94.67	131.11
HDC	450.75	550.02	97.26	120.74	84841.22	130912.09	1858.697	3019.51	108.46	69.13	124.77	152.65	534.22	734.95
MLC	382.69	486.45	104.36	127	56793.96	78087.81	2788.045	3812.14	101.78	48.87	189.95	238.72	625.82	812.46
CLC	469.68	558.86	121.28	142.9	41686.21	45632	774.457	790.94	80.96	0.5	268.26	311.71	1164.94	1310.54
KDC	464.28	540.89	207.41	295.59	57913.05	92777.17	1006.794	1423.72	194.3	149.21	571.6	783.46	3010.6	4358.59
VRDC	212.11	321.34	67.11	90.49	42105.87	50957.39	464.6742	474.06	81.36	38	64.78	76.52	209.44	285.75

Table C1 Continued: Initial Data used to compare the Handheld XRF to the Conventional XRF

Sample	Ca		K		Sc		Ti		V		Th		U	
	Conv	Hand	Conv	Hand	Conv	Hand	Conv	Hand	Conv	Hand	Conv	Hand	Conv	Hand
KPC	32661.84	31204.37	13780.44	11417.58	18.05	66.09	4136.605	3825.81	69.88	103.66	8.06	12.82	0.5	0.5
APC	9576.993	10463.18	5645	5065.58	10.99	27.44	3237.343	3340.65	54.76	106.87	3.76	39.25	0.42	9.57
BFPC	35592.11	36205.19	18595.29	15742.91	14.26	70.67	3417.196	3386.69	64.5	109.29	10.43	20.97	0.5	23.89
SPC	13293.44	13349.24	23742.2	19006.68	12.28	25.57	3776.9	3417.89	79.62	135.63	14.55	22.31	1.2	17.09
HDC	3287.625	4981.29	5728.014	5496.6	15.52	0.5	5275.67	4989.38	140.88	175.4	6.87	6.43	0.5	11.82
MLC	8004.651	8923.68	6558.161	5914.99	20.34	25.32	4436.359	4680.4	112.04	183.58	11.36	11.97	1.33	10.41
CLC	6003.488	7466.01	7471.323	6605.56	12.92	22.23	4676.162	4773.35	95.3	124.04	10.78	10.38	0.59	6.03
KDC	7861.711	8554.78	7886.397	6989.23	14.87	25.28	4196.556	4435.96	105.77	174.45	8.42	16.61	1.55	15.66
VRDC	3573.505	4919.28	14859.63	12030.96	11.95	0.5	4316.458	4338.68	88.44	135.4	21.76	28.9	3.78	36.07